Theoretical Applications of Non-Standard Cosmological and Gravitational Physics: Higher Spins and Modified Gravity

by
Leah Gabrielle Jenks
B.A., Colgate University, 2017
M.Sc., University of Edinburgh, 2018
Sc.M., Brown University, 2020

A dissertation submitted in partial fulfillment of the
requirements for the Degree of Doctor of Philosophy
in the Department of Physics at Brown University

Providence, Rhode Island
April 2022

This dissertation by Leah Gabrielle Jenks is accepted in its present form by the Department of Physics as satisfying the dissertation requirement for the degree of Doctor of Philosophy.

Date _____ _____

Professor Stephon Alexander, Advisor

Recommended to the Graduate Council

Date _____ _____

Professor S. James Gates, Jr., Reader

Date _____ _____

Professor David Lowe, Reader

Approved by the Graduate Council

Date _____ _____

Professor Andrew Campbell
Dean of the Graduate School

Per aspera ad astra

Through hardship to the stars

Vita

Leah Jenks completed her B.A. in Astronomy-Physics at Colgate University in 2017. As an undergraduate she worked on a range of topics, including observations of quasars with Professor Thomas Balonek, characterizing the morphologies of high-redshift galaxies with Professor Debra Elmegreen, and studying the production of superheavy dark matter with Professor Patrick Crotty. She then completed an M.Sc. in Theoretical Physics at the University of Edinburgh in 2018, where she wrote a masters thesis on higher-dimensional black hole mechanics with Professor James Lucietti. In Fall 2018 she began the Ph.D. program at Brown University and joined Professor Stephon Alexander's group. Her Ph.D. research has spanned a wide range of topics in theoretical cosmology and gravitation, including applications of higher spin fields to cosmology and explorations of modified gravity theories in the context of gravitational waves and black holes. Leah also participated in the 'Summer Brown' program, teaching a course 'Quantum Mechanics and the Nature of Reality' for high school students during summers 2019, 2021 and 2022. Furthermore, she has been an advocate for women and historically underrepresented groups in physics, co-leading the Graduate Women in Physics group and serving on the departmental DIAP committee during her time at Brown. Leah has been awarded a KICP Postdoctoral Fellowship at the University of Chicago and will begin in the Fall of 2022.

Preface

This thesis is based on the following six papers, completed during the author's PhD.

1. Higher Spin Supersymmetry at the Cosmological Collider: Sculpting SUSY Rilles in the CMB
   Journal of High Energy Physics, 10, 156 (2019)
   with Stephon Alexander, S. James Gates Jr., Konstantinos Koutrolikos, and Evan McDonough
2. Gravity Waves in Parity Violating Copernican Universes
   Physical Review D, 102, 4, 044039 (2020)
   with Stephon Alexander, Pavel Jirousek, João Magueijo, and Tom Zlosnik
3. Probing Noncommutative Gravity with Gravitational Waves and Binary Pulsar Observations
   Physical Review D, 102, 084022 (2020)
   with Stephon Alexander and Kent Yagi
4. Higher Spin Dark Matter
   Physics Letters B, 819, 136436 (2021)
   with Stephon Alexander and Evan McDonough
5. The Chern-Simons Caps for Rotating Black Holes
   Physical Review D, 104,6, 064033 (2021)
   with Stephon Alexander, Gregory Gabadadze, and Nicolás Yunes
6. Black Hole Superradiance in Dynamical Chern-Simons Gravity
   Under review, submitted to *Physical Review D* (2022)
   with Stephon Alexander, Gregory Gabadadze, and Nicolás Yunes

Acknowledgements

The completion of this PhD truly took a village and I am indebted to all of those who supported me along the way. First and foremost I would like to thank my wonderful PhD advisor, Stephon Alexander. I have developed into the scientist I am today due to his wisdom, patience, and guidance. I would not be at this point without him having taken a chance on me in 2018, and his persistent belief in me ever since. I am deeply grateful for everything he has taught me, from performing quantum field theory calculations to the minutae of being a member of the greater scientific community.

I would also like to thank Greg Gabadadze, Nico Yunes, and Evan McDonough for being incredible mentors and collaborators through my PhD. Again, this PhD would not have been possible without their support and I am motivated every day to push myself to be as good of a physicist as they think I am.

I have learned something from every collaborator I have had the pleasure working with over the last four years, and for that I thank Jim Gates, Konstantinos Koutrolikos, João Maguiejo, Tom Zlosnik, Pavel Jirousek, and Kent Yagi, in addition to Evan, Nico and Greg.

I would like thank Jim Gates and David Lowe for serving on my preliminary exam and thesis committees, as well as the administrative staff of the physics department, Pete Bilderback, Ida Alarcon, Mary Ellen Woyjik, and Morgan Latus.

I would like to thank the Alexander cosmology group past and present for creating a collaborative and intellectually stimulating environment: Mike Toomey, Alejandra Rosselli-Calderon, Tats Daniel, Christian Capanelli, Gabe Herczeg, Steven Clark, and Batia Friedman-Shaw, as well as my officemates past and present: Jatan Buch, John Leung, Kyriakos Vattis,

and Isabelle Goldstein.

I am fortunate to have had an outstanding cohort and support system in Providence: Farrah Simpson, Sammie Moreno-Ulibarri, Austin Vaitkus, Nick Pervan, Michael Lukasik, Lauren Hirai, Kara Fox, and Rutendo Jakachira.

I thank my family, John, Jennifer and Daniel Jenks for always believing in me and encouraging me to chase my dreams, and I thank Ishir Dutta for his love, support, and snacks as this PhD was being completed and thesis was being written.

I would like to thank my high school physics teacher, the late Kevin McCarron for sparking the desire to become a physicist, as well as Tom Balonek, Patrick Crotty, Debra Elmegreen for being my early research mentors, believing in me and supporting me.

Lastly, I would like to thank Dr. Rick Friedman, Dr. Marc Schwartz, and the entire UC San Diego Acoustic Neuroma program, head and neck surgery team, and neurosurgery team. Without their efforts in January of 2022, this thesis would not have been possible.

Contents

List of Tables

List of Figures

Chapter 1

Introduction

We are currently in the midst of an exciting era of physics, for both theorists and experimentalists alike. Now more than ever before, the theories which encode our understanding of the universe are able to be studied with a wide array of experimental and observational tools. For example, the Large Hadron Collider at CERN has confirmed the standard model (SM) of particle physics to high precision, the LIGO/Virgo/KAGRA collaboration has confirmed general relativity (GR) via observations of gravitational waves (GW), and careful measurements of the cosmic microwave background have made the case for ΛCDM cosmology. However, all is still not known. Fortunately for theorists who would be out of a job if the aforementioned theories described the universe perfectly and completely, there are still many unknowns and open questions in the realm of cosmology, gravitation and high-energy physics.

Some of these questions are as follows. Most notably, while quantum mechanics does an excellent job explaining physics on the smallest scales and general relativity the largest, we still do not have a verified theory of quantum gravity. If one attempts to quantize gravity directly, one runs into nonrenormalizability issues, among others. Thus, it seems that general relativity must be a low energy limit of some UV complete theory which accurately describes quantum gravity effects. The most prominent such theory is string theory, in which the fundamental object is no longer a particle, but a string. String theory and its variants have

been widely studied in a variety of contexts but there has still been no direct observational evidence for the theory, nor any other proposed theories of quantum gravity, such as loop quantum gravity.

Another open problem is that of dark matter. Dark matter makes up about 25% of the energy density of the universe and its presence has been observationally inferred through techniques including observations of spiral galaxy rotation curves and gravitational lensing. However, despite the critical role that dark matter plays in our universe, it has never been directly detected and its constituent particle remains a mystery. The leading paradigm since the discovery of dark matter has been the WIMP, or weakly interacting massive particle and efforts are ongoing to detect such a particle with experiments such as LZ and XENON. Thus far, these experiments have been unsuccessful in finding dark matter, but have been making the viable parameter space smaller and smaller. As such, other alternative dark matter candidates have gained popularity, including axion-like particles, primordial black holes and other exotic models. Despite the wide range of possible models though, the dark matter problem remains.

Beyond the puzzles of quantum gravity and dark matter, there are many other unsolved problems, including as the cosmological constant problem and the Hubble tension. Clearly, though our trusty theories such as the standard model, general relativity and ΛCDM cosmology have done a great job predicting the dynamics of the universe, there are still many open questions and puzzles to be solved. By looking for physics beyond the standard paradigms, we hope to glean insight into these questions and move towards a resolution. In the case of quantum gravity, it is useful to study theories which may not necessarily be quantum theories of gravity themselves, but that are derived from some UV complete theory in order to make progress towards the ultimate goal. Similarly, for dark matter, it is of significant interest to continue building models and think creatively about possible solutions to the dark matter problem.

Broadly motivated by these questions, this thesis will explore non-standard cosmological and gravitational theories and investigate both the theoretical nuances of such theories as well

as observational prospects and constraints. We focus specifically on cosmological implications of higher-spin particles and gravitational phenomena in various theories of modified gravity.

The structure of this thesis is as follows. We begin in Chapter 2 with a discussion of the relevant background information for the work presented. The remainder of the thesis is split into three pars. We first begin in Part I in the early universe and consider cosmological aspects of higher spin fields during inflation. Chapter 3 discusses higher spin supersymmetry in the context of the cosmological collider program and Chapter 4 investigates higher spin particles as a dark matter candidate. We then redshift our way to the late universe in Part II, where we discuss the propagation of gravitational waves, both in a modified theory of gravity in which the cosmological constant is dynamical in and noncommutative gravity in Chapter 6. Lastly, we remain in the late universe in Part III where we explore aspects of rotating black holes in another modified theory of gravity, dynamical Chern-Simons gravity. We study the 'Chern-Simons caps' in Chapter 7 and conclude with an investigation of superradiance for dCS black holes in Chapter 8. Finally, we present concluding remarks in Chapter 9.

Chapter 2

Background

2.1 General Relativity and Gravitational Waves

2.1.1 General Relativity

One of the most beautiful agreements of theory and experiment in physics is Einstein's theory of General Relativity, written down in 1915, and its confirmation by the LIGO experiment nearly 100 years later in 2015. Einstein's theory, motivated by special relativity and Newtonian gravity is built upon the following two principles [2]:

1. General principle of relativity: the general principle of relativity states that the laws of physics should remain the same in all reference. This generalizes the special principle of relativity, which postulates that the laws of physics are the same in all *inertial* reference frames.

2. Equivalence principle: the equivalence principle comes from the observation of the equivalence of gravitational and inertial mass, and has two formulations; the strong and weak equivalence principles. The weak equivalence principle states that locally, one can choose an inertial frame in which the laws of physics are identical to those in a frame in which gravity is absent. The strong equivalence principle extends the weak equivalence principle more generally to hold in a relativistic theory and for all the laws of physics.

As eloquently put by John Archibald Wheeler, general relativity can be summed up as 'spacetime tells matter how to move, matter tells spacetime how to curve.' This can be see quantitatively from the Einstein Field Equations,

$$R_{\mu\nu} - \frac{1}{2}Rg_{\mu\nu} + \Lambda g_{\mu\nu} = 8\pi T_{\mu\nu}, \tag{2.1}$$

where $g_{\mu\nu}$ is the spacetime metric, $R_{\mu\nu}$ is the Ricci curvature tensor, R the Ricci scalar and $T_{\mu\nu}$ the energy-momentum tensor of the spacetime. We have also included the cosmological constant, Λ. The above is written in geometric units such that $G = c = 1$. The left-hand side of Eq. (2.1) reflects the curvature of the spacetime, 'spacetime tells matter how to move,' and the right-hand side describes the matter present in the spacetime, 'matter tells spacetime how to curve.' Eq. (2.1) is a set of ten nonlinear partial differential equations. Luckily, employing the Bianchi identities can reduce this to six. Nonetheless, finding exact solutions of this system of equations is highly nontrivial. Such solutions of the Einstein field equations describe spacetimes, including black hole spacetimes and expanding cosmological spacetimes. The first exact solution to the Einstein equations was found by Karl Schwarzschild in 1915, which describes an uncharged and non-rotating black hole. According to Birkhoff's theorem, the Schwarzschild metric is the most general spherically symmetric solution of the Einstein equations. The Schwarzschild line element is given by

$$ds^2 = -f dt^2 + \frac{1}{f}dr^2 + r^2 d\theta^2 + r^2 \sin^2\theta d\phi^2, \tag{2.2}$$

where f is the so-called 'Schwarzschild factor'

$$f = 1 - \frac{2M}{r}, \tag{2.3}$$

where again we have worked in geometric units such that $G = c = 1$. In this expression, we can see that there is a singularity at $r = 2M$, known as the Schwarzschild horizon, as well as at $r = 0$. However, the singularity at $r = 2M$ is coordinate system dependent, whereas the singularity at $r = 0$ is a true curvature singularity.

Other notable solutions to the Einstein equations include the Kerr metric, which describes a rotating black hole, the Riessner-Nordstrom metric, describing a charged black hole, the Kerr-Newman metric, which describes a charged and rotating black hole, and the Friedmann-Lemaitre-Robertson-Walker metric (FLRW), which describes an expanding universe. The Einstein equations have also been solved in higher dimensions, giving rise to a 5D black ring solution, for example, as well as in various modified theories of gravity, such as the slowly rotating black hole in dynamical Chern-Simons gravity.

General relativity can also be written in terms of an action,

$$S = \int d^4x\sqrt{-g}R, \tag{2.4}$$

known as the Einstein-Hilbert action. The variation of this action with respect to the metric yields the Einstein equations.

2.1.2 Gravitational Waves

One of the most stunning predictions of general relativity is the existence of gravitational waves, spacetime ripples which propagate as a result of mergers of compact objects. To understand the emergence of gravitational waves from the Einstein field equations, first consider a perturbation to the metric such that [2]

$$g_{\mu\nu} = \eta_{\mu\nu} + h_{\mu\nu}, \tag{2.5}$$

where $\eta_{\mu\nu}$ is the Minkowski metric and $|h_{\mu\nu}| \ll 1$. This is considered a 'weak field approximation' in which we assume the gravitational field is weakly perturbed about a flat background. This allows us to linearize the Einstein equations and explore the gravitational wave behavior. Let us study this linearization further. The perturbation Eq. (2.5) leads to the following expression for the Christoffel symbols:

$$\Gamma^{\rho}_{\mu\nu} = \frac{1}{2}\eta^{\rho\lambda}\left(\partial_\mu h_{\nu\lambda} + \partial_\nu h_{\lambda\mu} - \partial_\lambda h_{\mu\nu}\right). \tag{2.6}$$

This allows us to linearize the Riemann tensor and the Ricci tensor:

$$R_{\mu\nu\rho\sigma} = \tfrac{1}{2}\left(\partial_\rho\partial_\nu h_{\mu\sigma} + \partial_\sigma\partial_\mu h_{\nu\rho} - \partial_\sigma\partial_\nu h_{\mu\rho} - \partial_\rho\partial_\mu h_{\nu\sigma}\right), \tag{2.7}$$

$$R_{\mu\nu} = \tfrac{1}{2}\left(\partial_\sigma\partial_\nu h^{\sigma_\mu} + \partial_\sigma\partial_\mu h^\sigma_\nu - \partial_\mu\partial_\nu h - \Box h_{\mu\nu}\right), \tag{2.8}$$

where h is the trace of the perturbation and $\Box$ is the d'Alembertian operator. Similarly, we can obtain the Ricci scalar via contraction:

$$R = \partial_\mu\partial_\nu h^{\mu\nu} - \Box h. \tag{2.9}$$

All together, these linearized quantities yield the Einstein equations, here in vacuum with zero cosmological constant:

$$G_{\mu\nu} = \frac{1}{2}\left(\partial_\sigma\partial_\mu h^\sigma_\nu + \partial_\sigma\partial_\nu h^\sigma_\mu - \partial_\mu\partial_\nu h - \Box h_{\mu\nu} - \eta_{\mu\nu}\partial_\rho\partial_\lambda h^{\rho\sigma} + \eta_{\mu\nu}\Box h\right) = 0. \tag{2.10}$$

One can choose a gauge to work in to make these equations more tractable. One common choice is the Lorentz gauge, which has the gauge condition:

$$\partial_\mu h^\mu_\lambda - \frac{1}{2}\partial_\lambda h = 0. \tag{2.11}$$

This condition leads to the following satisfying form for the vacuum Einstein equations:

$$\Box h_{\mu\nu} = 0. \tag{2.12}$$

It is clear to see that this choice has simply reduced the Einstein equations to a relativistic wave equation, for which we can find plane wave solutions. Consider one such solution

$$h_{\mu\nu} = A_{\mu\nu}e^{ik_\mu x^\mu}, \tag{2.13}$$

where $A_{\mu\nu}$ are constants. Note that to obtain true gravitational waves, we must have $k^2 = 0$. This itself necessitates that gravitational waves must travel at the speed of light (an

important test of GR which we will discuss in the next section).

Now, to account for gravitational waves which arise in nature, such as those emitted by merging black holes, we must consider the Einstein equations with a source,

$$\Box \bar{h}_{\mu\nu} = -16\pi T_{\mu\nu}, \tag{2.14}$$

where $\bar{h}_{\mu\nu}$ is the trace reversed perturbation. It is well known that this type of sourced wave equations can be solved with the Green's function method such that

$$\bar{h}_{\mu\nu}(x) = -16\pi \int G(x-y) T_{\mu\nu} d^4y. \tag{2.15}$$

The retarded Green's function is given by

$$G(x-y) = -\frac{1}{4\pi|\vec{x}-\vec{y}|}\delta\left[|\vec{x}-\vec{y}| - (x^0-y^0)\right]\theta(x^0-y^0). \tag{2.16}$$

Together, for the perturbation we then have

$$\bar{h}_{\mu\nu} = 4\int \frac{d^3y}{|\vec{x}-\vec{y}|} T_{\mu\nu}(t-|\vec{x}-\vec{y}|, \vec{y}). \tag{2.17}$$

With some manipulations we can define the quadrupole moment tensor of the system:

$$I_{ij} = \int d^3y T^{00} y^i y^j, \tag{2.18}$$

and find that for the spatial part of the gravitational wave, we have

$$\bar{h}_{ij}(\vec{x}, t') = \frac{2}{r}\left[\frac{d^2 I_{ij}(t')}{dt^2}\right]_{t'=t-r}, \tag{2.19}$$

where r is the distance to the source. This solution matches our physical intuition behind the gravitational wave processes from compact binary systems, namely that gravitational waves are emitted due to a change in the masses via the quadrupole moment.

Gravitational waves have a measureable effect. As the waves propagate away from their

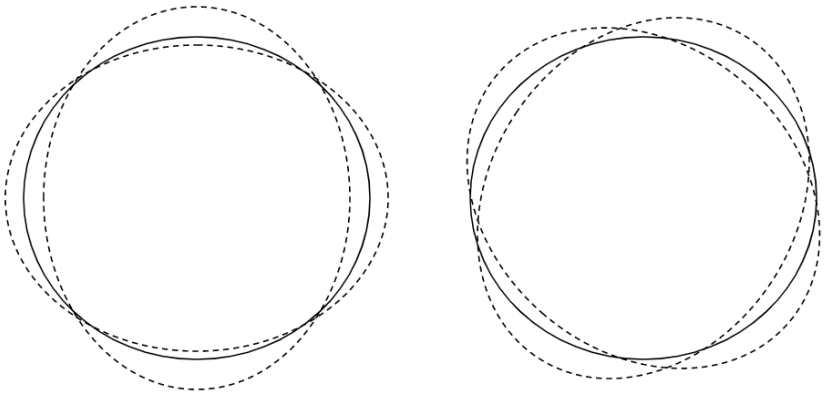

Figure 2.1: Effect of a + (left) and × (right) polarized gravitational wave on a ring of test particles.

source, they create tiny 'ripples' in spacetime itself. These ripples have the effect of distorting spacetime and it's contents. As an example, consider the impact of a gravitational wave on a circle of test particles. The two gravitational wave + and × polarizations each stretch the test particles in a characteristic way. In Figure 2.1 we see the effects of each on a ring of test particles, and specifically that each polarization mode has distinct behavior.

The GW polarizations can also be written in terms of handedness as h_R and h_L as a linear combination of the + and × modes.

These distortions can also be measured on earth, which is the key principle behind the LIGO experiment (now the LIGO/Virgo/KAGRA Collaboration). These experiments consist of Michelson inteferometers, as demonstrated in Figure 2.2.

As the gravitational wave propagates through spacetime and passes earth, it stretches the length of the detector arms by less than a proton width, which can then be observed. These theorized gravitational waves became a reality in 2015 when the first gravitational wave event from a binary black hole merger was detected by the LIGO and Virgo collaboration in 2015. Since then, 90 such detections have been made, including from binary black holes, from binary neutron stars and even binary black hole-neutron star systems.

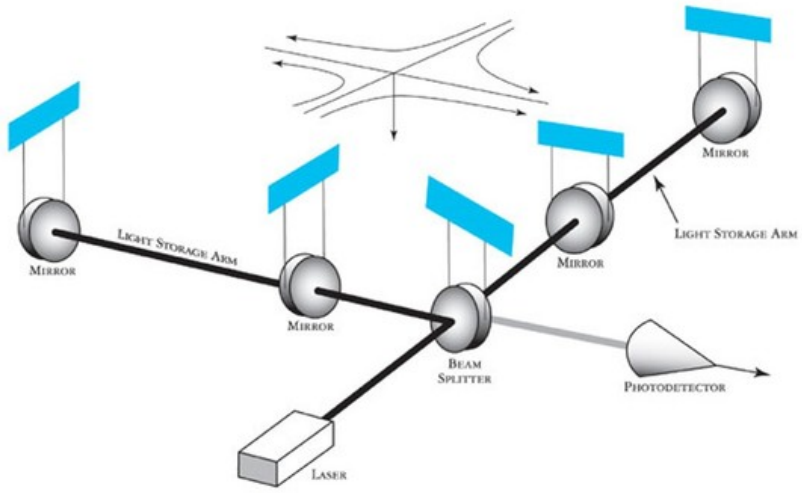

Figure 2.2: Schematic diagram showing the basic LIGO inteferometer setup. Image credit: Caltech/MIT LIGO Lab.

2.1.3 Tests of General Relativity

Multiple methods exists with which to test general relativity, and thus far the theory has withstood all of them. The first test that GR passed with flying colors took place in our own solar system backyard - the explanation of the perihelion precession of the planet Mercury. The fact that the perihelion, or point of closest approach, of Mercury's orbit precesses is an effect which can mostly, but not exactly, be explaned by the gravitational pull of the other planets in the solar system. However, there is a deviation of approximately 43 arcseconds per century between the measured effect and the predicted value by considering the impacts of the other planets with classical Newtonian mechanics. This discrepancy was first noticed in 1859 by Urbain Le Verrier and puzzled astronomers. Many solutions, including the existence of another planet were proposed, but ultimately all failed. It was not until Einstein introduced general relativity that it was realized that the missing 43 arcseconds/century could be exactly explained by post-Newtonian general relativistic effects. This explanation of Mercury's pericenter precession represented the first astrophysical test of GR [2]. Further solar system tests of GR have also proved robust, including observations of the bending of light around the sun.

Moving to the 21st century, GR has withstood further trials, the main test arising from

the aforementioned detection of gravitational waves as well as observations of binary pulsars. The existence of gravitational waves is itself a direct confirmation of general relativity, but studying the properties of the waves allows us to further test the theory and place constraints on any theories of modified gravity. The first such property is the propagation speed of the gravitational waves. General relativity predicts that gravitational waves travel at the speed of light, c, while many modified theories of gravity induce corrections such that the propagation speed is altered. The most stringent constraint on the speed of gravity comes from the binary neutron star event, GW170817, which observed both gravitational and electromagnetic emission from the merger. From the difference in arrival time of the electromagnetic and gravitational signals, the speed of gravity has been constrained to

$$|v_{\rm GW} - v_{\rm EM}| \lesssim 10^{-15}. \tag{2.20}$$

As we can see, the gravitational waves must travel either at the speed of light, or very close to it, up to one part in 10^{15}. Clearly, there is not much room for deviation here and this constraint has indeed ruled out many modified theories of gravity, such as certain formulations of scalar-tensor theory, Hordenski theory, and Horava-Lifshitz gravity. Nonetheless, many modified gravity theories do exist which do not modify the propagation speed or which have such small modifications to still respect this bound [3, 4].

Another way in which general relativity is tested with observations of gravitational waves is via the waveform. GR has made predictions for the waveform and waveform templates have been constructed using such predictions. These templates have generally been found to be a good match to the observed GW waveforms, but some theories such as dynamical Chern-Simons gravity or noncommutative gravity predict modifications to the waveform in distinctive ways. In particular, the phase of the wave is often modified in alternative theories, as we discuss explicitly for noncommutative gravity in Chapter 6. Any deviations from the phase have been constrained up to 3.5 post-Newtonian order [5].

General relativity can also be tested with binary neutron star and pulsar observations, as we will also discuss in Chapter 6 in the context of noncommutative gravity. In particular,

the Hulse-Taylor binary [6] and the binary pulsar system PSR J0737-3039 have been key observations [7]. The most recent test of GR comes from the first direct image of a black hole, taken by the Event Horizon Telescope (EHT) collaboration. Again, this observation does not immediately indicate any violations of GR [8]. However, it does provide a rich background on which to probe general relativity as more observations are available in the coming years.

2.1.4 First Order Formalism of General Relativity

One can also understand general relativity in a differential geometric context, in what is known as the 'first order' or Palatini formalism. In the second order, or metric formulation, the metric itself is the only independent variable, and all other quantities such as the connection and the curvature can be found in terms of $g_{\mu\nu}$. In the Palatini formalism, the metric and the connection are considered independent variables. This formulation of general relativity is attractive for several reason. First, this is the necessary framework with which to couple gravity to fermions. Additionally, the Palatini formalism can be related to Ashtekar variables and Ashtekar's formulation of canonical general relativity.

The Palatini formalism is characterized by the Palatini action,

$$S = \int \epsilon_{ABCD}(e^A \wedge e^B \wedge R^{CD}[\omega]), \tag{2.21}$$

where $\wedge$ is the antisymmetric wedge product, and we have introduced the following quantities. e^A is known equivalently as the 'tetrad,' 'frame field,' or 'vierbein,' which is defined in terms of the metric by

$$g_{\mu\nu} = e^A_\mu e^B_\nu \eta_{AB}, \tag{2.22}$$

where η_{AB} is the Minkowski metric. Here μ, ν are spacetime indices and A, B are SO(1,3) Lorentz indices. The frame field is a one-form, written as

$$e^A = e^A_\mu \wedge dx^\mu. \tag{2.23}$$

The spin connection, ω^{AB} is now, in general, independent from the frame field. If one is considering a torsion-free theory, then the spin connection can be written in terms of the frame field and Christoffel connection as

$$\omega_{\mu}^{ab} = e_{\nu}^{a}\Gamma^{\nu}{}_{\sigma\mu}e^{\sigma b} + {}_{\nu}^{a}\,\partial\mu e^{\nu b}. \tag{2.24}$$

If one is considering a theory in which the torsion is non-zero, then the above does not apply and one must consider the spin connection as independent from the frame field. The curvature two form and $R^{AB}[\omega]$ is a function of the connection and is defined by:

$$R^{AB} = D\omega^{AB} = d\omega^{AB} + \omega^{A}{}_{C} \wedge \omega^{CB}. \tag{2.25}$$

Here, D is the exterior covariant derivative.

One unique aspect of the Palatini formalism is that by considering the frame field and spin connection as independent variables, it allows for theories with non-zero torsion. The torsion is defined as

$$T^{A} = De^{A} = de^{A} + \omega^{A}{}_{B} \wedge e^{B}. \tag{2.26}$$

General relativity is a torsion-free theory, in which case the spin connection can be written as a a function of the frame field directly. However, if one wants to consider more exotic or beyond-GR theories, one must consider the effects of torsion on the spacetime.

Let us now consider some aspects of perturbation theory in the first order formalism. Recall that in the usual metric formulation, if one considers an inifintesimal spacetime diffeomorphism

$$x^{\mu} \to x^{\mu} + \xi^{\mu}, \tag{2.27}$$

then a tensor field, Y transforms as

$$Y \to Y + \mathcal{L}_{\xi}Y, \tag{2.28}$$

where $\mathcal{L}_{\xi}$ is the Lie derivative with respect to ξ^{μ}. This leads us to the standard perturbation

theory in the metric formulation. However, in the first order formalism, we must be careful with our transformation. Recall that in this formulation, we have two types of indices to keep track of, bot the spacetime indices as well as the SO(1,3) internal Lorentz indices. The transformation discussed above only takes into account the former and does not account for changes in the transformation due to the internal Lorentz structure. To resolve this predicament, we must now consider a combined diffeomorphism and Lorentz transformation to ensure that the combined transformation remains well behaved and gauge invariant. We will consider a Lorentz transformation given by

$$\Lambda^A_B = \delta^A_B + \lambda^A_B, \tag{2.29}$$

where we assume that λ is the same amount of small as ξ. Then, we can consider the combination, the 'Lorentzian Lie derivative,' $\mathcal{K}_\xi$, such that

$$\mathcal{K}_\xi = \mathcal{L}_\xi + \lambda^{\mathcal{A}}_{\mathcal{B}}. \tag{2.30}$$

Then, the transformation of any arbitrary tensor, Y, becomes

$$Y \to Y + \mathcal{K}_\xi Y. \tag{2.31}$$

This formulation of gauge invariant perturbation theory will be necessary for the discussion in Chapter 5 in order to study gravitional waves in a theory which is an extension of general relativity which contains a varying cosmological constant and non-zero torsion.

2.2 ΛCDM Cosmology

The current paradigm describing our universe is ΛCDM cosmology. To paraphrase Jo Dunkley from the 2022 American Physical Society April meeting, ΛCDM almost certainly seems correct, with the caveats that we don't know what Λ is and we don't know what CDM is. Although tongue in cheek, the above anecdote nicely sums up the state of cosmology. ΛCDM

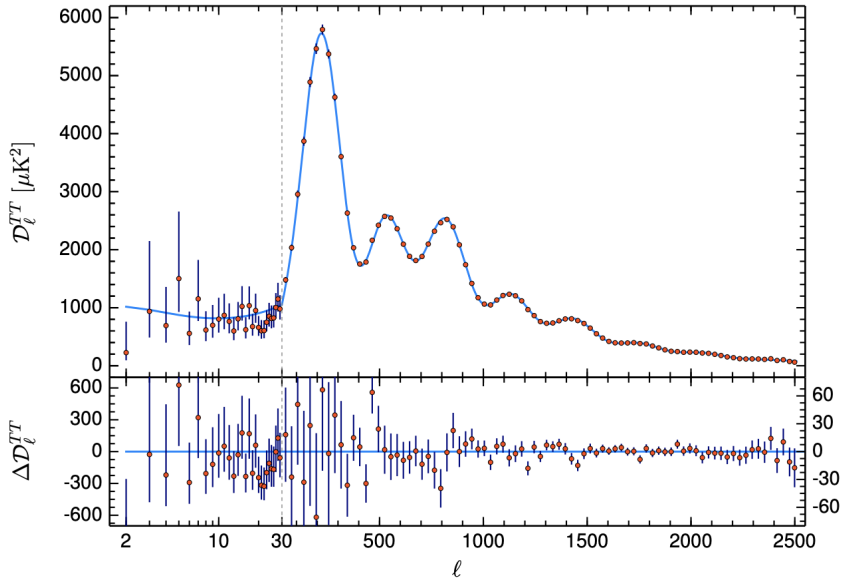

Figure 2.3: Plot showing the Planck 2018 temperature power spectrum and fit to ΛCDM parameters. The lower plot shows the residuals. Image via the Planck Collaboration [1].

is a standard model of big bang cosmology in which the universe is characterized mainly by the presence of a cosmological constant or dark energy, Λ and cold dark matter as well as ordinary matter. The model can be specified by six independent parameters, which are the dark matter density, $\Omega_c h^2$, the baryon density, $\Omega_b h^2$, the scalar spectral index, n_s, the optical depth, τ, the angular acoustic scale, $100\theta_*$, and the amplitude paramter, $\ln(10^{10}A_s)$. Other relevant parameters, including the Hubble tension and the age of the universe can be derived from these base ones. Figure 2.3 shows the Planck 2018 best fit for the temperature power spectrum, which we can see matches with stunning accuracy [1].

One may assume that this indicates that no open questions remain, but this is not the case. As alluded to previously, we still have not observed dark matter directly, we are still quite in the dark (no pun intended) as to the nature of dark energy, and other puzzles such as the Hubble tension and the σ_8 tension have crept up, all pointing towards the potential need for new physics.

2.3 Dark Matter

There is significant observational evidence for the existence of dark matter. The first hint that visible, baryonic matter is not all that comprises our universe can be found in rotation curves of spiral galaxies, which was first observed by Vera Rubin in 1978 [9]. In this seminal paper, Rubin noted that the rotation curves of spiral galaxies seemed to flatten out as a function of the distance from the center, rather than decrease, indicating that what was thought of as the edge of a galaxy was not in fact the edge - that there was a significant amount of additional mass present. This is what we now call 'dark matter.'

Other observed evidence for dark matter includes the bullet cluster and gravitational lensing. All of these observations indicate that there is missing mass in the universe that we cannot see, but they do little to give us a hint towards what that mass could be. In fact, we know very little about the nature of dark matter, beyond the fact that it must not interact (or interact extremely weakly) with the standard model. There have been a wide range of potential dark matter candidates over time, ranging from the ultra light axion with a mass of 10^{-22} eV to black holes with masses on the order of tens to thousands of solar masses. This range, spanning $\sim$80 orders of magnitude shows us how truly wide open the dark matter problem is.

The most prominent dark matter candidate in recent years is known as the WIMP, or weakly interacting massive particle. The WIMP satisfies the brief of a cold dark matter candidate, fitting nicely into the ΛCDM picture as discussed in the previous section. Many experiments are currently searching for WIMP dark matter, including the Lux-Zeppelin (LZ) and XenonNTon experiments. However, as of yet there have been no detections. Furthermore, there have been no fruitful searches for dark matter at collider experiments at CERN, or through indirect detection methods. This lack of observation is quickly shrinking the viable parameter space for the WIMP.

Given that the WIMP has not yet been detected and the parameter space seems to be shrinking, it is certainly of interest to explore alternative and more exotic models. Another

dark matter candidate which has gained popularity in recent years is the axion, or axion-like particle, which is an extremely light scalar field. Other models such as variations of WIMPS, primordial black holes, and neutrinos have all been proposed as potential solutions, but nothing has yet yielded any detection results. In Chapter 4 we propose another alternative model in which the dark matter is a higher spin ($s > 2$) particle.

2.4 Inflation

Inflation is a hypothesized epoch of the early universe, approximately 10^{-32} seconds after the big bang. This period is thought to consist of a rapid, non-adiabatic expansion of spacetime to 'inflate' the universe. Inflation was originally proposed to solve several puzzles in cosmology; notably the horizon problem and the flatness problem. They are as follows [10, 11].

Horizon problem: The horizon problem stems from the observation that the CMB is nearly perfectly homogeneous and isotropic, up to one part in 10^5. In all directions in the sky, the CMB has a temperature of $T \sim 2.7$ K. However, according to the standard cosmological model, these patches of the sky would never have been in causal contact with each other, making the uniformity of the CMB perplexing. We can see this explicitly by considering the particle horizon:

$$r_H = \int \frac{dt}{a(t)} = \int \frac{dz}{H(z)}, \tag{2.32}$$

which describes the maximum radius light can travel given the age of the universe. The physical size of the particle horizon, D_H is then given by

$$D_H(z) = a(z) r_H(z), \tag{2.33}$$

which, for a redshift of $z = 1100$ at last scattering, is ≈ 2 degrees. Clearly, based on our observations of the homogeneity and isotropy of the CMB extending further than 2 degrees, there must be a further explanation. Inflation resolves this issue by providing a model in which these regions of spacetime are indeed in causal contact prior to the inflationary

expansion.

Flatness problem: The flatness problem, as its name suggests, is the puzzle of why the universe appears to be spatially flat, and why the curvature is zero, or if nonzero, a very small number. This leads to a question of fine tuning of the initial cosmological parameters. To see this explicitly, we can write the Friedmann equation as

$$|\Omega_0 - 1| = \frac{|k|}{a^2 H^2} \tag{2.34}$$

Today, we measure the cosmic density parameter, Ω_0 to be extremely close to 1 within 1%, corresponding to the $k = 0$ flat universe that we observe ourselves to live in today. Notably, if the value of Ω_0 today is extremely close to 1, it must have always been - any small initial deviation from $\Omega = 1$ leads to an instability away from a flat universe, at odds with our observations. This fine tuning is as severe as one part in 10^{60} if one considers the initial time to be the Planck epoch.

Inflation addresses these problems by introducing a period of accelerated expansion in the early universe. The inflationary paradigm solves the horizon problem by allowing for the disparate regions of spacetime observed to be homogeneous at last scattering to in fact have been in causal contact at one point. Then, the rapid expansion moves the regions back *out* of causal contact, giving rise to what we observe today. Similarly, inflation provides an answer to the flatness problem by allowing the scale factor to dominate over the curvature and force Ω_0 close to one.

The inflationary universe is described the FRW metric,

$$ds^2 = -dt^2 + a(t)^2 d\vec{x}^2, \tag{2.35}$$

where $a(t)$ is the scale factor, describing the expansion of the universe. During inflation, the scale factor is given by

$$a(t) = e^{Ht}, \tag{2.36}$$

where H is the Hubble constant during this epoch, giving rise to the characteristic exponential

growth.

This process is thought to be driven by a scalar field, ϕ, known as the inflaton. The action for such a scalar field is given by

$$S = \int d^4x\sqrt{-g}\left(R + \frac{1}{2}\partial^\mu\phi\partial_\mu\phi - V(\phi)\right) \tag{2.37}$$

leading to the equations of motion for the inflaton field:

$$\ddot{\phi} + 3H\dot{\phi} - \nabla^2\phi + \frac{dV(\phi)}{d\phi} = 0. \tag{2.38}$$

To obtain the dynamics of inflation, we ignore spatial inhomogeneities and work in the so-called 'slow roll' regime, in which $\ddot{\phi}$ is neglible in comparison to the $3H\dot{\phi}$ and $dV/d\phi$ terms. We thus arrive at the slow roll condition:

$$3H\dot{\phi} = -\frac{dV}{d\phi}. \tag{2.39}$$

We can cast the inflationary slow roll conditions into dimensionless forms. The condition $V \gg \dot{\phi}^2$ can be written as

$$\epsilon = \frac{M_P^2}{16\pi}\left(\frac{V'}{V}\right)^2 \ll 1, \tag{2.40}$$

which also gives rise to

$$\eta = \frac{M_P^2}{16\pi}\left(\frac{V''}{V}\right) \ll 1. \tag{2.41}$$

Recently, it has been suggested that inflation can be used as a window into particle physics via the CMB; the 'cosmological collider' program. Aspects of this will be discussed further in Chapter 3 in the context of higher spin supersymmetry. Furthermore, inflation can give rise to a gravitational production of massive particles due to non-adiabatic fluctuations in a massive field. We discuss this mechanism as a potential genesis for a model of higher spin dark matter in Chapter 4.

Part I

Higher Spin Cosmology

Chapter 3

Higher Spin Supersymmetry at the Cosmological Collider: Sculpting SUSY Rilles in the CMB

3.1 Introduction

We begin our journey of this thesis in the inflationary epoch of the early universe. Inflationary cosmology provides the initial conditions of standard cosmology, and a mechanism to explain the origin of the large scale structure of the universe. These initial conditions are manifest in the statistical properties of anisotropies in the cosmic microwave background (CMB) radiation, which in addition to being measured to an incredible precision [12], are well described by linearized cosmological perturbation theory. This latter fact means the statistical properties of the CMB are calculable, and combined with the conservation of the primordial curvature perturbation on super-horizon scales [13, 14, 15, 16, 17, 18, 19], makes possible deductions as to the precise particle content of the very early universe.

In particular, while single-field slow-roll inflation predicts adiabatic, Gaussian, nearly-scale invariant perturbations, interactions of the primordial curvature perturbation with

new fields can generate deviations from Gaussianity, as encoded at lowest-order by the 3-point function $\langle\zeta\zeta\zeta\rangle$. Remarkably, this is sensitive even to fields that are heavier than the Hubble scale during inflation [20, 21, 22], and thus probes particles at energy scales far above those accessible by terrestrial colliders. The study of $\langle\zeta\zeta\zeta\rangle$ as a particle detector has been termed 'Cosmological Collider Physics' [23] (see also [24]), and gained significant momentum due to the realization that interactions with higher spin bosons, namely the exchange of a massive spin-s boson, impart a characteristic angular dependence on the non-Gaussianity, $\langle\zeta(k_1)\zeta(k_2)\zeta(k_3)\rangle \propto P_s(\hat{k}_1\cdot\hat{k}_3) + k_2 \leftrightarrow k_3$, with $P_s(\cos\theta)$ the degree-s Legendre polynomial.

The study of higher spins has a long history dating all the way back to the founding of relativistic field theory [1]. Since then, higher spins have gained fame and attention in large part due to their role in string theory[2], as well as their use in exploring the holographic principle[3]. Additionally, there is the old conjecture [28, 29, 30, 31] that physics beyond Planckian energy scales will have higher symmetries emerging. From this point of view the study of higher spins can be understood as an attempt to classify and realize the various possibilities for these emerging symmetries. The study of manifestly supersymmetric higher spins is a natural extension of the above program, both because supersymmetry is a property of the underlying theory (as in the example of (super)string theory) and, more generally, because it is compatible with the relevant structures (like the symmetries of S-matrix [32]).

For these reasons we are interested in using irreducible representations of the super-symmetric extension of appropriate spacetime symmetry groups which involve higher spin particles. These irreps are classified and labeled by the eigenvalues of the Casimir Operators. In $4D$ these are the mass (m) and the superspin (Y) which takes either integer ($\mathsf{Y} = s$) or half integer values ($\mathsf{Y} = s + 1/2$)[4]. These representations include multiple representations of the non-supersymmetric spacetime symmetry group: For the massless case ($m = 0$) a

[1] First paper by Majorana in 1932 [25] followed by Dirac, Pauli, Fierz, Wigner and others.

[2] For example, the UV softness of perturbative string scattering amplitudes originates from the freedom to exchange higher spin particles. More recently, higher spin fields have played a role in constraining the self-consistency of inflation in string theory [26, 27].

[3] All available, consistent, fully interacting higher spin theories (such as Vasiliev's or CS in 3D) require an AdS background and a spin two state. Both of these requirements are ingredients of AdS/CFT correspondence.

[4] For the purpose of this discussion we will ignore infinite sized representations that go under the name of continuous (super)spin representations [33].

supermultiplet with superspin Y includes massless particles with spins $j = \mathsf{Y} + 1/2$ and $j = \mathsf{Y}$, whereas for the massive case ($m \neq 0$) a supermultiplet with superspin Y includes massive particles with spins $j = \mathsf{Y} + 1/2$, $j = \mathsf{Y}$, $j = \mathsf{Y}$ and $j = \mathsf{Y} - 1/2$. This implies that supersymmetrizing the cosmological collider does not simply require adding a single higher spin fermion, but rather additional fields as well.

As a step towards combining this with inflationary cosmology, we consider an inflationary sector minimally coupled to a higher spin sector. The inflationary vacuum energy H^2 breaks supersymmetry, generating masses for the inflationary fermionic superpartners, while the higher spin sector, behaving as 'spectator fields' which do not contribute to H^2 and hence do not contribute to supersymmetry breaking, retain their on-shell supersymmetry. Given the candidate bosonic interactions proposed in the literature [23, 24], the remnant on-shell supersymmetry of the higher spin sector uniquely determines the interactions of the higher spin fermions with the primordial curvature perturbation. From this one can compute the statistical properties of anisotropies in the CMB, and in this way, use the CMB as a detector for higher spin supersymmetry at the early universe's collider.

Each higher spin particle, as enumerated by the corresponding irreducible representation, induces a contribution to the 3-point function $\langle\zeta\zeta\zeta\rangle$, i.e. a signal at the cosmological collider, and in this work we explicitly calculate the non-Gaussianity due to these contributions. Our primary result is the prediction of higher spin supersymmetry for the angular dependence of the non-Gaussianity: we find that the P_s contributions to the non-Gaussianity come in a characteristic pattern. Namely, every P_s contribution to the non-Gaussianity is accompanied by a P_{s+1} contribution and a tower of associated Legendre polynomials P_s^m. The magnitudes, while Boltzmann suppressed, are related by supersymmetric considerations.

This chapter is organized in the following way. In Section 2 we build the effective field theory that will be the framework for our calculations. Section 3, gives a very elementary review of massive, higher superspin supermultiplets focusing on the spectrum of propagating spin particles they include. Furthermore it demonstrates how to construct a supersymmetric extension of the previously studied class of effective field theories. In Section 4, using these

types of fermionic higher spin terms we consider an effective interacting Lagrangian up to first order in the higher spin fields. The effective Lagrangian is then used to calculate the contribution of higher spin fermions to the three point function $\langle\zeta\zeta\zeta\rangle$. The last section, Section 5, gives a summary of our results and a short discussion for future directions, including the tensor-scalar-scalar 3-point function $\langle\gamma\zeta\zeta\rangle$, which we compute for higher spin fermion exchange.

3.2 Setup in Effective Field Theory

In this work we consider a tripartite marriage of $4D, \mathcal{N} = 1$ supersymmetric higher spins [34, 35, 36, 37, 38, 39, 40, 41, 42, 43, 44, 45, 46, 47, 48] with the effective field theory (EFT) of inflation [49] and de Sitter supergravity [50, 51, 52]. We construct an effective field theory of a supersymmetric theory of higher spins in a quasi-de Sitter spacetime with spontaneously broken supersymmetry and spontaneously broken time-translation invariance. The goal of this construction is to minimally couple the higher spin sector and the inflationary sector, in such a way that the on-shell supersymmetry of the higher spin fields is maintained, despite supersymmetry being broken by the inflationary vacuum energy. The on-shell supersymmetry of the higher spin sector can then be used in conjunction with the effective field theory of inflation to dictate the couplings of higher spin fermions and bosons to primordial perturbations. This is distinct from the supersymmetric EFT of inflation [53] in that we do not focus on the gravity multiplet, but instead on the higher spin supermultiplets.

Our approach allows us to make progress despite not having a full theory of interacting higher spin de Sitter supergravity. While the setup may seem contrived, it bears some similarity with the interplay of supersymmetry and anomaly cancellation in string theory.

To appreciate this, one may recall that the interactions between effective field theory, supersymmetry and anomaly cancellation are not as direct as one might imagine. In some cases a complete superspace formulation or component-level supersymmetrization is known such as in the example of the $4D$, $\mathcal{N} = 1$ WZNW-QCD action [54, 55, 56]. In the development of

Heterotic theory, anomaly cancellation required the addition of a new term in the action a la the famous Green-Schwartz mechanism [57], and this term required yet more terms (and years of calculation) in order to restore supersymmetry to the action[58]. Similarly, in Type II/M theories the gravitational anomaly on D/M-branes induced by loops of chiral fermions is canceled via anomaly inflow by a higher-derivative correction to the bulk action [59, 60, 61], and despite the anomaly not playing any direct role in supersymmetry, as for Green-Schwarz the supersymmetrization of the anomaly-canceling terms requires yet more terms be added, the calculation of which requires a herculean level of technical skill and detail [62]. The same issue applies to the $SL(2,\mathbb{Z})$ symmetry of type IIB: restoring the invariance naively broken by the corrections requires the careful consideration of D-instantons [63] (and again these new terms must be supersymmetrized).

In each of these cases, a seemingly complete theory is found to be anomalous, and cancellation of the anomalies requires new terms. The new terms should respect the symmetries of the action, and generically additional terms must be found to accomplish this task. However, much can be learned even without a complete knowledge of all terms in the theory. For example, in the interim period between [59, 60, 61] and [62], the AdS/CFT correspondence was discovered [64]. Another example of this is of course the field of String Cosmology [65, 66], which makes no recourse to the precise manner in which $SL(2,\mathbb{Z})$ symmetry is maintained. With all this in mind, we construct an effective theory along the lines discussed above.

This approach can be illustrated with simple examples involving chiral superfields in $\mathcal{N}=1$ supersymmetry. The first non-trivial step is the 'sequestering' of supersymmetry breaking to the inflationary sector, analogous to the Randall-Sundrum scenario [67]. This can be done in a number of ways; one simple example is to take guidance from [68, 69] and allow for a non-minimal Kahler potential, as in

$$W = MX \quad , \quad K = X\bar{X}e^{Y\bar{Y}} + Y\bar{Y}. \tag{3.1}$$

This exhibits a vacuum at $X = \bar{X} = Y = \bar{Y} = 0$, wherein supersymmetry is broken by X, $D_X W = M$. The scalar potential evaluated for $X = \bar{X} = 0$ is given by a constant $V = M^2$,

leaving the scalar component of Y massless: $m_Y^2 \equiv \partial_{Y\bar{Y}} V = 0$ [5]. Similarly, the fermion component of Y remains massless since $D_Y W = 0$. Thus the breaking of supersymmetry is not communicated to the on-shell mass spectra of Y, and the Y superfield retains on-shell $\mathcal{N} = 1$ supersymmetry.

The utility of this approach is the enumeration of interactions and the tree-level couplings, since despite the sequestering of supersymmetry breaking, there are interactions between X and Y, which communicate the SUSY breaking at loop-level. Expanding $X \to \delta x$ and $Y \to \delta y$, $\delta x, \delta y \in \mathbb{R}$, one finds the interactions between scalar components,

$$\mathcal{L}_{int} = \delta y^2 (\partial \delta x)^2 + M^2 \delta y^2 \, \delta x^4 + ..., \tag{3.2}$$

where the ... are higher order terms. Similarly, there are interactions between the fermionic components of X and the fermionic components of Y, and these two sets of interactions will communicate the SUSY breaking to Y. The structure of these interactions is governed by the underlying supersymmetry, which is spontaneously broken by X, and this structure dictates the effect that δy interactions can have on δx correlators.

In our setup, the higher spin sector is analogous to Y while the inflationary sector is analogous to X. It is the above sense in which the HS sector in our setup has on-shell supersymmetry. This can be used to enumerate the interactions and estimate the amplitude of correlation functions. However, this is not the full story: The next puzzle piece is the embedding of supersymmetry and supergravity into cosmological spacetimes.

This can be done via the framework of *de Sitter supergravity* [50, 51, 52]. This theory describes the spontaneous breaking of supersymmetry with no field content other then the gravity multiplet and the goldstino of supersymmetry breaking. The latter can be expressed as a chiral superfield, S, satisfying a constraint equation,

$$S^2 = 0. \tag{3.3}$$

[5] For this simple example, also the scalar component of X is massless, but it can be made massive via an addition to the Kahler potential $\delta K = (X\bar{X})^2/\Lambda$. The fermionic component of X has mass set by M.

This constraint removes the scalar degree of freedom from S, leaving the fermionic component as the only propagating degree of freedom. The most general superpotential is given by,

$$W = W_0 + MS, \tag{3.4}$$

since any additional terms involving S vanish by the nilpotency constraint. Supersymmetry is broken by $D_S W = M$, and the resulting scalar potential, for a minimal Kahler potential $K = S\bar{S}$, is a cosmological constant given by

$$\Lambda \equiv V = M^2 - 3W_0^2, \tag{3.5}$$

which is positive for $M > \sqrt{3}W_0$, giving a de Sitter spacetime.

Any additional matter sectors in de Sitter supergravity can easily be sequestered from the breaking of supersymmetry. For example, endowing S with a non-trivial Kahler geometry [68, 69] and taking $W_0 = 0$,

$$W = MS \ \ , \ \ K = e^{T\bar{T}} S\bar{S} + T\bar{T} \ \ , \ \ S^2 = 0, \tag{3.6}$$

supersymmetry-breaking is purely in the S-direction provided that $D_T W = 0$ in vacuum, which is guaranteed to be the case since $D_T W \propto S = 0$, leaving the fermionic component of T massless. Meanwhile, SUSY is broken by S, $D_S W = M$, and the potential is a constant vacuum energy $V = \Lambda = M$, leaving the scalar components of T massless. Thus again, T retains on-shell supersymmetry.

To connect this with observational cosmology, and anisotropies in the cosmic microwave background radiation, it is necessary to consider fluctuations. Inflation models can be constructed in de Sitter supergravity along the lines of [68, 69, 70, 71]. Consider a superfield Φ with the real part of the scalar component of Φ identified as the inflaton φ. The fluctuations of φ in spatially flat gauge are related to the curvature perturbation on uniform density

hypersurfaces ζ in uniform field gauge via [72]

$$\zeta = \frac{H}{\dot{\varphi}}\delta\varphi = \frac{1}{\sqrt{2\epsilon}m_{pl}}\delta\varphi, \tag{3.7}$$

where $\epsilon \equiv -\dot{H}/H^2$ is the inflationary slow-roll parameter. This defines the primordial power spectrum, in dimensionless form,

$$\Delta^2_\zeta \equiv \frac{k^3}{2\pi^2}|\zeta_k|^2, \tag{3.8}$$

where ζ_k is a Fourier mode of the field $\zeta(x,t)$.

The curvature perturbation ζ can in turn be related to the Goldstone boson of spontaneously broken time-translation invariance, using the machinery of the effective field theory of inflation [49]. This starts from the realization that the time-dependence of the inflaton $\varphi(t)$ breaks the time diffeomorphisms. The Goldstone boson can be included in the theory by a redefinition of the time-coordinate,

$$t \to t - \pi(t,x), \tag{3.9}$$

with $\pi(t,x)$ the Goldstone boson. This induces a field fluctuation,

$$\varphi(t) \to \varphi(t) - \dot{\varphi}\pi(t,x) \tag{3.10}$$

and thus corresponds to a curvature perturbation,

$$\zeta = -H\pi. \tag{3.11}$$

This also generates a fluctuation to the 00 component of the metric,

$$\delta g^{00} = -2\dot{\pi}. \tag{3.12}$$

The interactions of π, and hence ζ, are dictated by the symmetry structure of the action, which is broken to invariance under spatial rotations. This allows δg^{00} to appear explicitly

in the action, while δg^{ij} can only appear with all indices contracted.

Similarly, the interactions of π, and hence ζ, with any additional fields are dictated by symmetry considerations. For fields with arbitrary spin, $\sigma_{\mu_1\ldots\mu_s}$, this leads to effective interactions of the form [23, 24]

$$\mathcal{L}_{int} \supset \frac{\lambda_s}{\Lambda^{s-3}}\partial_{i_1}\ldots\partial_{i_s}\zeta\sigma^{i_1\ldots i_s} + \frac{g_s}{\Lambda^{s-2}}\dot{\zeta}\partial_{i_1}\ldots\partial_{i_s}\zeta\sigma^{i_1\ldots i_s} \ , \tag{3.13}$$

where indices i runs over spatial directions: $1, 2, 3$, and Λ is a UV scale. These terms descend from higher-dimension operators built out of the metric and its derivatives, and have coupling constants that are a priori free parameters of the effective field theory. For example, in the spin-2 case, these terms arise from a coupling of a spin-2 field σ to the extrinsic curvature, $\sqrt{-g}K^{\mu\nu}\sigma_{\mu\nu}$. The first term in (3.13) descends from $\delta K^{\mu\nu}\sigma_{\mu\nu}$ while the second term arises from including the metric perturbation $\delta g^{00}\delta K^{\mu\nu}\sigma_{\mu\nu}$ [24]. There can also be additional terms at higher order in π and σ and terms with different distribution of derivatives (up to total derivatives).

We now arrive back at the tripartite marriage: We wish to connect the higher spin interactions in a quasi-dS space to supersymmetry. To do this, one could simply operate along effective field theory lines, and introduce interactions consistent with unbroken spatial rotations. However, an interesting possibility is to consider what we can learn from higher spin supersymmetry, and use this as guidance in constructing our effective field theory describing the interactions of the higher spin fermions. Towards this end, we now develop the machinery of higher spin supersymmetry.

3.3 Supersymmetric Higher Spins

The first Lagrangian description of supersymmetric, massless, higher spins in $4D$ Minkowski space was done in [73, 74], using components with on-shell supersymmetry. A natural approach to the off-shell formulation is to use the superspace and superfield methods (see e.g.[75, 76]). A superfield description of free supersymmetric massless, higher spin theories

was presented for the first time in [34, 35, 36] for both Minkowski and AdS spaces. This approach has been further explored in [37, 38, 39, 40]. Later studies of free supersymmetric, massless higher spin supermultiplets include [41, 42, 43, 44].

On the other hand, the Lagrangian description of 4D massive supersymmetric spins for arbitrary values of spin is only known in the component formulation with on-shell supersymmetry [45, 46], whereas the off-shell, superspace description has been developed up to superspin $\mathsf{Y} = 3/2$ supermultiplet [47, 48]. Nevertheless, independently of what the proper Lagrangian description is, we know that there are two types of such irreps (i) the integer superspin $\mathsf{Y} = s$ supermultiplets and (ii) the half integer superspin $\mathsf{Y} = s + 1/2$ supermultiplets. Moreover we know that on-shell they describe two bosonic and two fermionic massive higher spin particles with spin values $j = \mathsf{Y} + 1/2$, $j = \mathsf{Y}$, $j = \mathsf{Y}$ and $j = \mathsf{Y} - 1/2$. The half integer superspin $\mathsf{Y} = s + 1/2$ supermultiplet, consisting of components

$$\mathsf{Y} = s + 1/2 : \quad (s + 1,\ s + 1/2,\ s + 1/2,\ s) \tag{3.14}$$

and its on-shell, superspace description is given in terms of a real, bosonic superfield $H_{\alpha(s)\dot{\alpha}(s)}$[6] with the following on-shell conditions:

$$\mathrm{D}^{\alpha_s} H_{\alpha(s)\dot{\alpha}(s)} = 0 \ , \ \Box H_{\alpha(s)\dot{\alpha}(s)} = m^2 H_{\alpha(s)\dot{\alpha}(s)} \ , \tag{3.15}$$

where D^{α_s} is the superspace covariant derivative. Alternatively, the massive, integer $\mathsf{Y} = s$ superspin supermultiplet, comprised of components,

$$\mathsf{Y} = s : \quad (\ s + 1/2,\ s,\ s,\ s - 1/2) \tag{3.16}$$

has an on-shell superspace description in terms of a fermionic superfield $\Psi_{\alpha(s)\dot{\alpha}(s-1)}$ with the

[6]The notation $\alpha(s)$ signifies a string of s undotted indices $\alpha_1\alpha_2...\alpha_s$ which are symmetrized. This type of indices are the spinorial indices of a Weyl spinor of one chirality and take values 1 and 2 in $4D$. Similarly for $\dot{\alpha}(s)$, where $\dot{\alpha}$ are the spinorial indices of the opposite chirality Weyl spinor and take also two values $\dot{1}$ and $\dot{2}$ in $4D$.

on-shell equations:

$$\mathrm{D}^{\alpha_s}\Psi_{\alpha(s)\dot{\alpha}(s-1)}=0\ ,\ \bar{\mathrm{D}}^{\dot{\alpha}_{s-1}}\Psi_{\alpha(s)\dot{\alpha}(s-1)}=0\ ,\ i\partial_{\alpha_s}{}^{\dot{\alpha}_s}\bar{\Psi}_{\alpha(s-1)\dot{\alpha}(s)}+m\Psi_{\alpha(s)\dot{\alpha}(s-1)}=0\ . \quad (3.17)$$

We start with the assumption that the higher spin sector respects supersymmetry and therefore can be organized into higher spin supermultiplets. This is extremely useful because supersymmetry will guide us to the introduction of higher spin fermions which have been neglected so far. Once their contribution is better understood, one may choose to drop the assumption of supersymmetry and study these fermionic contributions independently.

The strategy for finding the fermionic higher spin contributions is: (a) Start with the family of effective actions that lead to (3.13) after breaking the time translation invariance, and elevate them to superspace. This will automatically introduce all fermionic partners. (b) We project back down to a component description to reveal the interactions of the higher spin fermions. (c) Finally, we break supersymmetry appropriately in the inflaton sector.

The first step is to embed the bosonic, massive spin s particle in a massive higher spin supermultiplet described by some higher spin superfield. As we have seen, there are two ways of doing that, we can either use the integer or the half-integer superspin supermultiplet, with components (3.16) and (3.14) respectively. For concreteness, we make the latter choice ($\mathsf{Y}=s+1/2$) which means that our spin s particle will be accompanied by one bosonic higher spin particle $j=s+1$ and two more fermionic higher spin particles $j=s+1/2$. In this choice the highest propagating spin is $s+1$. Similarly we embed the scalar curvature perturbation field in a scalar supermultiplet, which will of course introduce its fermionic superpartner, which we refer to as the inflatino [7]. A simple choice to describe such a scalar supermultiplet is to use a chiral superfield Φ.

Secondly, using superspace, we write quadratic and cubic interaction terms, between $H_{\alpha(s)\dot{\alpha}(s)}$ and Φ which are linear in the higher spin superfield. The family of such superspace

[7] In general the fermionic partner of the curvature perturbation field can be identified as a linear combination of the inflatino and other fermions in the theory.

effective Lagrangians takes the form:

$$\mathcal{L} = H^{\alpha(s)\dot{\alpha}(s)}\mathcal{I}_{\alpha(s)\dot{\alpha}(s)} \ + \ H^{\alpha(s)\dot{\alpha}(s)}\mathcal{J}_{\alpha(s)\dot{\alpha}(s)} \tag{3.18}$$

where $\mathcal{I}_{\alpha(s)\dot{\alpha}(s)}$ is linear in Φ and generates the quadratic interactions part, whereas $\mathcal{J}_{\alpha(s)\dot{\alpha}(s)}$ is quadratic in Φ and generates the cubic [8] part of the interactions. The most general ansatzes for $\mathcal{I}_{\alpha(s)\dot{\alpha}(s)}$ and $\mathcal{J}_{\alpha(s)\dot{\alpha}(s)}$ are,

$$\mathcal{I}_{\alpha(s)\dot{\alpha}(s)} = \partial^{(s)}(b\ \Phi + b^*\ \bar{\Phi}), \tag{3.19}$$

and

$$\mathcal{J}_{\alpha(s)\dot{\alpha}(s)} = \sum_{p=0}^{s}\Big\{d_p\ \partial^{(p)}\Phi\ \partial^{(s-p)}\bar{\Phi} + f_p\ \partial^{(p)}\mathrm{D}\Phi\ \partial^{(s-p-1)}\bar{\mathrm{D}}\bar{\Phi} + g_p\ \partial^{(p)}\Phi\ \partial^{(s-p)}\Phi + g_p^*\ \partial^{(p)}\bar{\Phi}\ \partial^{(s-p)}\bar{\Phi}\Big\} \tag{3.20}$$

Using this as a starting point, one can project the superspace Lagrangian to components and find the corresponding field theory (see [75, 76] and detailed examples can be found in [40, 80]). The result will include the entire spectrum of fields of the supersymmetric theory. In addition to the propagating spins, this includes the set of auxiliary fields required by supersymmetry in order to balance the bosonic and fermionic degrees of freedom and also make the symmetry manifest. However, these auxiliary fields do not have any dynamics and can be integrated out. By doing so, we obtain an effective theory with on-shell supersymmetry which includes two copies of the previously discussed bosonic higher spin interactions. That is because there are two higher spin bosons, one with spin s and one with spin $s+1$. Additionally, we obtain terms that depend on the higher spin fermions ($\psi_{\alpha(s+1)\dot{\alpha}(s)}$, $\xi_{\alpha(s+1)\dot{\alpha}(s)}$) and the 'inflatino' ($\chi_\alpha$). The interactions are given by,

$$\mathcal{L}_{\text{Bosonic}} = h^{\alpha(s+1)\dot{\alpha}(s+1)}\left[\frac{\lambda_{s+1}}{\Lambda^{s-2}}\ \partial^{(s+1)}\zeta + \sum_{p=0}^{s+1}\frac{\kappa_p^{s+1}}{\Lambda^{s-2}}\ \partial^{(p)}\zeta\ \partial^{(s+1-p)}\zeta + ...\right] \tag{3.21}$$

[8] The reason why we are considering massive higher spin supermultiplets is a consequence of the Higuchi bound [77, 78] plus the possibility of higher order mass-like interaction terms for the higher spin superfields, which we do not consider in this work. If that was not the case one should take into account the gauge symmetry of the higher spin (super)fields. The result of that would be that, the spectrum of the half integer supermultiplet will collapse from $(s+1,\ s+1/2,\ s+1/2,\ s)$ to $(s+1,\ s+1/2)$ and more importantly the generator of cubic interactions $\mathcal{J}_{\alpha(s)\dot{\alpha}(s)}$ in (3.18) will become conserved higher spin supercurrents. Such supercurrents have been found in [79, 80, 81, 82, 83, 84, 85, 86, 87] and their structure is consistent with (3.20).

$$+h^{\alpha(s)\dot{\alpha}(s)}\left[\frac{\lambda_s}{\Lambda^{s-3}}\,\partial^{(s)}\zeta+\sum_{p=0}^{s}\frac{\kappa_p^s}{\Lambda^{s-3}}\,\partial^{(p)}\zeta\,\partial^{(s-p)}\zeta+...\right]$$

$$\mathcal{L}_{\text{Fermionic}}=\psi^{\alpha(s+1)\dot{\alpha}(s)}\left[\frac{r_s}{\Lambda^{s-1}}\,\partial^{(s)}\chi_\alpha+\frac{\lambda_s}{\Lambda^{s-1}}\,\chi_\alpha\partial^{(s)}\zeta+\sum_{p=1}^{s}\frac{v_p}{\Lambda^{s-1}}\,\partial^{(p)}\chi\,\partial^{(s-p)}\zeta+...\right]+h.c. \tag{3.22}$$

$$+\xi^{\alpha(s+1)\dot{\alpha}(s)}\left[\frac{t_s}{\Lambda^{s-1}}\,\partial^{(s)}\chi_\alpha+\frac{\lambda_s}{\Lambda^{s-1}}\,\chi_\alpha\partial^{(s)}\zeta+\sum_{p=1}^{s}\frac{w_p}{\Lambda^{s-1}}\,\partial^{(p)}\chi\,\partial^{(s-p)}\zeta+...\right]+h.c.$$

where ... indicates additional and higher-order terms.

As discussed in section 3.2, on-shell supersymmetry should be preserved only in the higher spin sector, and not in inflaton sector which breaks supersymmetry with the inflationary vacuum energy H^2. In our effective Lagrangian this information can be entered by hand by removing any correlation between the coupling constants of the inflatino and those of the inflaton. For example we can assign the inflatino χ a mass $m_\chi \gtrsim H$. Typically one would then *integrate out* the inflatino, thereby eliminating all the contributions at linear order in the higher spin fermions (3.22). However it is the inclusion of such heavy fields that we are explicitly after in this work. Indeed, the higher spin fields themselves have mass $m > \sqrt{s(s-1)}H$ by the Higuchi bound [77, 78]. The breaking of supersymmetry will also induce differing loop corrections to the on-shell couplings of ζ to bosonic (3.22) and fermionic (3.22) higher spin fields. Depending on the precise details of the model, there may also be classical corrections to these parameters, for example, from a quartic interaction involving an additional scalar field that gains a VEV in the SUSY-breaking vacuum. For our analysis, we assume for simplicity that there are no such classical corrections, and that these couplings are equal at tree level. This does not alter the analysis in any way other then the overall prefactor of the result.

To make contact with the framework of effective field theories within we have to work, as presented in section 3.2, we must break the time translations part of the Poincaré group and write interaction terms which include fermionic higher spin particles up to linear order. From equation (3.22), and taking into account contributions coming from the $\sqrt{-g}$ part of

the action, one has to consider the following fermionic interaction Lagrangian for a spin-$s+1/2$ field:

$$\mathcal{L} \supset \frac{\lambda_s}{\Lambda^{s-1}}\partial_{i_1\ldots i_s}\zeta\bar{\chi}\psi^{i_1\ldots i_s} + \frac{g_s}{\Lambda^s}\dot{\zeta}\partial_{i_1\ldots i_s}\zeta\bar{\chi}\psi^{i_1\ldots i_s} + \frac{\kappa_s}{\Lambda^s}\dot{\zeta}\partial_{i_1\ldots i_s}\bar{\chi}\psi^{i_1\ldots i_s} + c.c., \tag{3.23}$$

where the coupling to $\dot{\zeta}$ enters from the metric perturbation δg^{00}, as in equation (3.13). The full fermionic interaction Lagrangian is composed of copies of (3.23) for the appropriate fermions in the supermultiplet. Armed with this, we can now return to the cosmological collider.

3.4 Higher Spin Supersymmetry at the Cosmological Collider

The statistical correlations of temperature fluctuations in the cosmic microwave background descend from the initial conditions prepared for it by inflation. This can be computed via the Schwinger-Keldysh formalism, colloquially called the 'In-In' formalism, in which the choice of integration contour allows for ignorance as to the future evolution of the universe. Introduced to cosmology in [88], there are now many excellent reviews on this topic, see e.g. [89, 90, 91], and see [92] for a textbook treatment of the field theory aspects.

Correlation functions can be computed in this framework by splitting the Hamiltonian into a free Hamiltonian H_0 and interaction Hamiltonian H_{int}. From this, one can define the interaction picture fields as having propagator determined solely by H_0, and correlation functions of operators built from the full fields can be computed as contractions of the interaction picture fields with the interaction Hamiltonian.

More precisely, the expectation value of an operator W is given by,

$$\langle W(t)\rangle = \langle \left[\bar{\mathrm{T}}e^{i\int_{-\infty(1-i\epsilon)}^{t} H^I_{int}(t')\mathrm{d}t'}\right] W^I(t) \left[\mathrm{T}e^{-i\int_{-\infty(1+i\epsilon)}^{t} H^I_{int}(t'')\mathrm{d}t''}\right]\rangle, \tag{3.24}$$

where H^I_{int} and W^I are the interaction Hamiltonian and the operator W built out of interaction picture fields. The simplest quantity one can compute from this is the expectation value given a single insertion of the interaction Hamiltonian. In that case, the above expression

reduces to

$$\langle W(t)\rangle = -2\,\mathrm{Re}\,\langle\, i\,W^I(t)\int_{-\infty(1-i\epsilon)}^{t} H^I_{int}(t')\mathrm{d}t'\,\rangle + ..., \tag{3.25}$$

where the ... corresponds to additional insertions of H_{int}.

For the case of the curvature perturbation 3-point function, $W = \zeta^3$, this picks out the intrinsic non-Gaussianity, first computed in [88]. This is the 3-point function induced by the self-interactions of ζ in an inflationary background. The result is given by

$$\begin{aligned}\langle\zeta(k_1,0)\zeta(k_2,0)\zeta(k_3,0)\rangle &= (2\pi)^3\delta(k_1+k_2+k_3)\frac{H^4}{m_{pl}^4}\frac{1}{(k_1k_2k_3)^3}\frac{1}{4\epsilon^2}\\ &\cdot\left[\frac{\eta}{8}\sum k_i^3 + \frac{\epsilon}{8}\left(-\sum k_i^3 + \sum_{i\neq j} k_i k_j^2 + \frac{8}{k_1+k_2+k_3}\sum_{i>j} k_i^2k_j^2\right)\right].\end{aligned} \tag{3.26}$$

This is typically expressed in the limit that one of the momenta is much smaller than the other two, in what is referred to as 'squeezed limit'. The result then takes a simplified form

$$\lim_{k_1\to 0}\langle\zeta(k_1,0)\zeta(k_2,0)\zeta(k_3,0)\rangle = (2\pi)^3 f_{NL}\delta(k_1+k_2+k_3)\frac{H^4}{16\epsilon^2 m_{pl}^4}\frac{1}{(k_1k_2k_3)^3}\sum k_i^3, \tag{3.27}$$

which corresponds to 'local shape' non-Gaussianity [93] with amplitude f_{NL} given by

$$f_{NL} = \frac{\eta}{2} + \epsilon. \tag{3.28}$$

The inflationary slow-roll conditions $\epsilon, \eta \ll 1$ thus imply the intrinsic non-Gaussianity in single-field slow-roll inflation is extremely small, $f_{NL} \ll 1$.

Additional insertions of H_{int} capture the effect of particle exchange. Given the slow-roll suppression of the intrinsic non-Gaussianity, this can easily be the dominant effect. It is in this sense that CMB non-Gaussianity is a particle detector, with inflation as the cosmological collider.

In this work we are concerned with the non-Gaussianity induced via the exchange of a higher spin particle, as described by the insertion of two interaction Hamiltonians. This is

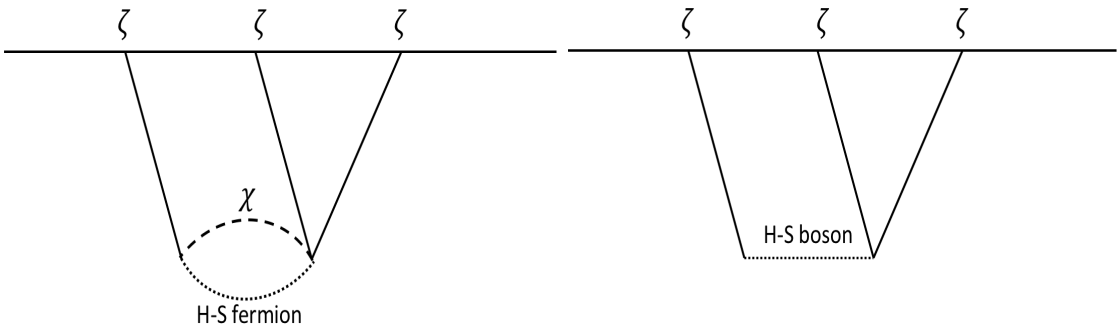

(a) Exchange of a higher spin Fermion (b) Exchange of a higher spin boson

Figure 3.1: In-In formalism Feynman Diagrams for exchange of a single higher spin particle.

captured by the quadratic terms in the expansion of (3.24), see e.g. [94],

$$\langle W(t)) \rangle = \int \mathrm{d}t' \int \mathrm{d}t'' \langle H^I(t') W(t) H^I(t'') \rangle - 2\,\mathrm{Re} \int \mathrm{d}t' \int \mathrm{d}t'' \langle W(t) H^I(t') H^I(t'') \rangle, \tag{3.29}$$

with appropriate $i\epsilon$ prescriptions in the integrations.

3.4.1 Effective Action and Relevant Interactions

We consider an effective action describing the interactions of a scalar ζ, a massive spin-1/2 field χ, and the propagating component fields of the massive, half-integer superspin $\mathsf{Y} = s + 1/2$ supermultiplet, as they have been discussed previously. We consider our action as an expansion in higher spin fields, keeping up to linear order terms. We consider

$$\mathcal{L} = \mathcal{L}_\zeta + \mathcal{L}_\chi + \mathcal{L}_{hs} + \mathcal{O}(hs^2)... \tag{3.30}$$

In this work we are particularly interested in the impact of the fermionic higher spin particles, which has thus far been left unstudied. Motivated from the discussion in section 3 and (3.23), we take the Lagrangian of one fermionic spin-$s+1/2$ particle ψ interacting with a dimensionless scalar ζ and the spin-1/2 particle χ,

$$\mathcal{L} \supset \frac{\lambda_s}{\Lambda^{s-1}} \partial_{i_1 \ldots i_s} \zeta \bar{\chi} \psi^{i_1 \ldots i_s} + \frac{g_s}{\Lambda^s} \dot{\zeta} \partial_{i_1 \ldots i_s} \zeta \bar{\chi} \psi^{i_1 \ldots i_s} + c.c., \tag{3.31}$$

where λ_s and g_s are dimensionless coupling constants, Λ is a UV cutoff, and fermionic indices are contracted between $\bar{\chi}$ and ψ. For simplicity we have taken $\kappa_s = 0$ in (3.23), which leads to the same angular dependence for $\langle\zeta\zeta\zeta\rangle$ as the two terms above. The relevant Feynman diagrams, or rather their equivalent in the Schwinger-Keldysh ("in-in" formalism) are shown in Figure 3.1.

3.4.2 Higher Spin Fields in de Sitter Space

To evaluate the three-point function in the Schwinger-Keldysh formalism, we first must have expressions for the free fields in de Sitter space.

To begin with, a scalar field ϕ is quantized in curved space as,

$$\phi(x,t) = \int \frac{\mathrm{d}^3k}{(2\pi)^3}\phi_k a_k e^{ik\cdot x} + \quad h.c.\,. \tag{3.32}$$

The coefficients $\phi_k(k,t)$ are referred to as "mode functions". The field $\phi(x)$ and mode functions ϕ_k are related to two-point correlation functions as follows. The position-space two point function of a free-field ϕ is given by,

$$\langle\phi(x)\phi(y)\rangle = \int \frac{\mathrm{d}^3k}{(2\pi)^3}\langle\phi_k\phi_k\rangle\, e^{ik(x-y)} = \int \mathrm{d}\log k\, \frac{k^3}{2\pi^2}|\phi_k|^2\, e^{ik(x-y)} \equiv \int \mathrm{d}\log k\, \Delta^2_\phi(k)\, e^{ik(x-y)}. \tag{3.33}$$

The last equality defines the dimensionless power spectrum, $\Delta^2_\phi(k) \equiv \frac{k^3}{2\pi^2}|\phi_k|^2$. A special case of the above is a scale-invariant spectrum. In this case, $\Delta^2_\phi(k)$ is a constant, which owes its name to the implied scaling symmetry of the two-point function, $\langle\phi(x)\phi(y)\rangle = \langle\phi(\lambda x)\varphi(\lambda y)\rangle$. During inflation, this scaling symmetry of a massless scalar has its origins in the dilatation symmetry at late times in de Sitter space.

An important example is the curvature perturbation on uniform density hypersurfaces, ζ. This has mode function given by,

$$\zeta_k \simeq \frac{H}{m_{pl}\sqrt{4\epsilon k^3}}(1 - ik\eta)e^{ik\eta}, \tag{3.34}$$

where $\epsilon = -\dot{H}/H^2 \ll 1$ is the inflationary slow-roll parameter, and η is conformal time $\mathrm{d}\eta \equiv a^{-1}\mathrm{d}t$, which in de Sitter space is given by $\eta = -1/(aH)$. This solution is found by explicitly solving the Klein-Gordon equation in de Sitter space. Inflation is a small deviation from de Sitter space, which converts the scaling with k to $k^{-3/2+(n_s-1)/2}$, where n_s defines the spectral index of the power spectrum,

$$\Delta^2_\zeta \equiv \frac{k^3}{2\pi^2}|\zeta_k|^2 \propto k^{n_s-1}. \tag{3.35}$$

Another important example is massless spin-2, e.g. the graviton. Expanded in helicity states $\lambda = \pm 2$, the mode functions are given by [65]

$$\gamma^\lambda_k = \frac{\sqrt{2}H}{m_{pl}}\frac{1}{\sqrt{k^3}}(1+ik\eta)e^{-ik\eta}, \tag{3.36}$$

which, importantly, differs from the curvature perturbation (3.34) in part by an factor of $1/\sqrt{\epsilon}$. The power spectrum of primordial gravitational waves on large scales $k\eta \to 0$ is then given by [65],

$$\Delta^2_\gamma \equiv \sum_\lambda \frac{k^3}{2\pi^2}|\gamma^\lambda_k| = \frac{2}{\pi^2}\frac{H^2}{m^2_{pl}}, \tag{3.37}$$

which is a direct probe of the energy scale of inflation [95]. The ratio of the tensor power spectrum (3.37) to scalar power spectrum, termed the 'tensor-to-scalar ratio', is given by

$$r \equiv \frac{\Delta^2_\gamma}{\Delta^2_\zeta} = 16\epsilon, \tag{3.38}$$

where again $\epsilon \ll 1$ is the inflationary slow-roll parameter.

In contrast with these two examples, for massive particles the two-point function and hence mode functions are suppressed on large scales and at late times. For a minimally-coupled massive scalar field σ, the two-point function has the exact solution[96]

$$\langle\sigma_k(\eta)\sigma_k(\eta')\rangle = \frac{\pi}{4}H^2(\eta\eta')^{3/2}e^{-\pi\mu}H^{(1)}_{i\mu}(-k\eta)H^{(1)*}_{i\mu}(-k\eta'), \tag{3.39}$$

where $\mu \equiv \sqrt{m/H^2 - 9/4}$, and $H^{(1)}_{i\mu}$ is the Hankel function of the first kind. This corresponds

to a mode function $\sigma_k \sim H\eta^{3/2}e^{-\pi\mu/2} = a(\eta)^{-3/2}e^{-\pi\mu/2}/\sqrt{H}$, the latter equality using $\eta = -1/aH$ during inflation.

Now we turn to massive particles with spin. These are constrained by the Higuchi bound to have mass satisfying $m^2 \geq s(s-1)H^2$. As for scalars, the isometries of dS fixes the scaling of the two-point correlation function of spinning fields [23], which takes the form

$$\langle \mathcal{O}_s(k)\mathcal{O}_s(k)\rangle \propto k^{2\Delta-3}, \tag{3.40}$$

where all Lorentz indices are contracted with s copies of a null vector, and Δ is the scaling dimension of the field,

$$\Delta = \frac{3}{2} - i\mu_s \ \ , \ \ \mu_s = \sqrt{\frac{m^2}{H^2} - \left(s - \frac{1}{2}\right)^2}. \tag{3.41}$$

For heavy fields, or more precisely the "principle series" [96], one has $\mathrm{Re}\Delta = 3/2$, and the mode function is simply

$$\langle \mathcal{O}_s(k)\mathcal{O}_s(k)\rangle \propto k^{-2i\mu_s}. \tag{3.42}$$

The prefactors follow from dimensional analysis, and intuition from solving the Klein-Gordon equation for heavy fields, which leads to an additional $e^{-\pi\mu_s}$ suppression. Importantly, this applies to general operators with spin, and not to just to bosonic (integer spin) operators, but to fermionic (half-integer spin) as well, and the two-point function of half-integer operators is similarly constrained to scale as $k^{2\Delta-3}$ as in (3.40).

In this work we will focus on the angular dependence of correlation functions. Given this, for simplicity we ignore the $e^{i\mu_s}$ phase, though we note that this can lead to oscillations in k-space [24], and thus is of potential interest. Dropping this phase, the mode functions for spin-s and spin-$(s+1/2)$ are at late times given by

$$\mathcal{O}_s(k,\eta) \simeq \frac{a(\eta)^{-3/2}}{\sqrt{H}}e^{-\pi\mu_s/2} \ \ , \ \ \mathcal{O}_{s+1/2}(k,\eta) \simeq a(\eta)^{-3/2}e^{-\pi\mu_{s+1/2}/2}. \tag{3.43}$$

The scaling with $a(\eta)$ follows from solving the mode-function equation of motion explicitly[9], while the differing factors of H follow from dimensional analysis[10]. This matches with the known result for a heavy spin-1/2 particle in de Sitter space[97]: a spin-1/2 fermion χ with mass $m > H$ has mode function given by,

$$\chi_k \simeq a(\eta)^{-3/2} e^{-\pi m_\chi / 2H}. \tag{3.45}$$

Now we can make this more precise. A massive spin-s boson may be split into helicity components as,

$$\sigma_{\mu_1 \ldots \mu_s} = \sum_{\lambda=-s}^{s} \sigma^{\lambda}_{\mu_1 \ldots \mu_s}, \tag{3.46}$$

and then decomposed into fields of n polarization directions by projecting the spinning field $\sigma_{\mu_1 \ldots \mu_s}$ onto spatial slices, i.e. via the decomposition

$$\sigma_{i_1 \ldots i_n \eta \ldots \eta} = \sum_{\lambda} \sigma^{\lambda}_{n,s} \varepsilon^{\lambda}_{i_1 \ldots i_n}, \tag{3.47}$$

where η is the time coordinate. Here, the s index refers to the spin, n refers to the 'spatial spin,' and λ is the helicity of the field. Thus $\varepsilon^{\lambda}_{i_s \ldots i_n}$ is a normalized, totally symmetric tensor with spin s and helicity λ. The $\sigma^{\lambda}_{n,s}$ satisfy $\sigma^{\lambda}_{n,s} = 0$ for $n < |\lambda|$ [24].

The quantity that appears in scattering with scalars is $\lambda = 0$ and $n = s$ (for more details see [24] or Appendix 3.A), i.e. the quantity $\sigma^0_{s,s}$. Explicitly solving for the mode function, one finds [24]

$$\sigma^0_{s,s}(k, \eta) \simeq \frac{a(\eta)^{s-3/2}}{\sqrt{H}} e^{-\pi \mu_s / 2}. \tag{3.48}$$

[9] In solving the Klein-Gordon equation explicitly, the scaling with $a(\eta)$ depends on the number of upper vs. lower indices, but this dependence cancels when all indices are contracted insider of correlation functions. For example, mode functions defined with respect to $\mathcal{O}_s$ with all lower indices are

$$\mathcal{O}_{i_1 \ldots . i_s}(k, \eta) \propto \frac{a(\eta)^{s-3/2}}{\sqrt{H}} \tag{3.44}$$

See (B.76) and (C.7) of [96]: Using $\eta{=}1/(aH)$ and $N_\lambda{=}(1/\sqrt{k})(k/H)^{s-1}$, one finds that $N_\lambda(k\eta)^{3/2-s}{=}(1/\sqrt{k})(k/H)^{s-1}(k/aH)^{3/2-s} {=}a^{s-3/2}/\sqrt{H}$.

[10] Bosons are defined as having mass term $m^2(\mathcal{O}^b(x))^2$ and hence mass dimension 1 while fermions are defined as having mass term $m\bar{\mathcal{O}}^f(x)\mathcal{O}^f(x)$ and hence mass dimension 3/2. The corresponding mode functions have dimension $-1/2$ and 0

Moreover, for the above $\lambda = 0$ helicity state, one has the important relation,

$$\hat{q}_{i_1}\hat{q}_{i_2}...\hat{q}_{i_s}\varepsilon^{\lambda=0}_{i_1...i_s}(\hat{k},\varepsilon) = P_s(\cos\theta), \tag{3.49}$$

with θ defined as the angle between $\hat{q}$ and $\hat{k}$. This follows from more general relations for spin-s polarization vectors, which are detailed in the thesis [96], and given in Appendix 3.A.

Similar to the bosonic case, a massive spin-$(s+1/2)$ 4-component fermion may be split into helicity components as,

$$\psi^{\alpha}_{\mu_1...\mu_s} = \sum_{\lambda} \psi^{\lambda\alpha}_{\mu_1...\mu_s}, \tag{3.50}$$

where α is a fermionic index and $\mu_1...\mu_s$ are bosonic indices, and projected onto spatial slices via the decomposition,

$$\psi^{\alpha}_{i_1...i_n\eta...\eta} = \sum_{\lambda} \psi^{\lambda}_{n,s}\epsilon^{\lambda\,\alpha}_{i_1...i_n}, \tag{3.51}$$

where again η is the time coordinate. We construct the spin-$(s+1/2)$ polarization vectors as a tensor product of spin-1/2 and spin-s. That is, we decompose,

$$\epsilon^{\lambda\alpha}_{i_1...i_s} = \sum_{\lambda'} \xi^{\alpha}_{\lambda'}\varepsilon^{\lambda}_{i_1...i_s}, \tag{3.52}$$

with $\xi_{\lambda'}$ a spin-1/2 eigenspinor of helicity λ' and ε^{λ} the spin-s polarization vector of helicity λ. The general decomposition of the fermion field can then be written as,

$$\psi^{\alpha}_{i_1...i_n\eta...\eta} = \sum_{\lambda,\lambda'} \psi^{\lambda\lambda'}_{n,s}\epsilon^{\lambda}_{i_1...i_n}\xi^{\lambda'\alpha}. \tag{3.53}$$

Similar to the bosonic case, the fermions can be split into helicity states, and it is the helicity $0 \pm 1/2$ which contributes to the loop in Figure 3.1a. More explicitly, the relevant mode function has the form,

$$\psi^{0\lambda'}_{s,s} \simeq a(\eta)^{s-3/2}e^{-\pi\mu_s/2}. \tag{3.54}$$

One can use this, along with the mode functions (3.45) and (3.34), and the interaction Lagrangian (3.31), to compute correlation functions of ζ involving intermediate states of

fermions.

3.4.3 Non-Gaussianity from higher spin Particle Exchange

The correlator we wish to compute is of three $\zeta(k,\eta)$ at lates times, $\eta \to 0$, and in the limit that one of the momenta is small $k_1 \ll k_2, k_3$, i.e. the quantity,

$$\langle \zeta(k_1,0)\zeta(k_2,0)\zeta(k_3,0)\rangle, \tag{3.55}$$

given the insertion of interaction vertices between the scalar ζ and higher spin fields. The result for exchange of a higher spin boson are given in [23, 24]. While [23] focused on the scaling and angular dependence, [24] explicitly solved the Klein-Gordon equation for higher spin bosonic fields and from this was able to compute all expressions exactly. In our analysis we will follow [23] and focus on the amplitude and angular dependence.

The 3-point function resulting from higher spin boson exchange, diagram 3.1b, is given by[24],

$$\lim_{k_1 \ll k_3, \eta \to 0} \frac{\langle \zeta(k_1)\zeta(k_2)\zeta(k_3)\rangle}{\Delta_\zeta^4} \;=\; \alpha_s \Delta_\zeta^{-1} \times P_s(\hat{k}_1 \cdot \hat{k}_3) \times \mathcal{I}^{(s)}(\mu_s, c_\pi, k_1, k_3, k_3)\delta(\sum k_i) + (k_2 \leftrightarrow k_3)\,, \tag{3.56}$$

where $\mathcal{I}^{(s)}(\mu_s, c_\pi, k_1, k_3, k_3)$ is a complicated function of momenta given in the Appendices of [24], and P_s the Legendre polynomial. This is characterized by a dimensionless coupling α_s, which in the notation of our (3.13), and taking the Goldstone boson parameters of [24] to be $c_\pi = 1$ and $f_\pi = m_{pl}$, is given by,

$$\alpha_s = \lambda_s g_s \left(\frac{\Lambda}{m_{pl}}\right)^6 \left(\frac{H}{\Lambda}\right)^{2s+1}. \tag{3.57}$$

This corresponds to a non-Gaussianity parameter of

$$f_{\rm NL} \equiv \frac{5}{18}\frac{\langle \zeta_k \zeta_k \zeta_k\rangle}{P_\zeta(k)^2} \;\sim\; e^{-\pi\mu_s}\alpha_s \Delta_\zeta^{-1}\,, \tag{3.58}$$

with shape function

$$\lim_{k_1 \ll k_3} \langle \zeta(k_1,0)\zeta(k_2,0)\zeta(k_3,0)\rangle \propto \frac{1}{k_1^3 k_3^3}\left(\frac{k_1}{k_3}\right)^2, \tag{3.59}$$

and a characteristic angular dependence,

$$\langle \zeta(k_1,0)\zeta(k_2,0)\zeta(k_3,0)\rangle \propto P_s(\cos\theta), \tag{3.60}$$

with θ the angle between k_1 and k_3.

We now turn to the fermions. Before we proceed, it is important to further clarify and emphasize the procedure. We approximate the fermionic mode functions by their super-horizon scaling (3.54), which neglects the sub-horizon oscillatory behavior of the exact solution (see [24] for the bosonic results). This is sufficient to compute the angular dependence of the 3-point function, as is our aim, but not the k-dependence and thus not the shape function. Additionally, we regulate the fermionic loop of Figure 3.1a by imposing a UV cutoff, which we choose to be the Hubble scale for self-consistency with our approximate form of the mode functions. The choice of cutoff does not qualitatively affect the result, and can be undone by a simple replacement $H \to \Lambda_{UV}$ in the loop integral.

To compute the fermion diagram Figure 3.1a there are two interaction Hamiltonians, which follow from the Lagrangian (3.31), given by

$$H_{int1} = \frac{\lambda_s}{\Lambda^{s-1}} \int d^3x \frac{1}{a^{2s-3}}\, \partial_{i_1\ldots i_s}\zeta\, \bar{\chi}\, \psi_{i_1\ldots i_s} + h.c., \tag{3.61}$$

and

$$H_{int2} = \frac{g_s}{\Lambda^{s}} \int d^3x \frac{1}{a^{2s-2}}\, \zeta' \partial_{i_1\ldots i_s}\zeta\, \bar{\chi}\, \psi_{i_1\ldots i_s} + h.c., \tag{3.62}$$

with i indices summed over, and where $'$ indicates a derivative with respect to conformal time. The 3-point function of three $\zeta(k,\eta)$, at late times $\eta \to 0$, is given by

$$\langle \zeta(k_1,0)\zeta(k_2,0)\zeta(k_3,0)\rangle = \mathrm{Re}4\langle \left[\zeta(k_1,0)\zeta(k_2,0)\zeta(k_3,0)\int a(\eta')\mathrm{d}\eta' H_{int1}(\eta')\int a(\eta'')\mathrm{d}\eta'' H_{int2}(\eta'')\right]\rangle, \tag{3.63}$$

where we focus on the second term in (3.29), which has the same angular dependence as the first term, the two terms differing in calculation only by the distribution of complex conjugation among the resulting ζ mode functions. The additional factor of 2 as compared to (3.29) is due to the two possibilities of time-ordering H_1 and H_2.

To compute this we expand H_{int1} and H_{int2} in momentum space, which results in 7 momentum integrals, $\mathrm{d}^3q_1....\mathrm{d}^3q_7$. We define the momenta as follows: let k_1 be the ζ in the left interaction vertex of Figure 3.1a, and ℓ the momentum of χ in the loop and $\ell + k_1$ the momentum of ψ in the loop. The 'outgoing' ζ momenta are defined as k_2 and k_3; under Wick contractions we will need to sum over $k_2 \to k_3$.

This gives, approximating the mode functions by their forms given in section 3.4.2,

$$\langle\zeta(k_1,0)\zeta(k_2,0)\zeta(k_3,0)\rangle = \frac{\lambda_s g_s}{\Lambda^{2s-1}}\mathrm{Re}\,8\zeta_{k_1}(0)\zeta_{k_2}(0)\zeta_{k_3}(0)\int\frac{\mathrm{d}\eta'}{a(\eta')^{s-1}}\int\frac{\mathrm{d}\eta''}{a(\eta'')^s}\zeta^*_{k_1}(\eta')\zeta'^*_{k_2}(\eta'')\zeta^*_{k_3}(\eta'')$$
$$\cdot|k_1|^s|k_3|^s e^{-\pi\mu_s}e^{-\pi m_\chi/H}\delta(\sum k_i)\int\frac{\mathrm{d}^3\ell}{(2\pi)^3}\,P_s(\hat{k}_1\cdot\hat{q})P_s(\hat{k}_3\cdot\hat{q})\left(\sum_\lambda\xi^\lambda(\hat{\ell})\xi^\dagger_\lambda(\hat{q})\right)^2 + k_2\leftrightarrow k_3, \quad (3.64)$$

where $\vec{q}\equiv\vec{\ell}+\vec{k_1}$. We can factorize this into three pieces:

$$\langle\zeta(k_1,0)\zeta(k_2,0)\zeta(k_3,0)\rangle \equiv \mathrm{Re}\mathcal{I}_1\mathcal{I}_2\mathcal{I}_3, \quad (3.65)$$

with time-integrals,

$$\mathcal{I}_1 \equiv \zeta_{k_1}(0)\zeta_{k_2}(0)\zeta_{k_3}(0)\int\frac{\mathrm{d}\eta'}{a(\eta')^{s-1}}\int\frac{\mathrm{d}\eta''}{a(\eta'')^s}\zeta^*_{k_1}(\eta')\zeta'^*_{k_2}(\eta'')\zeta^*_{k_3}(\eta''), \quad (3.66)$$

momentum integrals,

$$\mathcal{I}_2 \equiv \int\frac{\mathrm{d}^3\ell}{(2\pi)^3}\,P_s(\hat{k}_1\cdot\hat{q})P_s(\hat{k}_3\cdot\hat{q})\left(\sum_\lambda\xi^\lambda(\hat{\ell})\xi^\dagger_\lambda(\hat{q})\right)^2, \quad (3.67)$$

and an overall prefactor of

$$\mathcal{I}_3 \equiv \frac{\lambda_s g_s}{\Lambda^{2s-1}}8|k_1|^s|k_3|^s e^{-\pi\mu_s}e^{-\pi m_\chi/H}\delta(\sum k_i). \quad (3.68)$$

The loop integral $\mathcal{I}_2$ is UV-divergent, and we apply a cutoff at H,

$$\mathcal{I}_2 \simeq H^3 \int \mathrm{d}\Omega\, P_s(\hat{k}_1 \cdot \hat{q}) P_s(\hat{k}_3 \cdot \hat{q}) \left(\sum_\lambda \xi^\lambda(\hat{\ell}) \xi_\lambda(\hat{q}) \right)^2, \tag{3.69}$$

with $\hat{q}$ now given by

$$\hat{q} = \frac{H\hat{\ell} + k_1 \hat{k}_1}{\sqrt{H^2 + k_1^2}} \simeq \hat{\ell}, \tag{3.70}$$

where the latter equality follows working in the limit $k_1 \to 0$. This simplifies the sum over spin-1/2 helicities, as the $\xi(\hat{k})$ are normalized to 1. Thus we have,

$$\mathcal{I}_2 \simeq H^3 \int \frac{\mathrm{d}\Omega}{(2\pi^3)}\, P_s(\hat{k}_1 \cdot \hat{q}) P_s(\hat{k}_3 \cdot \hat{q}). \tag{3.71}$$

The remaining integral over angles can be performed analytically. Defining k_1 as making angle $\theta_1 = 0$ in the $\{x, y\}$ plane, and k_3 as making angle θ_{13}, such that $\hat{k}_1 \cdot \hat{k}_3 = \cos\theta_{13}$, $\hat{q} \cdot \hat{k}_1 = \cos\theta$, $\hat{q} \cdot k_3 = \cos(\theta - \theta_{13})$, the integral can be written as,

$$\mathcal{I}_2 \simeq \frac{H^3}{8\pi^2} \int \mathrm{d}\cos\theta\, P_s(\cos\theta) P_s(\cos(\theta - \theta_{13})). \tag{3.72}$$

We then use the identity[11],

$$P_\ell(\cos(a-b)) = \sum_{m=-\ell}^{\ell} P_\ell^m(\cos a) P_\ell^m(\cos b) \frac{(\ell - m)!}{(\ell + m)!}, \tag{3.73}$$

from which one can evaluate the integral explicitly. The result is

$$\mathcal{I}_2 = \frac{H^3}{8\pi^2} \sum_{m=-s}^{s} c_m P_s^m(\cos\theta_{13}), \tag{3.74}$$

with coefficients

$$c_m = \frac{(s-m)!}{(s+m)!} \int_{-1}^{1} \mathrm{d}x\, P_s(x) P_s^m(x) = \begin{cases} 2(-1)^{m/2} \frac{s!(2s)!}{(1+2s)!(s+m)!}, & \text{if } m \text{ even} \\ 0, & \text{if } m \text{ odd.} \end{cases} \tag{3.75}$$

[11] Using the spherical harmonics addition theorem with $\phi_1 = \phi_2 = 0$.

Finally we can perform the time integration. Using the explicit ζ mode function (3.34), one can analytically compute these integrals to find,

$$\mathcal{I}_1 = \frac{H^{2s+5}}{m_{pl}^6(4\epsilon)^3}\frac{1}{(k_1k_2k_3)^3}(1+s)\Gamma(s)\Gamma(2+s)\frac{k_2^3}{k_1^s(k_2+k_3)^{s+3}}\left(1+(s+3)\frac{k_3}{k_2}\right). \tag{3.76}$$

Putting the pieces together, we find for the non-Gaussianity,

$$\begin{aligned}\langle\zeta(k_1,0)\zeta(k_2,0)\zeta(k_3,0)\rangle \simeq \frac{1}{64\pi}\lambda_s g_s\frac{H^6}{m_{pl}^6\epsilon^3}(1+s)\Gamma(s)\Gamma(2+s)\left(\frac{H}{\Lambda}\right)^{2s-1}e^{-\pi\mu_s}e^{-\pi m_\chi/H}\\ \cdot\frac{\delta(\sum k_i)}{(k_1k_2k_3)^3}\frac{k_3^s}{(k_2+k_3)^s}\frac{k_2^3H^3}{(k_2+k_3)^3}\left(1+(s+1)\frac{k_3}{k_2}\right)\sum_{m=-s}^{s}c_m P_s^m(\hat{k}_1\cdot\hat{k}_3)+k_2\leftrightarrow k_3\end{aligned} \tag{3.77}$$

which can be brought to a canonical form,

$$\langle\zeta(k_1,0)\zeta(k_2,0)\zeta(k_3,0)\rangle \simeq \mathcal{A}_{s+1/2}\frac{\Delta_\zeta(k)^4}{k^6}\mathcal{S}(k_1,k_2,k_3)\delta(\sum k_i)\sum_{m=-s}^{s}c_m P_s^m(\hat{k}_1\cdot\hat{k}_3)+k_2\leftrightarrow k_3, \tag{3.78}$$

where Δ_ζ^2 is the dimensionless primordial power spectrum, $\mathcal{S}(k_1,k_2,k_3)$ is a function of the ratios of k_i, and $\mathcal{A}$ is all remaining prefactors.

The angular dependence of the non-Gaussianity is given by,

$$\langle\zeta(k_1,0)\zeta(k_2,0)\zeta(k_3,0)\rangle \propto \sum_{m=-s}^{s}c_m P_s^m(\hat{k}_1\cdot\hat{k}_3). \tag{3.79}$$

with the coefficients c_m given by (3.75). The schematic form of the shape function $\mathcal{S}$ can be read off from (3.77), but the exact expression requires solving for the exact mode-functions of the higher spin particles in de Sitter space.

The corresponding non-Gaussianity parameter is given by,

$$f_{NL} \simeq \lambda_s g_s(1+s)\Gamma(s)\Gamma(2+s)\left(\frac{H}{\Lambda}\right)^{2s-1}e^{-\pi\mu_s}e^{-\pi m_\chi/H}\Delta_\zeta^2, \tag{3.80}$$

where the factor $\Gamma(s)\Gamma(2+s)$ is a relic of not having normalized the mode functions; we expect that as in the bosonic case, equation (A.77) of [24], the normalization of the exact

solution of the mode functions scales with $1/\Gamma(s)^2$, cancelling the $\Gamma(s)$ dependence of the 3-point function. The robust result is the scaling with the couplings λ_s, g_s, the ratio H/Λ, and the Boltzmann suppression due to both the higher-spin fermion and the spin-1/2 fermion, $e^{-\pi\mu_s}e^{-\pi\mu_\chi}$.

3.4.4 The predictions of Higher Spin Supersymmetry

We can now read-off result for the three-point function $\langle\zeta\zeta\zeta\rangle$ given the higher spin supermultiplet. We simply add the contributions from the particle content of the half-integer superspin $\mathsf{Y} = s + 1/2$ supermultiplet (3.14), given the non-Gaussianity from each spin derived in the previous section. The result is

$$\begin{aligned}\langle\zeta(k_1,0)\zeta(k_2,0)\zeta(k_3,0)\rangle_{\text{HS}-\text{SUSY}} = \quad & \langle\zeta(k_1,0)\zeta(k_2,0)\zeta(k_3,0)\rangle_{s+1} \\ & +2\times\langle\zeta(k_1,0)\zeta(k_2,0)\zeta(k_3,0)\rangle_{s+1/2} \\ & +\langle\zeta(k_1,0)\zeta(k_2,0)\zeta(k_3,0)\rangle_{s} \qquad (3.81) \\ \propto \quad & P_{s+1}(\hat{k}_1\cdot\hat{k}_3)\ ,\ \sum_{m=-s}^{s} P_s^m(\hat{k}_1\cdot\hat{k}_3)\ ,\ P_s(\hat{k}_1\cdot\hat{k}_3) \qquad (3.82)\end{aligned}$$

where the last line indicates that the three terms in (3.81) have angular dependence given by P_{s+1}, $\sum_m P_s^m$, and P_s respectively. The relative amplitudes are determined by the mass spectrum of the theory.

The quantitative amplitude of this signal is, as in the non-supersymmetric bosonic case [24], generally small $f_{NL} \lesssim \mathcal{O}(1)$. The primary obstruction making f_{NL} any larger than this is perturbativity of the interaction strength, which at the very least, requires $\lambda_s(H/\Lambda)^{s-1} \ll 1$ and $g_s(H/\Lambda)^s \ll 1$, as these are the effective interaction strengths, e.g. appearing in (3.64). Non-Gaussianity of this size is not what would traditionally be referred to as 'large', but it can be considerably larger than the slow-roll suppressed single-field slow-roll value, and is within reach for CMB-S4 [95].

The analysis can be repeated for the case of embedding the higher spin particles inside the integer superspin supermultiplet (3.16) instead of the half integer one we have used as

an example. In that case the particle contained is ($s+1/2,\ s,\ s,\ s-1/2$) therefore one can immediately read off the result. The known $P_s(\cos\theta)$ dependence of spin-s bosons [23, 24] is accompanied by two towers of associated Legendre polynomials, $\sum_m P_s^m$ and $\sum_m P_{s-1}^m$, from the $s+1/2$ and $s-1/2$ fermions respectively.

3.5 Discussion

Precision measurements of the cosmic microwave background provide an unprecedented opportunity to search for new physics in the early universe. The 3-point function of primordial curvature perturbations, $\langle\zeta\zeta\zeta\rangle$, colloquially referred to as the non-Gaussianity, is sensitive to any new degrees of freedom, including those that are naively too heavy to be excited. One of the most striking results of this research program is the non-Gaussianity due to higher spin particles, and in particular the angular dependence $\langle\zeta\zeta\zeta\rangle \propto P_s(\cos\theta)$ due to the exchange of a single spin-s boson [23]. This prompted a flurry of activity, and possibilities for observing [98, 99, 100, 101, 102, 103, 104, 105, 106] the signature of higher spin particles.

Higher spin fermions have heretofore been left out of this discussion, but insofar as higher spin theory is understood as a limit of quantum gravity, namely superstring theory, fermions are built into the theory. This is required by the supersymmetric nature of the theory, which is itself a powerful tool for the incorporation of fermions into string theory, e.g. the construction of fermionic D-brane actions is accomplished by relying on the underlying supersymmetry of the theory [107, 108, 109, 110]. Guided by this, and building on recent developments in the construction of supersymmetric higher spin theories [34, 35, 36, 37, 38, 39, 40, 41, 42, 43, 45, 46, 47, 48], we have studied the imprint of higher spin supersymmetry at the cosmological collider.

The main result of this chapter is a characteristic pattern of the angular dependence of $\langle\zeta\zeta\zeta\rangle$ due to the exchange of higher spin superpartners. We find the $P_s(\cos\theta)$ signature of higher spin boson exchange, with θ the angle between the short and long wavelength modes, comes along with a $P_{s+1}(\cos\theta)$ and a tower of associated Legendre polynomials, arising from

a spin-$s+1$ boson and a pair of spin-$s+1/2$ fermions. For a variant description of higher spin supermultiplet, the partner contributions can be instead two towers of associated Legendre polynomials. The amplitude of the signal is generically not large by comparison to other known sources (e.g. [111, 112]), as already known for the non-supersymmetric bosonic case [24], so it is indeed the angular dependence which gives this signal its elevated status. Given this, in this work we have not endeavored to do a rigorous and precise calculation of the shape-function, which requires explicitly solving the mode-functions and computing involved integrals [24]. This latter difficulty motivated the development of the cosmological bootstrap [113], which might be a promising direction to take this work as well.

Remarkably, we have been able to derive these results despite not having a complete theory or model realization of higher spin supergravity inflation. Progress despite incomplete knowledge is a familiar situation in theoretical physics, for example, supersymmetry and the Green-Schwarz mechanism, all work to date pertaining to M-theory [114, 115], or in a more recent context, Double Field Theory [116]. To overcome this, we have constructed an effective theory that combines higher spin supersymmetry with de Sitter supergravity and the effective field theory of inflation, to describe a higher spin sector minimally coupled to the inflationary sector such that the higher spin sector retains on-shell supersymmetry. This allowed us to use supersymmetry considerations to deduce the field content and interactions of the higher spin fields with the curvature perturbation.

There are a number of ways forward from here. We have not considered yet the interactions with the graviton, or for that the matter, the gravitino. The former of these, corresponding to primordial gravitational waves γ, itself can lead to an interesting three point function, $\langle\gamma\zeta\zeta\rangle$, probed by cross-correlation with CMB B-mode polarization [117]. Starting from an effective field theory guided guess for the relevant interaction,

$$\mathcal{L}_{\gamma HS} = \frac{\hat{\lambda}_s}{\Lambda^{s-2}}\partial_{i_1\ldots i_{s-2}}\dot{\gamma}_{i_{s-1}i_s}\bar{\chi}\psi^{i_1\ldots i_s} + h.c., \tag{3.83}$$

the $\langle\gamma\zeta\zeta\rangle$ computed can be straight-forwardly worked out in a fashion similar to section 4.

We provide the calculations for this in Appendix 3.B, and here we give the result:

$$\lim_{k_1 \ll k_2, k_3} \langle \gamma^\lambda(k_1)\zeta(k_2)\zeta(k_3)\rangle = \hat{\lambda}_s g_s \left(\frac{H}{\Lambda}\right)^{2s-2} \frac{H^6}{m_{pl}^6}\frac{\sqrt{2}}{(4\epsilon)^2} e^{-\pi m_\chi/H} e^{-\pi\mu_s}\delta(\sum k_i)$$
$$\cdot\mathcal{S}(k_1,k_2,k_3)\int \frac{d\Omega}{(2\pi)^3} P_{s-2}(\hat{k}_1\cdot\hat{q})\varepsilon^\lambda_{ij}(\hat{k}_1)\sum_{\lambda'=\pm 2}\varepsilon^{\lambda' ij}(\hat{q})\hat{P}_s^{\lambda'}(\hat{k}_3\cdot\hat{q})\mathcal{E}_2^{\lambda'}(\hat{k}_3\cdot\hat{q}) + k_2 \leftrightarrow k_3, \tag{3.84}$$

where $\lambda = \pm 2$ is the helicity of the external graviton, ϵ_{ij} is the spin-2 polarization tensor, $\hat{P}_s^\lambda(x) \equiv (1-x^2)^{-\lambda/2}P_s^\lambda(x)$ and $\mathcal{E}_2^\lambda(\hat{k}_1\cdot\hat{k}_3) = \epsilon^\lambda_{ij}(\hat{k}_1)\hat{k}_3^i\hat{k}_3^j$ as in [24], and we have put all k-dependence in the function $\mathcal{S}$. This result is characterized by an angular dependence that is an integral over Legendre and associated Legendre polynomials,

$$\langle\gamma^\lambda\zeta\zeta\rangle \propto \sum_{\lambda'=\pm 2}\int d\cos\theta_q\, P_{s-2}(\hat{k}_1\cdot\hat{q})\varepsilon^\lambda_{ij}(\hat{k}_1)\varepsilon^{\lambda' ij}(\hat{q})\hat{P}_s^{\lambda'}(\hat{k}_3\cdot\hat{q})\mathcal{E}_2^{\lambda'}(\hat{k}_3\cdot\hat{q}), \tag{3.85}$$

where θ_q is the angle $\hat{q}$ makes in the plane. In the supersymmetric context, this would be joined with contributions from additional interactions. This requires careful consideration of the gravity multiplet, as is the focus of the supersymmetric EFT of inflation [53]. We postpone this analysis to future work.

On the theoretical front, an important next step is to construct the full theory of spontaneously broken supersymmetry (as in de Sitter supergravity and the supersymmetric EFT of inflation) and interacting higher spin fields. From this one can generalize the analysis here to situations where the higher spin fields themselves contribute to the supersymmetry breaking, or perhaps even drive inflation. We leave this possibility, and a host of observational implications, to future work.

As a concluding remark, we would like to express and share our enthusiasm for the work of scientists who are searching for signals of supersymmetry in the cosmos, a sentiment expressed by one of the authors in [118]. As argued for in this work, the non-Gaussianity of the CMB may prove to be a powerful tool of discovery, and with some good fortune, perhaps more and different such tools will later emerge for the SUSY search at the Cosmic Collider.

3.A Spin-s polarization vectors

This appendix discusses some relevant preliminaries and definitions relating to the free theory of higher spin fields in de Sitter space, which can also be found in [24]. Following [24], vectors will be denoted here in boldface, e.g. $\mathbf{k}$.

It is convenient to project the spinning field, $\sigma_{\mu_1\ldots\mu_s}$ onto spatial slices, which we can then write as

$$\sigma_{i_1\ldots i_n\eta\ldots\eta} = \sum_{\lambda} \sigma^{\lambda}_{n,s}\varepsilon^{\lambda}_{i_1\ldots i_n}. \tag{3.86}$$

Here, the s index refers to the spin, n refers to the 'spatial spin,' and λ is the helicity of the field. $\varepsilon^{\lambda}_{i_s\ldots i_n}$ is a normalized, totally symmetric tensor with spin s and helicity λ. It must satisfy:

$$\varepsilon^{\lambda}_{i_1\ldots i_s} = \varepsilon^{\lambda}_{(i_1\ldots i_s)} \;\;,\;\; \varepsilon^{\lambda}_{iii_3\ldots i_s} = 0 \quad , \quad \hat{k}_{i_1}\ldots\hat{k}_{i_r}\varepsilon^{\lambda}_{i_1\ldots i_s} = 0 \;\text{ for }\; r > s - |\lambda|, \tag{3.87}$$

corresponding to the symmetric, traceless, and transverse properties. These properties of the polarization tensor imply that we can decompose it into transverse and longitudinal parts as,

$$\varepsilon^{\lambda}_{i_1\ldots i_s}(\hat{\mathbf{k}},\varepsilon) = \varepsilon^{\lambda}_{(i_1\ldots i_\lambda}(\varepsilon) f_{i_{\lambda+1}\ldots i_s)}(\hat{\mathbf{k}}), \tag{3.88}$$

where $\varepsilon^{\lambda}_{i_1\ldots i_\lambda}$ is a maximally transverse polarization tensor, constructed out of polarization vectors $\varepsilon^{\pm}$ that are perpendicular to $\hat{\mathbf{k}}$. We must have that $\varepsilon^{+} = (\varepsilon^{-})*$, so that $\varepsilon^{\lambda}_{i_1\ldots i_\lambda}$ can be specified, up to a phase, by a single polarization vector ε. We have also defined $f_{i_{\lambda+1}\ldots i_s}$ as the longitudinal part of the associated Legendre polynomial, after contraction with momenta.

We then define,

$$F^{\lambda}_{s} = q_{i_1}....q_{i_s}\varepsilon^{\lambda}_{i_1\ldots i_s}(\mathbf{k}), \tag{3.89}$$

The symmetry properties of ε imply that F^{λ}_{s} takes the form [24], in d=3 spatial dimensions,

$$F^{\lambda}_{s} \propto z\hat{P}^{\lambda}_{s}, \tag{3.90}$$

where $z \equiv q_{i_1}...q_{i_\lambda}\varepsilon^{\lambda}_{i_1....i_\lambda}$, and $\hat{P}$ defined via

$$P_s^\lambda(\theta,\phi) = \sin^\lambda\theta \hat{P}_s^\lambda(\theta,\phi), \tag{3.91}$$

where P_s^λ is the associated Legendre polynomial. For the special case of $\lambda = 0$, which appears in the calculation of 3-point functions after enforcing momentum conservation, the othonormality of differing helicity states λ and λ', and the transverse property (3.87), one has

$$q_{i_1}....q_{i_s}\varepsilon^0_{i_1...i_s}(\hat{\mathbf{k}}) \propto P_s(\hat{\mathbf{q}}\cdot\hat{\mathbf{k}}), \tag{3.92}$$

with magnitude $|q_1|^s$, leading to the characteristic angular dependence of the three-point function for spin-s boson exchange. Moreover, the transverse property also implies that the only $\sigma^0_{n,s}$ that enters the correlation function is $n = s$.

3.B Details of $\langle\gamma\zeta\zeta\rangle$ Calculation

In this appendix, we further explicate the derivation of the tensor-scalar-scalar correlation function. We will limit our analysis to the single-exchange diagram shown in Figure 3.2.

This diagram has the same form as Figure 3.1a, however now we have an external graviton carrying momentum k_1 instead of ζ. The relevant interaction Lagrangian we will consider is

$$\mathcal{L} = \frac{\hat{\lambda}_s}{\Lambda^{s-2}}\partial_{i_1...i_{s-2}}\dot{\gamma}_{i_{s-1}i_s}\bar{\chi}\psi^{i_1...i_s} + \frac{g_s}{\Lambda^s}\dot{\zeta}\partial_{i_1...i_s}\zeta\bar{\chi}\psi^{i_1...i_s} + h.c., \tag{3.1}$$

which corresponds to two interaction Hamiltonians

$$H_{int_1} = \frac{\hat{\lambda}_s}{\Lambda^{s-2}}\int d^3x \frac{1}{a^{2s-2}}\partial_{i_1...i_{s-2}}\gamma'_{i_{s-1}i_s}\bar{\chi}\psi^{i_1...i_s} + h.c., \tag{3.2}$$

$$H_{int_2} = \frac{g_s}{\Lambda^s}\int d^3x \frac{1}{a^{2s-2}}\zeta'\partial_{i_1...i_s}\zeta\bar{\chi}\psi^{i_1...i_s} + h.c.. \tag{3.3}$$

As in the $\langle\zeta\zeta\zeta\rangle$ calculation, we would like to expand in Fourier modes. The graviton can be

expanded in helicity modes as given in [24]:

$$\gamma_{ij}(\mathbf{k},\eta) = \sum_{\lambda=\pm 2} \varepsilon_{ij}^{\lambda}(\mathbf{k})\gamma_k^{\lambda}(\eta)b(\mathbf{k},\lambda) + h.c., \tag{3.4}$$

where the graviton mode function, γ_k^{λ}, is given by

$$\gamma_k^{\lambda}(\eta) = \frac{\sqrt{2}H}{m_{pl}}\frac{1}{\sqrt{2k^3}}(1+ik\eta)e^{-ik\eta}. \tag{3.5}$$

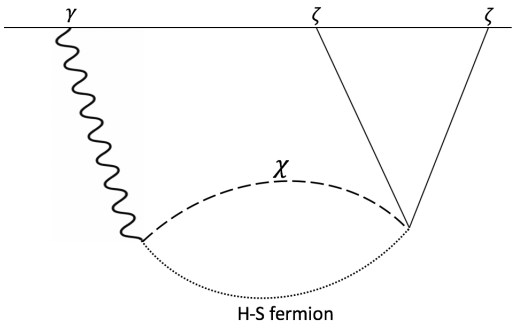

Figure 3.2: Diagram contributing to $\langle\gamma\zeta\zeta\rangle$.

With the mode functions in hand we can compute the tensor-scalar-scalar three point function $\langle\gamma\zeta\zeta\rangle$. As before, we would like to expand each interaction Hamiltonian in momentum space and compute the correlator. Much of the calculation remains the same as in the $\langle\zeta\zeta\zeta\rangle$ case, however, there are some subtleties. The angular dependence due to H_{int_2} remains largely the same, however now due to the fact that $\lambda \neq 0$, we have $H_{int_2} \propto \mathcal{E}_2^{\lambda}(\hat{k}_3\cdot\hat{q})\hat{P}_s^{\lambda}(\hat{k}_3\cdot\hat{q})$, rather than simply $P_s(\hat{k}_3\cdot\hat{q})$ as in the $\langle\zeta\zeta\zeta\rangle$ case. This arises from the definition (3.90), and we have defined $\mathcal{E}_2^{\lambda}(\hat{k}_3\cdot\hat{q}) = \varepsilon_{ij}^{\lambda}(\hat{k}_3)\hat{q}^i\hat{q}^j$. The angular dependence of H_{int_1} is similarly complicated due to the contraction with γ_{i_{s-1},i_s}.

After expanding in momentum space and following a similar procedure as in the $\langle\zeta\zeta\zeta\rangle$

calculation, we obtain

$$\begin{aligned}\langle\gamma^{\lambda}\zeta\zeta\rangle = 8\frac{\hat{\lambda}_s g_s}{\Lambda^{2s-2}}\mathrm{Re}\gamma^{\lambda}_{k_1}(0)\zeta_{k_2}(0)\zeta_{k_3}(0)\int\frac{d\eta'}{a(\eta')^{2s-3}}\int\frac{d\eta''}{a(\eta'')^{2s-3}}\int\frac{d^3\ell}{(2\pi)^3}\\ \cdot\gamma^{\lambda *'}_{k_1}(\eta')\zeta^{*'}_{k_2}(\eta'')\zeta^{*}_{k_3}(\eta'')\bar{\chi}_{\ell}(\eta')\chi_{\ell}(\eta'')\sum_{\lambda'=\pm 2}\psi^{\lambda'}_{s,s,\ell+k_1}(\eta')\bar{\psi}^{\lambda'}_{s,s,\ell+k_1}(\eta'')\\ \cdot|k_1|^{s-2}|k_3|^{s}P_{s-2}(\hat{k}_1\cdot\hat{q})\varepsilon^{\lambda}_{ij}(\hat{k}_1)\varepsilon^{\lambda' ij}(\hat{q})\hat{P}^{\lambda'}_{s}(\hat{k}_3\cdot\hat{q})\mathcal{E}^{\lambda'}_{2}(\hat{k}_3\cdot\hat{q})\delta(\sum k_i),\end{aligned} \tag{3.6}$$

where we have defined $\mathcal{E}$ as in [24] as $\mathcal{E}^{\lambda}_{2}(\hat{k}_1\cdot\hat{k}_3)=\epsilon^{\lambda}_{ij}(\hat{k}_1)\hat{k}^{i}_{3}\hat{k}^{j}_{3}$, and where $\vec{q}\equiv\vec{\ell}+\vec{k_1}$. The mode functions for χ remain the same as in the previous calculation, given by (3.45), and we approximate that $\psi^{\pm 2}_{s,s}$ by their super-horizon scaling, which is the same as (3.54). Plugging in the explicit expressions for the mode functions and substituting $a(\eta)=-\frac{1}{H\eta}$, we have ,

$$\begin{aligned}\langle\gamma^{\lambda}\zeta\zeta\rangle = \frac{\hat{\lambda}_s g_s}{\Lambda^{2s-2}}H^{2s}\frac{H^6}{m^6_{pl}}\frac{2\sqrt{2}}{(4\epsilon)^2}\frac{1}{k^3_1k^3_2k^3_3}e^{-\pi m_{\chi}/H}e^{-\pi\mu_s}|k_1|^{s-2}|k_3|^{s}\delta(\sum k_i)\\ \cdot\mathrm{Re}\int d\eta'\eta'^{s}(k^2_1\eta')e^{ik_1\eta'}\int d\eta''\eta''^{s}(k^2_2\eta'')(1+ik_3\eta'')e^{-i(k_2+k_3)\eta''}\\ \int\frac{d^3\ell}{(2\pi)^3}P_{s-2}(\hat{k}_1\cdot\hat{q})\varepsilon^{\lambda}_{ij}(\hat{k}_1)\sum_{\lambda'=\pm 2}\varepsilon^{\lambda' ij}(\hat{q})\hat{P}^{\lambda'}_{s}(\hat{k}_3\cdot\hat{q})\mathcal{E}^{\lambda'}_{2}(\hat{k}_3\cdot\hat{q})+k_2\leftrightarrow k_3.\end{aligned} \tag{3.7}$$

where $\hat{P}^{\lambda}_{s}(x)\equiv(1-x^2)^{-\lambda/2}P^{\lambda}_{s}(x)$ as in [24].

For ease of notation, let us denote this as,

$$\langle\gamma^{\lambda}\zeta\zeta\rangle=\mathcal{J}_1\mathcal{J}_2\mathcal{J}_3, \tag{3.8}$$

where $\mathcal{J}_1$ is the prefactor, $\mathcal{J}_2$ are the time integrals and $\mathcal{J}_3$ is the momentum integral. Performing the time integration and keeping only the real part yields

$$\mathcal{J}_2=\frac{k_1^{-s}k_2^2(k_2+k_3(s+3))\Gamma(s+2)^2}{(k_2+k_3)^{s+3}}. \tag{3.9}$$

In $\mathcal{J}_3$ we can perform the integration over ℓ, enforcing a cutoff at H, leaving only the angular

integral. Putting everything together, we obtain,

$$\begin{aligned}\lim_{k_1\ll k_2,k_3}\langle\gamma^\lambda(k_1)\zeta(k_2)\zeta(k_3)\rangle = \frac{\hat{\lambda}_s g_s}{\Lambda^{2s-2}}\frac{H^{2s+6}}{m_{pl}^6}\frac{2\sqrt{2}}{(4\epsilon)^2}e^{-\pi m_\chi/H}e^{-\pi\mu_s}\delta(\sum k_i)\\ \cdot\frac{H^3k_1^{-2}k_2^3k_3^s}{(k_1k_2k_3)^3(k_2+k_3)^{s+3}}\left(1+\frac{k_3}{k_2}(s+3)\right)\Gamma(s+2)^2\\ \cdot\int\frac{d\Omega}{(2\pi)^3}P_{s-2}(\hat{k}_1\cdot\hat{q})\varepsilon^\lambda_{ij}(\hat{k}_1)\varepsilon^{\lambda ij}(\hat{q})\hat{P}^\lambda_s(\hat{k}_3\cdot\hat{q})\mathcal{E}^\lambda_2(\hat{k}_3\cdot\hat{q})+k_2\leftrightarrow k_3.\end{aligned} \tag{3.10}$$

In a canonical form we can write this as,

$$\begin{aligned}\lim_{k_1\ll k_2,k_3}\langle\gamma^\lambda(k_1)\zeta(k_2)\zeta(k_3)\rangle = \hat{\lambda}_s g_s\left(\frac{H}{\Lambda}\right)^{2s-2}\frac{H^6}{m_{pl}^6}\frac{2\sqrt{2}}{(4\epsilon)^2}e^{-\pi m_\chi/H}e^{-\pi\mu_s}\delta(\sum k_i)\\ \cdot\mathcal{S}(k_1,k_2,k_3)\sum_{\lambda'=\pm2}\int\frac{d\Omega}{(2\pi)^3}P_{s-2}(\hat{k}_1\cdot\hat{q})\varepsilon^\lambda_{ij}(\hat{k}_1)\varepsilon^{\lambda' ij}(\hat{q})\hat{P}^{\lambda'}_s(\hat{k}_3\cdot\hat{q})\mathcal{E}^{\lambda'}_2(\hat{k}_3\cdot\hat{q})+k_2\leftrightarrow k_3.\end{aligned} \tag{3.11}$$

The angular dependence is given by

$$\langle\gamma^\lambda\zeta\zeta\rangle\propto\sum_{\lambda'=\pm2}\int d\cos\theta_q\, P_{s-2}(\hat{k}_1\cdot\hat{q})\varepsilon^\lambda_{ij}(\hat{k}_1)\varepsilon^{\lambda' ij}(\hat{q})\hat{P}^{\lambda'}_s(\hat{k}_3\cdot\hat{q})\mathcal{E}^{\lambda'}_2(\hat{k}_3\cdot\hat{q}), \tag{3.12}$$

where θ_q is the angle $\hat{q}$ makes in the plane.

Chapter 4

Higher Spin Dark Matter

4.1 Introduction

In the last chapter, we discussed the implications for higher spin fields (in the context of higher-spin supersymmetry) on the non-gaussianity of the cosmic microwave background. Given that these higher spin particles can be produced during inflation, it is a natural progression to then as whether the dark matter could be made up of higher spin particles, which we now discuss in this chapter. The precise identity of dark matter (DM) remains a mystery, despite decades of theorizing and detection efforts. Observations suggest that the dark matter does not interact with the standard model, or does so extremely weakly, creating significant room for model builders. Taken at face value, the observational evidence is at odds with the conventional origin story of dark matter, namely a thermal history, wherein the dark matter was initially in a state of thermal equilibrium with the standard model, sustained by interactions.

There are now many alternative dark matter origin stories. A particularly compelling possibility, by virtue of its simplicity, is the genesis of dark matter via gravitational particle production (GPP) in the early universe [119, 120, 121, 122, 123], e.g., during cosmic inflation. A generic feature of inflation is that the exponential expansion acts as a gravitational amplifier for particle production. While many of these particles would be redshifted, some, depending on their intrinsic properties such as mass and spin, can survive as a relic after

inflation ends. This idea was introduced in the context of superheavy 'WIMPzilla' dark matter, characterized by dark matter masses greater than the Hubble scale at the end of inflation ($m_{\rm DM} > H$) [119, 124, 120, 121, 122, 123], and has since been explored in a variety of cosmological contexts (see e.g. [125, 126, 127, 128, 129, 130]).

On the other hand, inflation is known to exhibit a UV sensitivity [131], motivating the search for a UV completion of inflation in theories beyond the standard model, such as string theory. In this context we may ask which states could be generically produced in an inflationary model that is connected to string theory. That massive higher spin particles are a natural consequence of string theory, and that generic cosmological inflation models induce particle production, is suggestive of the potential implications for connections to other physics, namely the dark matter problem. Moreover, the Higuchi bound on the mass of higher spin fields, $m^2 \geq s(s-1)H^2$, which must be satisfied at all times during an early universe genesis mechanism, naturally suggests dark matter in the superheavy regime, and hence, in light of [119, 120, 121, 122, 123], a gravitational origin of higher spin dark matter.

Despite the natural candidacy of higher spin fields as dark matter (and potentially an infinite tower of such fields), there has been little work done on investigating the feasibility of any such model beyond spin-3/2 [132, 133, 134], spin-2 [135, 136, 137, 138] and spin-3 [139, 140], aside from the suggestion in [141], and no work in a superheavy, gravitational production context. Additionally, there has been significant recent interest in the 'cosmological collider physics' program [142, 21, 22] (see also the related 'cosmological bootstrap' [113, 143, 144]) of studying the imprint in the cosmic microwave background (CMB) of fields with masses heavier than the Hubble scale during inflation, see e.g. [145, 146, 147, 148, 149, 150, 151]. This formalism has been applied to higher spin bosons [142, 24, 94], as well as higher spin fermions [152], and supersymmetric higher spin theory ([153, 154, 155, 156, 157]) [152]. However, thus far, no connections have been made between the massive higher spin particles produced by the cosmological collider and dark matter.

In this chapter we consider inflationary production and cosmological implications of higher spin particles and find that they can naturally serve as 100 percent of the dark matter: Higher

Spin Dark Matter (HSDM). We consider the implications of a small interaction of HSDM with the standard model, and find a characteristic angular dependence of nuclear recoil events for direct detection experiments. This mirrors the angular dependence in the cosmic microwave background non-Gaussianity that is predicted due to the the production of higher spins during inflation [142, 24, 152].

The structure of this chapter is as follows: in Section 6.2 we introduce the relevant higher spin formalism. In Section 6.3 we calculate the gravitational production of higher spin dark matter (HSDM) and show that there is a parameter space such that higher spin particles can account for all the dark matter. In Section 6.4 we discuss the possibilities for directional direct detection and show that there is a spin dependent contribution to the double differential recoil rate. Lastly, in Section 6.5 we speculate on other possible observable avenues and conclude with a discussion in Section 4.6.

4.2 Higher Spin Field Theory

The Standard Model of particle physics comprises particles with $s = 0, 1/2$ and 1, while gravity has spin $s = 2$. No fundamental particle with $s > 2$ has ever been observed in nature. However, there is a long history of the study of higher spins (HS). Beginning shortly after the advent of relativistic quantum field theory [25], the theory of higher spins has been developing for a century, notably [158, 159, 160, 153, 154, 161, 162, 163, 164, 165]; for recent work see e.g. [166, 167, 168, 169, 170, 171, 172, 173, 174, 175, 176, 177, 178, 179, 33, 180, 181, 182, 183, 184].

There are well known 'no-go' theorems that significantly limit the interactions of HS particles in a self-consistent quantum field theory. Generally, such theorems make it the case that in flat space, massless HS particles are forbidden from interacting with electromagnetism or gravity[1] [185, 186, 187, 188, 189, 190]. Two notable 'no-go' theorems are Weinberg's theorem [185], which necessitates that, in flat space, there are no long range interactions with spin greater than two, and the Coleman-Mandula theorem [186], which demonstrates

[1]Note that both during inflation and in the present day, the universe is de Sitter space

that, assuming an S-matrix and finite degrees of freedom, there can be no conserved higher spin charges associated with particles of $s > 2$.

A caveat to these arguments is *massive* higher spin theories. The mass term explicitly breaks the higher spin gauge invariance, such that there is no conserved current, and hence no conflict with the Coleman-Mandula theorem. As such, massive higher spins are not plagued by the same restrictions due to no-go theorems [191]. Indeed, massive higher spin excitations are intrinsic to string theory, and comprise the Regge trajectories. Higher spin fields have been considered in studies of inflation in string theory [26, 27, 192], and in the AdS/CFT correspondence [158, 160, 193]. It is thought that the tensionless limit of string theory is a higher spin field theory [194, 195, 196, 197, 198], and it has been suggested that string theory itself is a symmetry broken phase of a HS field theory [199, 200, 158, 201].

While the full theory of higher spins is not known, progress can be made by enumerating the irreducible representations of the spacetime symmetry group, thereby identifying the building the blocks of the theory. Although the representation theory of HS fields in a general Freidmann-Robertson-Walker spacetime is not known, the representations are known for flat space and (A)dS.

For cosmological purposes, in particular during inflation, we may make use of the results for de Sitter space. In this context, a lower bound on the higher spin mass is given by the Higuchi bound: $m^2 \geq s(s-1)H^2$ [77, 78]. Beyond this, fields can be organized into three categories of unitary, irreducible representations of the spacetime isometry group [202, 203]. They are the principal series:

$$\frac{m^2}{H^2} \geq \left(s - \frac{1}{2}\right)^2, \tag{4.1}$$

the complementary series:

$$s(s-1) < \frac{m^2}{H^2} < \left(s - \frac{1}{2}\right)^2, \tag{4.2}$$

and the discrete series:

$$\frac{m^2}{H^2} = s(s-1) - t(t+1). \tag{4.3}$$

In addition, In this work, we focus on the complementary series and principal series representations.

The evolution of HS fields in de Sitter space was derived in [24], which we summarize below. The spin-s generalization of Klein-Gordon equation is the Casimir eigenvalue equation of the de Sitter group [24],

$$\left(\Box - m^2 + (s^2 - 2s - 2)H^2\right)\sigma_{\mu_1\ldots\mu_s} = 0 \tag{4.4}$$

This is supplemented by constraint equations corresponding to transverse and traceless conditions on σ. To solve this equation, we expand the field $\sigma_{\mu_1\cdots\mu_s}$ into its different helicity components,

$$\sigma_{\mu_1\cdots\mu_s} = \sum_{\lambda=-s}^{s} \sigma^{(\lambda)}_{\mu_1\cdots\mu_s}\,. \tag{4.5}$$

A mode of helicity λ and n polarization directions can be written as,

$$\sigma^{(\lambda)}_{i_1\cdots i_n\eta\cdots\eta} = \sigma^{\lambda}_{n,s}\,\varepsilon^{\lambda}_{i_1\cdots i_n}\,, \tag{4.6}$$

where $\sigma^{\lambda}_{n,s} = 0$ for $n < |\lambda|$. The polarization vector $\varepsilon^{\lambda}_{i_1\cdots i_n}$ is symmetric, transverse, and traceless; for details, see [24].

The helicity-λ mode function with $n = |\lambda|$ number of polarization directions satisfies,

$$\begin{aligned}\sigma^{\lambda}_{|\lambda|,s} \quad & '' - \frac{2(1-\lambda)}{\eta}\sigma^{\lambda}_{|\lambda|,s}{}' \\ + \quad & \left(k^2 + \frac{m^2/H^2 - (s+\lambda-2)(s-\lambda+1)}{\eta^2}\right)\sigma^{\lambda}_{|\lambda|,s} = 0\,.\end{aligned} \tag{4.7}$$

This admits an exact solution, given by [24],

$$\sigma^{\lambda}_{|\lambda|,s} = \mathcal{A}_s\, Z^{\lambda}_s (-k\eta)^{3/2-\lambda} H^{(1)}_{i\mu_s}(k|\eta|)\,, \tag{4.8}$$

where μ_s is defined as

$$\mu_s = \sqrt{\frac{m^2}{H^2} - \left(s - \frac{1}{2}\right)^2}. \tag{4.9}$$

The normalization coefficients are given by,

$$\mathcal{A}_s = e^{i\pi/4} e^{-\pi\mu_s/2} \tag{4.10}$$

and

$$(Z_s^\lambda)^2 = \frac{1}{k}\left(\frac{k}{H}\right)^{2s-2} (\mathcal{Z}_s^\lambda)^2, \tag{4.11}$$

with

$$\begin{aligned}(\mathcal{Z}_s^\lambda)^2 = \quad & \frac{\pi}{4}\frac{[(2\lambda-1)!!]^2 s!(s-\lambda)!}{(2s-1)!!(s+\lambda)!} \\ & \cdot\frac{\Gamma(1/2+\lambda+i\mu_s)\Gamma(1/2+\lambda-i\mu_s)}{\Gamma(1/2+s+i\mu_S)\Gamma(1/2+s-i\mu_s)}.\end{aligned} \tag{4.12}$$

The other mode functions can then be obtained iteratively from the recursion relation:

$$\sigma_{n+1,s}^\lambda = -\frac{i}{k}\left(\sigma_{n,s}^{\lambda\ \prime} - \frac{2}{\eta}\sigma_{n,s}^\lambda\right) - \sum_{m=|\lambda|}^{n} B_{m,n+1}\,\sigma_{m,s}^\lambda\,, \tag{4.13}$$

where,

$$B_{m,n} \equiv \frac{2^n n!}{m!(n-m)!(2n-1)!!}\frac{\Gamma[\frac{1}{2}(1+m+n)]}{\Gamma[\frac{1}{2}(1+m-n)]}\,. \tag{4.14}$$

Care should be taken when considering these mode functions, since they are normalized with respect to σ with all lower indices. The quantity of physical interest is the two point function of two contracted σ, i.e.,

$$\langle \sigma_{i_1\ldots i_s}\sigma^{i_s\ldots i_s}\rangle = \frac{1}{a^{2s}}\langle \sigma_{i_1\ldots i_s}\sigma_{i_s\ldots i_s}\rangle. \tag{4.15}$$

More generally, for $\sigma_{n,s}^\lambda$, we are interested in the two-point correlation function,

$$\langle \sigma_{n,s}^\lambda \varepsilon_{i_1\ldots i_n}^\lambda \sigma_{n,s}^\lambda \varepsilon^{\lambda i_1\ldots i_n}\rangle = \frac{1}{a^{2n}}\langle \sigma_{n,s}^\lambda \varepsilon_{i_1\ldots i_n}^\lambda \sigma_{n,s}^\lambda \varepsilon_{i_1\ldots i_n}^\lambda\rangle. \tag{4.16}$$

The remaining contraction of polarization vectors can be computed from [24]

$$\varepsilon^{\lambda}_{i_1\cdots i_s}\varepsilon^{\lambda *}_{i_1\cdots i_s} = \frac{(2s-1)!!(s+\lambda)!}{[(2\lambda-1)!!]^2 s!(s-\lambda)!}, \tag{4.17}$$

where we have used the normalization $\varepsilon^{s}_{i_1\cdots i_s}\varepsilon^{s*}_{i_1\cdots i_s} = 2^s$ [24].

4.3 Gravitational Production of Higher Spin Dark Matter

The Higuchi bound $m^2 > s(s-1)H^2$ [77, 78] suggests that higher spin fields as realized in nature, insofar as they can be described by a single effective field theory in both the very early universe and in the late universe, should be cosmologically heavy. Guided by past literature [119, 120, 121, 122, 123], it is logical then to consider gravitational particle production as a genesis mechanism for higher spin dark matter. With this in mind, our first goal is to make a conservative estimate of the gravitational production of higher spin particles in the very early universe. This will serve as a proof of principle of gravitational particle production (GPP) as a genesis mechanism for higher spin dark matter (HSDM).

We will consider only the gravitational production *during* inflation, and not the transition between inflation and the radiation dominated phase that is the usual focus of works on GPP of dark matter [119, 120, 121, 122, 123, 127, 128]. This simplification is not made for convenience, but rather due to the limited knowledge of higher spin field theories as discussed previously. Our calculation provides a lower bound on the production, suitable for a demonstration that early universe GPP can provide enough higher spin particles to explain the observed DM abundance. We expect a more detailed analysis (e.g., directly from string theory) to change slightly the quantitative relationship between s, m, and H, that leads to the correct relic density, but not the qualitative result.

We focus on HS fields that during inflation are in either the complementary or principal series, defined by Eqs. (4.2) and (4.1) respectively. We make use of the fact that cosmic history is thought to be book-ended by de Sitter phases: cosmic inflation in the first moments and dark energy in the present. The full structure of the higher spin theory is not known in

for the intervening time period. However, post-inflation we are left with a collection of non-relativistic particles that simply redshift as matter, and hence we do not need to consider the detailed field theory dynamics. This negates the need to have complete knowledge of higher spin theories.

In general, gravitational particle production occurs when the field mass, including all contributions from quantum and gravitational effects, changes non-adiabatically. The canonical example is the primordial curvature, ζ, which obeys the equation of motion (in exact dS space)

$$v_k'' + \left(k^2 - \frac{2}{\eta^2}\right) v_k = 0. \tag{4.18}$$

Adiabaticity is violated when $k = \sqrt{2}/|\eta| \simeq aH$, i.e., when a given mode exits the horizon. The resulting particle production can be thought of as Hawking radiation emitted by the de Sitter horizon [204], see e.g. the discussion in [205], and indeed computed using conventional particle production methods [206, 207]. Alternatively, the equation of motion can be solved exactly at all times as a function of $k\eta$, see e.g. [208].

For a massive scalar field the effective mass is similarly given by [208]

$$\omega_k^2 = k^2 - \frac{2 - (m/H)^2}{\eta^2}. \tag{4.19}$$

For $m/H \gg 1$, adiabaticity is violated at $k \simeq \mu/|\eta| = \mu aH$ where $\mu \equiv m/H$ [128]. The scale $k_* = \mu aH$ defines an effective horizon, and all modes which have $k > k_*$ at the end of inflation, i.e. which have exited this effective horizon, have undergone particle production during inflation.

This is the principle behind superheavy dark matter. The total energy density in a massive scalar can be computed as

$$\rho_\varphi = m_\varphi^2 \langle \delta\varphi^2 \rangle \simeq m_\varphi^2 \int_0^{k_*} \mathrm{d}^3 k \, |\delta\varphi_k|^2, \tag{4.20}$$

corresponding to a particle number, $n = \rho_\varphi / m_\varphi$,

$$n = m_\varphi \int_0^{k_*} \mathrm{d}^3 k \, |\delta\varphi_k|^2. \tag{4.21}$$

The phenomenology of superheavy dark matter is thus determined by the dark matter mass and the energy scale of inflation. Due to the decay outside the horizon of the heavy field, along with the phase space suppression in the limit $k \to 0$, the integral is dominated by the contribution from the upper bound. The number density scales with H^3, where H is the Hubble constant during inflation. The relic density can be tuned to the observed value by tuning the mass $m_{\rm DM}$ as a function of H; for the canonical super-heavy dark matter, one finds $m_{\rm DM} \gtrsim H$ leads to the observed density [119, 120, 121, 122, 123].

The generalization of this to the energy density of a bosonic higher spin field σ produced gravitationally during inflation is given by,

$$\rho_\sigma \simeq m^2 \langle \sigma^2 \rangle = m^2 \sum_{n,\lambda} \varepsilon^{\lambda}_{i_1 \cdots i_n} \varepsilon^{\lambda *}_{i_1 \cdots i_n} \int \mathrm{d}^3 k \frac{|\sigma^\lambda_{n,s}|^2}{a^{2n}}, \tag{4.22}$$

where the sum is over all values of n and λ, and the contraction of polarization vectors is given by Eq. (4.17).

To evaluate this we begin from the equation of motion Eq. (4.8). To put this in a more familiar form, we rescale σ in Eq. (4.8) as $\hat{\sigma} = \eta^{1-\lambda}\sigma$. This removes the first-derivative term, leading to,

$$\hat{\sigma}^\lambda_{|\lambda|,s}{}'' + \left(k^2 - \frac{s(s-1) - \mu_s^2}{\eta^2} \right) \hat{\sigma}^\lambda_{|\lambda|,s} = 0, \tag{4.23}$$

which describes a simple harmonic oscillator with a time-dependent mass. We can see that the λ dependence has cancelled identically, and the effective mass is given by,

$$m^2_{\rm eff} = \mu_*^2 H^2 \equiv (s(s-1) - \mu_s^2) H^2, \tag{4.24}$$

where we define the quantity $\mu_* \equiv s(s-1) - \mu_s^2$, with μ_s given by Eq. (4.9).

In analogy with a massive scalar, adiabaticity is maximally violated ($|\dot{\omega}_k|/\omega_k^2$ is peaked)

when $k = \sqrt{2}\mu_* aH \simeq \mu_* aH$. Thus, we take the UV cutoff of the energy density integral to be this scale of adiabaticity violation. Incidentally, this cutoff is also the dividing line between relativistic and non-relativistic particles. Thus, independent of discussions of adiabaticity violation, this approach is equivalent to considering only those perturbations which become non-relativistic already during inflation and thus can be treated as non-relativistic at all times following inflation.

In principle, Eq. (4.22) involves the sum over all excitations of the spin-s field σ. However, the dominant excitation of a spin-s field near the Higuchi bound is $\sigma^0_{s,s}$. This can be seen qualitatively from Eqs. (4.8) and (4.13). Eq. (4.8) will have a maximum value at $\lambda = 0$ and all other modes with $\lambda > 0$ will be suppressed in comparison. It can then be seen from Eq. (4.13) that the dominant contribution will be the $n = s$ state, due to the contribution from $B_{m,n}$. Curiously, this is the same mode which is considered in the 'cosmological collider physics' program [142, 21, 22], leading to the characteristic Legendre polynomial angular dependence of 3-point functions [142, 24, 152].

Given the subdominance of all other modes, we approximate the full density as that which comes from $\sigma^0_{s,s}$. We use the recursion relation Eq. (4.13) to explicitly numerically calculate the mode functions, $\sigma^0_{n,s}$. We then calculate the density of excitations at the end of inflation using

$$\rho_{\sigma^0_{s,s}}(t_i) = m^2 \frac{(2s-1)!!}{s!} \int_0^{a\mu_* H} \mathrm{d}^3k\, a^{-2s} |\sigma^0_{s,s}|^2, \tag{4.25}$$

where t_i denotes the end of inflation, and μ_* is given by Eq. (4.24). The factorial prefactors come from evaluating the contraction of $\lambda = 0$, $n = s$, polarization vectors.

The integral is again dominated by the contribution from the upper bound, and in the numerics that follow we make use of this approximation. Further, since $\mu_* \gtrsim s > 1$, by the Higuchi bound, the DM density is dominated by particles that are still sub-horizon at the end of inflation ($k/a < H$) and those which re-enter the horizon immediately following inflation $k/a \sim H$. Since m/H is greater than 1 for all subsequent times, we can approximate these particles as non-relativistic for all times post-inflation. From this we define the present DM

density as,

$$\rho_{\text{today}} = \frac{\rho_{\text{inflation}}}{a(t_i)^3}, \tag{4.26}$$

where $\rho_{\text{inflation}}$ is defined by the integral Eq. (4.25), and $a(t_i)$ is the scale factor of the universe at the end of inflation (we normalize $a = 1$ today).

The acceptable parameter space for our HSDM model will be that for which the relic density Eq. (4.26) matches the observed dark matter abundance. The observed dark matter density is given by $\rho_{\text{DM0}} = 3m_{pl}^2 H_0^2 \Omega_{\text{CDM}}$ where Ω_{CDM} is the abundance observed to be $\Omega_{\text{CDM}} h^2 \simeq 0.12$ [209], and $H_0 \equiv 100h\,\text{km/s/Mpc} = 2.13h \times 10^{-33}\text{eV}$ with $h \simeq 0.7$. From this we find ρ_{DM0} evaluates to $\rho_{\text{DM0}} = 3.95 \times 10^{-11}\text{eV}^4$. Meanwhile, the redshift factor in Eq. (4.26) can be simplified by expand $a(t_i)$ as a ratio of redshifts,

$$a(t_i) = \frac{1 + z_{eq}}{1 + z_i} \frac{1}{1 + z_{eq}}, \tag{4.27}$$

where eq refers to matter-radiation equality. We have $z_{eq} \simeq 3400$ and $(1+z) \propto T$ for $z \gtrsim z_{eq}$. Taking $T_{eq} \simeq 0.8\text{eV} \simeq 1\text{eV}$ and instant reheating $T_{re} \simeq (g_*\pi^2/30)^{-1/4}\sqrt{Hm_{pl}}$, with $g_* \sim 100$, the above becomes $a(t_i) = 1.43 \times 10^{-18}\sqrt{\frac{\text{eV}}{H}}$.

Putting things together, we find that the DM density after inflation must satisfy,

$$\rho(t_i) = 1.17 \times 10^{37} \left(\frac{H}{\text{eV}}\right)^{3/2} \text{eV}^4, \tag{4.28}$$

with $\rho(t_i)$ given by Eq. (4.25).

To gain intuition as to the range of masses that can provide the correct relic density, we note the peculiar case of the complementary series, which occupies a narrow range of masses just above the Higuchi bound. At the saturation limit of the Higuchi bound, we approach partial masslessness and states become gauge redundancies [94]. To avoid this we deform away from the Higuchi bound by a small amount 2δ and consider $m^2/H^2 = s(s-1) + 2\delta$. In this limit, μ_s, Eq. (4.9), becomes

$$\mu_s \to \frac{i}{2}(1 - 4\delta)\,. \tag{4.29}$$

One can appreciate from the above that μ_s is purely *imaginary*. This is a feature of the complementary series Eq. (4.2), which corresponds to $0 < \delta < 1/4$. It follows that the exponential suppression, which one might anticipate for excitations of a heavy field, and is encoded in Eq. (4.10), becomes a phase factor – i.e., is not a suppression at all.

In Fig. 4.1 we illustrate the values of s and H for which the correct relic density of particles is produced. By varying the mass, points in the colored regions can achieve the correct relic density. The colors pink and blue denote masses in the complementary series and principle series respectively.

The lower and upper dashed lines of Fig. 4.1 denote the lower edge of the complementary series (the Higuchi bound) and upper edge of the complementary series. The parameter space below the lower edge is ruled out: the DM particle mass cannot be lower than the Higuchi bound, and decreasing H while leaving m/H fixed will lead to an underproduction of DM during inflation. The upper bound of this band represents the upper limit on particles with masses in the complementary series. If m/H and s remain fixed, increasing H will lead to an overproduction of the DM. A simple way out is to increase m/H, leaving the complementary series, and thereby generating an exponential suppression of the amount of DM, which is denoted by the light blue portion of Figure 4.1.

By considering masses slightly in the principal series we are able to obtain the correct relic density over the entire blue region of Fig. 4.1. This imposes a relation between m and H, at fixed values of s, as shown in Fig. 4.2. From left to right, fixed curves from $s = 2 - 8$, respectively show that for any spin, there is a continuous range of allowed H values with increasing mass. The allowed parameter space is bounded by the Planck mass, above which is forbidden and denoted by the grey shaded region. Although we have only explicitly shown up to $s = 8$, one can appreciate that there is a much larger space where solutions will be present, up to $m/H = 10^{18}$ and correspondingly increasing spin. This allows for a wide range of H and s values, which makes HSDM amenable to a variety of inflation models.

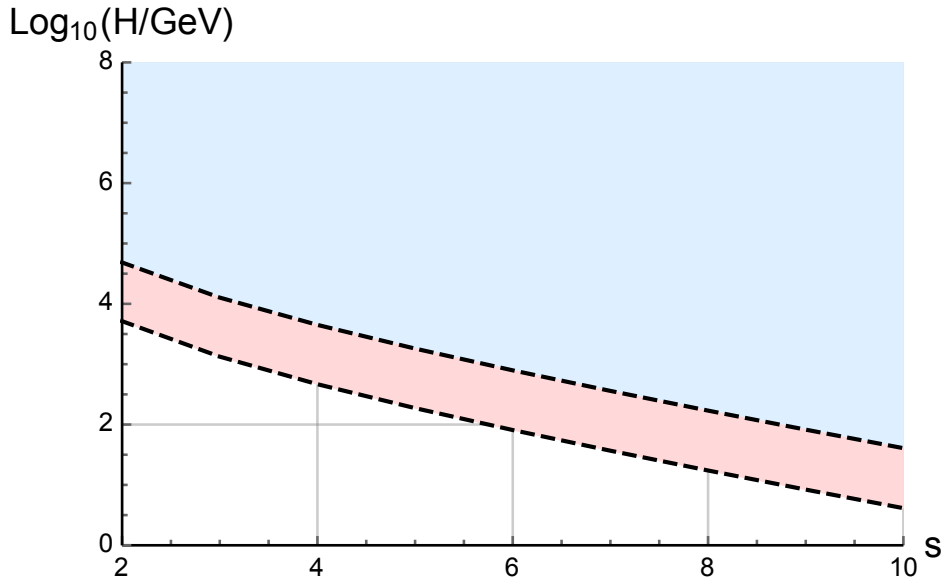

Figure 4.1: Regions of of $\{s, H\}$ values that give the observed density of higher spin dark matter, with mass in the complementary series (pink) or principal series (blue). The dashed lines denote the boundaries of the complementary series, i.e., assuming a mass that differs from the Higuchi bound by a fractional difference $\delta = 0.001$ and $\delta = 0.2499$ as the lower and upper bounds, respectively. The blue region extends up to Planck scale, $H = M_{\rm pl}$.

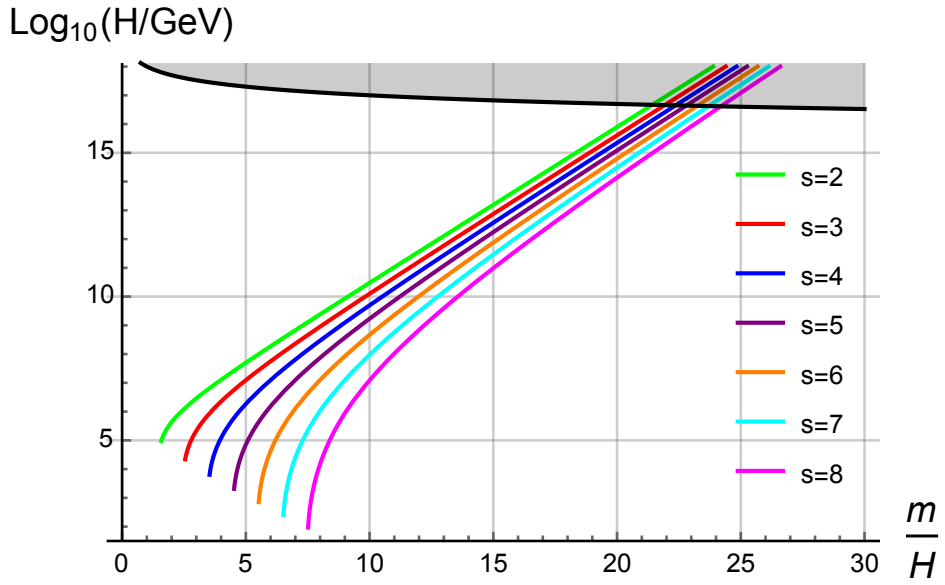

Figure 4.2: Sample parameter space for particles in the principal series. Lines of fixed s indicate allowable H values as a function of the HSDM mass. Each curve is truncated at the lower boundary of the principal series, i.e., the top dashed line of Fig. 4.1. The black curve corresponds to masses m equal to the Planck mass, $m = M_{\rm pl}$, and the grey region is super-Planckian masses $m > M_{\rm pl}$.

4.4 Directional Direct Detection

Direct detection is a prominent detection strategy for dark matter. In this approach, one hopes to observe nuclear recoil events generated by scattering of incoming dark matter particles. As realized early on [210], a signature prediction of the motion of the earth through the enveloping dark matter halo is a preferred direction of nuclear recoil events, suggesting an approach known as *directional direct detection* [211]. More recently, it has been demonstrated [212, 213, 214] that the angular dependence of the directional direct detection signal can distinguish between spin-0, and spin-1/2, and spin-1 dark matter. It is logical, therefore, to consider the directional direct detection signature of higher spin dark matter.

Any such direct detection signal is premised upon an interaction of dark matter with the standard model. As discussed in Sec. 6.2, while higher spin interactions are naively strongly constrained, this is relaxed for massive higher spins. The interactions of massive higher spin fields can be understood as a low energy effective field theory, with a UV completion given by string theory. The possible interactions have been studied in detail and enumerated in e.g. [174, 178, 175, 179].

We will consider a simple interaction between a higher spin boson and a standard model nucleus, eg., Xenon, that we model as a Dirac fermion. We construct an interaction through a derivative coupling of the higher spin boson to the fermion vector current. We consider the low energy effective interaction Lagrangian,

$$\mathcal{L}_{int} = \frac{g_s}{\Lambda^s}\partial_{\mu_1\ldots\mu_s}(\bar{\psi}\gamma^\mu\psi)\sigma_\mu^{\mu_1\ldots\mu_s} + \text{h.c.}, \tag{4.30}$$

where Λ is a UV scale that corresponds to the cutoff of the massive higher spin theory, and g_s is a coupling constant. Note that here σ refers to a spin-$(s+1)$ field, rather than spin-s. We compute the nuclear recoil scattering cross section in App. 4.A. We obtain,

$$\frac{d\sigma}{dE_r} \simeq \frac{m^3}{\pi v^2}\frac{1}{(2s+1)} \qquad \frac{g_s^4}{\Lambda^{4s}}\Big[p'^s P_s(\hat{k}'\cdot\hat{p}') + k^s P_s(\hat{k}'\cdot\hat{k})\Big]^2$$

$$\cdot\Big[p^s P_s(\hat{k}\cdot\hat{p})\Big]^2 \cdot \frac{32k^2}{(p\cdot k)^2}, \tag{4.31}$$

where p and p' and k and k' refer to the ingoing and outgoing momenta of the SM nucleus and DM, respectively, v is the relative velocity of the incoming DM particle, and P_s are the Legendre polynomials. The details of the computation of the cross section can be found in App. 4.A.

The quantity relevant to direct directional detection is the double differential rate of nuclear recoil events [212, 213]. This is given in standard notation by

$$\frac{d^2R}{dE_R d\Omega} = \kappa_{\rm DM}\int d^3\mathbf{v}\delta(\mathbf{v}\cdot\mathbf{w}-w_q)f(\mathbf{v}+v_\oplus(t))v^2\frac{d\sigma}{dE_R}. \tag{4.32}$$

Here, v is the relative velocity of the incoming DM particle relative to the target nucleus, $\kappa_{\rm DM}$ is related to the local halo density of DM near the earth ($\rho_{\rm DM}\simeq 0.3$ GeV/cm^3), f is the velocity distribution of DM in the galactic halo, which is dependent on $\mathbf{v}$ as well as $v_\oplus$, the time dependent Earth velocity in the galactic rest frame. We also define $\mathbf{w}$ as a unit vector pointing in the direction of nuclear recoil, $w_q = q/(2\mu)$. We will follow the methods in [213], outlined below, to obtain an expression for our particular case.

Following [213], we assume a Maxwell-Boltzmann velocity distribution $f(v)$, truncated at the galactic escape velocity, which we take to be $v_{esc} = 544$ km/s. The most probable speed is $v_0 = 220$ km/s, which is the circular speed of the local standard of rest. This can be written as

$$f(\vec{v}) = \frac{1}{N}e^{-(\vec{v}+\vec{v}_e^2)/v_0^2}, \tag{4.33}$$

where

$$|\vec{v}+\vec{v}_e| \le v_{esc}. \tag{4.34}$$

Here $\vec{v}_e$ is the Earth velocity in the galactic rest frame, which is generally a function of time, but for simplicity can be taken to be its constant magnitude, $\vec{v}_e = 232$ km/s. The overall

normalization N is a constant given by

$$N = \pi v_0^2 \left[\sqrt{\pi} v_0 \, \mathrm{erf}\left(\frac{v_{esc}}{v_0} \right) - 2 v_{esc} e^{-v_{esc}^2/v_0^2} \right]. \tag{4.35}$$

We can then break up the velocity integral into two parts:

$$\begin{aligned} \int \mathrm{d}^3 v = & \int_{v_{min}}^{v_{esc}-v_e} \mathrm{d}v v^2 \int_{-1}^{1} \mathrm{d}\cos\theta \int_0^{2\pi} \mathrm{d}\phi \\ + & \int_{v_{esc}-v_e}^{v_{esc}+v_e} \mathrm{d}v v^2 \int_{-1}^{\frac{v_{esc}^2 - v^2 - v_e^2}{2 v v_e}} \mathrm{d}\cos\theta \int_0^{2\pi} \mathrm{d}\phi. \end{aligned} \tag{4.36}$$

For simplicity here we focus on the first term; the resulting spin and angular dependence is the same in both cases. We make use of the identity,

$$\delta\left(\vec{v} \cdot \hat{q} - \frac{q}{2\mu} \right) = \frac{\delta(v - \bar{v})}{|\hat{v} \cdot \hat{q}|}, \tag{4.37}$$

where

$$\bar{v} = \frac{q}{2\mu(\hat{v} \cdot \hat{q})}, \tag{4.38}$$

where $\hat{v}$ is a unit vector in the direction of the incoming dark matter velocity, $\hat{q}$ is a unit vector in the recoil direction, and μ is the reduced mass of nucleon-DM system, $\mu = \frac{m_N m_{\mathrm{DM}}}{m_N + m_{\mathrm{DM}}}$. Then, performing the integral over the Dirac delta function we obtain,

$$\begin{aligned} \frac{d^2 R}{dE_R d\Omega} = & \quad \frac{\rho_{\mathrm{DM}}}{2N\pi m m_N} \int_{-1}^{1} \mathrm{d}\cos\theta \int_0^{2\pi} \mathrm{d}\phi \frac{\bar{v}^4}{|\hat{v} \cdot \hat{q}|} e^{-(\bar{v}+v_e)^2/v_0^2} \\ & \cdot \frac{d\sigma}{dE_R}(\bar{v}) \Theta(\bar{v} - v_{min}) \Theta((v_{esc} - v_e) - \bar{v}), \end{aligned} \tag{4.39}$$

where we have taken the dark matter mass to be m. Now let us define the angles α, β, θ, and ϕ, such that

$$\hat{q} = (\sin\alpha\cos\beta, \sin\alpha\sin\beta, \cos\alpha), \tag{4.40}$$

$$\hat{v} = (\sin\theta\cos\phi, \sin\theta\sin\phi, \cos\theta) \tag{4.41}$$

and

$$\hat{v}' = \frac{v}{v'}\hat{v} + \frac{q}{mv'}\hat{q}, \tag{4.42}$$

where $\hat{v}$ is the direction of the incoming DM particle, $\hat{q}$ is the direction of nuclear recoil, $\hat{v}'$ is the direction of the outgoing HS DM particle, and $\hat{p}$ is the unit vector in the direction of the incoming nucleus, which we will take to be in the $\hat{z}$ direction. One can deduce v' from conservation of momentum.

Substituting into Eq. (4.39) the cross section Eq. (4.31), we find the double differential recoil rate,

$$\begin{aligned}\frac{d^2R}{dE_R d\Omega} \simeq \frac{32\rho_{\rm DM} g_s^4 m_N^2}{2N(2s+1)\pi^2\Lambda^{4s}m}\int d\Omega' f_{\rm SI}(v) \\ \cdot\Big[q^s P_s(\hat{v}'\cdot\hat{q}) + m^s\bar{v}^s P_s(\hat{v}\cdot\hat{v}')\Big]^2 \cdot \Big[p^s P_s(\hat{p}\cdot\hat{v})\Big]^2,\end{aligned} \tag{4.43}$$

where $d\Omega'$ is the integration over incoming momenta, and $f_{\rm SI}(v)$ is the spin-independent contribution to the scattering rate, given by,

$$\begin{aligned}f_{\rm SI}(v) = \frac{\bar{v}^4}{|\hat{v}\cdot\hat{q}|(p\cdot\bar{v})^2}\cdot e^{-(\bar{v}^2+v_e^2+2\bar{v}v_e\cos\theta)/v_0^2} \\ \cdot\Theta(\bar{v}-v_{min})\Theta((v_{esc}-v_e)-\bar{v}).\end{aligned} \tag{4.44}$$

Finally, in the limit that the dark matter mass is larger than the momentum transfer, i.e., $m \gg q$, the term proportional to $m\bar{v}$ in the second line will be dominant over the first.

The final result is then given by,

$$\frac{d^2R}{dE_R d\Omega} = \frac{\mathcal{N}}{\Lambda^{4s}}\int d\Omega' f_{\rm SI}(v)\Big[m^s\bar{v}^s P_s(\hat{v}\cdot\hat{v}')\Big]^2\Big[p^s P_s(\hat{p}\cdot\hat{v})\Big]^2, \tag{4.45}$$

where the prefactor $\mathcal{N}$ is defined as,

$$\mathcal{N} = \frac{32\rho_{\rm DM} g_s^4 m_N^2}{2N(2s+1)\pi^2 m}. \tag{4.46}$$

Here, note the distinct dependence on the Legendre polynomials, P_s. The angular dependence in $f_{\rm SI}(v)$ is spin-independent and is present in conventional WIMP models.

The angular dependence on the Legendre polynomials, one the other hand, is a direct consequence of considering higher spins. This generalizes previous works (see e.g. [212, 213, 214, 215]) that considered the imprints of spin-0, 1/2, and 1 DM in the double differential recoil rate,leading to ring-like features. Our HSDM model modulates the bosonic signal further, with an added angular dependence on Legendre polynomials, P_s, due to scattering of a spin-$s+1$ boson.

This avenue for direct detection is complementary to work that has been done within the 'cosmological collider physics' program, which predicts that higher spin particles produced during inflation will leave behind a distinctive signature in the cosmic microwave background, proportional to Legendre polynomials [21, 24, 152]. An implication of our results is the potential for a dual 'smoking gun' signature and relationship between CMB experiments and dark matter direct detection experiments. We see that the angular dependence on Legendre polynomials in the CMB non-gaussianity is mirrored by the appearance of Legendre polynomials in the double differential recoil rate.

4.5 Other Observable Windows

Aside from direct detection, one might wonder what signature higher spin dark matter may leave at the other pillars of dark matter detection: collider production, and indirect detection (e.g., at the galactic center [216]). To this end, we consider the other possible interactions that could couple higher spin dark matter candidate to the Standard Model.

The simplest possibility is to directly couple a higher spin boson to the Standard Model Higgs boson. For example, an interaction of the form,

$$\mathcal{L}_{\sigma HH} = \frac{1}{\Lambda^{s-1}}\sigma^{(s)}\partial^{(s)}|H|^2, \tag{4.47}$$

where $\partial^{(s)}$ denotes s number of derivatives. From this interaction, a high energy Higgs boson, e.g. generated at a collider, could radiate a spin-s boson σ. At quadratic order in σ, one could have a $\sigma^2|H|^2$ interaction, allowing $2 \leftrightarrow 2$ scattering of the Higgs and HS boson.

The field content of the standard model is not restricted to bosons, and nor are higher spin field theories. Higher spin *fermions* are interesting in their own right, and may serve as their own dark matter candidate. Unfortunately, a relic density computation as has been done here is not readily repeated for fermions, since the exact solution of HS fermions in dS space is not known. Nonetheless, one may expect a higher spin fermon dark matter candidate to couple to the standard model fermions via 4-fermion interactions, e.g., of the form,

$$\mathcal{L}_{4f} = \frac{1}{\Lambda^2}\bar{\Psi}^{\mu_1\ldots\mu_s}\Psi_{\mu_1\ldots\mu_s}f\bar{f}, \tag{4.48}$$

where Ψ is a spin-$s+1/2$ fermion, and f is a standard model fermion. Such an interaction allows for signatures at precision electroweak experiments, and via annihilation of HS fermions into standard model fermions, a signature in the galactic center [216].

Finally, there is the possibility that the higher spin bosons and higher spin fermions could be organized into multiplets, that is, into *super*-multiplets of a supersymmetric theory of higher spin fields [155, 156, 157] (for recent work, see e.g. [166, 167, 168, 169, 171, 173, 174, 175, 176, 178, 179, 33, 180]). Supersymmetry constrains both the spectrum of the theory and the interactions, as discussed in a cosmological context in [152]. Even if supersymmetry is broken at a high scale, one would expect some remnant of this structure to remain at energies accessible by terrestrial experiments.

The cosmological collider analysis of higher spin supersymmetry [152] revealed correlated signals, with the usual $P_s(\cos\theta)$ angular dependence accompanied by superpartner contributions that scale as $P_{s+1}(\cos\theta)$ and $\sum_m P_s^m(\cos\theta)$. It will be interesting to compute the dual signal in directional direct detection.

4.6 Discussion

In this work we have considered gravitationally produced massive higher spin particles as a model of dark matter. We have shown that there is a wide range of parameter space for

superheavy particles with $s > 2$ for which the correct relic density of dark matter is produced. We have also explored a potential directional direct detection signature, showing that there is distinctive spin dependent angular dependence in the double differential recoil rate. This enters in the form of Legendre polynomials and is complementary to the 'cosmological collider' signature in the cosmic microwave background.

This opens up opportunities to explore a wide range of new models and parameter spaces to aid in the search for dark matter. We have mentioned several possibilities, but there is certainly much that is still unknown. In future work we will perform a more rigorous numerical exploration of our results in the context of directional direct detection, in order to show more explicitly the impact of the higher spin angular dependence in the double differential recoil rate. It would also be of interest to build a similar model for fermionic HSDM and build connections to HS supersymmetry. We leave these explorations and others to future work.

Comment added: During the final preparation of this manuscript on which this chapter is based we became aware of recent work [217] with thematic overlap to this paper. The effective field theory approach taken there is promising and may yield further directional direct detection signatures in addition to that considered here. There is no overlap in the content of the papers.

4.A Matrix Element Calculation

We here show technical details of the differential cross section used in Section 6.4. To calculate the differential cross section for a HSDM particle scattering off a SM fermion, there are several subtleties that must be considered. The vertex factor for scattering with $\sigma^0_{s,s}$ is given by

$$V = -i\frac{g_s}{\Lambda^s}\left[\sum_{n=0}^{s}\binom{s}{n}k_1^{i_1\ldots i_{s-n}}k_2^{i_n\ldots i_s}\right]\gamma^\mu, \tag{4.49}$$

where we have considered all possible combinations of derivatives on $\bar{\psi}\psi$, and k_1 and k_2 correspond to the momenta of the standard model nucleons. We assume that the incoming

nucleon is at rest, therefore the only terms that contributes to the vertex will be those which have either k_1^s or k_2^s. The helicity state of the higher spin particle is λ. Thus, this expression can be simplified as

$$V = -i\frac{g_s}{\Lambda^s}(k_{1_{i_1\ldots i_s}} + k_{2_{i_1\ldots i_s}})\gamma^\mu. \tag{4.50}$$

Each higher spin external leg carries a factor of the spin-s+1 polarization tensor $\epsilon_\mu^{[\lambda'']i_1\ldots i_s}(k_3)$. This can be decomposed into a spin-1 component and a spin-s component as follows:

$$\epsilon_\mu^{[\lambda'']i_1\ldots i_s}(k_3) = \epsilon_\mu^{[\lambda']}(k_3)\epsilon^{[\lambda]i_1\ldots i_s}(k_3), \tag{4.51}$$

where $\lambda' = -1, 0, 1$ and $\lambda = -s\ldots s$ are the possible helicity states of the spin-1 and spin-s components, respectively. Lastly, note that generally, working in an expanding background will lead to additional factors of the scale factor, $a(t)$. However, for the remainder of the calculation we normalize $a(t) = 1$, to account for the insensitivity of particle physics experiments today to the previous expansion of the universe. The matrix element can easily be found in analogy with standard QED computations, and with the use of the relation

$$\hat{q}_{i_1}\ldots\hat{q}_{i_s}\epsilon^\lambda_{i_1\ldots i_s} \equiv \mathcal{E}^\lambda_\lambda(\theta,\phi)P^\lambda_s(\cos\theta), \tag{4.52}$$

where $\cos\theta = \hat{\mathbf{q}}\cdot\hat{\mathbf{k}}$, $\cos\phi = \hat{\mathbf{q}}\cdot\epsilon$ and $\mathcal{E}^\lambda_\lambda$ and P^λ_s are the transverse and longitudinal parts of the spherical harmonics, respectively [24, 94], where for the $\lambda = 0$ modes we simply have $\hat{q}_{i_1}\ldots\hat{q}_{i_s}\epsilon^\lambda_{i_1\ldots i_s} = P_s(\cos\theta)$. Then, we find the matrix element to be

$$\begin{aligned}|\mathcal{M}|^2 = \frac{g_s^4}{\Lambda^{4s}}&\Big[p'^s P_s(\hat{k}'\cdot\hat{p}') + (p+k)^s P_s(\hat{k}'\cdot(\hat{p+k}))\Big]^2\\ &\cdot\Big[p^s P_s(\hat{k}\cdot\hat{p}) + (p+k)^s P_s(\hat{k}\cdot(\hat{p+k}))\Big]^2\\ &\cdot\frac{(2m)^2}{(2p\cdot k)^2}(16p^2 + 64p\cdot k + 32k^2),\end{aligned} \tag{4.53}$$

where k and k' refer to the incoming and outgoing HSDM particle, respectively,p and p' refer to the standard model nucleus, and we note $(\hat{p+k}) \equiv (\vec{p}+\vec{k})/|\vec{p}+\vec{k}|$. From the matrix

element, one can find the differential scattering cross section given by

$$\frac{d\sigma}{dE_R} = \frac{2m}{\pi v^2}\frac{1}{(2J+1)(2s_\chi+1)}|\mathcal{M}|^2. \tag{4.54}$$

We will simplify this by noting that in our construction, we assume that the standard model nucleus is stationary and the incoming HS particle has a much larger momentum, $k \gg p$. In this limit, we can also take $k' \cdot (p+k) = k' \cdot k$. Thus, keeping only the relevant dominant terms in k, we obtain for the cross section

$$\begin{aligned}\frac{d\sigma}{dE_R} \simeq \frac{m^3}{\pi v^2}\frac{1}{(2s+1)} \quad & \frac{g_s^4}{\Lambda^{4s}}\Big[p'^s P_s(\hat{k}'\cdot\hat{p}') + k^s P_s(\hat{k}'\cdot\hat{k})\Big]^2 \\ \cdot \quad & \Big[p^s P_s(\hat{k}\cdot\hat{p})\Big]^2 \cdot \frac{32k^2}{(p\cdot k)^2}.\end{aligned} \tag{4.55}$$

Part II

Gravitational Waves as a Probe of Modified Gravity

Chapter 5

Gravity Waves in Parity-Violating Copernican Universes

5.1 Introduction

In this section, we move to the late universe and begin by exploring the propagation of gravitational waves in modified theories of gravity. We begin with such a theory with a dynamical cosmological constant, Λ. The cosmological constant, Λ, and the Copernican principle are two cornerstones of modern cosmology. In this paper we explore the implications of the fact that their story may be more intricate than it is usually assumed. That the cosmological "constant" does not actually need to be constant in theories with torsion has been noted, for example, in [218, 219]. It is not new that torsion can change dramatically the perspective of many problems (for a selection of examples see [220, 221, 222, 223, 224, 225, 226, 227, 228, 229, 230, 231]). It has also been noted [222, 232] that under the shadow of torsion, homogeneity and isotropy do not imply parity invariance. The Copernican principle therefore has a choice between incorporating parity invariance or not. Parity odd solutions in homogeneous and isotropic models employ a geometrical structure which has been known since the inception of General Relativity: Cartan's spiral staircase [222, 233]. Thus, a varying Lambda may go hand in hand with parity violating Copernican models, creating an

interesting synergy.

Within the theories considered in [218, 232] the inverse of Lambda becomes canonically conjugate to the Chern-Simons invariant[1] [237, 238]. The radical implications of this fact in quantum cosmology were examined in [238] (see [239, 240] for the background problem). In the context of classical solutions, the dynamics are then ruled by two topological invariants, of which the Chern-Simons functional is the density. Depending on whether one considers the real or imaginary parts of the Chern-Simons term, these are the Pontryagin and the Euler (or Gauss-Bonnet) invariants. Since these terms appear in the action multiplied by Λ^{-1}, they are only topological invariants if Λ is a constant. The variability of Lambda disrupts their topological nature, and so they are *quasi*-topological terms (to use the terminology of [218]).

The theories considered in [218, 219, 232] have the virtue that they do not add new parameters to gravity with respect to Einstein's theory with a cosmological constant. The coefficient of the Euler term is fully fixed by the Bianchi identities (from solutions without matter), so that the only true new parameter is the numerical coefficient of the Pontryagin term, should we consider it. However, for these theories Λ is longer a free parameter, as it is in Einstein's theory. Hence, a theory with the Euler term alone would have *fewer* free parameters than General Relativity, as argued in [218]. As explained in [219] such a theory conflicts dramatically with basic Hot Big Bang cosmology (it refuses to accept a radiation epoch). The introduction of the Pontryagin term allows for a viable expansion history (as studied in [232]), leaving the working theory with the *same* number of free parameters as General Relativity.

It was found in [232] that the parity-even and parity-odd Copernican solutions belong to separate branches of the dynamics. Indeed, a Hamiltonian analysis revealed a different structure of constraints and consequently a different number of degrees of freedom. We are therefore talking about different phases of the same non-perturbative theory. The underlying gauge symmetry associated with the new constraint of the theory is a form of conformal invariance (generalized for theories with torsion). Lambda appears to be pure gauge with

[1] Models where Λ is directly conjugate to the Chern-Simons invariant (or similar quantities) have been considered within the context of unimodular gravity [234, 235, 236].

regards to this symmetry in the parity-even branch (in the absence of matter). The parity-odd branch breaks conformal invariance even in the absence of matter, giving a varying Lambda a physical meaning. Non-conformal matter does the same in the parity-even branch, but then Lambda becomes a slave to matter (much in the spirit of [241]). It is interesting to note that the (odd parity) Pontryagin term is only relevant for the homogeneous and isotropic dynamics in the parity-odd branch of the solutions.

A preliminary investigation [232] revealed that phenomenology in these theories (which, we stress, often have *fewer* free parameters than General Relativity, and rarely can be made to have more) shows a preference for the parity-odd branch in the presence of Pontryagin dynamics. These considerations concerned only the background solution, which is already very rich in the parity-odd branch. The next obvious step is to investigate the propagation of gravitational waves in the same branch. Such is the purpose of the current investigation.

The plan of this chapter is as follows. In Section 5.2 we start by reviewing previous results that will be needed in this paper, translating them into the notation we found most useful for establishing a perturbation calculation. In Section 5.3 we set up the tensor perturbation variables and work out the linearized equations in various forms (tetrad index and space-time index forms, and then decomposed in Fourier and helicity modes). The equations in general look ominous: we have to contend with first order equations in three variables – metric, and parity even and odd components of the connection – but in subsection 5.3 we condense them in a more aesthetically pleasing form, and lay out a strategy for their solution.

The rest of the chapter is spent on working out solutions for various parameter settings. In Section 5.4 we briefly discuss general properties of the perturbed equations. Next we discuss a number of limiting cases of interest. As a sanity check we find the General Relativity limit in Section 5.5, with reassuring results. In Section 5.6 we consider the case where the dynamics are ruled purely by an Euler pseudo-topological term. We unveil our first surprise: the tensor mode perturbation is left entirely undetermined by the equations of motion. This could well signify that they have become a gauge degree of freedom in this case.

The introduction of the Pontryagin term changes the picture. Physical propagating tensor

modes now do exist, but they are endowed with chiral modified dispersion relations. We concentrate on two limiting forms - in Section 5.7 the propagation of gravitational waves in the late universe is discussed, whilst in Section 5.8 their propagation at earlier stages when the evolution is dominated by matter and radiation components is discussed. Finally in Section 5.9 we summarize our results and discuss prospects for further development.

5.2 Review of previous results

Here we shall review some results, adapting the notation in previous literature to the notation that shall be more useful in this chapter. Specifically, we shall use the following conventions for indices:

- A, B, C, D: $SO(1,3)$ gauge indices.
- I, J, K, L: $SO(3)$ gauge indices.
- μ, ν, α, β: spacetime coordinate indices.
- t: time coordinate index.
- $i, j, k, l,$: spatial coordinate indices.

5.2.1 The full theory and its equations

The theories we analyze can be written as:

$$S^g[e,\omega,\Lambda] = -\int \frac{3}{2\Lambda}\left(\epsilon_{ABCD} + \frac{2}{\gamma}\eta_{AC}\eta_{BD}\right)\left(R^{AB} - \frac{\Lambda}{3}e^A e^B\right)\left(R^{CD} - \frac{\Lambda}{3}e^C e^D\right) - \frac{2}{\gamma}\int T^A T_A. \tag{5.1}$$

where $R^{AB} \equiv d\omega^{AB} + \omega^A{}_C \omega^{CB}$, $T^A \equiv de^A + \omega^A{}_B e^B$ and unless otherwise stated, multiplication of differential forms is via the wedge product [2].The action can be rewritten as proportional

[2]If the parameter $\gamma \to \infty$ and Λ is constrained to be a constant, the resulting theory is the Einstein-Cartan theory alongside an Euler boundary term; the particular coefficient of this boundary term has been found to be associated with interesting properties of Noether charges in gravity [242, 243]

to four terms $S^g = S_{Pal} + S_{Eul} + S_{NY} + S_{Pont}$, with

$$\begin{aligned} S_{Pal} &= \int \epsilon_{ABCD}\left(e^A e^B R^{CD} - \frac{\Lambda}{6} e^A e^B e^C e^D\right), && (5.2)\\ S_{Eul} &= -\frac{3}{2}\int \frac{1}{\Lambda}\epsilon_{ABCD} R^{AB} R^{CD}, && (5.3)\\ S_{NY} &= \frac{2}{\gamma}\int e^A e^B R_{AB} - T^A T_A, && (5.4)\\ S_{Pont} &= -\frac{3}{\gamma}\int \frac{1}{\Lambda} R^{AB} R_{AB}. && (5.5) \end{aligned}$$

The first term is the Palatini action, though differs from that of the Einstein-Cartan theory in that we allow Λ vary as a dynamical field rather than fixing it to be a constant. The second term is the quasi-Euler term of [218]. The third term is the Nieh-Yan topological invariant (replacing the Holst term should there be torsion). The last term is the quasi-Pontryagin term studied in [232]. We stress that the connection proposed here between γ and the pre-factor of the quasi-Pontryagin term can be broken, and is not strictly needed. More generally, we could also look at theories with arbitrary numerical factors in front of the quasi-Euler and quasi-Pontryagin terms.

As usual, matter can be added to the gravitational action, to yield a total action:

$$S = \frac{1}{2\kappa} S^g(e, \omega, \Lambda) + S_M(\Phi, e, \omega, \Lambda), \tag{5.6}$$

where Φ denote matter fields. The full gravitational equations of motion of this theory are then:

$$\begin{aligned} \epsilon_{ABCD}\left(e^B R^{CD} - \frac{1}{3}\Lambda e^B e^C e^D\right) &= -2\kappa\tau_A && (5.7)\\ T^{[A} e^{B]} + \frac{3}{2\Lambda^2} d\Lambda R^{AB} - \frac{3}{4\gamma\Lambda^2}\epsilon^{ABCD} d\Lambda R_{CD} &= \kappa \mathcal{S}^{AB} && (5.8)\\ \epsilon_{ABCD}\left(R^{AB} R^{CD} - \frac{1}{9}\Lambda^2 e^A e^B e^C e^D\right) + \frac{2}{\gamma} R^{AB} R_{AB} &= -2\kappa\mathcal{J} && (5.9) \end{aligned}$$

where $\kappa \equiv 8\pi G$ and we have defined energy momentum 3-form $\tau_A = \frac{1}{2}\frac{\delta S_M}{\delta e^A}$, the spin-current 3-form $\mathcal{S}^{AB} \equiv -(1/2)\epsilon^{ABCD}\delta S_M/\delta\omega^{CD}$ and the Λ-source 4-form $\mathcal{J} \equiv (2/3)\delta S/\delta\Lambda$. They are

obtained by varying (5.1) together with the action for matter with respect to e, ω and Λ, respectively. A key property of these models is that Einstein's equation (5.7) takes the same form in the Einstein-Cartan formulation of gravity (where $\Lambda = cst.$). Any dynamics for Λ will arise from the gravitational field ω^{AB} rather than via the addition of explicit kinetic terms for Λ in the Lagrangian.

In this chapter we will confine ourselves to situations where the quantities $\mathcal{S}^{AB}$ and $\mathcal{J}$ both are negligible. For standard 'minimal' coupling between fermions and the spin connection, the quantity $\mathcal{S}^{AB}$ is sourced by the axial spinor current; much of our focus will be on the behaviour of certain cosmological perturbations in 'recent' post-recombination cosmological history where this quantity is expected to be negligible [220]. The assumption that $\mathcal{J}$ is negligible must be regarded as a simplifying assumption and more detailed analysis is needed to determine its expected coupling to matter. For the particular cosmological consequences of the theory examined here, it will suffice to that the matter content is describable in terms of perfect fluids. By way of example, a perfect fluid with density ρ, pressure p and four-velocity $U^{\mu} = e^{\mu}_{A}U^{A}$ will have stress-energy 3-form:

$$\tau^{A} = -\frac{1}{6}(\rho + p)U^{A}\epsilon_{BCDE}U^{B}e^{C}e^{D}e^{E} - \frac{1}{6}p\epsilon^{A}{}_{BCD}e^{B}e^{C}e^{D} \tag{5.10}$$

5.2.2 The background solution

We now look at the behaviour of the theory in situations where spacetime has Friedmann-Robertson-Walker (FRW) symmetry. This symmetry is widely considered to well approximate the geometry of the universe on large scales and there exist strong constraints on the evolution of the universe within this framework. We will henceforth refer to possible solutions with this symmetry as 'background' solutions as later we will consider the behaviour of small perturbations around them. It is important then to demonstrate that the combined action (5.6) yields solutions that are consistent with these constraints.

We shall denote all background quantities by a bar over the respective variable. For

simplicity we assume that the background spatial curvature is zero, so that we can use Cartesian coordinates with

$$\bar{e}^0 = N(t)dt \tag{5.11}$$

$$\bar{e}^I = a(t)\delta^I_i dx^i \tag{5.12}$$

where $N(t)$ is the lapse function ($N = 1$ for proper time) and $a(t)$ is the expansion factor. Note that $\bar{e}^I_i = a\delta^I_i$ and $\bar{e}^i_I = a^{-1}\delta^i_I$. Then, the spin connection will be given by:

$$\bar{\omega}^{0I} = g(t)a(t)\delta^I_i dx^i \tag{5.13}$$

$$\bar{\omega}^{IJ} = -P(t)a(t)\epsilon^{IJ}{}_K\delta^K_k dx^k \tag{5.14}$$

where g and P are its parity even and odd components, respectively. A connection of the form (5.14) was considered by Cartan as an extension to Riemannian geometry, with parallel transport according to this connection yielding a rotation of vectors with a 'handedness' dictated by the sign of P. This effect has been termed Cartan's spiral staircase and we will see that all parity violating effects in this gravitational model appear only when $P \neq 0$. The torsion associated with (5.13) and (5.14) is given by:

$$\bar{T}^0 = 0 \tag{5.15}$$

$$\bar{T}^I = T\bar{e}^I\bar{e}^0 + P\epsilon^{IJK}\bar{e}_J\bar{e}_K \tag{5.16}$$

with the parity even component T related to g by:

$$T = \left(g - \frac{1}{N}\frac{\dot{a}}{a}\right). \tag{5.17}$$

The field strength is:

$$\bar{R}^{0I} = \frac{1}{N}\left(\dot{g} + \frac{\dot{a}}{a}g\right)\bar{e}^0\bar{e}^I + gP\epsilon^{IJK}\bar{e}_J\bar{e}_K \tag{5.18}$$

$$\bar{R}^{IJ} = \frac{1}{N}\left(\dot{P} + P\frac{\dot{a}}{a}\right)\epsilon^{IJ}{}_{K}\bar{e}^{K}\bar{e}^{0} + \left(g^2 - P^2\right)\bar{e}^{I}\bar{e}^{J}. \tag{5.19}$$

It can be shown that with this "Copernican" ansatz, equations (5.7) to (5.9) become:

$$g^2 - P^2 = \frac{\Lambda + \kappa\rho}{3} \tag{5.20}$$

$$\frac{(ag)^{\cdot}}{a} = \frac{\Lambda}{3} - \frac{\kappa}{6}(\rho + 3p) \tag{5.21}$$

$$T = \frac{\dot{\Lambda}}{2\Lambda^2}\left(\Lambda + \kappa\rho - \frac{6}{\gamma}gP\right) \tag{5.22}$$

$$P = \frac{3\dot{\Lambda}}{\Lambda^2}\left(gP + \frac{\Lambda + \kappa\rho}{6\gamma}\right) \tag{5.23}$$

$$\begin{aligned}(\Lambda + \kappa\rho)\left(\Lambda - \frac{\kappa}{2}(\rho + 3p)\right) - \Lambda^2 &= 18gP\frac{(aP)^{\cdot}}{a} \\ &+ \frac{9}{\gamma}\left(\frac{\Lambda + \kappa\rho}{3}\frac{(aP)^{\cdot}}{a} + \frac{2}{3}\left(\Lambda - \kappa\frac{\rho + 3p}{2}\right)gP\right)\end{aligned} \tag{5.24}$$

As shown in Appendix 5.A, this system can be cast in the form of a first-order system of evolution equations for $\{a, g, \Lambda, P\}$ plus a constraint (the Hamiltonian constraint/Friedmann's equation). Reference to these background equations will be made at several points in this paper, to simplify the perturbation equations.

5.2.3 Background evolution

We now discuss solutions to equations (5.20)-(5.24) with an emphasis on solutions that appear likely to be most consistent with the observed expansion history of the universe. Care must be taken here as many probes of background quantities are additionally sensitive to details of cosmological perturbations. For example, the position of the first peak of temperature anisotropies in the cosmic microwave background (CMB) is sensitive to both the distance to last scattering (a background quantity) and the sound horizon at last scattering (a quantity which additionally depends on the form of equations describing cosmological perturbations) [244].

The system of equations (5.20)-(5.24) is rather complicated and must be solved numerically. However, relevant approximate solutions do exist, which we will now discuss.

Early times

There is strong evidence that the universe has undergone an early period ('the radiation era') where relativistic species (such as photons and relativistic neutrinos) dominate the evolution of the universe for a time before the universe cools down enough such that the gravitational effect of near-pressureless/dustlike matter (baryons and dark matter) dominates ('the matter era'), before eventually a new source of energy - typically termed dark energy - begins to dominate and cause the expansion of the universe to accelerate [245]. We will look to see whether the theory (5.6) permits this kind of cosmological history, whilst ascribing the recent cosmological acceleration to - now dynamical - Λ. An important part of this is that the gravitational effect of new degrees of freedom quantities such as Λ and the torsion P do not contradict the above picture.

It can be shown that when $|\gamma| \ll 1$, to first order in γ there exists a solution for the field P in the limit $\Lambda \to 0$

$$P = P_{(\rho)} = \frac{\gamma}{3}\sqrt{\frac{\kappa\rho}{3}} \tag{5.25}$$

We see then that when this solution holds, the torsion field P is proportional to γ and so a smaller value of γ suppresses torsion in the cosmological background. Neglecting the contribution of Λ is expected to be a good approximation in the earlier universe where the 'dark energy' is a sub-dominant contributor to the universe's expansion. When (5.25) holds it may be shown that the Friedmann equation can be recovered in approximation:

$$3\left(\frac{\dot{a}}{a}\right)^2 = \left(1 - \frac{\gamma^2}{9}\right)\kappa\rho + \mathcal{O}(\gamma^3) \tag{5.26}$$

where we have adopted the $N = 1$ spacetime gauge. Hence the solution (5.25) acts to rescale the bare Newton's constant G during times when the effect of Λ is negligible. The degree to which this effect is observable depends on how the value of Newton's constant G_N measured

in tabletop experiments is related to G. If $G \neq G_N$, then the rate of expansion $\dot{a}/a$ due to a given ρ will be different from as is the case in General Relativity and so in principle γ could be constrained by probes of the expansion rate during big bang nucleosynthesis [246].

However, importantly, the solution (5.25) is not stable. By way of illustration, we may consider the evolution of small, homogeneous perturbations $P = P_{(\rho)}(1 + \delta_P(t))$. It can be shown that deep in the radiation era where $\kappa\rho/3 \sim H_0^2\Omega_r/a^4$ - where H_0 is the Hubble constant today - that

$$P_{(\rho)} = \frac{\gamma}{3a^2} H_0 \sqrt{\Omega_r} \tag{5.27}$$

$$\delta_P = \mathcal{C}a^3 \tag{5.28}$$

Therefore δ_P grows as a increases. By way of example, if $\delta_P \ll 1$ at $a \sim 10^{-15}$ then for it to remain smaller than unity at $a \sim 10^{-5}$ we must have $\delta_P(a = 10^{-15}) < 10^{-30}$. This indicates that significant fine-tuning of initial data is required for the spiral staircase field P to find itself following the solution (5.25).

If P deviates considerably from the tracking solution, the tendency is for P to evolve to dominate the evolution of the universe. In this case it may be shown that $P = P_0/a$ where P_0 is a constant and $a \sim (1+\gamma)(t-t_0)$ - here the evolution of the universe due to P resembles a General-Relativistic empty universe with negative spatial curvature. It is hard to see how such a universe could be consistent with experiment. This is the case even if P is initially negligible. Therefore, the phenomenological viability of the model rests on P being able to initially find itself sufficiently close to the form (5.25) to avoid dominating the evolution of the universe.

Late times

During late time cosmological evolution for realistic cosmologies we expect that universe to begin accelerating and we look to ascribe this to Λ and P beginning to dominate cosmic

evolution. Again assuming $|\gamma| \ll 1$ and now assuming $P^2 \ll \Lambda$ and taking the limit $\rho \to 0$ we have the following evolution equations for Λ and P:

$$\frac{dP}{d\ln a} = -3P, \quad \frac{d\Lambda}{d\ln a} = 2\sqrt{3}\gamma P\sqrt{\Lambda} \tag{5.29}$$

which possess solutions

$$P = \frac{P_i}{a^3} \tag{5.30}$$

$$\Lambda = \Lambda_0 - \frac{2\gamma}{\sqrt{3}a^3}P_i\sqrt{\Lambda_0} \tag{5.31}$$

So, asymptotically for large a, $\Lambda \to \Lambda_0$ and $P \to 0$, leading to a confluence with the current standard cosmological picture of the late-time universe's evolution being dominated by a cosmological constant of magnitude Λ_0. The contribution of P to the Hamiltonian constraint goes as $\sim P^2$ so we see that in this regime P evolves like a shear component, its energy density diluting as a^{-6}. For realistic cosmologies a typical value for P_i will be given by its value when Λ begins to dominate the evolution of the universe at a scale factor $a \sim a_i$ following a period of matter domination during which $P \sim (\gamma/3)H_0 a_i^{-3/2}$ (from the solution (5.25)). We expect then $P_i \sim (\gamma/3)H_0 a_i^{3/2}$. This has important implications: if phenomenologically viable cosmologies involve P staying on the tracking solution (5.25) for an appreciable amount of time, this means that fixing γ fixes the size of P during matter domination, and the size of P_i as the cosmological constant begins to dominate.

We now discuss the evolution of Λ. It can be seen from (5.25) that the tracking solution can exist if $\mathrm{sign}(P) = \mathrm{sign}(\gamma)$. Recall that the Λ equation of motion is $\dot{\Lambda} = 2\gamma\Lambda^2 P/(6\gamma g P + \Lambda + \kappa\rho)$ and therefore in the earlier universe if $\kappa\rho$ is initially greater than Λ it will tend to suppress time variation of Λ. Furthermore, we will have $\dot{\Lambda} > 0$ throughout, meaning that Λ must be of smaller magnitude in the past than today. A typical evolution of Λ and P are shown in Figure 5.1.

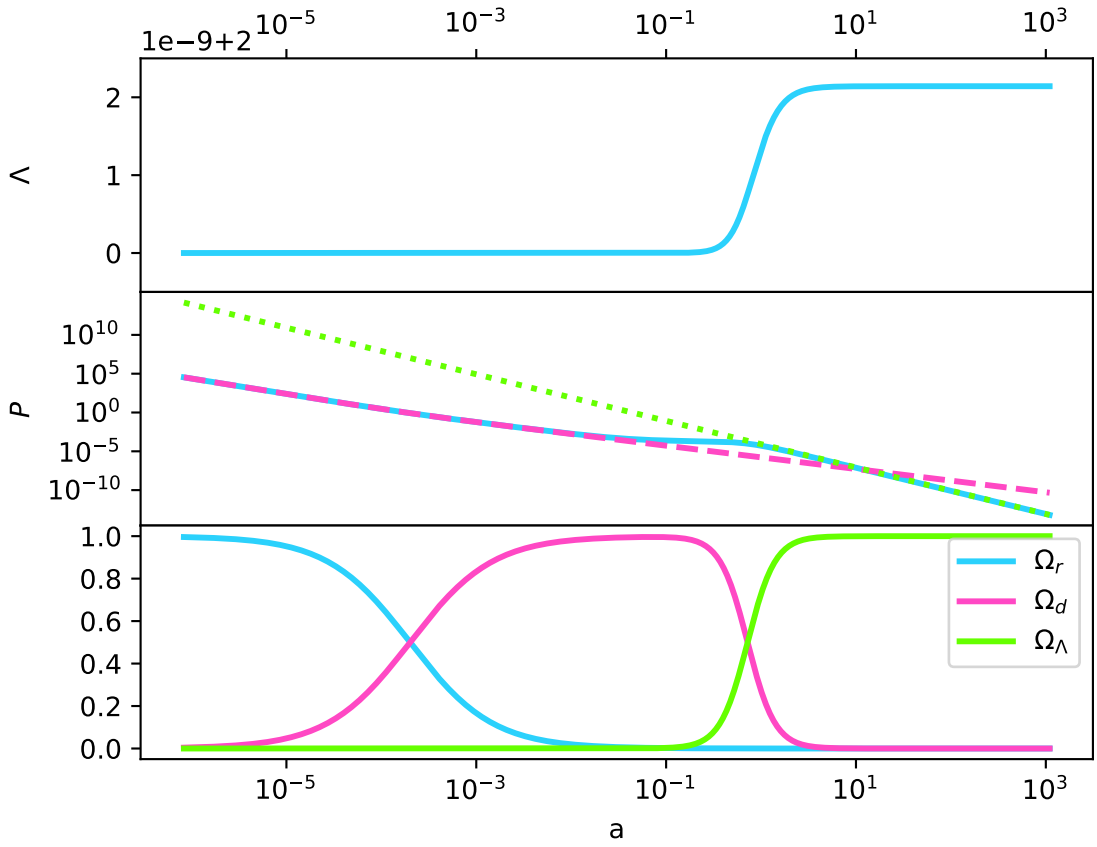

Figure 5.1: The numerical evolution of various quantities for the parameter choice $\gamma = 10^{-5}$. In the upper plot the evolution of Λ is shown; it can be seen that the field changes by roughly one part in 10^9 over cosmic history. In the middle plot the solid line shows the exact evolution of the torsion field P whilst dashed line shows the solution (5.25) and the dotted line shows the solution (5.30). The lower plot shows evolution of Ω quantities (here defined as fractional contributions to g^2 in the Hamiltonian constraint) and P (solid lines) as a function of $\ln a$ for a realistic universe. Subscripts d and r denote dust and radiation-like components of the universe. The scale factor is fixed to be $a = 1$ at the present moment, and units where the present day Hubble parameter H_0 is set to unity are used.

In summary then, numerical exploration suggests that unless P finds itself on the tracking solution (5.25) for much of cosmic history, it will tend to dominate the evolution of the universe and therefore very likely in conflict with cosmological data. This requires fine tuning of the initial value of P so that it begins close to the tracking solution. During the tracking stage, the effect of P is to rescale Newton's constant G. We will find later that deviations of gravitational wave speed from unity tend to be of order γ^2. This justifies our assumption that $|\gamma| \ll 1$ and - in conjunction with recent constraints on the speed of gravity - restricts the fractional rescaling of G to be $\mathcal{O}(10^{-15})$, which is well within bounds that will be placed by BBN constraints for the foreseeable future [246]. Additionally we see that a smaller value of γ tends to lower the total time variation of Λ over cosmic history, making it more difficult to distinguish from a genuine cosmological constant.

5.3 The perturbed equations of motion for tensor modes

We now look at the evolution of small perturbations to the cosmological background. We perturb the tetrad and connection as:

$$\delta e^0 = 0 \tag{5.32}$$

$$\delta e^I = \frac{1}{2}\mathcal{H}^{IJ}\bar{e}_J \tag{5.33}$$

$$\delta\omega^{0I} = \frac{1}{2}\mathcal{E}^{IJ}\bar{e}_J \tag{5.34}$$

$$\delta\omega^{IJ} = \frac{1}{2}\epsilon^{IJ}{}_K\mathcal{B}^{KL}\bar{e}_L \tag{5.35}$$

where $\mathcal{H}^{[IJ]} = \mathcal{E}^{[IJ]} = \mathcal{B}^{[IJ]} = 0$ and $\mathcal{H}^I{}_I = \mathcal{E}^I{}_I = \mathcal{B}^I{}_I = 0$. In addition we apply the restriction of looking at tensor (transverse traceless) modes, so that we impose:

$$\dot{\beta}_I\mathcal{H}^{IJ} = \dot{\beta}_I\mathcal{E}^{IJ} = \dot{\beta}_I\mathcal{B}^{IJ} = 0. \tag{5.36}$$

where $\bar{D}_I \equiv \bar{e}^i_I\bar{D}_i$ and $\bar{D}_i$ is the covariant derivative according to $\bar{\omega}^{IJ}{}_i$. Note the field P does not contribute to the expressions (5.36) and so the equations are equivalent to

$\bar{e}^i_I \partial_i \mathcal{H}^{IJ} = \bar{e}^i_I \partial_i \mathcal{E}^{IJ} = \bar{e}^i_I \partial_i \mathcal{B}^{IJ} = 0$.

Given a quantity Y_{IJ} that represents a small perturbation, it can be converted into a tensor Y_{ij} in the spatial coordinate basis via $Y_{ij} \equiv \bar{e}^I_i \bar{e}^J_j Y_{IJ}$. Given our assumption of vanishing spatial curvature, a 'co-moving' tensor $\tilde{Y}_{ij} = Y_{ij}/a^2$ can further be constructed.

The linearly-perturbed form of equations (5.7)-(5.9) can be written as linear partial differential equations in (t, x^i) and they are written in this form in Appendix 5.C. For simplicity we decompose these perturbations into plane-wave Fourier components labelled by wave number k. As a further simplification we decompose each co-moving tensor mode Fourier mode into helicity eigenstates:

$$\tilde{\mathcal{H}}_{ij} = \sum_{\pm} \mathcal{H}^{\pm}(k,t) e^{ik_i x^i} \tilde{\mathcal{P}}^{\pm}_{ij} \tag{5.37}$$

$$\tilde{\mathcal{E}}_{ij} = \sum_{\pm} \mathcal{E}^{\pm}(k,t) e^{ik_i x^i} \tilde{\mathcal{P}}^{\pm}_{ij} \tag{5.38}$$

$$\tilde{\mathcal{B}}_{ij} = \sum_{\pm} \mathcal{B}^{\pm}(k,t) e^{ik_i x^i} \tilde{\mathcal{P}}^{\pm}_{ij}. \tag{5.39}$$

Here $\tilde{\mathcal{P}}^{\pm}_{ij}$ are co-moving polarization tensors for $+$ and $-$ helicity components. For a plane-wave perturbation with wavenumber k^i we have the important identities, $ik^m \tilde{\epsilon}_{im}{}^l \tilde{\mathcal{P}}^{\pm}_{lj} = \pm k \tilde{\mathcal{P}}^{\pm}_{ij}$ and $\tilde{\mathcal{P}}^{\lambda}_{ij} \tilde{\mathcal{P}}^{\lambda' ij} = 2\delta^{\lambda\lambda'}$ where $\lambda = +, -$ and $\tilde{\epsilon}_{ijk}$ is the co-moving three dimensional Levi-Civita symbol. Indices of co-moving tensors are taken to be raised and lowered with the Kronecker delta symbol.

After some algebra, it can be shown that the spin connection equations of motion yield the following equations:

$$\begin{pmatrix} \mathcal{B}^{\pm} \\ \mathcal{E}^{\pm} \end{pmatrix} = \frac{1}{A^2 + B^2} \begin{pmatrix} A & B \\ -B & A \end{pmatrix} \begin{pmatrix} -k_P^{\pm} \mathcal{H}^{\pm} \\ \dot{\mathcal{H}}^{\pm} + \left(2\frac{\dot{a}}{a} - g \right) \mathcal{H}^{\pm} \end{pmatrix} \tag{5.40}$$

where here and subsequently we choose the spacetime gauge $N = 1$ (proper time) and where

$$A = 1 - \frac{3\dot{\Lambda}}{\Lambda^2}\left(g - k_P^{\pm}\gamma^{-1}\right) \tag{5.41}$$

$$B = \frac{3\dot{\Lambda}}{\Lambda^2}\left(k_P^{\pm} + g\gamma^{-1}\right) \tag{5.42}$$

We have introduced the polarization-dependent torsion-adjusted proper wavenumber $k_P^{\pm}$ according to:

$$k_P^{\pm} \equiv \pm\frac{k}{a} - P \tag{5.43}$$

For reference, in the usual Einstein-Cartan theory we have $A = 1$, $B = 0$; in that case, $\mathcal{B}^{\pm}$ is related to spatial derivatives of $\mathcal{H}^{\pm}$ and $\mathcal{E}^{\pm}$ is related to time variations of $\mathcal{H}^{\pm}$. All modifications to the relation between $\{\mathcal{E}^{\pm}, \mathcal{B}^{\pm}\}$ and $\mathcal{H}^{\pm}$ stem from non-constancy of Λ. Hence the connection equations imply that in general the parity even and odd components of the connection ($\mathcal{E}$ and $\mathcal{B}$) can be obtained from their Einstein-Cartan expressions via a rotation, with an angle θ satisfying:

$$\tan\theta = \frac{B}{A} = \frac{\frac{3\dot{\Lambda}}{\Lambda^2}(g + \gamma k_P^{\pm})\gamma^{-1}}{1 - \frac{3\dot{\Lambda}}{\Lambda^2}(g - k_P^{\pm}\gamma^{-1})} \tag{5.44}$$

followed by a dilatation by $1/\sqrt{A^2 + B^2}$.

Then we may look to find the "second order" evolution equation for $\mathcal{H}^{\pm}$ by inserting the solution (5.40) for $\mathcal{B}^{\pm}$ and $\mathcal{E}^{\pm}$ into the Einstein equation:

$$\begin{aligned} 0 = {} & \dot{\mathcal{E}}^{\pm} + \left(\frac{\dot{a}}{a} + g\right)\mathcal{E}^{\pm} - k_P^{\pm}\mathcal{B}^{\pm} \\ & - \left(\frac{2}{3}\Lambda + \frac{\kappa}{6}(\rho - 3p)\right)\mathcal{H}^{\pm} \end{aligned} \tag{5.45}$$

We now look at solutions to the system (5.40) and (5.45).

5.4 General features

Generally, if the solution (5.40) is inserted into (5.45) then the resulting coefficient of $\ddot{\mathcal{H}}^{\pm}$ is proportional to:

$$\left(1+\frac{6P}{\Lambda+\kappa\rho}k_P^{\pm}\right). \tag{5.46}$$

We see that the coefficient is not positive-definite and hits zero when $k=k_*^{\pm}$:

$$k_*^{\pm}=\mp\frac{a}{6P}\left(\Lambda+\kappa\rho-6P^2\right) \tag{5.47}$$

signalling a divergence in the frequency. For example in the very late universe we may expect $\Lambda\sim\Lambda_0=cst.$ to dominate the evolution of the universe hence then:

$$k_*^{\pm}\sim\mp\frac{a}{6P}\Lambda_0 \tag{5.48}$$

where we've assumed that $P^2/\Lambda_0\ll 1$.

Following the arguments proposed in Subsections 5.2.3 and 5.2.3, we have that $k_*^{\pm}\sim\mp 2a^4\Lambda_0/\gamma$ for realistic cosmologies. Reaching $k_*^{\pm}$ will correspond to $\omega_{\pm}^2(k,t)$ and $f_{\pm}(k,t)$ diverging and therefore likely signals a breakdown in the applicability of linear perturbation theory. As for the case of $P(t)$, we see that a key parameter for the size of $k_*^{\pm}$ is γ.

When $k\neq k_*^{\pm}$ and with the important exception of the limit $|\gamma|\to\infty$ (see Section 5.6), it is possible to write the Einstein equation (5.45) in the following form :

$$\ddot{\mathcal{H}}^{\pm}=-\omega_{\pm}^2(k,t)\mathcal{H}^{\pm}-f_{\pm}(k,t)\dot{\mathcal{H}}^{\pm} \tag{5.49}$$

For arbitrarily values of γ, the form of $\omega_{\pm}^2(k,t)$ and $f_{\pm}(k,t)$ will be extremely complicated and so we will concentrate in detail on how (5.49) looks in relevant, limiting cases.

5.5 The Einstein-Cartan limit

We start by finding the Einstein-Cartan limit of these theories, noting that when γ is finite and $\rho = p = 0$ there are solutions where $P = 0$, $g = \dot{a}/a$ and Λ is constant [232]. Taking these background solutions we should obtain the Einstein-Cartan limit for our theory, which is equivalent to General Relativity in this situation. Inserting these conditions into the formalism just developed, we find $\dot{\Lambda} = 0$, and so $A = 1$ and $B = 0$, as already announced in the previous Section. The connection equations are therefore:

$$\mathcal{B}^{\pm} = -k_P^{\pm}\mathcal{H}^{\pm} \tag{5.50}$$

$$\mathcal{E}^{\pm} = \left(\frac{d}{dt} + \frac{\dot{a}}{a}\right)\mathcal{H}^{\pm}. \tag{5.51}$$

Note that since $P = 0$ we have $k_P^{\pm} = \pm k/a$, and so for gravity waves in Einstein-Cartan theory, the parity-odd connection perturbation, $\mathcal{B}$, is a spatial gradient of the metric, whereas the parity-even component, $\mathcal{E}$, is a time derivative of the metric (cf. Eqs (5.35) and (5.34)). Inserting these expressions into the Einstein equation (5.45), as prescribed, we find:

$$\ddot{\mathcal{H}}^{\pm} + 3\frac{\dot{a}}{a}\dot{\mathcal{H}}^{\pm} + \left(\dot{g} + 2g^2 - \frac{2}{3}\Lambda\right)\mathcal{H}^{\pm} + (k_P^{\pm})^2\mathcal{H}^{\pm} = 0 \tag{5.52}$$

where the dot denotes derivative with respect to the background proper time. In the Einstein-Cartan theory we have $T = 0$ in the absence of background sources of torsion, so $g = \dot{a}/a$, and the background equations of motion read (see (5.20) and (5.21)):

$$g^2 = \frac{\Lambda}{3} \tag{5.53}$$

$$\dot{g} + \frac{\dot{a}}{a}g = \dot{g} + g^2 = \frac{\Lambda}{3}. \tag{5.54}$$

Therefore we find:

$$\ddot{\mathcal{H}}^{\pm} + 3\frac{\dot{a}}{a}\dot{\mathcal{H}}^{\pm} = -(k_P^{\pm})^2\mathcal{H}^{\pm}$$

$$= -\left(\frac{k}{a}\right)^2 \mathcal{H}^{\pm} \tag{5.55}$$

Thus, our formalism for gravity waves reduces to the textbook equations for gravity waves in General Relativity in this limit.

5.6 Euler theory ($\gamma \to \infty$) in a parity-odd background ($P \neq 0$)

Our first surprise arises when we consider a theory with the Euler pseudo-topological term only, by letting $\gamma \to \infty$, but with a background with $P \neq 0$. Then, as the background Equation (5.23) shows (with $P \neq 0$ and $\gamma \to \infty$), we must have $3\dot{\Lambda}g = \Lambda^2$. Therefore, the definitions of A and B (Eqns. (5.41) and (5.42)) lead to:

$$A = 0, \quad B = \frac{k_P^{\pm}}{g} \tag{5.56}$$

These are orthogonal to the Einstein-Cartan values, in the sense that for the latter the matrix (5.40) is diagonal, whereas here the matrix is purely off-diagonal. Indeed the rotation part of the transformation is now $\theta = \pi/2$. This is reflected in the way the connection is related to the metric. the Einstein-Cartan case (cf. Eqns. (5.50) and (5.51)) we have:

$$\mathcal{E}^{\pm} = g\mathcal{H}^{\pm} \tag{5.57}$$

$$k_P^{\pm}\mathcal{B}^{\pm} = g\left(\dot{\mathcal{H}}^{\pm} + \left(\frac{2\dot{a}}{a} - g\right)\mathcal{H}^{\pm}\right) \tag{5.58}$$

Inserting into the Einstein equation (5.45) we find that not only does this imply an absence of second order time derivatives for $\mathcal{H}^{\pm}$, but the first time derivatives cancel out. In addition the algebraic equation obtained is

$$\left(\frac{1}{2}\dot{g} + g^2 - \frac{g}{2}\frac{\dot{a}}{a} - \frac{\Lambda}{3} + \frac{1}{12}(3p - \rho)\right)\mathcal{H}^{\pm} = 0 \tag{5.59}$$

The term in brackets in (5.59) vanishes due to the equations of motion, therefore the tensor mode perturbation is $\mathcal{H}^{\pm}$ completely undetermined by the perturbed equations of motion [3].

One may wonder to what extent this is a result of the particular choice for our action. For example, if the coefficient $-\frac{3}{2}$ in the term (5.3) is replaced by $-\frac{3}{2\xi}$ then it can be shown that Einstein's equation instead becomes:

$$\frac{1}{\xi}\Big(1-\xi\Big)\Big(4\Lambda+\rho-3p\Big)\mathcal{H}^{\pm}=0 \tag{5.60}$$

Thus in the case when $\Lambda \neq 0$, $\rho \neq 3p$ and $\xi \neq 1$, the perturbation $\mathcal{H}^{\pm}$ is not undetermined but fixed to vanish. It appears that the presence of the Euler term in the absence of the Pontryagin term is sufficient to nullify the dynamics of the perturbation $\mathcal{H}^{\pm}$ with the special case $\xi = 1$, which leaves them undetermined by the perturbed equations of motion. Note that the case of simultaneous vanishing of the Euler and Pontryagin term ($\xi \to \infty$) does not correspond to General Relativity. In fact such limit yields a rather exotic background solution $a = 0$ due to Λ being a dynamical field.

5.7 The leading order solution for the general case in the late universe

We now consider a general finite value of γ and look at the perturbed equations in a regime where the evolution of the universe is dominated by Λ. We define a dimensionless parameter $\epsilon_P \equiv P/\sqrt{\Lambda}$ which is expected to be of magnitude much smaller than unity in the late universe. Furthermore we assume that $|\gamma| \ll 1$. Inserting the solutions for $\mathcal{E}^{\pm}$ and $\mathcal{B}^{\pm}$ from (5.40) into the Einstein equations and keeping only terms up to second order in $\{\epsilon_P, \gamma\}$ we find:

$$\ddot{\mathcal{H}}^{\pm} = -\omega_{\pm}^2(k,t)\mathcal{H}^{\pm} - f_{\pm}(k,t)\dot{\mathcal{H}}^{\pm}$$

[3] This would appear to contradict the result found in [247] which says that tensor modes propagate luminally as in General Relativity in a model with tensor mode perturbation equations that should be mappable to the ones considered here.

$$\omega_{\pm}^2(k,t) \equiv \Bigg[4\Lambda\epsilon_P^2 \mp 4\sqrt{\Lambda}\epsilon_P\left(\frac{k}{a}\right) + \Bigg(1 + \frac{(\kappa\Lambda\rho - 3\kappa\Lambda p - \kappa^2\rho^2 - 3\kappa^2 p\rho)}{(\kappa\rho+\Lambda)^2}\gamma^2$$
$$+ \frac{8\left(\sqrt{3}\Lambda^{5/2} + \sqrt{3}\kappa\Lambda^{3/2}\rho - \sqrt{3}\kappa^2\sqrt{\Lambda}\rho^2 - 3\sqrt{3}\kappa^2\sqrt{\Lambda}p\rho - 3\sqrt{3}\kappa\Lambda^{3/2}p\right)}{(\kappa\rho+\Lambda)^{5/2}}\gamma\epsilon_P \tag{5.61}$$
$$+ \frac{42\left(2\Lambda^2 - \kappa\Lambda\rho - 3\kappa\Lambda p\right)}{(\kappa\rho+\Lambda)^2}\epsilon_P^2\Bigg)\left(\frac{k}{a}\right)^2\Bigg]$$
$$+ \mathcal{O}(\epsilon_P,\gamma)^3 \tag{5.62}$$

$$f_{\pm}(k,t) \equiv \sqrt{3(\Lambda+\kappa\rho)}$$
$$\pm \left[\frac{4\sqrt{3}\sqrt{\Lambda}\sqrt{\kappa\rho+\Lambda}(2\Lambda-\kappa\rho)\epsilon_P + \kappa\rho(\kappa\rho-\Lambda)\gamma + 3\kappa p\left((\kappa\rho+\Lambda)\gamma - 4\sqrt{3}\sqrt{\Lambda}\sqrt{\kappa\rho+\Lambda}\epsilon_P\right)}{(\kappa\rho+\Lambda)^2}\right]\left(\frac{k}{a}\right)$$
$$+ \mathcal{O}(\epsilon_P,\gamma)^2 \tag{5.63}$$

where it is assumed that $|k| \ll k_*$. Roughly speaking, positivity of both $\omega_{\pm}^2(k,t)$ and $f_{\pm}(k,t)$ imply that $\mathcal{H}^{\pm}$ evolves in a stable manner.

We immediately see from (5.61) that novel features are generally present in the propagation of $\mathcal{H}^{\pm}$. In the limit $k \to 0$ we see that

$$\lim_{k\to 0}\omega_{\pm}^2(k,t) = 4\Lambda\epsilon_P^2 \equiv \mathcal{M}_G^2(P) \tag{5.64}$$

i.e. the non-Riemannian background curvature provided by the spiral staircase field P gives what may be interpreted as contributing to a non-zero effective mass to the graviton.

At non-zero k we see that there exist terms linear in k in $\omega_{\pm}^2(k,t)$ alongside the term proportional to k^2 familiar from General Relativity present in equation (5.55). We may consider the wavenumber $k_{(\omega)12}$ at which the term linear in k is of comparable size to the term quadratic in k^2. It can be calculated to be, to leading order in small quantities:

$$k_{(\omega)12}^{\pm} \equiv \pm 4a\epsilon_P\sqrt{\Lambda} = \pm 4aP \tag{5.65}$$

For realistic background cosmologies we expect in this regime that $P \approx (\gamma/3)H_0 a_i^{3/2} a^{-3}$ so $k^{\pm}_{(\omega)12} \approx \pm 4(\gamma/3)a_i^{3/2}a^{-2}H_0$, where a_i will be the scale factor where Λ begins to dominate the evolution of the universe. As $|\gamma| \ll 1$ then $k^{\pm}_{(\omega)12}$ is expected to be on scales far larger than the characteristic cosmological horizon scale $k_H \equiv H_0$ today. We note that the mass term and chirality-dependent leading term linear in k are due to the tensor perturbation $\mathcal{H}^{ij}$ coupling to the parity-violating torsionful generalization of the Laplacian operator.

Following [248] (see also [249, 250, 251]) the speed of monochromatic tensor modes today $c_T^{\pm}$ (taking $a = 1$) is given by $c_T^{\pm} = \frac{\omega_{\pm}}{k}$. In general our expression for c_T will be rather complicated but it is instructive to detail the order of magnitude of terms appearing in its expressions. Given how we expect $P(t)$ to scale with γ from the results of Section 5.2.3 we find that:

$$\begin{aligned} c_T^{\pm} \sim 1 \pm \mathcal{O}\left(\frac{H_0}{k}\gamma\right) + \mathcal{O}\left(\gamma^2\right) + \mathcal{O}\left(\frac{H_0^2}{k^2}\gamma^2\right) \\ \pm \mathcal{O}\left(\frac{H_0^3}{k^3}\gamma^3\right) \pm \mathcal{O}\left(\frac{k}{k_*}\gamma^2\right) + \mathcal{O}\left(\frac{k^2}{k_*^2}\gamma^2\right) + \dots \end{aligned} \tag{5.66}$$

The above shows the leading contribution to each k dependence; these get further corrections by higher powers of γ as appropriate. Note that the terms involving k_*, which are important in terms of telling us when breakdown happens for higher k, appear at leading order cubic in $\{\epsilon_P, \gamma\}$ and that the next-to-leading contribution to $c_T^{\pm}$ involving k_* is a factor (k/k_*) smaller than the leading one, implying that the leading term is the dominant one as long as $|k/k_*| \ll 1$. Constraints from the LIGO experiment roughly constrain the deviation of $c_T^{\pm}$ from unity by approximately 10^{-15}. This will generally imply that each of the terms in (5.66) that cause deviations from unity should be no bigger than 10^{-15}. If we take a typical wavelength of gravitational waves probed by LIGO to be $\lambda_{LIGO} \sim 1000km$ then $k_{LIGO} = 2\pi/\lambda_{LIGO} \sim 6 \times 10^{-3} km^{-1}$. Taking a value $H_0 \sim (2/3)10^{-23} km^{-1}$ (corresponding to $H_0 \sim 70 km/s/Mpc$) we have $H_0/k_{LIGO} \sim 10^{-21}$. As we expect $\gamma^2 < 1$, the leading H_0/k chirality-dependent modification ot the speed of gravity is not constrained by existing data.

The constraint on the speed of gravitational wave speed then places the following restriction on γ:

$$\gamma^2 \lesssim \mathcal{O}(10^{-15}) \tag{5.67}$$

Given this constraint and the small value of H_0/k_{LIGO}, the remaining immediate constraint from $c_T^{\pm}$ is that

$$|k_*^{\pm}| \gg \mathcal{O}(k_{LIGO}) \tag{5.68}$$

which is necessary for the consistency of our use of the linearly perturbed equations of motion; as the breakdown of the applicability of these equations is approached, significant deviations of $c_T^{\pm}$ from unity are expected. We can translate this into a constraint on γ by assuming as above that $P \sim (\gamma/3)H_0 a_i^{3/2} a^{-3}$ and so using equation 5.47 we have $k_*^{\pm} \sim \mp H_0/\gamma$ and so

$$|\gamma| \ll \mathcal{O}(10^{-21}) \tag{5.69}$$

5.8 Perfect fluid domination

In this limit, we consider the evolution of perturbations on a background where the evolution is dominated by a combination of perfect fluids. It was shown in 5.2.3 that there exist solutions where $\Lambda \sim 0$ and $P^2 = \gamma^2 \kappa \rho/27$ with $\gamma \ll 1$ and that these seem to be the solutions that yield a realistic cosmology. Assuming that these solutions hold then to quartic order in the small parameter γ we have that:

$$\ddot{\mathcal{H}}^{\pm} = -\omega_{\pm}^2(k,t)\mathcal{H}^{\pm} - f_{\pm}(k,t)\dot{\mathcal{H}}^{\pm} \tag{5.70}$$

$$\omega_{\pm}^2(k,t) \equiv \left[\frac{4}{27}\left(1-\frac{1}{9}(1+3w)\gamma^2\right)\gamma^2\kappa\rho \mp \frac{4}{3}\sqrt{\frac{\kappa\rho}{3}}\gamma\left(\frac{k}{a}\right) + \left(1+\frac{1}{9}(1+3w)\gamma^2+\frac{12}{243}(1+3w)\gamma^4\right)\left(\frac{k}{a}\right)^2 \right.$$
$$\left. \mp \frac{2}{9}(1+3w)\sqrt{\frac{3}{\kappa\rho}}\gamma^3\left(\frac{k}{a}\right)^3 + \frac{20}{27}\frac{(1+3w)}{\kappa\rho}\gamma^4\left(\frac{k}{a}\right)^4\right] + \mathcal{O}(\gamma^5) \tag{5.71}$$

$$f_{\pm}(k,t) \equiv \left[\sqrt{3\kappa\rho}\left(1-\frac{1}{18}\gamma^2+\frac{217}{1944}\gamma^4+\frac{13}{162}w\gamma^4\right) \mp \frac{1}{9}(1+3w)\left(1+4\gamma^2\right)\gamma\left(\frac{k}{a}\right)\right.$$
$$\left. + (1+3w)\sqrt{\frac{3}{\kappa\rho}}\frac{2}{9}\left(1+\frac{16}{9}\gamma^2\right)\gamma^2\left(\frac{k}{a}\right)^2 \mp \frac{4}{9}\frac{(1+3w)}{\kappa\rho}\gamma^3\left(\frac{k}{a}\right)^3 + \frac{8}{27}(1+3w)\frac{\sqrt{3}}{(\kappa\rho)^{3/2}}\gamma^4\left(\frac{k}{a}\right)^4\right]$$
$$+ \mathcal{O}(\gamma^5) \tag{5.72}$$

where $w \equiv p/\rho$. Note that as in the case of the late time solution discussed in Section 5.7 the leading term in $\omega_{\pm}^2$ to leading order in γ^2 as $k \to 0$ corresponds to $\mathcal{M}_G^2 = 4P^2$, and this term grows more quickly than $(k/a)^2$ as the scale factor a decreases. By numerical inspection, $\omega_{\pm}^2$ to arbitrary order in γ has a minimum during fluid domination (if $a = 1$ today)

$$a \sim \frac{2\left(\gamma^2 H_0^2\Omega_d + \sqrt{\gamma^4 H_0^4\Omega_d^2 + 9\gamma^2 H_0^2 k^2\Omega_r}\right)}{9k^2} \tag{5.73}$$

where $k > 0$ for the $+$ polarization, and $k < 0$ for the $-$ polarization where we've defined Ω_d and Ω_r for dust and radiation respectively via $\kappa\rho_d/3 \equiv H_0^2\Omega_d/a^3$ and $\kappa\rho_r/3 \equiv H_0^2\Omega_r/a^4$. This behaviour can be seen for ω_+^2 in Figure 5.2 and appears to mark a brief transition between ω_+^2 being dominated by the mass term at earlier times and the more familiar $(k/a)^2$ term at later times. Indeed, one can see that generally the effective mass term in (5.71) - proportional to ρ- grows more quickly than $(k/a)^2$ as a decreases so will tend to dominate at early times.

5.9 Outlook

In this chapter we revisited models of the Universe where the cosmological constant is allowed to vary as a result of a balancing torsion. Such theories potentially have fewer free parameters than General Relativity, but we need to consider parity violating backgrounds so that they

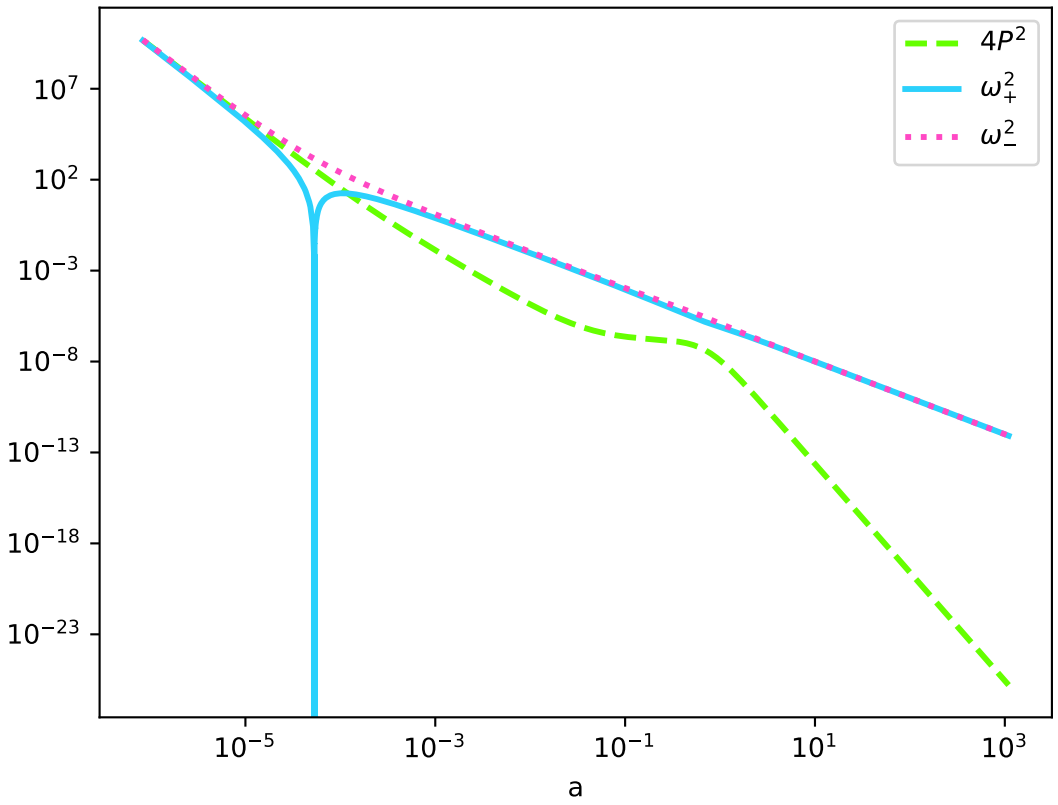

Figure 5.2: Plot of the exact forms of ω_+^2 and ω_-^2 (correct up to any order in γ) and $4P^2$ for the background cosmology depicted in Figure 5.1 and with $k = 10^{-3}H_0$, $\gamma = 10^{-5}$. It can be seen that both ω_+^2 and ω_-^2 asymptote at early times to the $4P^2$, whereas at later times each evolves as $(k/a)^2$.

display acceptable late time phenomenology even at the level of background cosmological evolution [232]. Going beyond the homogeneous and isotropic approximation, the most obvious question concerns the propagating modes of the theory, specifically gravitational waves. We found that indeed dramatic results and severe constraints arise in this respect.

We developed the required perturbation theory within the first order formulation, taking into account that the connection has parity-odd and -even components, with both potentially receiving zeroth order terms. We also proposed a strategy for solving the more involved equations one has to contend with in this setting. We recovered the usual result for gravity waves if we assume the Einstein-Cartan theory (or solutions to our theory that reduce to it). For a theory with a pure Euler term we found a remarkable result that the linearly perturbed equations of motion leave the tensor perturbations either entirely undetermined (or fixed to vanish, if the term has a factor different from the one imposed by self-duality). This may well be hinting at the fact that gravity waves become 'pure gauge' in this case (in analogy with what happens for a varying Lambda in the parity even branch of the background solutions).

In the more general case, with a Pontryagin-type quasi-topological term, the situation is more promising. There are exotic effects, but these need not contradict observations in particular if we restrict ourselves to viable background solutions that may be currently indistinguishable from the standard ΛCDM cosmological mode. At the level of perturbations, results will necessarily differ from General Relativity for some wavenumbers k, with the speed of tensor modes in the late universe receiving large modifications as $|k| \sim \gamma H_0$ (the scale of the graviton mass) and as $|k| \sim H_0/\gamma$ (the scale $k_* \sim H_0/\gamma$ where linear perturbation theory is expected to break down in these models). As one approaches each of these values, the speed of gravity is predicted to diverge substantially from unity in a chirality-dependent manner. All these effects occur only when the parity-violating torsion field $P(t) \neq 0$ and - via equation 5.76 - equivalently when the time derivative of $\Lambda(t)$ is non-zero.

Thus, our results are potentially very useful as a new model relating observations on the accelerating Universe (possibly implying of a non-constant deceleration parameter) and other gravitational observations. But even more originally, our conclusions may be of great value

for in phenomenological quantum gravity. Modified dispersion relations are a major feature of phenomenological approaches to quantum gravity (see, for example, [252, 253, 254, 255]). Our work has added a layer to this approach by introducing *chiral* modified dispersion relations. It has been speculated that the concept of parity requires severe revision at the Planck scale [256]. Furthermore, our results supplement existing findings regarding how parity violation in theories of gravity involving to extensions to Riemannian geometry can affect the propagation of gravitational waves (for example see [247, 257] for cases where the gravitational connection field has torsion and non-metricity respectively).

A number of open questions remain. Firstly, we have only considered tensor perturbations in this theory. It is expected that in the vector mode sector, there will be no new degrees of freedom present - as in the tensor mode case, a relic of the polynomial nature of the new ΛRR terms in the Lagrangian is that modifications will always only be enabled by a non-zero time derivative of $\Lambda(t)$ which concomitantly implies that time derivatives of the spin-connection perturbation will not appear. In the scalar sector, a new scalar degree of freedom $\delta\Lambda(x^i, t)$ is expected to propagate and it will be important to see its effect on the cosmic microwave background CMB) and the growth of large scale structure.

There are also several avenues to study further observational signatures of this parity violation. The gravitational wave waveform will show deviations from General Relativity in both the amplitude and phase, due to amplitude and velocity birefringence effects, respectively, which both arise as a result of parity violation [258, 259]. Some of these effects could potentially be constrained in second generation gravitational wave detectors, and it would be interesting to derive the modifications to the waveform due to these effects. In addition to observable signatures in propagation, there is potential to detect parity violation at the gravitational wave source through study of various types of astrophysical binary systems as proposed by [260, 261]. It has also been suggested that parity violation in the gravitational sector could leave distinct signatures in the CMB to be detected with future experiments (see e.g., [262, 263, 264, 265, 266, 267, 268]), which could also be worth further exploration in the context of our theory.

It remains to understand our results in the light of a Hamiltonian analysis of the theory to second order, or even non-perturbatively, to all orders. A clear direction of further development would be to present the Hamiltonian structure of the full theory, with an examination of its number of degrees of freedom. It is curious that the mini-superspace approximation reveals two branches with different symmetries and degrees of freedom. We have now discovered that the fluctuations about them have rather exotic properties. In particular, the under-determination of the perturbed tensor equations of motion for a theory with a pure Euler term hints that a novel type of gauge symmetry may exist.

5.A Alternative form of the background equations of motion

It is possible to write down the field equations (5.7)-(5.9) as a system of first-order ordinary differential equations for variables $\{P, g, \Lambda, a\}$ along with a constraint equation:

$$\dot{P} = \frac{-6P\kappa\rho\left(6\gamma Pg^2 + 3g\left(\Lambda + 2P^2\right) - \Lambda\gamma P\right) + \kappa^2\rho(6P(3gp + \gamma P\rho) + \gamma\Lambda\kappa(\rho - 3p)) - \gamma\kappa^3\rho^2(3p + \rho)}{6\kappa\rho(6\gamma Pg + \Lambda\kappa + \rho)} \tag{5.74}$$

$$\dot{g} = -\frac{6\left(\gamma^2 + 1\right)g^2P^2}{6\gamma Pg + \Lambda + \kappa\rho} - g^2 + g\gamma P + \frac{\Lambda}{3} - \frac{\kappa}{6}(\rho + 3P) \tag{5.75}$$

$$\dot{\Lambda} = \frac{2\gamma P\Lambda^2}{6\gamma Pg + \Lambda + \kappa\rho} \tag{5.76}$$

$$\dot{a} = a\left(\frac{6\left(\gamma^2 + 1\right)gP^2}{6\gamma Pg + \Lambda + \kappa\rho} + g - \gamma P\right) \tag{5.77}$$

$$\frac{\Lambda}{3} = g^2 - P^2 - \kappa\frac{\rho}{3} \tag{5.78}$$

It can be checked via differentiation of the constraint equation that $\dot{\rho} = -3\frac{\dot{a}}{a}(\rho + p)$ as in the case of a perfect fluid in General Relativity. Using the constraint equation we can rewrite the evolution equation as $\dot{\Lambda} = (2/3)\gamma P\Lambda^2/(g^2 - P^2 + 2g\gamma P)$. From this perspective, the dynamics for Λ can be seen as arising from the spin connection components g and P.

5.B Linearly perturbed field strength and torsion

Central objects in the field equations (5.7)-(5.9) are the curvature and torsion two-forms R^{AB} and T^A. Their linearly-perturbed forms around the cosmological background are found to be:

$$\begin{aligned}\delta R^{0I} = &-\epsilon^I{}_{JK} g\mathcal{B}^J{}_L \bar{e}^L \bar{e}^K + \left(\frac{1}{N}\frac{\partial}{\partial t}\mathcal{E}^{IJ} + \frac{1}{N}\frac{\dot{a}}{a}\mathcal{E}^{IJ}\right)\bar{e}^0\bar{e}_J \\ &+ \bar{D}^K\mathcal{E}^{IJ}\bar{e}_K\bar{e}_J + P\mathcal{E}^I{}_J\epsilon^{JKL}\bar{e}_K\bar{e}_L \end{aligned} \tag{5.79}$$

$$\begin{aligned}\delta R^{IJ} = &\, 2g\mathcal{E}_L{}^{[I}\bar{e}^{|L|}\bar{e}^{J]} + \epsilon^{IJ}{}_K\Bigg(\left(\frac{1}{N}\frac{\partial}{\partial t}\mathcal{B}^{KL} + \frac{1}{N}\frac{\dot{a}}{a}\mathcal{B}^{KL}\right)\bar{e}^0\bar{e}_L \\ &+ (\bar{D}_L\mathcal{B}^{KM})\bar{e}^L\bar{e}_M + P\mathcal{B}^K{}_P\epsilon^{PMN}\bar{e}_M\bar{e}_N\Bigg) \end{aligned} \tag{5.80}$$

$$\begin{aligned}\delta T^I = &\left(\frac{1}{N}\frac{\partial}{\partial t}\mathcal{H}^{IM} + \frac{1}{N}\frac{\dot{a}}{a}\mathcal{H}^{IM} - \mathcal{E}^{IM}\right)\bar{e}^0\bar{e}_M \\ &+ \left(\dot{\beta}^L\mathcal{H}^{IJ} + P\mathcal{H}^I{}_K\epsilon^{KLJ} + \epsilon^{IJ}{}_K\mathcal{B}^{KL}\right)\bar{e}_L\bar{e}_J \end{aligned} \tag{5.81}$$

where $\dot{\beta}_I \equiv e_I^i\dot{\beta}_i$ where $\dot{\beta}_i$ is the covariant derivative according to $\bar{\omega}^{IJ}$.

5.C Perturbed equations of motion

For completeness we provide the full form of the perturbed equations of motion for the fields $\{H^{IJ}, \mathcal{B}^{IJ}, \mathcal{E}^{IJ}\}$:

$$\begin{aligned}-\left(\dot{\beta}^K H^{IM}\epsilon_{KM}{}^J + 2PH^{IJ}\right) - \left(\frac{\Lambda + 12P^2}{\Lambda + 6g\gamma P}\right)\mathcal{B}^{IJ} = &-\frac{3}{\Lambda^2}\dot{\Lambda}\left(\bar{D}^K\mathcal{E}^{IM}\epsilon_{KM}{}^J + 2P\mathcal{E}^{IJ}\right) \\ &- \frac{3}{\Lambda^2\gamma}\dot{\Lambda}\left(g\mathcal{E}^{IJ} - \bar{D}^K\mathcal{B}^{IM}\epsilon_{KMJ}\right) \end{aligned} \tag{5.82}$$

$$-\left(\frac{\partial}{\partial t}H^{IJ}+\left(2\frac{\dot{a}}{a}-g\right)H^{IJ}\right)+\left(\frac{\Lambda+12P^2}{\Lambda+6g\gamma P}\right)\mathcal{E}^{IJ}=-\frac{3}{\Lambda^2}\dot{\Lambda}\left(\bar{D}^K\mathcal{B}^{IM}\epsilon_{KM}{}^{J}+2P\mathcal{B}^{IJ}\right)$$
$$-\frac{3}{\Lambda^2\gamma}\dot{\Lambda}\left(g\mathcal{B}^{IJ}+\bar{D}^K\mathcal{E}^{IM}\epsilon_{KMJ}\right) \quad (5.83)$$

$$\frac{\partial}{\partial t}\mathcal{E}^{IJ}+\left(\frac{\dot{a}}{a}+g\right)\mathcal{E}^{IJ}=\frac{2}{3}\Lambda H^{IJ}+\bar{D}_K\mathcal{B}^{(I}{}_{L}\epsilon^{J)KL}+2P\mathcal{B}^{IJ}$$
$$+\left(\frac{2}{3}\Lambda+\frac{\kappa}{6}\left(\rho-3p\right)\right)H^{IJ} \quad (5.84)$$

where ϵ_{IJK} is the three-dimensional Levi-Civita symbol and we have chosen the $N=1$ spacetime gauge.

Chapter 6

Probing Noncommutative Gravity with Gravitational Wave and Binary Pulsar Observations

6.1 Introduction

We now turn to another modified theory of gravity; noncommutative gravity. Since the advent of gravitational wave astronomy with the detection of gravitational waves (GWs) by the LIGO/Virgo collaboration (LVC), the theory of general relativity (GR) has been directly testable to greater precision than previously possible. Although no observations have yet indicated any compelling deviations from GR, we are able to study modifications to GR, alternative theories of gravity and other fundamental physics using gravitational waves as a probe [269, 270, 271, 272, 273, 274]. Particularly, non-GR effects are highly constrained by GW observations, which can be used to explore many different theories. This has been done, for example for Einstein-Aether theory [275], Einstein-dilaton-Gauss-Bonet gravity [276, 277], dynamical Chern-Simons gravity [276] and others [278, 279].

In addition to gravitational waves, pulsar timing observations are valuable tool in probing

modifications to GR. The system that we will be using to place constraints via pulsar observations is the double pulsar binary system PSR J0737-3039A/B. This system is quite unique, as both neutron stars are radio pulsars, which allows for extremely precise measurements and provides a rich background for tests of general relativity and modified theories of gravity [280, 281].

In this chapter, we will employ a combination of gravitational wave and pulsar analysis to introduce two independent constraints on noncommutative theories. Various noncommutative theories have been proposed previously, originally introduced as a method of quantizing spacetime [282]. The introduction of noncommutative geometry [283] allowed this idea to be applied more broadly, with a focus on noncommutative quantum field theories [284, 285] as well as multiple formulations of a noncommutative extension to the Standard Model [286, 287, 288, 289]. The idea of noncommutative gravity stems from these theories. Non-commuting conjugate variables are a cornerstone of quantum mechanics, and it seems natural that one could apply the same conventions that give rise to, for example, the Heisenberg uncertainty principle in quantum mechanics, to a gravitational setting [284, 285]. Noncommutative gravity also has string theory implications [290, 291] and thus we have a wide range of motivations for its study. The version that we will be focused on is characterized by promoting spacetime coordinates to operators which satisfy the following canonical commutation relation

$$[\hat{x}^\mu, \hat{x}^\nu] = i\theta^{\mu\nu}. \tag{6.1}$$

Here, $\theta^{\mu\nu}$ introduces a new fundamental quantum scale which represents the "quantum fuzziness" of spacetime, in analogy to $\hbar$ in quantum mechanics.

Previous work [292] has placed a bound on the time component of the noncommutativity scale θ^{0i} using GW150914. The authors worked in the post-Newtonian (PN) formalism, in which quantities are expanded in powers of $(v/c)^n$ with v representing the relative velocity of the binary constituents, which are considered order $(n/2)$PN [293]. Reference [292] found corrections entering at 2PN in the acceleration and the waveform phase. The authors

introduce the notation

$$\Lambda\theta^i = \frac{\theta^{0i}}{l_p t_p}, \tag{6.2}$$

where θ^i represent the components of a three-dimensional unit vector $\boldsymbol{\theta}$, which acts as a preferred direction that induces precession of the orbital plane. For calculational simplicity, the authors assumed that the orientation of the $\boldsymbol{\theta}$ is orthogonal to the orbital plane as to place an approximate upper bound on $\sqrt{\Lambda}$, which was found to be $\sqrt{\Lambda} \lesssim 3.5$, at the order of the Planck scale (see [294, 295] for related works).

In this work we extend and generalize the above analysis by considering the general case for the orientation of the preferred direction $\boldsymbol{\theta}$ with respect to the orbital plane by adopting orbital averaging. We then place constraints by employing posterior samples from the GWTC-1 catalog as in [276], rather than explicitly using the bound on the non-GR parameter at 2PN order found by LVC [269] as done in [292]. This new approach properly accounts for the uncertainties in the masses. We derive bounds from four different gravitational wave events with relatively small masses, namely GW151226, GW170608, GW170814 and GW170817.

We also place constraints on the the time component of the noncommutative tensor using the binary pulsar system PSR J0737-3039A/B to act as an independent check on the gravitational wave constraints. In the binary pulsar system, the noncommutativity induces an additional contribution in the pericenter precession beyond GR at 1PN, due to the preferred direction $\boldsymbol{\theta}$ that is induced by the inclusion of noncommutative terms. Corrections to other observables, such as the mass ratio and Shapiro delay, enter at higher PN orders. Thus, we use the latter to determine the masses of the double pulsar binary and use the pericenter precession to constrain the theory (see e.g. [296] for a related work on constraining noncommutative gravity from the pericenter precession of binary pulsars). We find that such bounds are slightly weaker than the ones from gravitational wave events.

The structure of the chapter is as follows. In Section 6.2 we derive the lowest order 2PN noncommutative corrections to the binary system acceleration, beginning from the energy-momentum tensor. We proceed to constrain the noncommutative parameter with LVC data

in Section 6.3 by computing the 2PN non-commutative correction to the gravitational waveform. We then use posterior samples for two different waveform templates to constrain the noncommutativity parameter, $\sqrt{\Lambda}$, in terms of the quantity $\hat{\boldsymbol{L}} \cdot \boldsymbol{\theta}$. In Section 6.4 we then independently constrain $\sqrt{\Lambda}$ as a function of $\hat{\boldsymbol{L}} \cdot \boldsymbol{\theta}$, where $\hat{\boldsymbol{L}}$ is a unit vector orthogonal to the orbital plane, by computing the noncommutative correction to the GR pericenter precession and using the binary pulsar event PSR J0737-3039A/B. Finally, In section 6.5, we summarize our results, and provide some concluding remarks as well as directions for future work. We work in the geometric units $c = G = 1$.

6.2 Noncommutative Corrections to the Acceleration and Energy

In GR, one can approximate a binary system as two point masses which have an energy momentum tensor given by

$$T^{\mu\nu}_{\text{GR}}(\boldsymbol{x}, t) = m_1 \gamma_1(t) v_1^{\mu}(t) v_1^{\nu}(t) \delta^3[\boldsymbol{x} - \boldsymbol{y}_1(t)] + 1 \leftrightarrow 2. \tag{6.3}$$

Here, m_i are the masses of each body, $\boldsymbol{y}_i$ the positions and v_i^{μ} the four velocities. γ_i is given by

$$\gamma_i = \frac{1}{\sqrt{g_i (g_{\alpha\beta})_i (v_i^{\alpha} v_i^{\beta}/c^2)}}, \tag{6.4}$$

where $g_{\mu\nu}$ is the metric, g its determinant and $i = 1, 2$ [293]. It was previously shown in [292] that noncommutative corrections to the expression 6.3 can be found by considering that the black holes are sourced by a massive real scalar field ϕ and incorporating the noncommuting operators $\hat{x}^{\mu}$ by replacing the product of any two functions with a Moyal product. It was found that the energy-momentum tensor, including noncommutative corrections, can be written as

$$\begin{aligned} T^{\mu\nu}_{\text{NC}}(\boldsymbol{x}, t) = {} & m \gamma_L(t) v^{\mu}(t) v^{\nu}(t) \delta^3[\boldsymbol{x} - \boldsymbol{y}_1(t)] + \frac{m^3 \gamma_L^3}{8} v^{\mu} v^{\nu} \Theta^{kl} \partial_k \partial_l \delta^3[\boldsymbol{x} - \boldsymbol{y}_1(t)] \\ & + (\eta^{\mu m} \eta^{\nu n} \partial_m \partial_n - \eta^{\mu\nu} \partial_i \partial^i) \left(\frac{\hbar^2}{4 m \gamma_L} + \frac{m \gamma_L \hbar^2}{32} \Theta^{kl} \partial_k \partial_l \right) \delta^3[\boldsymbol{x} - \boldsymbol{y}_1(t)], \end{aligned} \tag{6.5}$$

where γ_L is the Lorentz factor and we define

$$\Theta^{kl} = \frac{\theta^{0k}\theta^{0l}}{l_p^2 t_p^2} + 2v_p \frac{\theta^{0k}\theta^{pl}}{l_p^3 t_p} + v_p v_q \frac{\theta^{kp}\theta^{lq}}{l_p^4}. \tag{6.6}$$

Here, θ is the noncommutativity parameter defined by Eq. (6.1) while l_p and t_p are the Planck length and time respectively. The second term in Eq. (6.5) is suppressed by a factor of $\hbar^2$ and can be neglected. We will consider the contribution from the first term in Eq. (6.6), which using the convention that a term of order $(v/c)^n$ is of order $(n/2)$PN, enters as a correction at the second Post-Newtonian order (2PN). We will consider only lowest order noncommutative corrections, and thus can make the approximation $\gamma_L = 1$. Then, for a binary system which considers only the lowest order noncommutative corrections, the energy-momentum tensor simplifies to

$$\begin{aligned} T^{\mu\nu}_{\text{NC}}(\mathbf{x}, t) &= m_1 \gamma_1(t) v_1^\mu(t) v_1^\nu(t) \delta^3(\mathbf{x} - \mathbf{y}_1(t)) \\ &+ \frac{m_1^3 \Lambda^2}{8} v_1^\mu(t) v_1^\nu(t) \theta^k \theta^l \partial_k \partial_l \delta^3(\mathbf{x} - \mathbf{y}_1(t)) + 1 \leftrightarrow 2, \end{aligned} \tag{6.7}$$

where we have defined a normalization of the noncommutative tensor, Λ as in Eq. 6.2. In analogy to [292], we follow the standard procedure to arrive at the acceleration, where we consider only the leading order GR contribution and the lowest order noncommutative correction entering at 2PN:

$$a_i = (a_i)_{\text{GR}} - \frac{15 M^3 (1 - 2\nu) \Lambda^2}{8 r^4} \theta^k \theta^l \hat{n}_{ikl}. \tag{6.8}$$

Here, $M = m_1 + m_2$ is the total mass, $\nu = m_1 m_2 / M^2$ is the symmetric mass ratio, and r is the binary separation $r = |\boldsymbol{y}_1 - \boldsymbol{y}_2|$. We have also introduced the quantity $\boldsymbol{n}$ such that $\boldsymbol{n} = (\boldsymbol{y}_1 - \boldsymbol{y}_2)/r$ to define

$$\hat{n}_{ikl} = n_i n_k n_l - \frac{1}{5}(\delta_{kl} n_i + \delta_{il} n_k + \delta_{ki} n_l). \tag{6.9}$$

From the acceleration we can also determine the correction to the GR Lagrangian

$$L = L_{\rm GR} + \frac{3M^3\mu(1-2\nu)\Lambda^2}{8r^3}\theta^k\theta^l\hat{n}_{kl}, \tag{6.10}$$

and the conserved energy:

$$E = E_{\rm GR} - \frac{3M^3\mu(1-2\nu)\Lambda^2}{8r^3}\theta^k\theta^l\hat{n}_{kl}. \tag{6.11}$$

Here, $\mu = m_1m_2/M$ is the reduced mass and

$$\hat{n}_{kl} = n_k n_l - \frac{\delta_{kl}}{3}. \tag{6.12}$$

In these expressions for the acceleration, conserved energy and Lagrangian, the vector $\boldsymbol{\theta}$ acts as a preferred direction and will in general induce precession in the orbital plane. Previous work simplified these expressions for the acceleration, Lagrangian and conserved energy by assuming a constrained case in which the orbital plane is perpendicular to the preferred direction, $\boldsymbol{\theta}$[292]. Given that each binary is expected to be oriented randomly with respect to the preferred direction, the chance of the above assumption being satisfied is extremely low. To overcome this, we perform an orbital averaging procedure as is typically done for precessing [297, 298] and magnetized [299] binaries. We will consider the following relation as an orbital average over the unit vector $\boldsymbol{n}$ and the preferred direction $\boldsymbol{\theta}$ as follows:

$$\overline{(\mathbf{n}\cdot\boldsymbol{\theta})(\mathbf{n}\cdot\boldsymbol{\theta})} = \frac{1}{2}\left(1 - (\hat{\boldsymbol{L}}\cdot\boldsymbol{\theta})^2\right). \tag{6.13}$$

Here, $\hat{\boldsymbol{L}}$ is a unit vector orthogonal to the orbital plane, as the projection of the angular momentum of the binary system. $\hat{\boldsymbol{L}}\cdot\boldsymbol{\theta} = 1$ corresponds to the limiting case in which the preferred direction is perpendicular to the orbital plane. Employing the orbital averaging procedure, we obtain for the acceleration and conserved energy:

$$a_i = (a_i)_{\rm GR} - \frac{15M^3(1-2\nu)\Lambda^2}{8r^4}$$

$$\times \left(n_i (\mathbf{n}\cdot\boldsymbol{\theta})^2 - \frac{1}{5} n_i - \frac{2}{5}\theta_i (\mathbf{n}\cdot\boldsymbol{\theta}) \right), \tag{6.14}$$

and

$$E = E_{\rm GR} - \frac{M^3 \mu (1-2\nu)\Lambda^2}{16 r^3} \left(1 - 3(\hat{\boldsymbol{L}}\cdot\boldsymbol{\theta})^2 \right). \tag{6.15}$$

6.3 Gravitational Wave Constraints

In this section, we study bounds on noncommutative gravity with gravitational wave observations. We first derive corrections to the gravitational waveform phase. We then find bounds on $\sqrt{\Lambda}$ using posterior samples of selected gravitational wave events produced by LVC.

6.3.1 Gravitational Waveform

From the acceleration and the conserved energy, we can compute noncommutative corrections to the gravitational waveform to constrain the theory. We focus on a quasicircular orbit such that r is a constant. Defining the relative position $\mathbf{y}(t) = \mathbf{y}_1(t) - \mathbf{y}_2(t)$, we can rewrite Eq. (6.14) as

$$\mathbf{a} = -\Omega^2 \mathbf{y} + \mathcal{O}(1/c^5). \tag{6.16}$$

In order to find the leading noncommutatice correction to the waveform, we keep only the leading GR and 2PN NC term. The angular velocity Ω is given by

$$\Omega^2 = \frac{M}{r^3}\left[1 + \frac{3(1-2\nu)\Lambda^2}{16}(1 - 3(\hat{\boldsymbol{L}}\cdot\boldsymbol{\theta})^2)\gamma^2 \right], \tag{6.17}$$

where we have defined the quantity

$$\gamma = \frac{M}{r}. \tag{6.18}$$

Similarly, taking into account both the explicit 2PN contribution to the energy as well as the 2PN correction to Ω^2 in the leading order GR contribution, we have

$$E = -\frac{\mu\gamma}{2}\left[1 - \frac{1}{16}(1-2\nu)\Lambda^2\left(1 - 3(\hat{\boldsymbol{L}}\cdot\boldsymbol{\theta})^2\right)\gamma^2\right]. \tag{6.19}$$

Then, inverting Eq. (6.17) and defining the quantity $x = (M\Omega)^{2/3}$ which corresponds to relative velocity squared, we can rewrite the conserved energy in terms of x:

$$E = -\frac{\mu x}{2}\left[1 - \frac{1}{8}(1-2\nu)\Lambda^2\left(1 - 3(\hat{\boldsymbol{L}}\cdot\boldsymbol{\theta})^2\right)x^2\right]. \tag{6.20}$$

To determine the lowest order noncommutative corrections to the energy radiated by gravitational waves, we assume the energy balance equation

$$\frac{dE}{dt} = -\mathcal{L}. \tag{6.21}$$

Here, $\mathcal{L}$ is the gravitational wave luminosity, which is defined by

$$\mathcal{L} = \left[\frac{1}{5}\frac{d^3I_{ij}}{dt^3}\frac{d^3I_{ij}}{dt^3} + \mathcal{O}(1/c^2)\right], \tag{6.22}$$

where I_{ij} is the traceless mass quadrupole moment. There are two noncommutative corrections to the quadrupole moment. The explicit 2PN noncommutative contribution is time independent, as shown in [292], and will not contribute to the gravitational wave luminosity. Thus, we only need to consider the Newtonian part of I_{ij}, which will lead to noncommutative corrections through the acceleration. For the leading order and 2PN noncommutative corrections to the third derivative of the quadrupole moment, we find

$$\begin{aligned}\dddot{I}_{ij} = &-\frac{8\nu M^2}{r^3}\left(\frac{y_iv_j + v_iy_j}{2}\right)\\ &\times\left[1 + \frac{15}{8}\Lambda^2(1-2\nu)\left((\boldsymbol{n}\cdot\boldsymbol{\theta})^2 - \frac{1}{5}\right)\gamma^2\right]\\ &+\frac{9\nu M^4}{4r^4}\Lambda^2(1-2\nu)(\boldsymbol{n}\cdot\boldsymbol{\theta})(\theta_iv_j + \theta_jv_i).\end{aligned} \tag{6.23}$$

Squaring and keeping only the relevant lowest order terms, we find after orbital averaging and inserting the result into Eq. (6.22) that the full expression for the luminosity is

$$\mathcal{L} = \frac{32}{5}\nu^2 x^5 \left[1 + \frac{\Lambda^2(1-2\nu)}{32}\left(23 - 39(\hat{\boldsymbol{L}}\cdot\boldsymbol{\theta})^2\right)x^2\right]. \tag{6.24}$$

It is then straightforward to determine the evolution of the orbital phase of the binary system. We define a new parameter

$$\Theta \equiv \frac{\nu}{5GM}(t_c - t), \tag{6.25}$$

where t_c is the coalescence time, such that the energy balance equation can be written as

$$\frac{dE}{dx}\frac{dx}{d\Theta} = \frac{5M}{\nu}\mathcal{L}. \tag{6.26}$$

This can then be solved order by order to find

$$x = \frac{1}{4}\Theta^{-1/4}\left\{1 - \frac{\Lambda^2(1-2\nu)}{1024}[35 - 75(\hat{\boldsymbol{L}}\cdot\boldsymbol{\theta})^2]\Theta^{-1/2}\right\}. \tag{6.27}$$

We then invert this expression for x to find Θ,

$$\Theta = \frac{1}{256x^4}\left\{1 - \frac{\Lambda^2(1-2\nu)}{16}\left[35 - 75(\hat{\boldsymbol{L}}\cdot\boldsymbol{\theta})^2\right]x^2\right\}. \tag{6.28}$$

Θ is related to the orbital phase by the following

$$\frac{d\phi}{d\Theta} = -\frac{5}{\nu}x^{3/2}, \tag{6.29}$$

which can easily be solved to find

$$\phi = -\frac{x^{-5/2}}{32\nu}\left\{1 - \frac{5}{32}\Lambda^2(1-2\nu)\left[35 - 75(\hat{\boldsymbol{L}}\cdot\boldsymbol{\theta})^2\right]x^2\right\}. \tag{6.30}$$

Then, as we have assumed that the velocity of each binary component is small compared to c, we may use the stationary phase approximation (SPA) [300], under which the phase of

the waveform in Fourier domain can be written as

$$\psi(f) = 2\pi f t_f - \frac{\pi}{4} - \Phi(t_f). \tag{6.31}$$

t_f is the time such that $d\Phi(t_f)/dt = f$. It can be found from (6.28), and $\Phi(t_f)$ is found from (6.30) to obtain the full expression for the inspiral phase including the leading order term and explicit 2PN noncommutative correction:

$$\begin{aligned} \psi_I(f) = 2\pi f t_c - \phi_c - \frac{\pi}{4} + \frac{3}{128\nu}\left(\pi M f\right)^{-5/3} \\ \times \left\{1 - \frac{5}{16}\Lambda^2(1-2\nu)\left[35 - 75(\hat{\boldsymbol{L}}\cdot\boldsymbol{\theta})^2\right]\left(\pi M f\right)^{4/3}\right\}. \end{aligned} \tag{6.32}$$

This expression follows the standard PN waveform format,

$$\psi_I(f) = 2\pi f t_c - \phi_c - \frac{\pi}{4} + \frac{3}{128\nu}\sum_{j=0}^{4}\varphi_j\left(\pi M f\right)^{(j-5/3)}. \tag{6.33}$$

We will be interested in the φ_4 coefficient, which enters at 2PN. With the NC correction and the full 2PN GR contribution [301], φ_4 is

$$\begin{aligned} \varphi_4 =& \frac{15293365}{508032} + \frac{27145}{504}\nu + \frac{3085}{72}\nu^2 \\ & - \frac{5}{16}\Lambda^2(1-2\nu)\left[35 - 75(\hat{\boldsymbol{L}}\cdot\boldsymbol{\theta})^2\right]. \end{aligned} \tag{6.34}$$

We can then define the fractional deviation from GR as

$$\begin{aligned} \delta\varphi_4^{\rm NC} \equiv& \frac{\varphi_4^{\rm NC}}{\varphi_4^{\rm GR}} \\ =& \frac{158760(1-2\nu)}{4353552\nu^2 + 5472432\nu + 3058673} \\ & \times \left[-7 + 15(\hat{\boldsymbol{L}}\cdot\boldsymbol{\theta})^2\right]\Lambda^2. \end{aligned} \tag{6.35}$$

We now employ this result to constrain the quantity $\left[-7 + 15(\hat{\boldsymbol{L}}\cdot\boldsymbol{\theta})^2\right]\Lambda^2$ from gravitational wave events.

6.3.2 Bounds on $\sqrt{\Lambda}$

Now that we have obtained the expression for the noncommutative correction to φ_4, it is straightforward to compute bounds. However, one issue we still face is the presence of ν, the symmetric mass ratio, in the expression $\delta\varphi_4^{NC}$. One could simply take the central values given for each binary component mass to compute ν, however this method lacks in precision, as it does not take into account the uncertainties in the binary masses. As an alternative, we will follow the method outlined in [276] and make use of the LVC posterior samples for multiple events in order to obtain 90% confidence bounds on the noncommutative parameter. This follows from the LVC approach [273, 274] in which Markov-Chain Monte-Carlo simulations are performed to obtain posterior distributions of the binary parameters. This theory-independent approach allows one to test GR and constrain non-GR theories in a systematic way.

We use posterior samples from the GWTC-1 catalog for gravitational wave events GW 151226, GW170608 and GW170814 [302, 273], as well as the binary neutron star event GW170817, for which posterior samples are also available [3, 274]. Data for events GW150914 and GW170104 are also available, however these two events are characterized by large masses and thus a short inspiral period. This makes it difficult to reliably probe non-GR effects through corrections to the waveform [269], thus we do not include constraints from these events.

Inverting Eq. (6.35) allows us to obtain an expression for $\left(-7+15(\hat{\boldsymbol{L}}\cdot\boldsymbol{\theta})^2\right)\Lambda^2$ in terms of $\delta\varphi_4$, m_1 and m_2. Then, using posterior samples for the two waveform templates IMRPhenomPv2 (IMRP) and SEOBNRv4 (SEOB), we are able to plot the histograms and probability distribution functions (PDFs) for each event, shown in Fig. 6.1.

From the PDFs for each event, we calculate 90% constraints on $\Lambda^2[-7+15(\hat{\boldsymbol{L}}\cdot\boldsymbol{\theta})^2]$ as an upper and lower bound. We can then use these upper and lower bounds to constrain $\sqrt{\Lambda}$ as a function of $\hat{\boldsymbol{L}}\cdot\boldsymbol{\theta}$. These constraints are shown in Fig. 6.2 for both waveform templates. From Fig. 6.2, we see that there is a region of the $\hat{\boldsymbol{L}}\cdot\boldsymbol{\theta}$ plane in which we cannot constrain the noncommutativity parameter, specifically when $\hat{\boldsymbol{L}}\cdot\boldsymbol{\theta}=\sqrt{7/15}$. However, given that we are

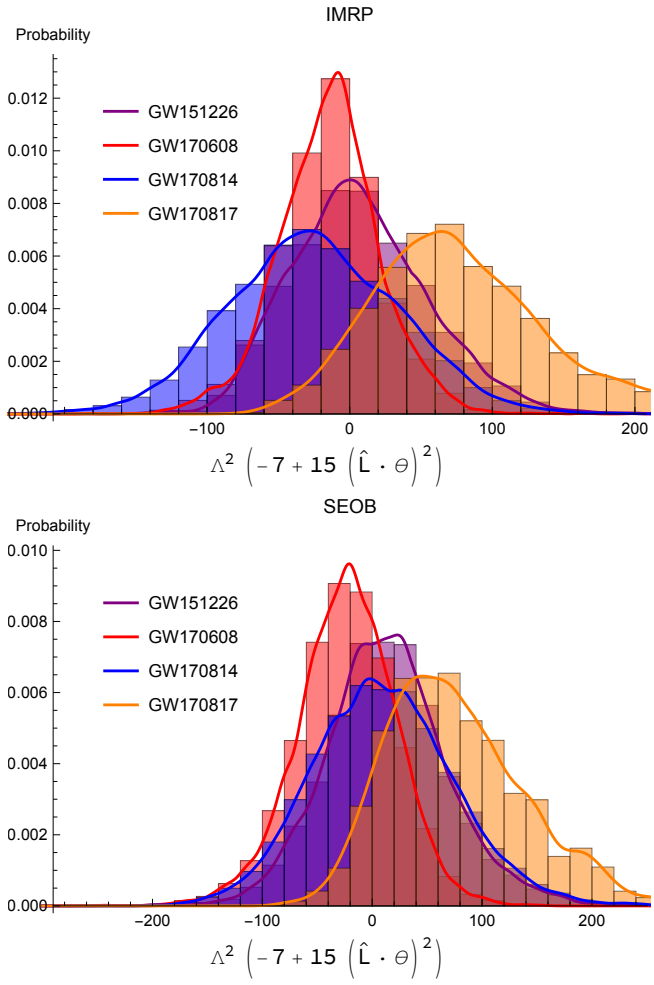

Figure 6.1: Posterior distributions of $\Lambda^2(-7+15(\hat{\boldsymbol{L}}\cdot\boldsymbol{\theta})^2)$ for various gravitational wave events derived from the posterior samples using the IMRP (left) and SEOB (right) waveform templates.

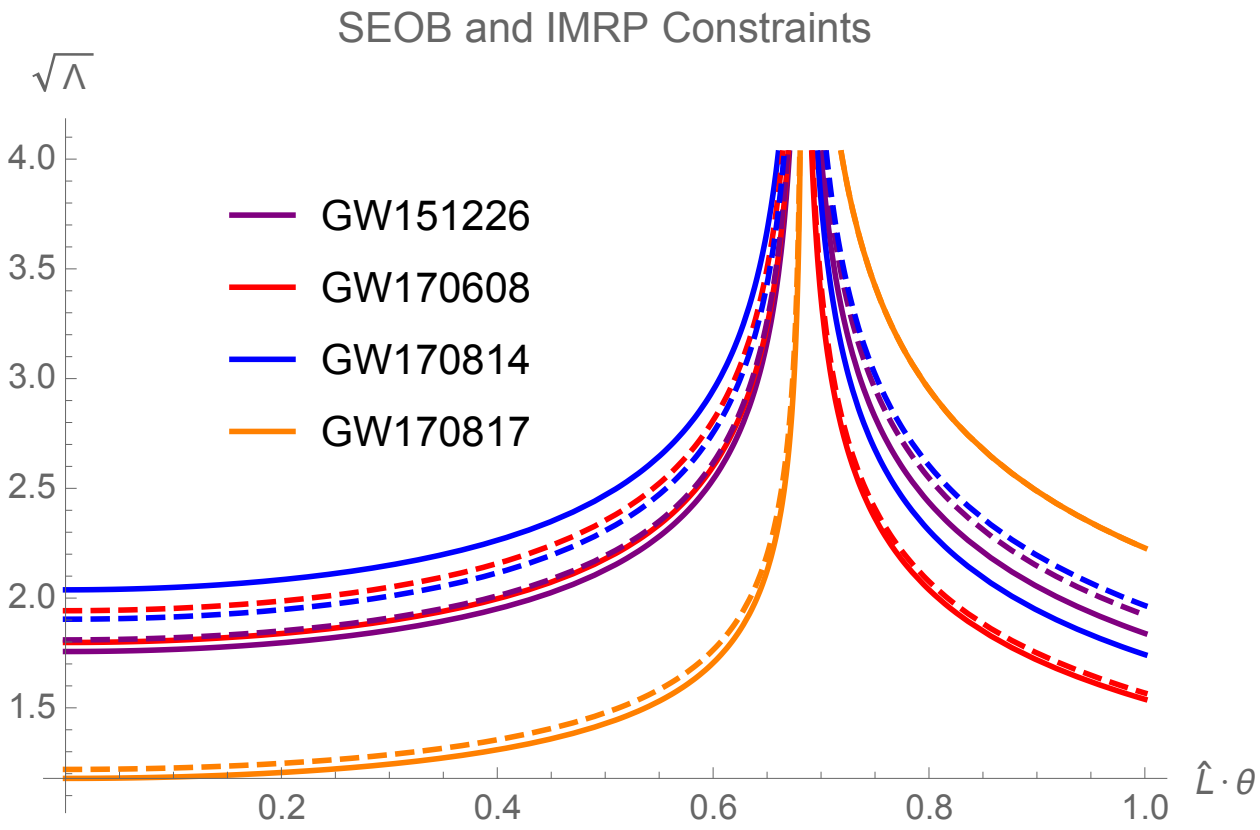

Figure 6.2: Constraints on the noncommutative parameter Λ for each gravitational wave event from SEOB (dashed) and IMRP (solid) waveform templates.

considering multiple gravitational wave events and $\hat{\boldsymbol{L}} \cdot \boldsymbol{\theta}$ varies from one binary to another, statistically the chance that each of those events would be specifically at $\hat{\boldsymbol{L}} \cdot \boldsymbol{\theta} = \sqrt{7/15}$ is low, thus we expect we can still place meaningful bounds. In total, we can see that the 90% confidence constraints on $\sqrt{\Lambda}$ as a function of $\hat{\boldsymbol{L}} \cdot \boldsymbol{\theta}$ is constrained to be of order unity, in agreement with [292].

6.4 Binary Pulsar Constraints

We now turn to constraints on the noncommutativity tensor from the double pulsar binary system PSR J0737-3039A/B [280]. We first derive noncommutative corrections to the pericenter precession. We then find bounds on $\sqrt{\Lambda}$ using the double pulsar system.

6.4.1 Pericenter Precession

Beginning from the acceleration, Eq. (6.14), we can easily calculate the correction to the pericenter precession to provide another independent bound on $\sqrt{\Lambda}$. We will treat the noncommutative correction to the acceleration as a perturbing acceleration $\delta\boldsymbol{a}$. We can then define the orbital parameters following a standard formulation of osculating orbits explained e.g. in [303] and find the correction to the pericenter precession, given by

$$\frac{d\omega}{dt} = \frac{1}{e}\sqrt{\frac{p}{M}}\Bigg[-\cos f\mathcal{R} + \frac{2+e\cos\bar{f}}{1+e\cos\bar{f}}\sin\bar{f}\mathcal{S} - e\cot\iota\frac{\sin(\omega+\bar{f})}{1+e\cos\bar{f}}\mathcal{W}\Bigg]. \tag{6.36}$$

The relevant orbital elements here are the eccentricity e, the inclination ι, the nodal angle Ω, the pericenter angle ω and the semilatus rectum p, defined by $p = a(1-e^2)$ where a is the semi-major axis. Then, ϕ is the orbital phase as measured from the ascending node, and $\bar{f}$ is the true anomaly, defined by $\bar{f} \equiv \phi - \omega$. Here the noncommutative correction to the radial, cross-track and out-of-plane components of the perturbing acceleration, $\mathcal{R}, \mathcal{S}$, and $\mathcal{W}$

are given by

$$\mathcal{R}_{\rm NC} = -\frac{9M^3(1-2\nu)\Lambda^2}{8r^4}\left((\mathbf{n}\cdot\boldsymbol{\theta})^2 - \frac{1}{3}\right), \tag{6.37}$$

$$\mathcal{S}_{\rm NC} = \frac{3M^3(1-2\nu)\Lambda^2}{4r^4}(\boldsymbol{\lambda}\cdot\boldsymbol{\theta})(\boldsymbol{n}\cdot\boldsymbol{\theta}), \tag{6.38}$$

$$\mathcal{W}_{\rm NC} = \frac{3M^3(1-2\nu)\Lambda^2}{4r^4}(\hat{\boldsymbol{h}}\cdot\boldsymbol{\theta})(\boldsymbol{n}\cdot\boldsymbol{\theta}), \tag{6.39}$$

where $\boldsymbol{\lambda}$ is defined as $\partial\boldsymbol{n}/\partial\phi$ and $\hat{\boldsymbol{h}} = \boldsymbol{n}\times\boldsymbol{\lambda}$. Expanding out these expressions in Cartesian coordinates in the equations of motion yields a complicated expression that can be further simplified as in [304] by introducing the variables

$$\boldsymbol{e}_P \equiv \boldsymbol{n}|_{\phi=\omega} = \boldsymbol{e}_\Omega\cos\omega + \boldsymbol{e}_\perp\sin\omega, \tag{6.40}$$

$$\boldsymbol{e}_Q \equiv \boldsymbol{\lambda}|_{\phi=\omega} = -\boldsymbol{e}_\Omega\sin\omega + \boldsymbol{e}_\perp\cos\omega, \tag{6.41}$$

$$\hat{\boldsymbol{h}} \equiv \boldsymbol{e}_P\times\boldsymbol{e}_Q = \boldsymbol{e}_\Omega\times\boldsymbol{e}_\perp. \tag{6.42}$$

Here, $\boldsymbol{e}_P$ is a unit vector pointing towards the pericenter and $\boldsymbol{e}_Q = \hat{\boldsymbol{h}}\times\boldsymbol{e}_P$. $\boldsymbol{e}_\Omega$ is a unit vector which points along the ascending node, and $\boldsymbol{e}_\perp = \hat{\boldsymbol{h}}\times\boldsymbol{e}_\Omega$. $\boldsymbol{n}$ and $\boldsymbol{\lambda}$ can be analogously translated into the P, Q, and h coordinates.

Next, we integrate Eq. (6.36) from 0 to 2π to find the noncommutative correction to $\Delta\omega$. We find

$$\begin{aligned}\Delta\omega_{\rm NC} = &-\frac{3\pi M^2\Lambda^2(1-2\nu)}{8p}[2-3\theta_P^2-3\theta_Q^2+2(\hat{\boldsymbol{L}}\cdot\boldsymbol{\theta})\cot\iota]\\ &\times(\theta_p\cos\omega+\theta_Q\sin\omega).\end{aligned} \tag{6.43}$$

In this expression there is both explicit ω dependence, as well as implicit ω dependence in θ_p and θ_Q. Thus, it is more enlightening to express everything in terms of $\boldsymbol{e}_\Omega$ and $\boldsymbol{e}_\perp$. We can then expand $\omega = \omega_0 + \omega'\phi$ and integrate over ϕ. For ω', it is sufficient to consider the GR contribution only since $\Delta\omega_{\rm NC}$ above is already proportional to Λ^2. Noting that $\theta_\Omega^2 + \theta_\perp^2 + (\hat{\boldsymbol{L}}\cdot\boldsymbol{\theta})^2 = 1$ and that for the J0737-3039A/B system, $\iota \approx \pi/2$, we obtain the

correction to the pericenter precession as

$$\Delta\omega_{\rm NC} = \frac{3\pi M^2\Lambda^2(1-2\nu)}{8p^2}\left[1-3(\hat{\boldsymbol{L}}\cdot\boldsymbol{\theta})^2\right]. \tag{6.44}$$

Then, the noncommutative correction to the observable quantity of pericenter precession $\dot{\omega}$, which can be found by dividing $\Delta\omega$ by the orbital period, P_b is

$$\dot{\omega}_{\rm NC} = \frac{3}{16}\frac{M^{4/3}}{(1-e^2)^2}\left(\frac{P_b}{2\pi}\right)^{-7/3}\Lambda^2(1-2\nu)\left[1-3(\hat{\boldsymbol{L}}\cdot\boldsymbol{\theta})^2\right], \tag{6.45}$$

where we have used Kepler's law to write p^2 in terms of the orbital period. Adding this to the GR expression for $\dot{\omega}$ [305] we obtain

$$\begin{aligned}\dot{\omega} =& 3\left(\frac{P_b}{2\pi}\right)^{-5/3}\frac{M^{2/3}}{1-e^2}\left\{1+\frac{1}{16}\frac{1}{1-e^2}\left(\frac{P_b}{2\pi M}\right)^{-2/3}\right.\\ &\left.\times\Lambda^2(1-2\nu)\left[1-3(\hat{\boldsymbol{L}}\cdot\boldsymbol{\theta})^2\right]\right\}.\end{aligned} \tag{6.46}$$

For completeness, we present the noncommutative corrections to other orbital elements in Appendix 6.A.

6.4.2 Bounds on $\sqrt{\Lambda}$

We now derive constraints on $\sqrt{\Lambda}$ with the double pulsar system PSR J0737-3039A/B. We wish to use $\dot{\omega}$ to constrain the theory. To do so, we need to determine the masses from other observables. Here, we use the Shapiro delay s, masss ratio R, and the mass functions f_A. The noncommutative correction to these observables enter through the Kepler's law at 2PN or higher (see [306] for a similar analysis when the metric is modified at 1PN order within the parameterized PN formalism), while the one in $\dot{\omega}$ in Eq. (6.46) enters at 1PN order. This justifies us to use the GR expressions for s, R and f_A to determine the masses and use $\dot{\omega}$ to test the noncommutative gravity.

Figure 6.3 shows these observables plotted as a function of the pulsar masses. The GR

expressions for R, s, and the region for which $\sin\iota$ (obtained from the mass function measurements) is less than one are plotted. The overlapping shaded region corresponds to the allowed mass parameter space from these measurements. Any correction to $\dot{\omega}$ must remain within the region of overlap. The upper and lower bounds for $\dot{\omega}$ correspond to variations in the expression $\Lambda^2\left[1-3(\hat{\boldsymbol{L}}\cdot\boldsymbol{\theta})^2\right]$ such that the $\dot{\omega}$ curve marginally passes through the overlapping region. The thickness in each of the curves corresponds to the uncertainty in the $\dot{\omega}$ measurement and the two curves correspond to the upper and lower bounds on $\Lambda^2\left[1-3(\hat{\boldsymbol{L}}\cdot\boldsymbol{\theta})^2\right]$. We find that the acceptable range for the noncommutative contribution is

$$-15600 \lesssim \Lambda^2\left[1-3(\hat{\boldsymbol{L}}\cdot\boldsymbol{\theta})^2\right] \lesssim 1100. \tag{6.47}$$

Then, as we did in the gravitational wave analysis, taking this upper and lower bound, we can plot $\sqrt{\Lambda}$ as a function of $(\hat{\boldsymbol{L}}\cdot\boldsymbol{\theta})$ as in Fig. 6.4. We can see that there is again a particular value of $(\hat{\boldsymbol{L}}\cdot\boldsymbol{\theta}) = \sqrt{1/3}$ that we are not able to place a constraint as was the case for the GW analysis, however we are still able to place bounds for the rest of the range. We find that the binary pulsar bounds are actually less stringent than those found from the gravitational wave events by approximately an order of magnitude. However, these constraints remain consistent with the general statement that the noncommutativity parameter must be of order unity.

6.5 Conclusion

We have explored noncommutative gravity in light of observations from LVC gravitational wave events as well as the binary pulsar system J0737-3039A/B. We have focused on the lowest order noncommutative effects entering at 2PN in the binary system acceleration. The time component of the noncommutative tensor, θ^{0i} enters as a 2PN correction to the acceleration. When this effect is propagated through, we find that there is a phase shift in the gravitational waveform again entering at 2PN, shifting the φ_4 coefficient. Similarly, in the case of binary pulsar dynamics, we find that the correction to the acceleration leads to

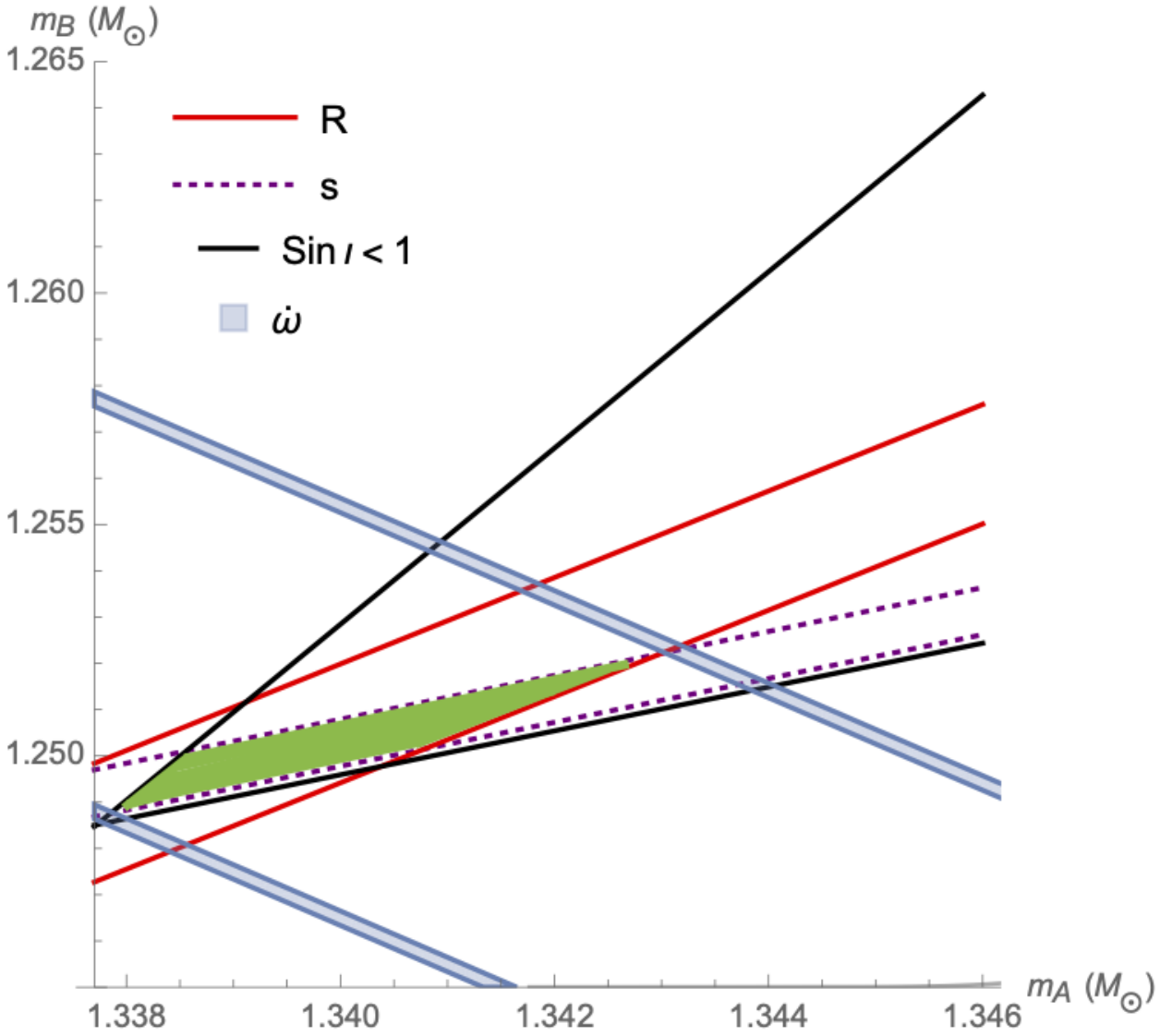

Figure 6.3: Testing noncommutative gravity with the double pulsar binary. The two masses are determined from the mass ratio R, the Shapiro delay parameter s and $\sin\iota < 1$ using the GR expressions (since the noncommutative corrections to these observables enter at higher PN orders than that for $\dot{\omega}$), with the allowed region shown by the green shade. We then vary the noncommutative parameter Λ in $\dot{\omega}$ such that it is consistent with the green shaded region to determined the bound on Λ. The thickness of $\dot{\omega}$ in blue corresponds to the measurement error on $\dot{\omega}$.

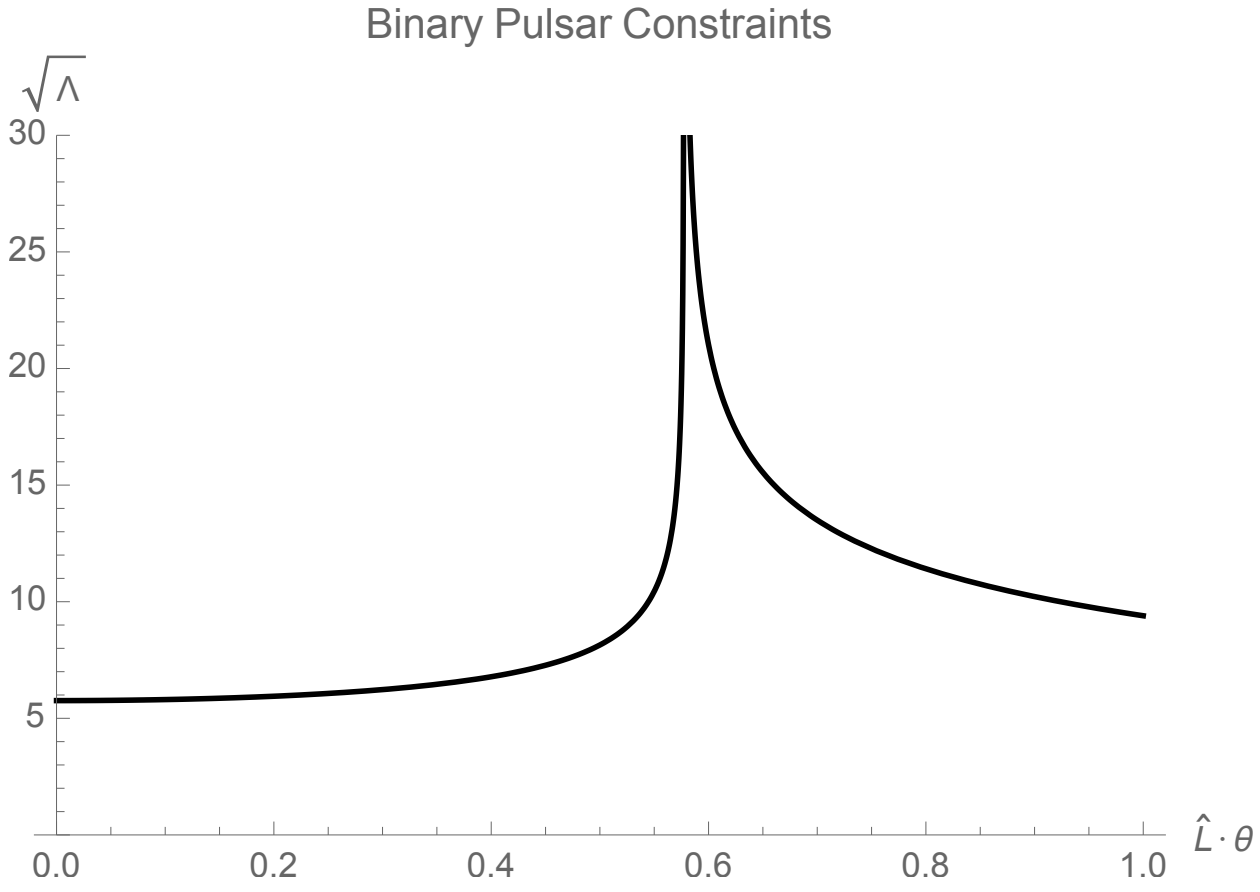

Figure 6.4: Bounds on $\sqrt{\Lambda}$ as a function of $(\hat{\boldsymbol{L}} \cdot \boldsymbol{\theta})$ for the double pulsar binary.

a noncommutative contribution to the pericenter precession.

An updated and more rigorous analysis than in previous work has been performed to use gravitational wave events and the binary pulsar system PSR J0737-3039A/B to constrain the space-time component of the noncommutativity tensor. We find that the gravitational wave events including GW151226, GW170608, GW170814 and GW170817 are more constraining than the binary pulsar event PSR J0363-3039A/B by approximately an order of magnitude. However, the more stringent GW constraints are consistent with previous results, findng that the the quantity $\sqrt{\Lambda}$ is constrained to be of order unity.

A few different avenues exist for future work. For example, it would be interesting to constrain the theory from the preferred frame effect [304]. It would also be of interest to investigate the effects of the spatial component of the noncommutative tensor, θ^{ij}, which enters at 3PN and has potential implications for e.g. string theory. Additionally, it would be valuable to explore the model dependence of the effects that we have discussed, and work towards a more general understanding of how noncommutative gravity may come into play with these observables.

6.A Noncommutative Corrections to Osculating Orbits

In addition to the noncommutative correction to the pericenter precession, $\dot{\omega}$, the noncommutative correction to the acceleration also induces corrections to the other orbital parameters, p, e, i, and Ω, described in Section 6.4. The "Lagrange planetary equations" for these quantities are [303]

$$\frac{dp}{dt} = 2\sqrt{\frac{p^3}{M}}\frac{\mathcal{S}}{1+e\cos\bar{f}}, \tag{6.48}$$

$$\frac{de}{dt} = \sqrt{\frac{p}{M}}\left[\sin\bar{f}\mathcal{R} + \frac{2\cos\bar{f}+e+e\cos^2\bar{f}}{1+e\cos\bar{f}}\mathcal{S}\right], \tag{6.49}$$

$$\frac{d\iota}{dt} = \sqrt{\frac{p}{M}}\mathcal{W}\left(\frac{r}{p}\right)\cos\phi, \tag{6.50}$$

$$\frac{d\Omega}{dt} = \sqrt{\frac{p}{M}}\mathcal{W}\left(\frac{r}{p}\right)\frac{\sin\theta}{\sin\iota}. \tag{6.51}$$

Plugging in the expressions for $\mathcal{S}, \mathcal{W}$, and $\mathcal{R}$ obtained in Section 6.4, it is straightforward to obtain

$$\Delta p_{\text{NC}} = 0, \tag{6.52}$$

$$\Delta e_{\text{NC}} = 0, \tag{6.53}$$

$$\Delta \iota_{\text{NC}} = \frac{3\pi M^2 \Lambda^2 (1-2\nu)}{4p} (\hat{\boldsymbol{L}} \cdot \boldsymbol{\theta})(\theta_p \cos\omega - \theta_Q \sin\omega), \tag{6.54}$$

$$\Delta \Omega_{\text{NC}} = \frac{3\pi M^2 \Lambda^2 (1-2\nu)}{4p} (\hat{\boldsymbol{L}} \cdot \boldsymbol{\theta})(\theta_p \cos\omega + \theta_Q \sin\omega) \csc i. \tag{6.55}$$

As in $\Delta\omega$ there is both explicit and implicit ω dependence in these expressions. Using the same expansion method, we obtain for the noncommutative contributions to the orbital parameters:

$$\Delta p_{\text{NC}} = 0, \tag{6.56}$$

$$\Delta e_{\text{NC}} = 0, \tag{6.57}$$

$$\Delta \iota_{\text{NC}} = \frac{3\pi M^2 \Lambda^2 (1-2\nu)}{4p^2} (\hat{\boldsymbol{L}} \cdot \boldsymbol{\theta}) \theta_\Omega, \tag{6.58}$$

$$\Delta \Omega_{\text{NC}} = \frac{3\pi M^2 \Lambda^2 (1-2\nu)}{4p^2} (\hat{\boldsymbol{L}} \cdot \boldsymbol{\theta}) \theta_\perp \csc i. \tag{6.59}$$

Part III

Black Holes as a Probe of Modified Gravity

Chapter 7

The Chern-Simons Caps for Rotating Black Holes

7.1 Introduction and outline

In this last section, we turn towards a discussion of black holes in modified gravity. We consider another string theory inspired modified gravity theory, dynamical Chern-Simons gravity. Dynamical Chern-Simons (dCS) gravity [307, 308] modifies the Einstein-Hilbert action with the addition of a parity-violating Chern-Simons form coupled to a derivative of a pseudo-scalar field. dCS gravity is not an arbitrary extension of general relativity (GR), but rather has physical roots in particle physics [309] and string theory [310, 311, 312]. dCS gravity naturally emerges as an anomaly-canceling term through the Green-Schwarz mechanism [313]. It is often the case that the scale at which the dCS term becomes significant is inseparable from the scale where other higher dimensional terms become significant, too.

In this work we regard the stand-alone dCS action as a low energy effective field theory. In order for us to be able to keep the dCS term in the action, while neglecting an infinite number of the Planck mass suppressed terms, we require that the scale where the CS term becomes relevant is much smaller than the Planck mass. We specify a field theory mechanism that can lead to such a hierarchy of scales without unnatural fine tunings, and discuss a broad

range of the parameter space where our approach is justified. The above discussions are presented in Section 2.

Within the range of validity of the effective field theory we then look for certain novel characteristics of rotating black hole solutions in Section 3. Previous work has shown that dCS gravity admits some solutions of GR without any obstruction, while predicting modifications to GR solutions that lack a sufficiently high degree of symmetry [314, 315, 316, 317]. In particular, the dCS theory supplies an additional term in the Einstein equation, which can be thought of as a new "stress-energy tensor" in the right-hand side of the equation. Since this new term descends from a quantum anomaly, it does not have to obey the classical positivity conditions. The latter feature manifests itself in the properties of the solutions of the theory that have a nonzero new "stress-energy tensor." Such are the rotating black hole solutions carrying dCS pseudoscalar hair [318, 319, 320].

We show, in Section 3, that the rotating black holes possess a novel geometric structure due to the dCS term. In particular, the solutions get endowed with two, cap-like domains, emanating from the north and south poles of the black holes expressed in the standard Boyer-Lindquist coordinates. These new domains, referred to here as "CS caps," extend out to a distance that is approximately a few percent of the black hole's size. The CS caps have an unusual equation of state, which leads to the violation of the focusing condition for geodesics.

While the CS caps of the rotating black holes may have some interesting observational consequences (to be investigated in subsequent works), the fact that they violate the focusing condition calls for rethinking of the Hawking-Penrose (HP) theorem [321, 322], as we discuss in Section 4. According to our findings, the HP theorem cannot be applied to geodesics of external probe matter placed within the CS caps, where the focusing condition is violated. While this fact itself says nothing about the singularity (non)formation for external matter in those domains, it nevertheless represents an existence proof of a stable spatial domains where the main condition of the HP theorem is not fulfilled.

We use the following conventions in this chapter: we work exclusively in four spacetime dimensions with signature $(-,+,+,+)$, with Latin letters $(a,b,\ldots,h)$ ranging over all spacetime coordinates; round and square brackets around indices denote symmetrization and anti-symmetrization respectively, namely $T_{(ab)} := \frac{1}{2}(T_{ab}+T_{ba})$ and $T_{[ab]} := \frac{1}{2}(T_{ab}-T_{ba})$; partial derivatives are sometimes denoted by commas, e.g. $\partial\theta/\partial r = \partial_r\theta = \theta_{,r}$. The Einstein summation convention is employed unless otherwise specified.

7.2 DCS as an Effective Field Theory

Let us begin by defining the action of dCS gravity [314]:

$$S = \int d^4x\sqrt{-g}\left[\kappa R + \frac{\sigma}{4\mu}\ {}^*R\,R - \frac{1}{2}\left(\nabla_a\sigma\right)\left(\nabla^a\sigma\right)\right], \tag{7.1}$$

where $\kappa = (16\pi G_N)^{-1}$, g is the determinant of the metric, the integral extends over all spacetime, R is the Ricci scalar, and the pseudo-scalar field σ couples to the Pontryagin invariant ${}^*R\,R$, defined as follows

$${}^*R\,R := {}^*R^a{}_b{}^{cd}R^b{}_{acd}\,, \tag{7.2}$$

where the dual Riemann-tensor is given by

$${}^*R^a{}_b{}^{cd} := \frac{1}{2}\epsilon^{cdef}R^a{}_{bef}\,, \tag{7.3}$$

with ϵ^{cdef} the 4-dimensional Levi-Civita tensor[1]. The Pontryagin term [Eq. (8.3)] can be expressed as the divergence

$$\nabla_a K^a = \frac{1}{4}\,{}^*R\,R \tag{7.4}$$

of the Chern-Simons topological current (Γ is the Christoffel connection),

$$K^a := \epsilon^{abcd}\left(\Gamma^n{}_{bm}\partial_c\Gamma^m{}_{dn} + \frac{2}{3}\Gamma^n{}_{bm}\Gamma^m{}_{cl}\Gamma^l{}_{dn}\right). \tag{7.5}$$

[1] We prefer to work with tensors rather than with tensor densities, so some expressions might appear to differ by factors of $\sqrt{-g}$ from [307].

Hence, the interaction term of σ can be rewritten, up to a total derivative, as follows

$$-\frac{1}{\mu}\int d^4x\sqrt{-g}\, g_{ab}\,\partial^a\sigma\, K^b\,. \tag{7.6}$$

We will use interchangeably the term in Eq. (7.6) with its counterpart in Eq. (7.1), keeping in mind that there is a total derivative distinguishing the two. Note that the action in Eq. (7.6) makes the shift symmetry of the pseudoscalar field manifest, $\sigma \to \sigma + const.$ In this formulation, the shift symmetry current on a non-interacting theory, $\partial_b\sigma$, couples to the Chern-Simons current, K^b, thus the name "Chern-Simons modified gravity"[2].

General Relativity is not a renormalizable theory, and hence, the action in Eq. (7.1) could only be part of an effective field theory that contains an infinite number of higher curvature terms, proportional to R^2, R^3 and so on, and their derivatives, suppressed by the respective powers of the Planck mass, $M_P = 1/\sqrt{G_N}$. In order for the higher dimensional terms to be negligible as compared to the term $\sigma\, {}^*R\, R/(4\mu)$ kept in Eq. (7.1), we should require

$$\mu << M_P\,. \tag{7.7}$$

Since the term $\sigma\, {}^*R\, R/(4\mu)$ is not renormalizable either, its presence would then imply some new physics at the scale $\mu << M_P$. The new physics would generate the term $\sigma\, {}^*R\, R/(4\mu)$ at low energies, $E << \mu$, while above the energy scale μ, the term $\sigma\, {}^*R\, R/(4\mu)$ would ascend to certain renormalizable terms.

In particular, the term $\sigma\, {}^*R\, R/(4\mu)$ can be generated by the gravitational axial anomaly [323]. At energies above μ, one starts with a gravitational theory of a massless fermion Ψ, coupled to a complex scalar field Σ with strength set by a Yukawa coupling λ,

$$\lambda\,(\bar{\Psi}_L\Sigma\Psi_R + \bar{\Psi}_R\Sigma^+\Psi_L)\,. \tag{7.8}$$

Furthermore, the complex scalar has its own conventional kinetic term and a quartic potential. All these term are symmetric with respect to a global $U(1)$ axial Peccei-Quinn (PQ)

[2] If $\nabla_a K^a$ is converted into $1/\sqrt{g}\,\partial_a(\sqrt{g}K^a)$ the results (2.4) and (2.5) of [307] are recovered.

transformations

$$\Sigma \to e^{i\beta}\Sigma, \quad \Psi_R \to e^{-i\beta/2}\Psi_R, \quad \Psi_L \to e^{i\beta/2}\Psi_L\,. \tag{7.9}$$

The PQ symmetry is spontaneously broken by a nonzero vacuum expectation value of the scalar $\langle\Sigma\rangle = \mu$, due to the symmetry breaking scalar potential. Both the fermion and modulus of the scalar, $\rho = \sqrt{\Sigma^{+}\Sigma}$, acquire their masses due to the vacuum expectation value $\langle\Sigma\rangle = \mu$. These masses are proportional to the respective coupling constants and the energy scale μ. Furthermore, these massive field can be integrated out below their mass scales. However, the phase of the scalar field, σ, remains massless as it is a Nambu-Goldstone (NG) mode of the spontaneously broken PQ symmetry. At low energies only this massless state is kept, and its low energy action can be deduced by substituting $\Sigma = \mu\exp(\sigma/\mu)$ and calculating the anomalous diagrams, giving rise to the term proportional to $\sigma\, {}^{*}R\, R/4\mu$.

We have already specified that μ is considered to be much smaller than the Planck mass. The question though is how small can μ be. The fermion Ψ and the scalar ρ have masses proportional to μ and would have been accessible to accelerator experiments for $\mu < \ TeV$; however, the fermion and scalar do not couple to any other fields besides gravity, and can only be produced in the accelerators via gravity mediated processes, which are very much suppressed at energies below $\ TeV$.

For low values of μ one may worry about nonlinear interactions of gravitons becoming strong at energies much lower that the Planck mass due to the new vertices introduced by Eq. (7.6). For instance, the four graviton scattering amplitude of GR will be amended by a set of new diagrams using the exchange of σ due to the cubic vertex given by Eq. (7.6). To get a sense of the magnitude of these corrections, we expand over a flat spacetime metric, $g_{ab} = \eta_{ab} + h_{ab}$, and rescale $h \to h/M_P$, to normalize canonically h's kinetic term. As a result, we get from Eq. (7.6) the scaling of the new cubic vertex

$$\frac{\partial\sigma(\partial h)(\partial\partial h)}{\mu M_P^2}\,. \tag{7.10}$$

Thus, the strong scale is given by

$$\Lambda_s = (\mu M_P^2)^{1/3} \,. \tag{7.11}$$

Furthermore, the dCS term in Eq. (7.6) will generate higher order vertices, such as the one containing $\partial\sigma$ and three powers of ∂h, but those terms will be suppressed by the scale, $(\mu\, M_P^3)^{1/4}$, which is higher than Λ_s. All other higher vertices obtained from Eq. (7.6) will give even higher scales, and hence, Λ_s is the lowest one to worry about.[3]

For the value of μ as astonishingly small as the present day Hubble constant, $\mu \sim H_0 \sim 10^{-33}\, eV$, the corresponding value of the strong scale is $\Lambda_s \sim 5 \cdot 10^7\, eV$. The latter is much higher than the scale of $10^{-2} eV$, up to which precision gravity measurements have so far probed deviations from conventional gravity.

What is the range of μ in dCS that is allowed by non perturbative physics? The most stringent constraint on dCS gravity to date was established in Ref. [325], which used the gravitational wave data obtained by the LIGO/Virgo collaboration for the merger of two neutron stars [3], as well as the X-ray data obtained by the NICER collaboration for the pulse profile emitted by a rotating neutron star [326, 327]. This constraint requires that $\mu \gtrsim 4 \times 10^{-50} eV$ (or $\alpha^{1/2} \lesssim 8.5$km, in the notation of the next section) to 90% confidence. Note in passing that binary pulsar observations cannot yet be used to place stringent constraints on dCS gravity because such binaries are widely separated, and thus, the Pontryagin source to the pseudo-scalar field is too small [328].

Before moving on, let us make a final comment about the mass of the pseudoscalar field σ. There is no mass or potential terms associated with the pseudoscalar field σ in Eq. (7.1), since σ is a NG boson of spontaneously broken PQ symmetry. In the perturbative approximation, quantum corrections will not generate a nonzero mass and potential for σ because of the shift symmetry, $\sigma \to \sigma + const.$ However, this symmetry is expected to be broken by non-perturbative quantum gravity effects and the pseudoscalar field would then acquire a mass [329]. The induced mass can be estimated; when the saddle-point approximation for the

[3] One can also realize the Chern-Simons term from a BF theory perspective, see e.g. [324].

quantum gravity path integral is justified, the induced mass ends up being small by an exponential factor, e^{-x} with $x >> 100$ and $\mu << M_P$ [329]. In what follows we will consider distance scales much shorter than the inverse of the induced pseudoscalar mass, and hence we will ignore the small induced mass term in the action.

7.3 CS Caps for Rotating Black Holes

Let us rescale the σ field in Eq. (7.1) as $\sigma = M_P\,\vartheta$, and pull out the overall factor of M_P^2 in front of the action; having done that, let us set $M_P = 1/\sqrt{G_N} = 1$. In these geometric units the dCS gravity action reads [314]:

$$S = \int d^4x\sqrt{-g}\left[\kappa R + \frac{\alpha}{4}\vartheta\ {}^*R\,R - \frac{1}{2}\left(\nabla_a\vartheta\right)\left(\nabla^a\vartheta\right)\right], \tag{7.12}$$

where $\kappa = (16\pi)^{-1}$, and $\alpha \equiv 1/(\mu M_P)$. Therefore, although μ has units of energy in natural units, α has units of km^2 in geometric units.

The modified field equations can be obtained by varying the action in Eq. (8.2) with respect to the metric:

$$G_{ab} + \frac{\alpha}{\kappa}\,C_{ab} = \frac{1}{2\kappa}T_{ab}\,, \tag{7.13}$$

where G_{ab} is the Einstein tensor, and the traceless 'C-tensor' is defined as

$$C^{ab} = \left(\nabla_c\vartheta\right)\ \epsilon^{cde(a}\nabla_e R^{b)}{}_d + \left(\nabla_c\nabla_d\vartheta\right)\ {}^*R^{d(ab)c}\,. \tag{7.14}$$

The stress-energy tensor for the scalar is

$$T_{ab} := \left(\nabla_a\vartheta\right)\left(\nabla_b\vartheta\right) - \frac{1}{2}g_{ab}\left(\nabla_c\vartheta\right)\left(\nabla^c\vartheta\right)\,, \tag{7.15}$$

and we will assume that apart from this scalar field the spacetime is empty. Variation of the

action with respect to the scalar field yields its evolution equation

$$\Box\vartheta = -\frac{\alpha}{4\kappa}\, {}^*R\, R\,, \tag{7.16}$$

where $\Box$ stands for the d'Alembertian operator.

The field equations are given by Eqs. (8.7) and (8.10), but they simplify somewhat in trace-reversed form:

$$R_{ab} = 8\pi \bar{T}_{ab} - 16\pi\alpha C_{ab}, \tag{7.17}$$

because the C-tensor is traceless, $C^a{}_a = 0$, where

$$\bar{T}_{ab} := (\nabla_a\vartheta)\,(\nabla_b\vartheta)\ , \tag{7.18}$$

is the trace-reversed stress-energy tensor of the scalar field. From this formulation, it is clear that in the pure vacuum case, i.e. when $\bar{T}_{ab} = 0$, then the pseudo-scalar field must be a constant and dCS gravity reduces continuously to GR.

When the so-called Pontryagin constraint holds on a subspace of solutions, i.e. when ${}^*R\, R = 0$ on shell, then dCS gravity simplifies significantly. One can show that ${}^*R\, R = 0$ for any spherically symmetric spacetime, regardless of whether it is static or not [317, 330]. If so, the pseudo-scalar field then satisfies an unsourced wave equation, $\Box\vartheta = 0$. If one imposes a "no-cosmological scalar field" boundary condition, i.e. $\nabla_a\vartheta = 0$ at spatial infinity, then $T_{ab} = 0 = C_{ab}$ for stationary solutions. In this case, all spherically symmetric, stationary, spacetimes must be Ricci flat, and one concludes that all spherically symmetric, vacuum solutions in dCS gravity must be identical to those in GR [317]. In particular, this implies that the Schwarzschild metric continues to be a solution of dCS gravity.

When we consider spacetimes that break spherical symmetry, however, then the Pontryagin density does not vanish and GR solutions will not be solutions of dCS gravity. For example, when considering spacetimes that are stationary but axisymmetric, then the Pontryagin density sources a non-trivial scalar field, which then back-reacts on the metric to induce non-GR modifications. Such an analysis can be carried out to find slowly-rotating

black hole solutions in dCS gravity, as done first in [318], and then extended to second-order and fifth order in rotation in [319] and [320] respectively.

Let us consider the dCS gravity solution that represents a stationary and axisymmetric spacetime [318, 319, 320] valid to fifth order in a slow-rotation expansion in Boyer-Lindquist-like coordinates, with ADM angular momentum $J_{\rm ADM} = Ma$ and ADM mass $M_{\rm ADM} = M$. To leading order in $a/M \ll 1$, the modified rotating black-hole solution in dCS gravity using Boyer-Lindquist-like coordinates (t, r, θ, ϕ) is

$$ds^2 = ds^2_K + \frac{5}{4}\zeta M\chi \frac{M^4}{r^4}\left(1 + \frac{12}{7}\frac{M}{r} + \frac{27}{10}\frac{M^2}{r^2}\right)\sin^2\theta dt d\phi\,, \tag{7.19}$$

where ds^2_K is the Kerr solution of general relativity, $\chi = a/M$ is the dimensionless spin parameter, and

$$\zeta = \frac{16\pi\alpha^2}{(G_N M)^4}\,, \tag{7.20}$$

is a dimensionless coupling parameter. The higher order in spin terms introduce modifications to all other components of the metric that can be found in [320], but their expressions to $\mathcal{O}(a^5/M^5)$ are long and un-illuminating, so we will not present them here.

Let us us consider the behavior of both null and timelike geodesics in this spacetime. First, consider a static timelike observer in this spacetime. The tangent to such an observer's geodesic is $k^a_{\rm st} = \gamma_{\rm st}[1, 0, 0, 0]$ and $\gamma_{\rm st}$ is a normalization constant to ensure $k^{\rm st}_a k^a_{\rm st} = -1$. With that in hand, employing Maple and the GRTensorIII software [331], we calculate the quantity whose sign defines whether the geodesic congruences are converging or diverging:

$$\begin{aligned} R_{ab}\, k^a_{\rm st} k^b_{\rm st} = \frac{45}{4}\,\zeta\chi^2\, f\frac{\gamma^8}{M^2}\Bigg[1 + 2c^2_\theta + \frac{40\gamma}{15}\left(1 + \frac{3}{4}c^2_\theta\right) \\ + 6\gamma^2\left(1 + \frac{1}{3}c^2_\theta\right) - \frac{312}{5}\gamma^3 c^2_\theta\Bigg] + \mathcal{O}(\zeta\chi^4)\,, \end{aligned} \tag{7.21}$$

where $f := 1 - 2\gamma$, $\gamma := M/r$, and $c_\theta := \cos\theta$. Similarly, consider a null observer with tangent vector $l^a = [l, g(r,\theta), 0, 0]$, where $g(r,\theta)$ is a function such that the null condition

$l_a l^a = 0$ is satisfied. In this case we have:

$$R_{ab}\, l^a l^b = \frac{25}{32}\,\zeta\chi^2\, f\frac{\gamma^6}{M^2}\left[c_\theta^2 + 4\gamma c_\theta^2 + \frac{72}{5}\gamma^2\left(1+\frac{43}{24}c_\theta^2\right)\right.$$
$$+\frac{192}{5}\gamma^3\left(1+\frac{13}{32}c_\theta^2\right) + \frac{432}{5}\gamma^4\left(1-\frac{1}{15}c_\theta^2\right)$$
$$\left.-\frac{19872}{25}\gamma^5 c_\theta^2\right] + \mathcal{O}(\zeta\chi^4)\,, \tag{7.22}$$

One can check by direct evaluation that both of these quantities are positive definite almost everywhere. In those regions the geodesics will be focusing. However, there are regions where the quantities in Eq. (7.21) and Eq. (7.22) are negative. In particular, when one looks at spacetime regions near the polar axis (i.e. near $\theta = 0$) and close to the horizon, one finds that the above contractions changes their signs. Note that, as we will show below, the location of the ergosphere coincides with the location of the event horizon along the polar axis in this solution, just like it does for the Kerr metric, so static observers do exist right outside the horizon along the polar axis.

Let us discuss these unusual regions further. The considered solution is known to have an event horizon located at

$$r_{\text{EH}} = r_{\text{EH},\mathcal{K}} - \zeta M\left[\frac{915}{28672}\chi^2 + \frac{351479}{13762560}\chi^4 + \mathcal{O}(\zeta\chi^6)\right]\,, \tag{7.23}$$

and an ergosphere whose outer edge is located at

$$r_{\text{ergo}} = r_{\text{ergo},\mathcal{K}} - \zeta M\left[\left(\frac{915}{28672} + \frac{709}{7168}s_\theta^2\right)\chi^2 + \right.$$
$$\left(\frac{351479}{13762560} - \frac{336421}{2408448}s_\theta^2 + \frac{151229}{1605632}s_\theta^4\right)\chi^4$$
$$\left.+\mathcal{O}(\zeta\chi^6)\right]\,, \tag{7.24}$$

where $s_\theta := \sin\theta$, while $r_{\text{EH},\mathcal{K}} = M + M(1-\chi^2)^{1/2}$ and $r_{\text{ergo},\mathcal{K}} = M + M(1-\chi^2 c_\theta^2)^{1/2}$ are the locations of the event horizon and the outer-edge of the ergosphere for the Kerr metric respectively [318, 319, 320]; notice that the outer edges of the ergosphere coincide on the

polar axis $\theta = 0$.

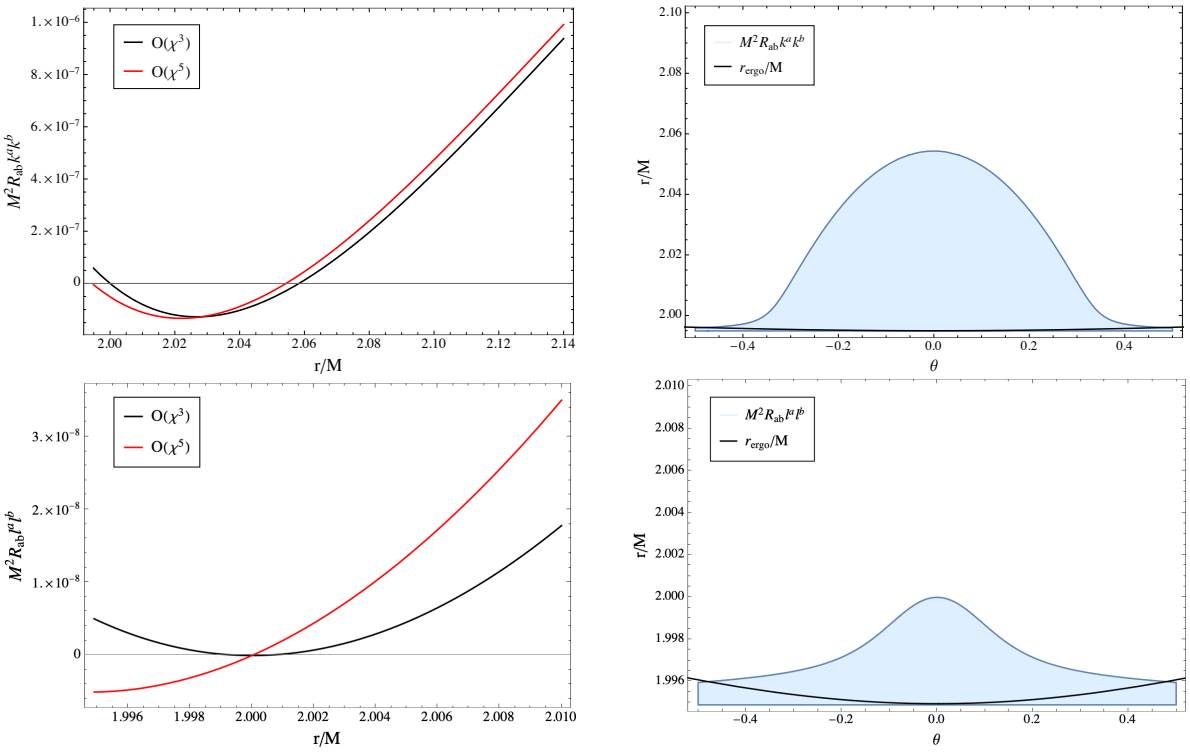

Figure 7.1: (color online) Dimensionless contraction of the Ricci tensor with the tangent vector of timelike (top) and null (bottom) congruences $M^2E[k] = M^2R_{ab}k^ak^b$ and $M^2E[k] = M^2R_{ab}l^al^b$ computed along the ($\theta = 0$) polar axis (left panels) and in the r–θ plane (right panels). In the left panels, the red and blue curves denote $M^2E[k]$ calculated with a BH solution in dCS gravity to third- and fifth-order in rotation, respectively, both for a black hole with dimensionless spin $\chi = 0.1$ and dimensionless dCS coupling $\zeta = 0.1$. In the right panels, we present $M^2E[k]$ computed with a fifth-order in rotation dCS BH metric (blue shaded region) assuming $\chi = 0.1$ and $\zeta = 0.1$, and for comparison, we also present the outer edge of the ergosphere in dCS gravity. Observe that the contractions $R_{ab}k^ak^b$ and $R_{ab}l^al^b$ switch sign close to the horizon, in a cup-shaped region around the polar axis. Note that the x-axis on the right panels is given in θ, not in r/M.

The top left panel of Fig. 7.1 shows the contraction $R_{ab}k^ak^b$ (timelike geodesics) to third- and to fifth-order in the slow-rotation approximation on the polar axis close to but outside of the event horizon. Observe that this contraction flips sign, regardless of the order of the slow-rotation approximation used for the metric. Extending this analysis to all θ, we see that indeed there is a cone shaped region near the horizon extending from the pole up to $\sim 20°$ on either side where the sign of the contraction $R_{ab}k^ak^b$ flips and becomes negative. This is shown in the top right panel of Fig. 7.1 (blue region) with a metric valid to to $\mathcal{O}(\chi^5)$, where we also include the location of the outer edge of the ergosphere (black curve) for comparison.

The bottom left and right panels show the contraction $R_{ab}l^al^b$ (null geodesics) on the

polar axis to third- and fifth-order in rotation, and extended to all θ, respectively. We see that there is a similar, much smaller region close to the horizon where the null contraction flips sign. Note that in order to obtain the negative region, one must go to $\mathcal{O}(\zeta\chi^5)$ in perturbation. We expect that going to higher orders in the perturbative expansion will yield small corrections and will not change the negative result.

The size of the regions of interest do not depend on the value of ζ, which is proportional to the coupling α^2, see Eq. (7.20). In order to remain in the regime of validity of the slow rotation approximation, we must have $\zeta \ll 1$, so we have taken $\zeta = 0.1$ as a representative example in Fig. 7.1. Varying this value changes the magnitude of negativity for the contractions $R_{ab}k^a k^b$ and $R_{ab}l^a l^b$ in the CS caps, but it does *not* change the boundaries of the caps. That is, we have explored versions of Fig. 7.1 evaluated with various values of ζ (e.g. $\zeta = (10^{-3}, 10^{-2}, 10^{-1})$) and in all cases the change in sign occurs roughly along the boundary of the same caps shown in the right panel of that figure (although how negative the contraction is does scale with ζ).

This technical point – that we are necessarily constrained to consider small values of ζ because of the lack of an exact solution – also forces us to consider black holes that are not too small To see this, let us use the definition in Eq. (7.20), and require that $\zeta \leq 0.1$ to find

$$M \geq 3M_\odot \left(\frac{\alpha}{1\text{ km}}\right)^{1/2}, \tag{7.25}$$

or restoring the powers of the Planck mass

$$M \geq 2M_\odot \left(\frac{10^{-47}\ eV}{\mu}\right)^{1/2}. \tag{7.26}$$

If Nature is described by dCS gravity as an effective theory, then depending on Nature's value of μ (or α), our calculations would be valid for black holes of a different mass. More specifically, for our calculations to be valid, the smaller Nature's μ is (or the larger Nature's α is), the heavier the black holes we can consider would have to be.

The above limitation on the BH mass is a result of our small coupling approximation

(ie. $\zeta \ll 1$) when finding slowly rotating BH solutions. However, it might well be that the CS caps are universal for all rotating black holes in the dCS theory. Such an outcome is not ruled out by general arguments of continuity in the value of the parameter ζ, and by the considerations of the focusing theorem in the next section showing that the dCS can in general permit negative values for the contraction in Eq. (7.21), irrespective of the approximation used.

One may be worried that the curvatures close to the horizon are so large that we are exploring these slowly-rotating solutions outside of the regime of validity of the effective field theory, where these solutions are calculated in the first place. The cut-off scale of the theory, i.e. the scale inside which the small-GR-deformation approximation of effective field theory breaks down, can be approximated by computing the Pontryagin density with the approximate black hole solutions. Figure 7.2 presents the Pontryagin density computed with the Kerr metric and with the dCS metric for a slowly-rotating black hole. Observe that the dCS correction to the Pontryagin density, i.e. the term proportional to α^2 in the calculation of R^*R with the dCS metric, exceeds the GR value only deep inside the event horizon for $r/M < 0.75$, and nowhere near the regime where the contraction, $R_{ab}k^a k^b$ flips sign (which from Fig. 7.1 we recall occurs for $2.06 \lesssim r/M \gtrsim 2$ for timelike geodesics).[4]

An agreement emerges between our result and both analytic [318, 319, 320] and numerical [332, 333] studies that have found black hole spacetimes. Those studies found stationary and axisymmetric solutions in dCS gravity that differ from the Kerr spacetime everywhere on the manifold, leading for example to dCS corrections to the location of the event horizon and the ergosphere. These solutions agree with the Kerr metric in that they both posses spacetime regions inside their respective event horizons where curvature invariants diverge, which is why we say these solutions represent black holes. The dCS corrections to the metric, however, become dominant over the GR terms inside the event horizon, as shown in Fig. 7.2, and in particular before reaching the singularity. As usual, the curvature singularities in these modified solutions are outside the validity of the effective theory. It is entirely possible

[4]Even though we are working here in Boyer-Lindquist coordinates, the statement that the curvature becomes large only deep inside the horizon is also true in horizon-penetrating coordinate systems.

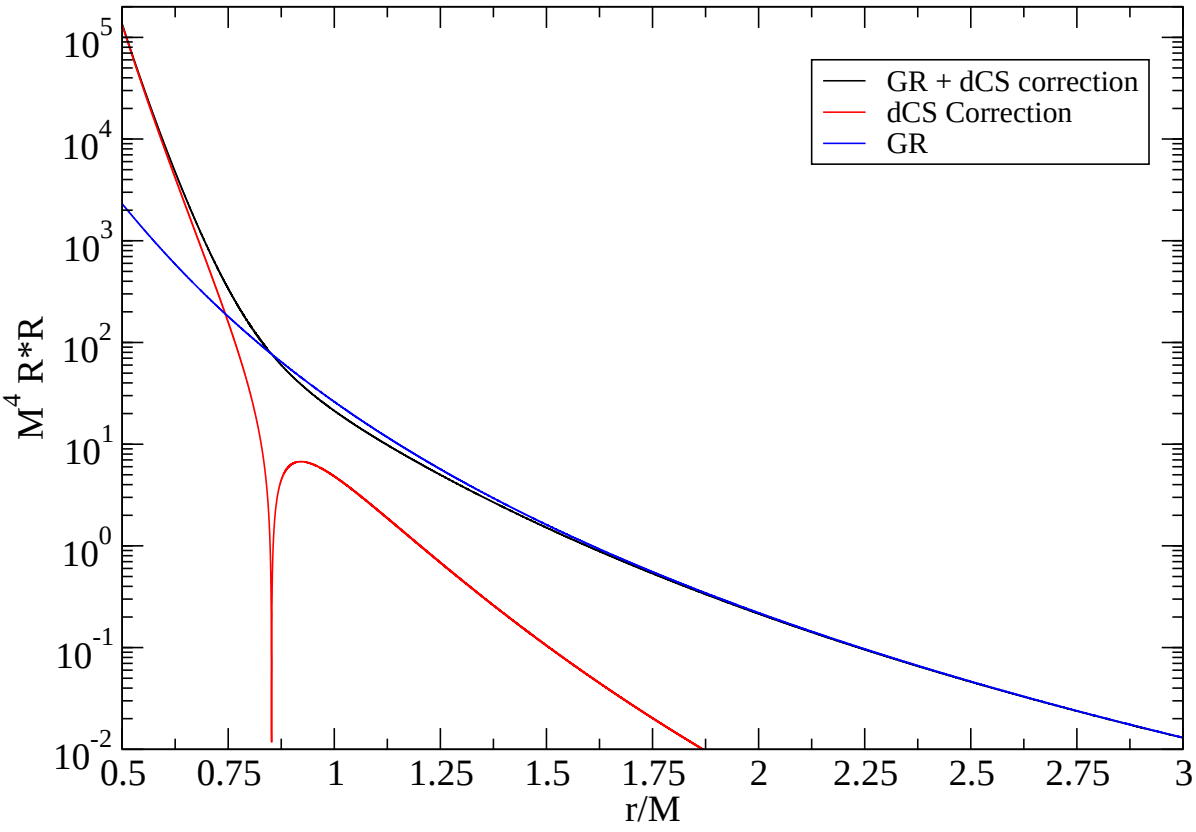

Figure 7.2: (color online) Dimensionless Pontryagin density of a slowly-rotating black hole solution computed to fifth order in slow rotation in GR (blue), in dCS gravity (black) and using only the α^2 correction to the GR solution in dCS gravity (red) for a black hole with spin $\chi = 0.1$ and dCS coupling $\zeta = 0.1$. Observe that the α^2 correction to the Pontryagin density is much smaller than the GR contribution outside the horizon ($r/M \gtrsim 2$), which is precisely where $R_{ab}k^a k^b$ becomes negative.

that these singularities could then be cured by higher order terms in the action that have been neglected. It would be interesting to see if higher curvature corrections related to a stringy excitations in higher dimensions may become relevant near the singularity to resolve it, in the spirit of topological stars [334].

7.4 Geodesic (de)focusing and dCS Gravity

7.4.1 Focusing and the Hawking-Penrose Theorem

To review the well-known focusing theorem [335], one starts from the Ricci identity,

$$(\nabla_a \nabla_b - \nabla_b \nabla_a) k^a = R^a{}_{cab} k^c, \tag{7.27}$$

and derives the Raychaudhuri equation [335],

$$\dot{\Theta} = -\sigma_{ab}\sigma^{ab} - \frac{1}{3}\Theta^2 - E[k]\,, \tag{7.28}$$

for vorticity-free congruences of non-intersecting world lines. The quantity σ_{ab} is the shear tensor of this congruence, while $\Theta = \nabla_c k^c$ is the expansion scalar, and $E[k] := R_{cd}k^c k^d$, where k^c is the timelike or null tangent vector field of the congruence.

The focusing theorem for timelike geodesics states that if the strong-energy condition $\bar{T}_{ab}k^a k^b > 0$ holds, then vorticity-free geodesics will focus in GR. This result is established directly from the Raychaudhuri equation presented above, upon the use of the Einstein equations to write $E[k] = 8\pi \bar{T}_{cd}k^c k^d$, where $\bar{T}_{ab}$ is the trace-reversed stress-energy tensor. Using the Einstein equations and the strong-energy condition, it is obvious that the right-hand side of the Raychaudhuri equation is negative because $E[k] > 0$, which then means that the rate of change of the expansion scalar with respect to the geodesic's affine parameter is negative, and the worldlines will focus within a finite value of the affine parameter, reflecting the attractive nature of gravity. An analogous argument holds for null geodesics, provided that the null energy condition is satisfied.

The focusing theorem leads to the Hawking-Penrose singularity theorem as follows. Consider two events A and B in a globally hyperbolic spacetime which contains a trapped surface, that are connected via a timelike or null curve. If this is the case, there must exist a geodesic of maximal length γ that connects these two points, on which there are no conjugate points. The focusing theorem, however, establishes that all geodesics emanating from A will focus in finite affine parameter, leading to conjugate points. Intuitively, a geodesic cannot be extended beyond a conjugate point, and therefore one cannot reach point B, so the spacetime must be geodesically incomplete. In summary [322]:

Theorem 1(Hawking-Penrose singularity theorem).*If a globally-hyperbolic spacetime contains a non-compact Cauchy hypersurface* Σ *and a closed future-trapped surface, and if the convergence condition,* $R_{ab}u^a u^b \geq 0$ *holds for null* u^a*, then there are future incomplete null geodesics.*

Einstein's theory of general relativity predicts that singularities are unavoidable, since the energy momentum tensor along timelike or null geodesics, will be positive definite according to the Einstein field equations if the strong energy condition holds. On the other hand, consistent modifications of general relativity that violate the strong energy condition can lead to violations of the focusing theorem, and therefore the evasion of singularities. Clearly, if the discriminant $E[k] < 0$, then it could be that $\dot{\Theta} > 0$, which would imply that geodesics defocus, leading to gravitational repulsion and the possibility of an evasion of singularities. We have shown in Section 8.2.1 that the slowly rotating dCS solution contains geodesics for which $E[k] < 0$ close to the black hole. Note, however that due to the smallness of the dCS caps, both the null and strong *average* energy conditions [336] remain satisfied. In what follows, we show that dCS gravity naturally has the mathematical and physical features needed to violate the conditions of the focusing theorem.

7.4.2 The Focusing and Hawking-Penrose Theorems in dCS Gravity

Recall that both the focusing and Hawking-Penrose theorem rely on satisfying the constraint $R_{ab}k^a k^b \geq 0$ with R_{ab} the Ricci tensor and k^a the tangent to a timelike or a null geodesic

congruence. Using the modified field equations in dCS gravity, this condition becomes,

$$\bar{T}_{ab}k^a k^b \geq 2\alpha C_{ab}k^a k^b \,, \tag{7.29}$$

and we see that in general this need not be satisfied allowing for the possibility that timelike or null congruences will defocus, avoiding a singularity.

When precisely do we have a violation of the focusing theorem? Using the definition of the scalar-field stress-energy tensor and the C-tensor, this occurs when

$$\begin{aligned} &2\alpha \left(\nabla_c \vartheta\right) \, \epsilon^{cdea} \left(\nabla_e R^b{}_d\right) k_a k_b \\ &+ 2\alpha \left(\nabla_c \nabla_d \vartheta\right) \, {}^*R^{dabc} k_a k_b > \left(\nabla_a \vartheta\right) \left(\nabla_b \vartheta\right) k^a k^b \,, \end{aligned} \tag{7.30}$$

where we have removed the symmetrization parenthesis in the C-tensor because we are contracting it with the symmetric tensor $k_a k_b$. We recognize the right-hand side as a total square of the directional derivative of the scalar field in the direction of the tangent to the congruence. Therefore, a sufficient (but not necessary) conditions for the Hawking-Penrose theorems to be violated is simply

$$\left(\nabla_c \nabla_d \vartheta\right) \, {}^*R^{dabc} k_a k_b > \left(\nabla_c \vartheta\right) \, \epsilon^{dcea} \left(\nabla_e R^b{}_d\right) k_a k_b \,, \tag{7.31}$$

where we have eliminated the minus sign through a permutation of the indices in the Levi-Civita tensor.

The above inequality is the best one can do without using additional approximations. Note that the equation of motion for the scalar field cannot be used to simplify the left-hand side of the above equation, because the double covariant derivative acting on the scalar field is not contracted into a d'Alembertian operator. A simplification one can do, however, is to work in an effective field theory approach. In the latter, one can substitute the modified field equations into the right-hand side of the above equations to find

$$\left(\nabla_c \nabla_d \vartheta\right) \, {}^*R^{dabc} k_a k_b > \left(\nabla_c \vartheta\right) \, k_a k_b \, \epsilon^{dcea}$$

$$\times \nabla_e \left(8\pi \bar{T}^b{}_d - 16\pi\alpha C^b{}_d\right) , \tag{7.32}$$

The right-hand side of this equation is quadratic in α because because the equation of motion of the scalar field ϑ is linear in α. Therefore, to leading order in α, the condition to ensure the Hawking-Penrose theorem is violated reduces to

$$\left(\nabla_c \nabla_d \vartheta\right) \, {}^*R^{dabc} k_a k_b > 0 \, . \tag{7.33}$$

There is no reason to expect that the left-hand side of the above equation will have a definite sign. Thus, in general, it would seem the assumptions required in the Hawking-Penrose theorem do not hold. Notice, moreover, that in the above derivation, we never used the fact that k^a is the tangent vector to a timelike geodesic congruence, and so, this result also applies to null geodesic congruences. We then conclude that the usual proof of the Hawking-Penrose theorem does not go through in dCS gravity.

The lesson we have learned from this first study is that timelike and null geodesics can, and in general will defocus in dCS gravity, yielding a violation of the conditions required by the Hawking-Penrose singularity theorem. By itself, this does *not* however mean that dCS gravity resolves the black hole singularity. At shorter distances, the dCS term would transform into the terms that gave rise to it in the low-energy approximation, as was was discussed in Section 2. To fully understand this, we plan to study Oppenheimer-Snyder-like collapse of a rotating dust ellipsoid and neutron star collapse in dCS gravity and its short-distance completion to see if, when and how a singularity forms [337]. Moreover, in another upcoming study we will analyze solutions, including dynamical black hole and cosmological solutions, that obey the $R_{ab}k^a k^b < 0$ condition, and explore the prospect of what new physical effects this violation is signaling, including a potential new regime of super-radiance outside the rotating black holes [338].

Chapter 8

Black Hole Superradiance in Dynamical Chern-Simons Gravity

8.1 Introduction

The discussion in the previous chapter showed that rotating black holes in dCS become endowed with 'caps' which have a unique equation of state that leads to a violation of the null and strong energy conditions. As a next step, it is of interest to consider the behavior of matter close to such black holes. One obvious process to consider is black hole superradiance, which is the focus of this chapter. Dynamical Chern-Simons (dCS) gravity [307, 308] is an extension of general relativity (GR) in which the parity-violating Chern-Simons form coupled to a pseudo-scalar field is added to the Einstein-Hilbert action of GR. This addition is well motivated from particle physics [309] and string theory [310, 311, 313, 312] perspectives. While non-rotating black holes in dCS gravity possess the same properties as those in GR [317, 330], those which are rotating are subject to corrections to the metric that are sourced by the Chern-Simons pseudo-scalar [318, 319, 320]. As such, dCS gravity provides a vast playground on which to study deviations from GR and has been considered in a wide variety of gravitational and astrophysical contexts [339, 340, 341, 342, 343, 344, 345, 346, 347, 348, 328, 349, 332, 350, 351]. The most stringent constraints on dCS gravity arise from combining

gravitational wave observations and X-ray observations of isolated pulsars [325], while solar system experiments and pure gravitational wave observations or binary pulsar tests generally have so far left the theory unconstrained [352, 328, 276, 353].

DCS gravity can be reliably treated as a low-energy effective field theory (EFT) valid below a certain energy scale, μ, that can be near, or below the Planck scale [354]. In the past and present work we consider μ to be below the Planck scale by at least a few orders of magnitude, $\mu \ll M_{\rm P}$. The dCS term itself is the first leading term among an infinite number of terms of the EFT. All these terms can be obtained from a conventional high-energy quantum field theory of a complex scalar and fermion which are coupled to each other in a specific way and also coupled to gravity. The quantum field theory is valid above μ and below the Planck scale (see [354]). The anomalous triangle diagram of this high energy theory is what is responsible for generating the dCS term in the low energy approximation.

The above comments should make it clear that certain classical solutions – which emerge in dCS theory due to the higher derivative nature of its equations of motion – are connected to physics at the scale μ, and therefore, cannot be justified since they would be modified by the infinite number of higher dimensional terms, if the latter were kept in the theory. Likewise, any statement about ghost states of mass μ, inferred from the dCS theory would not be justified. Moreover, the high energy theory that completes dCS at the scale μ does not have such ghost states in its spectrum [354]. The solutions that can reliably be discussed within dCS theory are the ones present in GR but now modified due to the dCS term treated as a small correction. We will continue to be interested only in these solutions.

Recently, we showed that dCS gravity naturally possesses a mathematical structure that leads to the violation of the conditions for geodesic focusing. More precisely, slowly rotating black holes in the theory become endowed with two "cap-like" structures at the north and south poles in which the focusing theorem is violated [354]. It is thus of significant interest to investigate the behavior of matter or fields near these black hole regions. While these caps are small regions compared to the size of the black hole, if they alter the behavior of matter in a meaningful way, it may be possible to point to observable signatures that could

be distinct from those in GR.

One obvious physical process that might lead to deviations from GR is black hole superradiance. In general, superradiance describes a radiative enhancement process that applies to many areas in physics, first put forth by Dicke, who coined the term "superradiance" in describing coherent radiation [355]. Zeldovich then showed that superradiant scattering could also be sourced by a rotating surface [356, 357]. In particular, ultralight scalar fields can exhibit superradiance when they scatter off a rotating black holes, leading to a growing instability of this field. The latter can lead to "clouds" around the rotating black hole that have a variety of observable implications.

Mathematically, the study of the superradiant growth of a massive scalar field around a rotating black hole requires the solution to the Klein-Gordon equation on a rotating black hole background. The machinery for finding these solutions was first developed by Starobinsky [358]. Black hole superradiance has since been studied for a wide range of cases, including for scalars in a variety of limits [359, 360, 358, 361, 362, 363, 364, 365, 366, 367, 368, 369, 370, 371], as well as for vector and tensor fields [372, 373, 374, 375, 376, 377, 378, 379]. Superradiance has also been studied in a range of modified theories of gravity [380, 381, 382, 383], however a full analytical analysis of black hole superradiance in dCS gravity is missing from the literature until now.

Black hole superradiance is an example of the Penrose process, in which energy and angular momentum can be extracted from a rotating black hole [384]. As such, it provides a landscape to probe unseen scalar sectors. In particular, superradiance is a powerful tool that can be used to constrain ultra-light dark matter (see e.g. [385] for a review). The hypothesis here is that dark matter is perhaps an ultralight scalar field that grows around rotating black holes, leading to a scalar cloud that spins black holes down as it grows. This process leads to two observational consequences, the first of which arises from the emission of monochromatic gravitational waves from the dissipation of the scalar cloud, as discussed in [366, 386, 387, 388, 376, 389, 390]. The second is the spin-down of the black hole, in which the amplification of the scalar field reduces the black hole spin and mass [391, 392, 369].

These processes can be a key tool to investigate the existence of massive particles and one could ask whether one could use them to distinguish between a Kerr black hole and a slowly rotating dCS black hole.

In what follows, we will study a dCS black hole that is accompanied by an ultra-light scalar field in addition to the massless dCS pseudo-scalar. As an approximation, we will be working in the "probe" limit, in which the backreaction of the ultra-light scalar onto the spacetime itself, as well as the backreaction onto the massless dCS pseudo-scalar, can be neglected. As long as $\mu M \ll 1$ this approximation scheme is valid, so we will restrict our analysis to the parameter space in which this inequality is satisfied. We consider a scenario in which an ultra-light scalar field is amplified by the rotation of the black hole, which itself contains a massless pseudo-scalar cloud sourced by the parity-violating Pontryagin density. Working with the same machinery developed by Detweiler [363], we solve the Klein-Gordon equation on the dCS background through a procedure of matching asymptotic expansions. We find that additional modes of the ultralight massive scalar are amplified as compared to the solution for a ultralight massive scalar field on a Kerr background; we obtain contributions from $\ell, \ell+2$, and $\ell-2$ modes for every ℓ. The ultralight massive scalar field does indeed possess an instability that is significantly dominated by the $\ell = 1, m = 1, n = 0$ mode, in agreement with the GR case. Lastly, we comment on how the addition of these extra modes, while small, may impact future observable endeavors.

The structure of this chapter is as follows. In Sec. 8.2, we review dCS gravity and the properties of the ultralight scalar field. In Sec. 8.3, we review the known studies of black hole superradiance in GR, focusing particularly on the well-known solution by Detweiler [363]. We then extend this analysis to dCS gravity in Sec. 8.4 and discuss specific properties of the solution in Sec. 8.5. Finally, conclude with a discussion of implications and future work in Sec. 8.6. Throughout the paper, we use the following conventions. We work in four spacetime dimensions with signature (-,+,+,+). Latin letters (a,b,...,h) range over all spacetime indices with round and square brackets denoting symmetrization and antisymmetrization, respectively. We work in geometric units such that $G = 1 = c$, unless otherwise specified.

8.2 dCS Black Hole With an External Scalar Field

We will be considering a slowly-rotating dCS black hole which is accompanied by an ultralight scalar field in addition to the massless pseudo-scalar field associated with dCS gravity. We emphasize that this massless pseudo-scalar field is distinct from the ultralight scalar, which we will probe for superradiant behavior. The full action is as follows:

$$S = S_{\text{EH}} + S_{\text{dCS}} + S_{\vartheta} + S_{\varphi}, \tag{8.1}$$

where S_{EH} is the Einstein-Hilbert action of GR, S_{dCS} contains the Chern-Simons term, S_{ϑ} is the action for the dCS pseudo-scalar ϑ, and S_{φ} is the action of the external ultralight scalar field φ. In the following, we will review the basics of dCS gravity in vacuum, as well as rotating black holes in dCS gravity, and the ultralight scalar separately, before considering the dCS black hole and scalar together.

8.2.1 Dynamical Chern-Simons Gravity in Vacuum

The *vacuum* action of dCS gravity is given by $S_{\text{vac}} = S_{\text{EH}} + S_{\text{dCS}} + S_{\vartheta}$. Explicitly,

$$S_{\text{vac}} = \int d^4x\sqrt{-g}\left[\kappa R + \frac{\alpha}{4}\vartheta\ {}^*R\,R - \frac{1}{2}\left(\nabla_a\vartheta\right)\left(\nabla^a\vartheta\right)\right], \tag{8.2}$$

where κR is the usual Einstein-Hilbert term with $\kappa = (16\pi)^{-1}$ and R the Ricci scalar [307, 308]. The Chern-Simons term consists of a dynamical pseudo-scalar field, ϑ, which couples to the Pontryagin density of the spacetime. The Pontryagin density is defined as

$${}^*R\,R := {}^*R^a{}_b{}^{cd}R^b{}_{acd}\,, \tag{8.3}$$

where the Hodge dual to the Riemann tensor is

$${}^*R^a{}_b{}^{cd} := \frac{1}{2}\epsilon^{cdef}R^a{}_{bef}\,, \tag{8.4}$$

and ϵ^{cdef} is the Levi-Civita tensor. The Pontryagin density can also be written in terms of divergence of the Chern-Simons topological current,

$$\nabla_a K^a = \frac{1}{4}\, {}^*R\, R, \tag{8.5}$$

where

$$K^a := \epsilon^{abcd}\left(\Gamma^n{}_{bm}\partial_c\Gamma^m{}_{dn} + \frac{2}{3}\Gamma^n{}_{bm}\Gamma^m{}_{cl}\Gamma^l{}_{dn}\right), \tag{8.6}$$

giving rise to the name "Chern-Simons gravity". Varying the action, Eq. (8.2) yields the modified *vacuum* field equations,

$$G_{ab} + \frac{\alpha}{\kappa}\, C_{ab} = \frac{1}{2\kappa} T_{ab}\,, \tag{8.7}$$

which include a modification from the C-tensor, defined as

$$C^{ab} = (\nabla_c \vartheta)\ \epsilon^{cde(a}\nabla_e R^{b)}{}_d + (\nabla_c\nabla_d\vartheta)\ {}^*R^{d(ab)c}\,. \tag{8.8}$$

The total energy-momentum tensor T_{ab} is the sum of any matter stress-energy tensor (assumed in this subsection to be zero) and the stress-energy tensor of the pseudo-scalar ϑ, which is given by

$$T^{(\vartheta)}_{ab} = (\nabla_a\vartheta)\,(\nabla_b\vartheta) - \frac{1}{2} g_{ab}\,(\nabla_c\vartheta)\,(\nabla^c\vartheta)\ . \tag{8.9}$$

The pseudo-scalar field ϑ itself obeys the following *vacuum* equation of motion

$$\Box\vartheta = -\frac{\alpha}{4\kappa}\ {}^*R\, R\,, \tag{8.10}$$

which can be obtained by varying the action, Eq. (8.2), with respect to ϑ.

8.2.2 Slowly Rotating Black Holes in dCS gravity

For spherically symmetric spacetimes, one can show that the Pontryagin density, $*RR$ must vanish [317, 330]. If this is the case, and the spacetime is assumed to be static, then the scalar, ϑ must be a constant, which implies $T_{ab} = 0 = C_{ab}$. Then, all dCS solutions must reduce to the static and spherically symmetric solutions of GR, and more precisely, must reduce to the Schwarzschild spacetime [317], which is a solution of dCS gravity. However, spacetimes which lack spherical symmetry, such as the Kerr solution of GR for rotating black holes, are no longer solutions of dCS gravity, even if they are stationary; this is because the Pontryagin density is nonzero in non-spherically symmetric spacetimes, and thus, it sources a non-trivial pseudo-scalar field by Eq. (8.10).

The first such solution was found by Yunes and Pretorius [318], by considering a black hole in a slow rotation expansion. This solution has since been extended to second order [319] and fifth order in rotation [320]. An extremal solution for the scalar field was found in [393], and a non-perturbative numerical solution for the metric was found in [332]. The leading order correction to the metric in the slowly rotating solution is as follows:

$$ds^2 = ds^2_{\mathcal{K}} + \frac{5}{4}\zeta M\chi \frac{M^4}{r^4}\left(1 + \frac{12}{7}\frac{M}{r} + \frac{27}{10}\frac{M^2}{r^2}\right)\sin^2\theta dt d\phi\,, \tag{8.11}$$

where M is the ADM mass, ζ is related to the CS coupling α by

$$\zeta = \frac{\alpha^2}{\kappa M^4}, \tag{8.12}$$

χ is the dimensionless spin parameter, defined in terms of the ADM angular momentum via $|S| = Ma = M^2\chi$, so that $\chi = a/M$ is dimensionless, and $ds^2_{\mathcal{K}}$ is the usual line element of the Kerr metric in Boyer-Lindquist coordinates. Explicit forms for the higher-order corrections to all terms in the metric can be found in [319, 320], but for simplicity we will not write them here. The associated pseudo-scalar to leading order in rotation is

$$\vartheta = \frac{5}{8}\alpha\chi\frac{\cos\theta}{r^2}\left(1 + 2\frac{M}{r} + \frac{18}{5}\frac{M^2}{r^2}\right). \tag{8.13}$$

At $\mathcal{O}(\zeta\chi^2)$, this solution has an event horizon, r_+ and an inner apparent horizon, r_- given by

$$r_\pm = r_{\pm,\mathcal{K}} \mp \frac{915}{28672} M\zeta\chi^2, \tag{8.14}$$

where $r_{\pm,\mathcal{K}}$ denotes the outer and inner Kerr horizons, respectively. The location of the ergosphere is given by

$$r_{\text{ergo}} = r_{\text{ergo},\mathcal{K}} - \frac{915}{28672} M\zeta\chi^2 \left(1 + \frac{2836}{915}\sin^2\theta\right). \tag{8.15}$$

For the remainder of the paper we will be considering the slowly rotating dCS metric up to $\mathcal{O}(\zeta\chi^2)$, given by

$$g_{\mu\nu} = g^{\mathcal{K}}_{\mu\nu} + g^{\text{dCS}}_{\mu\nu}\left[\mathcal{O}(\zeta\chi^2)\right], \tag{8.16}$$

where $g^K_{\mu\nu}$ is the Kerr metric in Boyer-Lindquist coordinates and $g^{\text{dCS}}_{\mu\nu}\left[\mathcal{O}(\zeta\chi^2)\right]$ is the dCS metric correction up to quadratic order in the rotation[319].

This metric is a valid approximation sufficiently far away from the black hole event horizon, since otherwise the $\mathcal{O}(\zeta)$ term in Eq. (8.11), which decays as $1/r^4$, would dominate over the GR term, which decays as $1/r^3$. However, close to the horizon we must take into account that its location is slightly shifted from its location in the Kerr spacetime, as we can see in Eq. (8.14). This shift leads to spurious divergences of Eq. (8.16) at the location of the Schwarzschild and Kerr horizons, which we will address by resumming the metric in χ. There are in principle an infinite number of ways in which the metric can be resummed, so long as the resummed metric:

1. identically reduces to the non-resummed metric, order by order in χ, when expanded in small $\chi \ll 1$,

2. has each component remain finite everywhere outside the dCS horizon, e.g. that there are no divergences at the Schwarzschild or Kerr horizon.

One way to perform the resummation is to consider a transformation $\Delta \to \bar{\Delta}$, where

$$\bar{\Delta} = \Delta + \frac{915}{14336} M^2 \zeta \chi^2, \tag{8.17}$$

which we have found by demanding that $\bar{\Delta}(r = r_{+,\rm dCS}) = 0$. By taking $\Delta \to \bar{\Delta}$ and the Schwarzschild factor $f \to \bar{\Delta}/r^2$ in the metric of Eq. (8.16), and expanding in $\chi \ll 1$, we find that the two counterterms that we need to add in order to retain the desired asymptotic behavior are

$$\delta g_{rr} = \frac{915}{14336} \frac{M^2 r^2 \zeta \chi^2}{\bar{\Delta}^2}, \tag{8.18}$$

and

$$\delta g_{tt} = \frac{915}{14336} \frac{M^2 \zeta \chi^2}{r^2}. \tag{8.19}$$

We also obtain counterterms for the $g_{t\phi}$ and $g_{\phi\phi}$ components, which are

$$\delta g_{t\phi} = -\frac{915}{14336} \frac{M^3 \sin^2\theta \zeta \chi^3}{r^2}, \tag{8.20}$$

$$\delta g_{\phi\phi} = \frac{915}{14336} \frac{M^4 \sin^4\theta \zeta \chi^4}{r^2}. \tag{8.21}$$

We include these terms for completeness, but note that they are $\mathcal{O}(\zeta\chi^3)$ and $\mathcal{O}(\zeta\chi^4)$ and will not contribute to our resummed metric, which we limit to $\mathcal{O}(\zeta\chi^2)$. The $g_{\theta\theta}$ term is unaffected by the resummation. Then, our full resummed metric is

$$\begin{aligned} g_{tt,\rm resum} &= g_{tt,\mathcal{K}}(\Delta \to \bar{\Delta}) + g_{tt,\rm dCS}(f \to \bar{\Delta}/r^2) + \delta g_{tt}\,, \\ g_{rr,\rm resum} &= g_{rr,\mathcal{K}}(\Delta \to \bar{\Delta}) + g_{rr,\rm dCS}(f \to \bar{\Delta}/r^2) + \delta g_{rr}, \end{aligned} \tag{8.22}$$

where $g_{tt/rr,\mathcal{K}}$ are the usual components of the Kerr metric in Boyer-Lindquist coordinates and $g_{tt/rr,\rm dCS}$ is the $\mathcal{O}(\zeta\chi^2)$ dCS correction described previously. All other metric components remain unchaged at $\mathcal{O}(\zeta\chi^2)$

8.2.3 dCS gravity Coupled to an Ultralight Scalar Field

In this paper, we will not be concerned with the vacuum field equations, but rather with those arising in the presence of an additional massive scalar field φ. The action is then as given in Eq. (8.1), where the action of the massive scalar field is

$$S_\varphi = \int d^4x\sqrt{-g}\left[-\frac{1}{2}g^{ab}\nabla_a\varphi\nabla_b\varphi - \frac{1}{2}\mu^2\varphi^2\right], \tag{8.23}$$

with μ the mass of the scalar. The energy-momentum tensor associated with the massive field is then

$$T^{(\varphi)}_{ab} = (\nabla_a\varphi)(\nabla_b\varphi) - \frac{1}{2}g_{ab}(\nabla_a\varphi\nabla^a\varphi + \mu^2\varphi^2), \tag{8.24}$$

which must be added to the pseudo-scalar stress-energy tensor $T^{(\vartheta)}_{ab}$ to compose the total energy-momentum tensor T_{ab}. The massive scalar field φ obeys the Klein-Gordon equation,

$$(\Box + \mu^2)\varphi = 0\,, \tag{8.25}$$

where $\Box = \nabla_a\nabla^a$ is the d'Alembertian operator.

In what follows, we will neglect any backreaction of the ultra-light scalar onto both the metric and the dCS pseudo-scalar, working in the probe limit. Previous work [394, 395] has considered the inclusion of these backreaction effects for scalar and vector fields for near-extremal black holes in GR using numerical methods. However, we will be working in the slow rotation and $\mu M \ll 1$ limit in which these effects are negligible. The equation of motion for the scalar field then becomes

$$(\Box_{\rm vac} + \mu^2)\varphi = 0\,, \tag{8.26}$$

where the d'Alembertian operator $\Box_{\rm vac}$ is that associated with the vacuum dCS spacetime solution discussed in the previous subsection.

8.3 Superradiance in GR

For completeness and to make more clear the methods we will use in Sec. 8.4, we will first review Detweiler's solution for the superradiant behavior of an ultralight scalar field in a Kerr background [363]. We will specifically work in the $\omega M \ll 1$ and $\mu M \ll 1$ limit in order to obtain an analytical solution and determine what parameters lead to the presence of the superradiant instability, which will be determined by the imaginary part of the frequency of the radiating modes.

We begin by considering a massive scalar field which obeys the Klein-Gordon equation,

$$(\Box_{\mathcal{K}} - \mu^2)\varphi_{\mathcal{K}}(t, r, \theta, \phi) = 0, \tag{8.27}$$

where μ is the field mass, and $\Box_{\mathcal{K}}$ and $\varphi_{\mathcal{K}}$ denote the d'Alembertian operator and scalar field, respectively for a Kerr black hole. The Klein-Gordon equation on a Kerr background is well studied to be separable in the $\omega M \ll 1$ and $\mu M \ll 1$ limit by making an ansatz

$$\varphi_{\mathcal{K}}(t, r, \theta, \phi) = \sum_{\ell=0}^{\infty} \sum_{m=-\ell}^{\ell} \varphi^{\mathcal{K}}_{\ell,m}, \tag{8.28}$$

where

$$\varphi^{\mathcal{K}}_{\ell,m} = e^{-i\omega t} e^{im\phi} S^{\mathcal{K}}_{\ell,m}(\theta) R^{\mathcal{K}}_{\ell,m}(r). \tag{8.29}$$

We can see from this expression that if the frequency, $\omega_{\mathcal{K}}$, has a positive, imaginary contribution then this expression will exponentially increase; this is the key component for the field to possess a superradiant instability. Upon applying the ansatz and separating Eq. (8.27), we find that the resulting differential equation for $S^{\mathcal{K}}_{\ell,m}(\theta)$ gives $S^{\mathcal{K}}_{\ell,m}(\theta) = P^m_\ell(\cos\theta)$, where $P^m_\ell(\cos\theta)$ are associated Legendre polynomials.

In order to analytically solve the radial differential equation arising from the separation of variables, we will perform a matching of asymptotic expansions. We will consider two zones: the far zone, where $r \gg M$ and the near zone, where $r - r_{\text{H},\mathcal{K}} \ll \max(\ell/\omega, \ell/\mu)$. We emphasize here that our use of the label "near zone" is distinct from the definition of the

near zone in post-Newtonian theory. With the solutions in both zones in hand, we will then match the expansions of the solutions in each zone in the opposite limit inside a buffer zone, where both expansions are simultaneously valid.

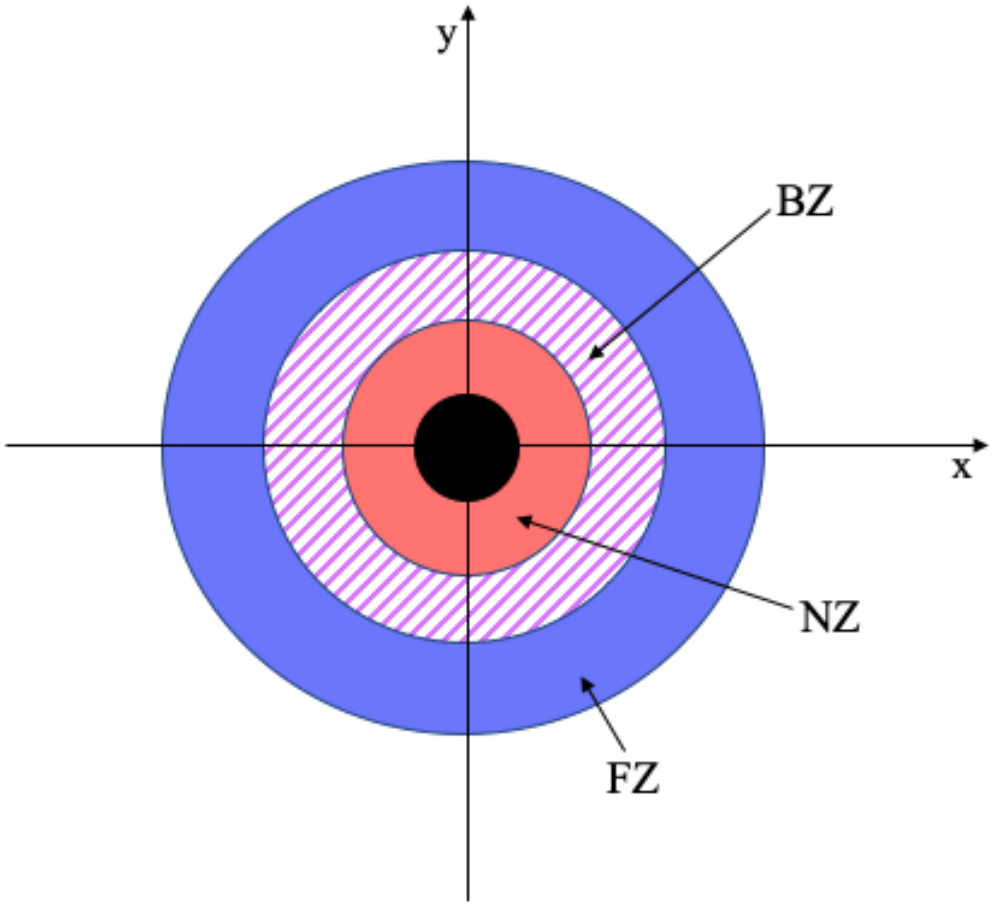

Figure 8.1: (Color online) Schematic diagram showing the relevant geometry. The black hole is denoted by the black circle at the center, the near zone (NZ) is in red, the far zone (FZ) is in blue and the intermediate buffer zone, where the expansions can be asymptotically matched, is shown in the purple striped region.

Figure 8.1 shows a schematic diagram of the three zones; this figure is meant to be an illustrative example of each of the zones, so it does not exactly represent the geometry of the black hole spacetime. The black circular region in Fig. 8.1 represents the black hole. The far zone (FZ), defined as the region in which $r \gg M$, is denoted in blue, and the near zone (NZ), defined by the region in which $r - r_{\text{H},\mathcal{K}} \ll \max(\ell/\omega, \ell/\mu)$, is denoted in red. The intermediate buffer zone (BZ) is the purple striped region and is characterized by $r \gg M$

and $r - r_{\text{H},\mathcal{K}} \ll \min(\ell/\omega, \ell/\mu)$ such that near-horizon expansion of the far zone solution and the large radius expansion of the near-horizon zone solution are *both* simultaneously valid and can thus be asymptotically matched.

First, we will consider the far zone, $r \gg M$. Solving the radial part of the Klein-Gordon equation in this zone and taking the appropriate boundary conditions at infinity, i.e., that the wave must be outgoing, we obtain

$$R_{\ell}^{\mathcal{K},\text{FZ}} = x^{\ell} e^{-x/2} U(\ell + 1 - \nu, 2\ell + 2, x), \tag{8.30}$$

where U is a confluent hypergeometric function [396] and we have defined

$$x = 2kr, \tag{8.31}$$

$$\nu = M\mu^2/k, \tag{8.32}$$

$$k^2 = \mu^2 - \omega^2, \tag{8.33}$$

$$\omega = \sigma + i\gamma. \tag{8.34}$$

Now consider the near zone, $r - r_{\text{H},\mathcal{K}} \ll \max(\ell/\omega, \ell/\mu)$. Let us define the quantity

$$z_{\mathcal{K}} = \frac{r - r_{+,\mathcal{K}}}{r_{+,\mathcal{K}} - r_{-,\mathcal{K}}}, \tag{8.35}$$

where $r_{+,\mathcal{K}}$ and $r_{-,\mathcal{K}}$ are the outer and inner Kerr horizons respectively, so that the defining relation of the near zone becomes $z_{\mathcal{K}} \ll \max(\ell/\omega, \ell/\mu)$. The solution to the radial part of the Klein-Gordon equation in the near zone is then

$$R_{\ell,m}^{\mathcal{K},\text{NZ}} = \left(\frac{z_{\mathcal{K}}}{z_{\mathcal{K}} + 1}\right)^{iP_{\mathcal{K}}} {}_2F_1(-\ell, \ell + 1, \ell - 2iP_{\mathcal{K}}, z_{\mathcal{K}} + 1), \tag{8.36}$$

where again we have imposed appropriate boundary conditions at the horizon in order to obtain a single independent solution. Here, ${}_2F_1$ is the ordinary hypergeometric function and $P_{\mathcal{K}}$ is a constant, defined as

$$P_{\mathcal{K}} = \frac{am - 2Mr_{+,\mathcal{K}}\omega}{r_{+,\mathcal{K}} - r_{-,\mathcal{K}}}, \tag{8.37}$$

where recall that a is the (dimensionful) spin parameter for a Kerr black hole.

Now, we can consider the intermediate buffer zone region. Defining the small-x expansion of the far zone solution in Eq. (8.30) as $\tilde{R}_\ell^{\mathcal{K},\text{FZ}}$, and the large-z expansion of the near-horizon solution in Eq. (8.36) as $\tilde{R}_{\ell,m}^{\mathcal{K},\text{NZ}}$, asymptotic matching then requires that

$$\tilde{R}_\ell^{\mathcal{K},\text{FZ}} \sim \tilde{R}_{\ell,m}^{\mathcal{K},\text{NZ}}, \tag{8.38}$$

inside the buffer zone, where the $\sim$ symbol here means "asymptotic to." This condition can only be satisfied by a set of frequencies that ensures both expressions are matched in the buffer region, and this, in turn allows us to determine the superradiance spectrum of perturbations.

Let us now carry out this matching in detail. First, following Detweiler [363], we introduce the ansatz

$$\nu = \frac{M\mu^2}{\sqrt{\mu^2 - \omega^2}} = \ell + 1 + n + \delta\nu, \tag{8.39}$$

where the first equality comes from Eqs. (8.32)–(8.33), and $\delta\nu$ is a function to be determined. With this ansatz, we use Eqs. (8.32)–(8.34) to find that this function must be related to the imaginary part of the frequencies γ via

$$\delta\nu = iM\gamma \left(\frac{\mu M}{l+1+n}\right)^{-3}. \tag{8.40}$$

Using our knowledge that γ scales as $(\mu M)^8$ (which we will prove in the following), it is clear that $\delta\nu = \mathcal{O}(\mu^5 M^5)$, and since $\mu M \ll 1$, then $\delta\nu \ll 1$. Assuming that $\mathcal{O}(\delta\nu) = \mathcal{O}(x^{2\ell+1})$ (which we will also prove in the following), we then have that the small x and $\delta\nu$ expansion of Eq. (8.30) is

$$\begin{aligned}\tilde{R}_\ell^{\mathcal{K},\text{FZ}} \approx (-1)^n \frac{(2\ell+1+n)!}{(2\ell+1)!}(2k_{\mathcal{K}} r)^\ell \\ +(-1)^{n+1}(2\ell)!n!(2kr)^{-\ell-1}\delta\nu_{\mathcal{K}},\end{aligned} \tag{8.41}$$

For the near-horizon solution, expanding in $z \gg 1$ gives

$$\tilde{R}^{\mathcal{K},\text{NZ}}_{\ell,m} \approx \frac{(-1)^{\ell}\Gamma(1+2\ell)\Gamma(1-2iP_{\mathcal{K}})}{\Gamma(\ell+1)\Gamma(\ell+1-2iP_{\mathcal{K}})}\left(\frac{r}{r_{+,\mathcal{K}}-r_{-,\mathcal{K}}}\right)^{\ell} + \frac{(-1)^{\ell-1}\Gamma(-1-2\ell)\Gamma(1-2iP_{\mathcal{K}})}{\Gamma(-\ell)\Gamma(-\ell-2iP_{\mathcal{K}})}\left(\frac{r}{r_{+,\mathcal{K}}-r_{-,\mathcal{K}}}\right)^{-\ell-1}. \tag{8.42}$$

We can now match these two asymptotic expansions to each other. That is, given two asymptotic expansions of the form $\tilde{f} \sim A\, r^{l} + B\, r^{-l-1}$ and $\tilde{g} \sim C\, r^{l} + D\, r^{-l-1}$ inside some common buffer zone, then asymptotic matching $\tilde{f} \sim \tilde{g}$ requires that $A = C$ and $B = D$. Using this to asymptotically match $\tilde{R}^{\mathcal{K},\text{FZ}}_{\ell}$ and $\tilde{R}^{\mathcal{K},\text{NZ}}_{\ell,m}$ we find relations for the coefficients of the r^{ℓ} and $r^{-\ell-1}$ terms that allow us to solve for $\delta\nu_{\mathcal{K}}$, namely

$$\delta\nu_{\mathcal{K}} = (2iP_{\mathcal{K}})\left[2k(r_{+,\mathcal{K}}-r_{-,\mathcal{K}})\right]^{2\ell+1}\frac{(2\ell+n+1)!}{n!} \times\left[\frac{\ell!}{(2\ell+1)!(2\ell)!}\right]^{2}\prod_{j=1}^{l}(j^{2}+4P^{2}_{\mathcal{K}}). \tag{8.43}$$

Observe that indeed, as we expected, $\delta\nu_{\mathcal{K}} = \mathcal{O}(x^{2\ell+1})$.

In order to find the dominant contribution to the superradiant spectrum, we need to consider the maximum positive value of $\delta\nu$. In GR, this occurs when $\ell = 1$, $m = 1$, and $n = 0$, corresponding to

$$\gamma_{\mathcal{K}} \approx \mu\frac{(\mu M)^{8}}{24}\left(a/M - 2\mu r_{+,\mathcal{K}}\right), \tag{8.44}$$

and a growth time of

$$\tau_{\mathcal{K}} \approx 24(\mu M)^{-8}\mu^{-1}\left(a/M - 2\mu r_{+,\mathcal{K}}\right)^{-1}. \tag{8.45}$$

Observe that indeed, as we expected, $\gamma_{\mathcal{K}} = \mathcal{O}[(\mu M)^{8}]$.

8.4 Superradiance in dCS gravity

Having reviewed the superradiant instability for a Kerr black hole, we now turn to an investigation of superradiance in dCS gravity. We will consider the slowly rotating black hole solution in dCS gravity [318, 319, 320] up to second order in the spin, $\mathcal{O}(\zeta\chi^2)$, appropriately resumed as explained in Sec. 8.2.2. We will follow Detweiler's method [363] as described in the previous section, and determine the behavior of the scalar field by solving the Klein-Gordon equation in both the far and near zones, as defined in Fig. 8.1, but now the metric will be given by the dCS black hole solution. We will then perform asymptotic matching on the asymptotic expansions of the approximate solutions to find the relevant frequencies for the spectrum of superradiant perturbations.

8.4.1 The Far Zone

We first consider the Klein-Gordon equation in the far zone, $r \gg M$. The metric is given in Eq. (8.16) because the resummed metric reduces to this equation in the far zone. With this, the Klein-Gordon equation becomes

$$(\Box_{\mathcal{K}} + \Box_{\rm dCS} - \mu^2)\varphi = 0, \tag{8.46}$$

to leading order in the dCS deformation, where $\Box_{\mathcal{K}}$ is the d'Alembertian operator of the Kerr background, $\Box_{\rm dCS}$ is a modification induced by the dCS corrections to the metric, and μ is again the mass of the ultralight scalar field. The full expression for $\Box_{\rm dCS}$ is rather complicated and can be found in Appendix 8.C.

Given that the dCS contribution itself is a small correction that is subdominant to the GR contribution, we can perform an asymptotic expansion of $\Box_{\rm dCS}$ in the far zone and simply consider the leading order contribution. This leading order contribution, acting on a function $g(t, r, \theta, \phi) = e^{-i\omega t}e^{im\phi}g(r, \theta)$ is

$$\Box_{\rm dCS} g(t, r, \theta, \phi) \approx \frac{603}{1792}\chi^2\zeta\frac{M^3\omega^2}{r^3}\left(\cos^2\theta - \frac{1}{3}\right)$$

$$\times\, g(r,\theta)e^{-i\omega t}e^{im\phi} \tag{8.47}$$

to leading order in $r \gg M$. Observe that $\Box_{\rm dCS} g \sim \zeta\chi^2/r^3$, where the $\mathcal{O}(\zeta\chi)$ term does not show up because it decays as r^{-6}.

In order to solve the wave equation in Eq. (8.46), we will consider a perturbative solution such that

$$\varphi_{\rm FZ} = \varphi_{0,\rm FZ} + \delta\varphi_{\rm FZ}, \tag{8.48}$$

where $\varphi_{0,\rm FZ}$ is simply the solution on the unperturbed Kerr background and $\delta\varphi$ is the dCS correction. We take $\delta\varphi_{\rm FZ}$ to be $\mathcal{O}(\zeta\chi^2)$ to match the expansion order of the metric and of the d'Alembertian operator. From [363] and the discussion in Sec. 8.3, we know that $\varphi_{0,\rm FZ}$ is given by Eq. (8.28). We can thus make a similar ansatz for $\delta\varphi_{\rm FZ}$:

$$\delta\varphi_{\rm FZ} = \sum_{\ell=0}^{\infty}\sum_{m=-\ell}^{\ell}\left(\delta\varphi^{\rm FZ}_{\ell,m} + \delta\varphi^{\rm FZ}_{\ell+2,m}\right) + \sum_{\ell=2}^{\infty}\sum_{m=-\ell}^{\ell}\delta\varphi^{\rm FZ}_{\ell-2,m}, \tag{8.49}$$

where

$$\delta\varphi^{\rm FZ}_{\ell,m} = e^{-i\omega t}e^{im\phi}f^{\rm FZ}_{\ell,m}(r,\theta), \tag{8.50}$$

$$\delta\varphi^{\rm FZ}_{\ell+2,m} = e^{-i\omega_{\ell+2} t}e^{im\phi}f^{\rm FZ}_{\ell+2,m}(r,\theta), \tag{8.51}$$

$$\delta\varphi^{\rm FZ}_{\ell-2,m} = e^{-i\omega_{\ell-2} t}e^{im\phi}f^{\rm FZ}_{\ell+2,m}(r,\theta). \tag{8.52}$$

We will show soon that the solution is indeed made up of a linear combination of the $\ell, \ell+2$ and $\ell-2$ modes, but one could also foresee that this must be the case due to the $\cos^2\theta$ dependence of Eq. (8.47), which will act as a source term. Note that in order to separate Eq. (8.46) in our perturbative expansion, the time dependence in $\delta\varphi_{\rm FZ}$ must be the same as that of $\varphi_{0,\rm FZ}$, namely $e^{-i\omega t}$, where the frequency ω remains the same as in the background case. In order to ensure that there is matching of the solutions and that this construction is valid, we will explicitly solve for the frequencies of the perturbed contribution via asymptotic matching and show that this is the case.

With the ansatz in Eq. (8.48), the Klein-Gordon equation reduces to

$$
\begin{aligned}
&r^2\left[\frac{1}{\sin\theta}\frac{\partial}{\partial\theta}\left(\sin\theta\frac{\partial f^{\text{FZ}}_{\ell,m}(r,\theta)}{\partial\theta}\right)-m^2\csc^2\theta f^{\text{FZ}}_{\ell,m}(r,\theta)\right]+r^2\frac{\partial}{\partial r}\left[r^2\frac{\partial f^{\text{FZ}}_{\ell,m}(r,\theta)}{\partial r}\right]\\
&+\left(\omega^2r^4-\mu^2r^4+2M\mu r^3\right)f^{\text{FZ}}_{\ell,m}(r,\theta)\\
&+r^2\left[\frac{1}{\sin\theta}\frac{\partial}{\partial\theta}\left(\sin\theta\frac{\partial f^{\text{FZ}}_{\ell+2,m}(r,\theta)}{\partial\theta}\right)-m^2\csc^2\theta f^{\text{FZ}}_{\ell+2,m}(r,\theta)\right]+r^2\frac{\partial}{\partial r}\left[r^2\frac{\partial f^{\text{FZ}}_{\ell+2,m}(r,\theta)}{\partial r}\right]\\
&+\left(\omega^2_{\ell+2}r^4-\mu^2r^4+2M\mu r^3\right)f^{\text{FZ}}_{\ell+2,m}(r,\theta)\\
&+r^2\left[\frac{1}{\sin\theta}\frac{\partial}{\partial\theta}\left(\sin\theta\frac{\partial f^{\text{FZ}}_{\ell-2,m}(r,\theta)}{\partial\theta}\right)-m^2\csc^2\theta f^{\text{FZ}}_{\ell-2,m}(r,\theta)\right]+r^2\frac{\partial}{\partial r}\left[r^2\frac{\partial f^{\text{FZ}}_{\ell-2,m}(r,\theta)}{\partial r}\right]\\
&+\left(\omega^2_{\ell-2}r^4-\mu^2r^4+2M\mu r^3\right)f^{\text{FZ}}_{\ell-2,m}(r,\theta)\\
&=-\frac{201M^3}{1792}r\omega^2(3\cos^2\theta-1)P^m_\ell(\cos\theta)R^{\text{FZ}}_{\mathcal{K},\ell}(r)\zeta\chi^2,
\end{aligned}
\tag{8.53}
$$

where $R_{\mathcal{K},\ell}(r)$ is given by Eq. (8.30). In order to fully separate this equation, we will make use of the Legendre polynomial recurrence relation to rewrite the angular dependence on the right-hand side of Eq. (8.53) as a linear combination of modes $\ell, \ell+2$ and $\ell-2$ modes. We thus make the following ansatzes:

$$
\begin{aligned}
f^{\text{FZ}}_{\ell,m}(r,\theta)&=A_{\ell,m}\,P^m_\ell(\cos\theta)g_\ell(r)\\
f^{\text{FZ}}_{\ell-2,m}(r,\theta)&=B_{\ell,m}\,P^m_{\ell-2}(\cos\theta)g_{\ell-2}(r)\\
f^{\text{FZ}}_{\ell+2,m}(r,\theta)&=C_{\ell,m}\,P^m_{\ell+2}(\cos\theta)g_{\ell+2}(r),
\end{aligned}
\tag{8.54}
$$

where $g_{\ell,\ell\pm2}(r)$ describes the radial dependence of each mode and $A_{\ell,m}, B_{\ell,m}$, and $C_{\ell,m}$ are constants given by

$$
\begin{aligned}
A_{\ell,m}&=\frac{(\ell+\ell^2-3m^2)}{4\ell(\ell+1)-3},\\
B_{\ell,m}&=\frac{3(\ell-1+m)(\ell+m)}{8\ell^2-2},\\
C_{\ell,m}&=\frac{3(\ell+1-m)(2+\ell-m)}{8\ell(2+\ell)+6}\,.
\end{aligned}
\tag{8.55}
$$

These constants can be derived from the recurrence relation, shown in detail in Appendix 8.A. Then, Eq. (8.53) separates into three separate equations for the $\ell, \ell+2$ and $\ell-2$ modes. We will only explicitly show the solution for the ℓ mode, as the others trivially follow by substituting $\ell \to l+2$ and $A_{\ell,m} \to B_{\ell,m}$ or $\ell \to l-2$ and $A_{\ell,m} \to C_{\ell,m}$.

The radial equation for the ℓ mode becomes

$$\begin{aligned}\frac{d^2}{dr^2}[r g_\ell(r)] + \left[\omega^2 - \mu^2 + \frac{2M\mu^2}{r} - \frac{\ell(\ell+1)}{r^2}\right] r g_\ell(r) \\ = -\frac{201}{1792}\frac{M^3\omega^2\zeta\chi^2}{r^2} R^{\rm FZ}_{\mathcal{K},\ell}(r)\,.\end{aligned} \tag{8.56}$$

We will again define x and ν as in Eqs. (8.31) and (8.32) and for convenience, let us write the confluent hypergeometric function U in terms of a WhittakerW function W. Doing so, the radial equation for the ℓ mode becomes

$$\begin{aligned}\frac{d^2[x g_\ell(x)]}{dx^2} + \left[-\frac{1}{4} + \frac{\nu}{x} - \frac{\ell(\ell+1)}{x^2}\right] x g_\ell(x) \\ = -\frac{402}{1792}\frac{M^3\omega^2 k\zeta\chi^2}{x^2}\frac{\mathrm{W}(\nu,\ell+1/2,\mathrm{x})}{x}\,, \\ = -\zeta\chi^2\Omega_1^{\rm FZ}\frac{\mathrm{W}(\nu,\ell+1/2,\mathrm{x})}{x^3}\,,\end{aligned} \tag{8.57}$$

where we have defined the overall prefactor $\Omega_1^{\rm FZ} = 402M^3\omega^2 k/1792$.

The solution to this differential equation is the sum of the homogeneous solution and a particular solution, the later of which we shall call $g_{p,\ell}(r)$. The homogeneous solution is the same as in GR, and thus, we drop it so as to not double-count the background solution. The particular solution is the dCS correction to the GR solution, and thus, solving Eq. (8.57) with a Green functions method, we find

$$\begin{aligned}g^p_\ell = \frac{\Omega_1^{\rm FZ}\zeta\chi^2}{x}\Big[\mathrm{W}(\nu,\ell+1/2,\mathrm{x})\int \mathcal{I}_1 \mathrm{dx} \\ - \mathrm{M}(\nu,\ell+1/2,\mathrm{x})\int \mathcal{I}_2 \mathrm{dx}\Big],\end{aligned} \tag{8.58}$$

where W and M refer to the WhittakerW and WhittakerM functions, respectively, and the

integrands, $\mathcal{I}_1$ and $\mathcal{I}_2$ are

$$\mathcal{I}_1 = \frac{\mathrm{M}(\nu,\ell+1/2,\mathrm{x})\mathrm{W}(\nu,\ell+1/2,\mathrm{x})}{x^2\Big[\mathrm{W}(\nu,\ell+1/2,\mathrm{x})\mathrm{M}(1+\nu,\ell+1/2,\mathrm{x})(1+\nu+\ell)+\mathrm{M}(\nu,\ell+1/2,\mathrm{x})\mathrm{W}(1+\nu,\ell+1/2,\mathrm{x})\Big]}, \tag{8.59}$$

$$\mathcal{I}_2 = \frac{\mathrm{W}(\nu,\ell+1/2,\mathrm{x})^2}{x^2\Big[\mathrm{W}(\nu,\ell+1/2,\mathrm{x})\mathrm{M}(1+\nu,\ell+1/2,\mathrm{x})(1+\nu+\ell)+\mathrm{M}(\nu,\ell+1/2,\mathrm{x})\mathrm{W}(1+\nu,\ell+1/2,\mathrm{x})\Big]}, \tag{8.60}$$

Equation (8.58) describes the radial behavior of φ in the far zone for the ℓ mode. Analogous expressions can be found for the $\ell \pm 2$ modes by taking $\ell \to l+2$ and $A_{\ell,m} \to B_{\ell,m}$ or $\ell \to l-2$ and $A_{\ell,m} \to C_{\ell,m}$.

8.4.2 The Near Zone

Let us now investigate the dynamics of the scalar field in the near zone region. We will again generally follow the same method as in [363], however we now must use the resummed metric described in Sec. 8.2 to account for the shift in the horizon location of the dCS black hole and avoid spurious divergences. Given the use of the resummed metric, we now also must account for the fact that the background solution is no longer strictly Kerr, but is the leading order contribution from the full resummed metric.

With this in mind, we investigate the near zone ansatz

$$\varphi_{\mathrm{NZ}} = \varphi_{0,\mathrm{NZ}} + \delta\varphi_{\mathrm{NZ}}. \tag{8.61}$$

where $\varphi_{0,\mathrm{NZ}}$ is the background solution and $\delta\varphi_{\mathrm{NZ}}$ is a perturbation. In order to find the background solution, we will consider the Klein-Gordon equation

$$\left\{\Box_{\mathrm{resum}}\left[\mathcal{O}(\zeta^0)\right]-\mu^2\right\}\varphi_{0,\mathrm{NZ}} = 0\,, \tag{8.62}$$

where we use the decomposition

$$\varphi_{0,\mathrm{NZ}} = e^{-i\omega t} e^{im\phi} S_{\ell,m}(\theta) G^{0,\mathrm{NZ}}_{\ell,m}\,, \tag{8.63}$$

for some background angular functions $S_{\ell,m}$ and some background radial functions $G^{0,\mathrm{NZ}}_{\ell,m}$. The background Klein-Gordon equation can be separated into

$$\begin{aligned}
&\frac{1}{\sin\theta}\frac{d}{d\theta}\left(\sin\theta\frac{dS_{\ell,m}(\theta)}{d\theta}\right) + \left(M^2\chi^2(\omega^2-\mu^2)\cos^2\theta - \frac{m^2}{\sin^2\theta} + \lambda\right) S_{\ell,m}(\theta) = 0,\\
&\bar{\Delta}\frac{d}{dr}\left(\frac{\bar{\Delta} dG^{0,\mathrm{NZ}}_{\ell,m}(r)}{dr}\right) + \Big[\omega^2(r^2+M^2\chi^2) + M^2\chi^2m^2 - \bar{\Delta}(\mu^2r^2 + M^2\chi^2\omega^2 + \lambda)\\
&\qquad\qquad - 2M\chi m\omega(r^2+M^2\chi^2-\bar{\Delta})\Big] G^{0,\mathrm{NZ}}_{\ell,m}(r) = 0.
\end{aligned} \tag{8.64}$$

Then, working in the $M\omega \ll 1$ and $M\mu \ll 1$ limit once again gives Legendre polynomials for the angular functions. For the radial functions, we first define z such that

$$z = \frac{r - r_{+}}{r_{+} - r_{-}}, \tag{8.65}$$

where r_{+} and r_{-} are the locations of the outer and inner horizons in the dCS solution, explicitly given in Eq. (8.14). Then, substituting for z and taking the appropriate limits, $\mu M \ll 1$, $\omega M \ll 1$, and $r - r_{+} \sim z \ll max(\ell/\omega, l/\mu)$, and near-horizon boundary conditions, we find that the $\mathcal{O}(\zeta^0)$ radial solution is

$$G^{0,\mathrm{NZ}}_{\ell,m} = \left(\frac{z}{z+1}\right)^{iP} {}_2F_1(-\ell, \ell+1, \ell-2iP, z+1), \tag{8.66}$$

where P is now defined with the dCS horizon as

$$P = \frac{am - 2Mr_{+}\omega}{r_{+} - r_{-}}, \tag{8.67}$$

and ${}_2F_1$ is again the ordinary hypergeometric function. Note that this solution has the same form as Eq. (8.36), but z and P are now defined with the horizon locations of the dCS black hole rather than the Kerr solution, so it is slightly shifted from the near zone GR solution.

Now, with the background solution in hand we can consider the full perturbative solution at $\mathcal{O}(\zeta\chi^2)$. We will consider the wave equation in the near zone using the resummed metric, Eq. (8.22), for which the d'Alembertian operator separates as

$$\Box = \Box_{\rm resum}\left[\mathcal{O}(\zeta^0)\right] + \Box_{\rm dCS}\left[\mathcal{O}(\zeta\chi^2)\right], \tag{8.68}$$

where for any function $f(t,r,\theta,\phi)$ we have

$$\begin{aligned}\Box_{\rm dCS} f(t,r,\theta,\phi) \approx & -\frac{27\omega^2 M^2\zeta\chi^2}{r_+^6\bar{\Delta}^2}\left(M-\frac{r_+}{2}\right)\left[M\hat{A}(r_+)\cos^2\theta+\hat{B}(r_+)\right]f(r,\theta)\\ & -\frac{\omega^2M^2\chi^2\zeta}{150528\bar{\Delta}^2 r_+^7}\left[\hat{C}(r_+)\cos^2\theta+\hat{D}(r_+)\right]f(r,\theta)\left(\frac{r-r_+}{r_+-r_-}\right)(r_+-r_-).\end{aligned} \tag{8.69}$$

and the coefficients are

$$\hat{A}(r_+) = -\frac{149\,M^5r_+}{2016}+\frac{445\,M^4r_+^2}{2016}+\frac{235\,M^3r_+^3}{1568}+\frac{3725\,M^2r_+^4}{21168}+\frac{67\,Mr_+^5}{896}+M^6+\frac{67\,r_+^6}{2688}, \tag{8.70}$$

$$\hat{B}(r_+) = -\frac{M^7}{3}-\frac{733\,M^6r_+}{6048}-\frac{155\,M^5r_+^2}{2016}-\frac{2785\,M^4r_+^3}{254016}-\frac{11075\,M^3r_+^4}{508032}-\frac{97\,M^2r_+^5}{16128}+\frac{37\,Mr_+^6}{32256}+\frac{305\,r_+^7}{64512}, \tag{8.71}$$

$$\begin{aligned}\hat{C}(r_+) = & \,24385536\,M^8-11662560\,M^7r_+ + 4189248\,M^6{r_+}^{*2}+481680\,M^5{r_+}^3\\ & +821280\,M^4{r_+}^4-53688\,M^3{r_+}^5+50652\,M{r_+}^7,\end{aligned} \tag{8.72}$$

$$\begin{aligned}\hat{D}(r_+) = & -8128512\,M^8+924000\,M^7r_+-264768\,M^6{r_+}^2+335040\,M^5r{+}^3\\ & -132640\,M^4r^4+19856\,M^3r^5-16884\,Mr^7+19215\,r{+}^8.\end{aligned} \tag{8.73}$$

Let us now consider the ansatz for the perturbation

$$\delta\varphi_{\rm NZ} = \sum_{\ell=0}^{\infty}\sum_{m=-\ell}^{\ell}\left(\delta\varphi^{\rm NZ}_{\ell,m}+\delta\varphi^{\rm NZ}_{\ell+2,m}\right)+\sum_{\ell=2}^{\infty}\sum_{m=-\ell}^{\ell}\delta\varphi^{\rm NZ}_{\ell-2,m}, \tag{8.74}$$

with

$$\delta\varphi^{\rm NZ}_{\ell,m} = e^{-i\omega_\ell t}e^{im\phi}f^{\rm NZ}_{\ell,m}(r,\theta), \tag{8.75}$$

$$\delta\varphi^{\rm NZ}_{\ell+2,m} = e^{-i\omega_{\ell+2}t}e^{im\phi}f^{\rm NZ}_{\ell+2,m}(r,\theta), \tag{8.76}$$

$$\delta\varphi^{\rm NZ}_{\ell-2,m} = e^{-i\omega_{\ell-2}t}e^{im\phi}f^{\rm NZ}_{\ell-2,m}(r,\theta). \tag{8.77}$$

Then, the full Klein-Gordon equation becomes

$$\begin{aligned}
&\frac{1}{\bar{\Delta}\Sigma}\Bigg\{\Big[(M^2\chi^2+r^2)^2 - M^2\chi^2\bar{\Delta}\sin^2\theta\Big]\omega^2 - 2M\chi m\omega(M^2\chi^2+r^2-\bar{\Delta}) \\
&- \Big(\bar{\Delta}\csc^2\theta - \chi^2M^2\Big)m^2 + \bar{\Delta}\partial_\theta^2 + \bar{\Delta}^2\partial_r^2 + \bar{\Delta}\cot\theta\partial_\theta + 2(r-M)\bar{\Delta}\partial_r\Bigg\}f^{\rm NZ}_{\ell,m}(r,\theta) \\
&+ \frac{1}{\bar{\Delta}\Sigma}\Bigg\{\Big[(M^2\chi^2+r^2)^2 - M^2\chi^2\bar{\Delta}\sin^2\theta\Big]\omega^2_{\ell+2} - 2M\chi m\omega_{\ell+2}(M^2\chi^2+r^2-\bar{\Delta}) \\
&- \Big(\bar{\Delta}\csc^2\theta - \chi^2M^2\Big)m^2 + \bar{\Delta}\partial_\theta^2 + \bar{\Delta}^2\partial_r^2 + \bar{\Delta}\cot\theta\partial_\theta + 2(r-M)\bar{\Delta}\partial_r\Bigg\}f^{\rm NZ}_{\ell-2,m}(r,\theta) \\
&+ \frac{1}{\bar{\Delta}\Sigma}\Bigg\{\Big[(M^2\chi^2+r^2)^2 - M^2\chi^2\bar{\Delta}\sin^2\theta\Big]\omega^2_{\ell-2} - 2M\chi m\omega_{\ell-2}(M^2\chi^2+r^2-\bar{\Delta}) \\
&- \Big(\bar{\Delta}\csc^2\theta - \chi^2M^2\Big)m^2 + \bar{\Delta}\partial_\theta^2 + \bar{\Delta}^2\partial_r^2 + \bar{\Delta}\cot\theta\partial_\theta + 2(r-M)\bar{\Delta}\partial_r\Bigg\}f^{\rm NZ}_{\ell-2,m}(r,\theta) \\
&+ \mu^2(f^{\rm NZ}_{\ell,m} + f^{\rm NZ}_{\ell+2,m} + f^{\rm NZ}_{\ell-2,m})(r,\theta) = \frac{27\omega^2M^2\zeta\chi^2}{r_+^6\bar{\Delta}^2}\left(M - \frac{r_+}{2}\right)\Big[M\hat{A}(r_+)\cos^2\theta + \hat{B}(r_+)\Big]P^m_\ell(\cos\theta)G^{0,\rm NZ}_{\ell,m}(r) \\
&+ \frac{\omega^2M^2\zeta\chi^2}{150528\bar{\Delta}^2r_+^7}\Big[\hat{C}(r_+)\cos^2\theta + \hat{D}(r_+)\Big]\left(\frac{r-r_+}{r_+-r_-}\right)(r_+-r_-), P^m_\ell(\cos\theta)G^{0,\rm NZ}_{\ell,m}(r)
\end{aligned} \tag{8.78}$$

Using our intuition about the angular dependence on the right-hand side being a linear combination of ℓ, $\ell+2$ and $\ell-2$ modes, we can now make the ansatzes

$$\begin{aligned}
f^{\rm NZ}_{\ell,m}(r,\theta) &= h_{\ell,m}(r)P^m_\ell(\cos\theta) \\
f^{\rm NZ}_{\ell-2,m}(r,\theta) &= h_{\ell-2,m}(r)P^m_{\ell-2}(\cos\theta) \\
f^{\rm NZ}_{\ell+2,m}(r,\theta) &= h_{\ell+2,m}(r)P^m_{\ell+2}(\cos\theta),
\end{aligned} \tag{8.79}$$

which allows us to separate the equation. More details can be found in Appendix 8.A.

The functions $h_{\ell,m}$ and $h_{\ell\pm2,m}$ describe the radial behavior of the perturbation. As before, let us focus on the ℓth mode solution, since the $\ell\pm2$ solutions can be found by taking $\ell \to \ell\pm2$

and the appropriate coefficients. Decoupling the three equations and writing everything in terms of z, we obtain

$$z(z+1)\frac{d}{dz}\left[z(z+1)\frac{dh_{\ell,m}(z)}{dz}\right]+\left[P^2-\ell(\ell+1)z(z+1)\right]h_{\ell,m}(z)$$
$$=\Omega_1^{\rm NZ}\tilde{A}_{\ell,m}+\Omega_2^{\rm NZ}\bar{A}_{\ell,m}z)\zeta\chi^2\frac{[z(r_+-r_-)+r_+]^2}{z(z+1)}\left(\frac{z}{z+1}\right)^{iP}{}_2F_1([-\ell,\ell+1],[1+2iP],-z), \tag{8.80}$$

where the prefactors have been defined as $\Omega_1^{\rm NZ}=27\omega^2M^2/[r_+^6(r_+-r_-)^4]$, $\Omega_2^{\rm NZ}=\omega^2M^2/(150528r_+^7(r_+-r_-)^4)$, and $\tilde{A}$ and $\bar{A}$ are constant coefficients which are derived from the Legendre polynomial recurrence relation given by

$$\tilde{A}_{\ell,m}=\hat{B}(r_+)+\hat{A}(r_+)\frac{(-\ell+2\ell(1+\ell)-2m^2)}{-3+4\ell(\ell+1)}, \tag{8.81}$$
$$\bar{A}_{\ell,m}=\hat{D}(r_+)+\hat{C}(r_+)\frac{(-\ell+2\ell(1+\ell)-2m^2)}{-3+4\ell(\ell+1)}, \tag{8.82}$$

whose derivations can be found in Appendix 8.A along with the relevant coefficients for the $\ell\pm2$ modes. Solving Eq. (8.80) again gives a homogeneous solution, which is just the background solution at $\mathcal{O}(\zeta^0)$, Eq. (8.66), and we thus discard to avoid double counting. The particular solution at $\mathcal{O}(\zeta\chi^2)$, $h_{p,\ell}$, is

$$h^p_{\ell,m}(z)=\zeta\chi^2(4P^2+1)\left(\frac{z}{z+1}\right)^{iP}{}_2F_1([-\ell,\ell+1],[1+2iP],-z)\int\mathcal{J}_1dz$$
$$-\zeta\chi^2(4P^2+1)\Big[z(z+1)\Big]^{-iP}{}_2F_1([-\ell-2iP,\ell+1-2iP],[1-2iP],-z)\int\mathcal{J}_2dz, \tag{8.83}$$

where

$$\mathcal{J}_1=\frac{1}{D_{\rm NZ}}{}_2F_1\Big([-\ell,\ell+1],[1+2iP],-z\Big){}_2F_1\Big([-\ell-2iP,\ell+1-2iP],[1+2iP],-z\Big)$$
$$\times\Big[z(r_+-r_-)+r_+\Big]^2\left(\Omega_1^{\rm NZ}\tilde{A}_{\ell,m}+z\Omega_2^{\rm NZ}\bar{A}_{\ell,m}\right), \tag{8.84}$$

$$\mathcal{J}_2 = \frac{{}_2F_1\Big([-\ell,\ell+1],[1+2iP],-z\Big)^2 [z(z+1)]^{iP} z^{iP}(z+1)^{-iP}\Big[z(r_+ - r_-)+r_+\Big]^2\Big(\Omega_1^{\rm NZ}\tilde{A}_{\ell,m}+z\Omega_2^{\rm NZ}\bar{A}_{\ell,m}\Big)}{D_{\rm NZ}}. \tag{8.85}$$

and the denominator is

$$\begin{aligned} D_{\rm NZ} = 8z^2(z+1)^3\Bigg\{ & iPz\left[P^2+\frac{1}{4}(\ell^2+\ell+1)+\frac{1}{8}(\ell^2+\ell)\right]{}_2F_1\Big([-\ell,\ell+1],[1+2iP],-z\Big) \\ & \times {}_2F_1\Big([-\ell-2iP+1,\ell+2-2iP],[2-2iP],-z\Big) \\ & -\Bigg[-\frac{z(\ell+1)(iP-1/2)\ell}{4}{}_2F_1\Big([-\ell+1,\ell+2],[2+2iP],-z\Big)+iP\Big(P^2 \\ & +\frac{1}{4}{}_2F_1\Big([-\ell,\ell+1],[1+2iP]\Big) \\ & \times {}_2F_1\Big([-\ell-2iP,\ell+1-2iP],[-2iP+1],-z\Big)\Bigg\}. \end{aligned} \tag{8.86}$$

We have thus obtained the radial behavior of solution for the scalar field in the near zone, Eq. (8.83).

8.4.3 Asymptotic Matching

With the near and far zone solutions, given by Eqs. (8.83) and 8.58, in hand, we now move on to matching them asymptotically in the buffer zone. In general, both of these solutions are complicated integral expressions. In order to perform these integrals and find the conditions on the frequency to obtain the superradiant instability, we focus on an intermediate regime of overlap, the 'buffer zone,' as described previously in Figure 8.1. As long as $r \gg M$ and $r - r_{\rm H,dCS} \ll \min(\ell/\omega, \ell/\mu)$, both the large-z expansion of Eq. (8.83) and the small-x expansion of Eq. (8.58) will be valid. As long as $\omega M \ll 1$ and $\mu M \ll 1$, there exists a region where this is the case and the two solutions will be asymptotic to each other.

First, let us consider the two asymptotic expansions of the approximate solution, beginning with the far zone solution. Defining $\delta\nu_\ell$ in analogy to Eq. (8.39), expanding Eq. (8.58)

in small x and small $\delta\nu_\ell$, recalling that $\delta\nu_\ell \ll 1$, and performing the integral, we obtain

$$\tilde{g}^p_\ell(x) \approx \frac{(1+\ell)\Gamma(-2\ell-2)}{\ell\Gamma(-1-2\ell-n)} x^{\ell-1}\Omega_1^{\text{FZ}}\zeta\chi^2 + \frac{(-1)^{1+n}\ell n!\Gamma[2\ell]}{1+\ell}\delta\nu_\ell x^{-\ell-2}\Omega_1^{\text{FZ}}\zeta\chi^2 \tag{8.87}$$

For details of this expansion, see Appendix 8.B. Let us now focus on the near zone solution. Similarly simplifying and expanding Eq. (8.83) in large z, we can perform the integration to obtain

$$\begin{aligned}\tilde{h}^p_{\ell,m}(z) \approx &\left[\frac{-2^{2\ell-1}(r_+ - r_-)^2\Gamma(\ell+1/2)\Gamma(1+2iP)}{\ell(1+4P^2)\sqrt{\pi}\Gamma(1+l+2iP)} z^{\ell-1}\right. \\ &\left. + \frac{(r_+ - r_-)^2\Gamma(-2\ell-1)\Gamma(\ell+1)\Gamma(1+2iP)\sin(\ell\pi)}{(1+4P^2)\pi\Gamma(-\ell+2iP)} z^{-\ell-2}\right] \\ &\times\Omega_2^{\text{NZ}}\bar{A}_{\ell,m}\zeta\chi^2\end{aligned} \tag{8.88}$$

The details of this expansion can also be found in Appendix 8.B. Both asymptotic expansions of the approximate solutions are suppressed by an overall factor of r relative to the asymptotic expansions of the GR solutions, in addition to the suppression due to the expansion in small $\zeta\chi^2$.

Asymptotic matching requires that in the buffer zone $\tilde{g}(r) \sim \tilde{h}(r)$. Using Eqs. (8.87) and (8.88), we can then match coefficients to find $\delta\nu_\ell$, namely

$$\delta\nu_\ell = 2iP[2k(r_+ - r_-)]^{2\ell+1}\frac{(2\ell+n+1)!}{n!}\left[\frac{\ell!}{(2\ell+1)!(2\ell)!}\right]^2\prod_{j=1}^{\ell}(j^2+4P^2), \tag{8.89}$$

where we have made use of the well-known identity $\Gamma(1+x) = x\Gamma(x)$ and variations thereof. For details of this matching, see Appendix 8.B.

As expected, this expression yields the same result as for the background solution. The ℓth contributions are maximized for $\ell = 1, m = 1$ and $n = 0$ and have a dominant imaginary frequency contribution and growth rate of

$$\gamma_\ell^{\text{max}} \approx \mu\frac{(\mu M)^8}{24}(\chi - 2\mu r_+)$$

$$\tau_{\ell}^{\max} \approx 24(\mu M)^{-8}\mu^{-1}\left(\chi - 2\mu r_{+}\right)^{-1}. \tag{8.90}$$

The $(\ell-2)$th contributions are maximized for $\ell = 3, m = 1$, and $n = 0$ and have the same dominant frequency and growth rate as the $\ell = 1$ ℓth contribution such that $\gamma_{\ell-2}^{\max} = \gamma_{\ell}^{\max}$ and $\tau_{\ell-2}^{\max} = \tau_{\ell}^{\max}$. The $(\ell+2)$th contribution is again maximized for $\ell = 1, m = 1$, and $n = 0$, but will be highly suppressed for all ℓ. The maximum imaginary frequency contribution and growth time are

$$\begin{aligned}\gamma_{\ell+2}^{\max} &\approx \mu\frac{(\mu M)^{16}}{129024000}\left(\chi - 2\mu r_{+}\right)\\ \tau_{\ell+2}^{\max} &\approx 129024000(\mu M)^{-16}\mu^{-1}\left(\chi - 2\mu r_{+}\right)^{-1}.\end{aligned} \tag{8.91}$$

8.5 Properties of the Superradiant Instability in dCS Gravity

Let us now consider the specific ways in which the solution found in Sec. 8.4 differs from the standard GR solution found in [363] and discussed in Sec. 8.3. Let us then recap the solution as

$$\varphi = \varphi_0 + \delta\varphi\,, \tag{8.92}$$

where

$$\varphi_0 = \sum_{\ell=0}\sum_{m=-\ell}^{\ell}\varphi^0_{\ell,m}(r,\theta,\phi)e^{-i\omega_{\ell}t}\,, \tag{8.93}$$

is the background solution (which itself has dCS modification) and

$$\begin{aligned}\delta\varphi = &\sum_{\ell=0}\sum_{m=-\ell}^{\ell}\left[\delta\varphi_{\ell,m}(r,\theta,\phi)e^{-i\omega_{\ell}t} + \delta\varphi_{\ell+2,m}(r,\theta,\phi)e^{-i\omega_{\ell+2,m}t}\right]\\ &+\sum_{\ell=2}\sum_{m=-\ell}^{\ell}\delta\varphi_{\ell-2,m}(r,\theta,\phi)e^{-i\omega_{\ell-2}t}.\end{aligned} \tag{8.94}$$

The first question one may look to answer is which of these terms dominates the growth of the ultralight scalar. The larger ℓ is, the smaller the frequency ω_{ℓ}, and thus, the slower the mode will grow. Therefore, the dominant contributions come from the most rapidly

growing modes, which have the largest frequencies and thus the smallest ℓs. The fastest growing mode in φ_0 is simply the $\ell = 1$ one, just as in the GR case. The fastest growing mode in $\delta\varphi$ is given by the $\ell = 1$ mode of $\delta\varphi_\ell$ ($\delta\varphi_{\ell+2}$ is always subdominant) and the $\ell = 3$ mode of $\delta\varphi_{\ell-2}$. This can be seen in Fig. 8.2, which shows the $\mathrm{Im}(\omega)$ as a function of μM for various values of dimensionless spin parameter $\chi = a/M$, and for the ℓth mode (solid line), $(\ell + 2)$th mode (dot-dashed line) and the $(\ell - 2)$th mode (dotted line), when $\ell = 1$ (left panel) and $\ell = 3$ (right panel). When $\ell = 1$ (left panel), the dominant contribution is given by the ℓth mode, since the $\ell + 2$ mode is suppressed. When $\ell = 3$ (right panel), the dominant contribution is given by the $(\ell - 2)$th mode, since the other two are suppressed. Therefore, in general, the $(\ell - 2)$th mode will dominate, except when it is not present in the spectrum (ie. when $\ell = 1$ or $\ell = 2$).

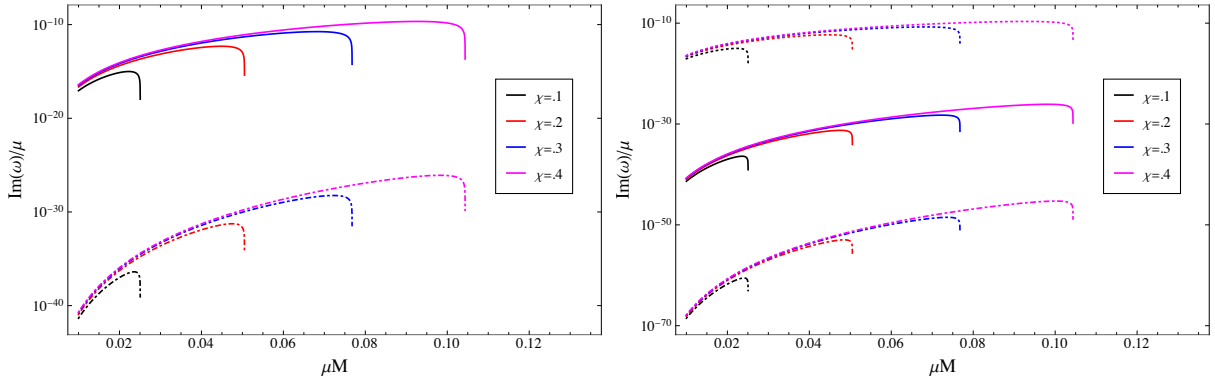

Figure 8.2: (Color online) Imaginary part of the frequency of the dCS contribution, $\mathrm{Im}(\omega)$ for $\ell = 1$ (right) and $\ell = 3$ (left). The solid lines correspond to ℓ, the dot-dashed lines correspond to $\ell + 2$, and the dotted lines correspond to $\ell - 2$. Note the different scaling of the two axes.

Another question one may wish to ask is whether the angular spectrum is modified in dCS gravity. Because we know that the dCS contribution excites additional modes (i.e. the $P^m_{\ell\pm2}(\cos\theta)$ as well as $P^m_\ell(\cos\theta)$), we expect the angular spectrum to change. The traditional behavior of the superradiant instability in GR leads to two clouds emanating from the equator of the black hole in analogy to the p-orbital of an electron. In Figure 8.3, we show the angular dependence of φ_0 and $\delta\varphi$ evaluated in the buffer zone (Eq. (8.29) and Eq. (8.52) respectively) for the $l = 1$ and $l = 3$ modes. As expected, the solution is dominated by the $\ell = 1$ part of φ_0, leading to a cloud that is still shapped like a p-orbital of an electron. There will

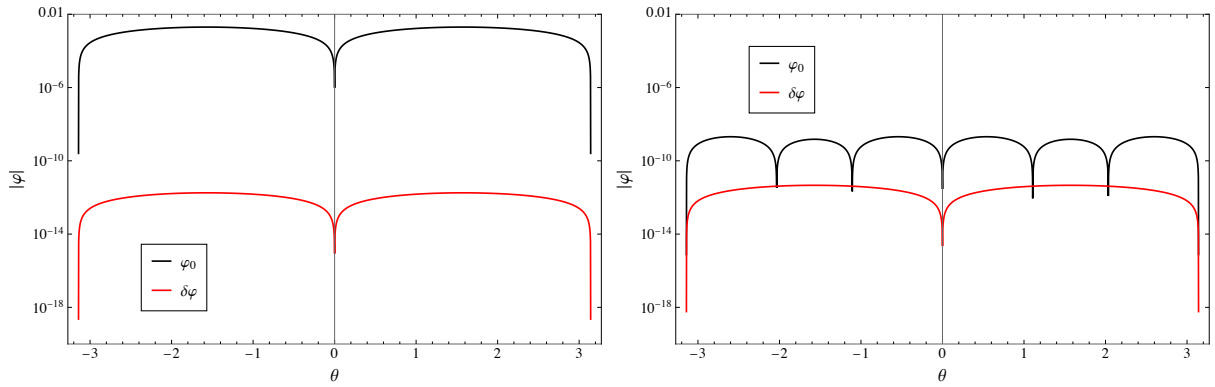

Figure 8.3: (Color online) Angular dependence of the magnitude of the solution for $|\varphi_0|$ (black) compared to $|\delta\varphi|$ (red), where φ_0 is given by Eq. (8.29) and $\delta\varphi$ is given by Eq. (8.41). For the radial dependence, we consider the buffer zone expansion of the far zone solution, Eq. (8.49) for φ_0 and Eq. (8.87) for $\delta\varphi$. We show the solutions for $\ell = 1$ (left panel) and $\ell = 3$ (right panel). We take $\zeta = .1, \chi = .1, M = 1, \mu M = .02$, and $r = 5M$. For illustrative purposes we take $t/M = 1$, but note that the actual timescale of the instability will be much greater.

be corrections to this, in the form of additional lower order harmonics introduced by $\delta\varphi$, but these will be subdominant. Note that the amplitude of $|\delta\varphi|$ is significantly suppressed compared to that of $|\varphi^0|$. This can be seen from considering the solution in Eq. (8.87) and observing that in addition to the suppression by $\zeta\chi^2$ and the additional factor of r^{-1} compared to the background solution, there is an overall factor of $\omega^2 k$ in the coefficient Ω_1^{FZ}. This factor is $\mathcal{O}(\mu^3)$. All together, this gives an overall suppression of $\mathcal{O}(10^{-9})$ for the chosen values of μ, ζ and χ, which is what we observe for the $\ell = 1$ mode, shown on the left.

Lastly, we consider the time evolution of the solution. Taking the same buffer zone approximation discussed above, Fig. 8.4 compares the growth of φ_0 to that of $\delta\varphi$ on the equator for the $\ell = 1$ (left panel) and $\ell = 3$ (right panel) modes. Observe that in the $\ell = 1$ case the growth of the instability is dominated by φ_0. The $\ell = 3$ mode is smaller than the $\ell = 1$, but it becomes dominated by $\delta\varphi$ at some finite time, because the $(\ell - 2)$th contribution to $\delta\varphi$ dominates over the ℓth contribution of φ_0. Although not shown in the figure, there is a large time (about $t/M \sim 10^{22}$, corresponding to $t \sim 10^9$ years, or roughly 10% of a Hubble time, for a $M = 10^6 M_\odot$ black hole) at which $\delta\varphi$ dominates over φ_0 and our perturbative expansions cease to be valid. This, however, will typically occur after the superradiant instability is quenched due to the draining of spin angular momentum from the

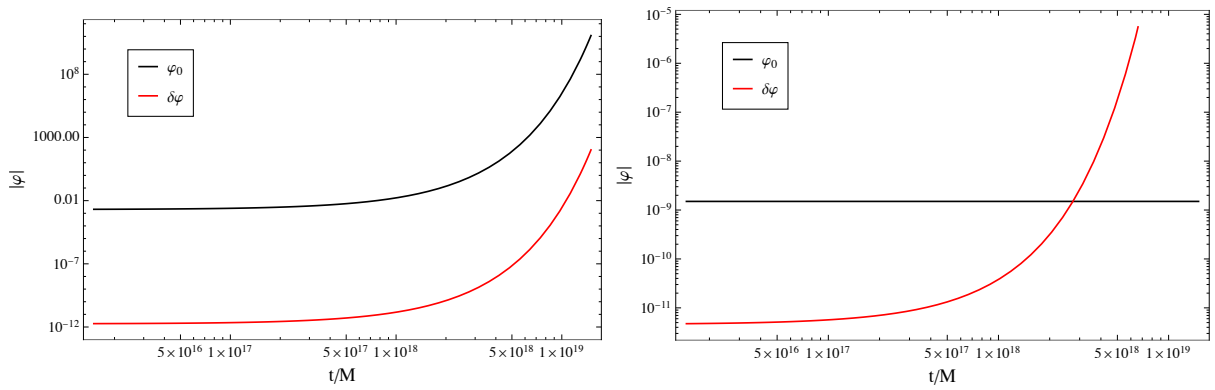

Figure 8.4: (Color online) Time evolution of the magnitude of the solution for $|\varphi_0|$ (black) compared to $|\delta\varphi|$ (red), where φ_0 is given by Eq. (8.29) and $\delta\varphi$ is given by Eq. (8.41). For the radial dependence, we consider the buffer zone expansion of the far zone solution, Eq. (8.49) for φ_0 and Eq. (8.87) for $\delta\varphi$. We show the solutions for $\ell = 1$ (left panel) and $\ell = 3$ (right panel). We take $\zeta = .1, \chi = .1, M = 1, \mu M = .02$, $r = 5M$, and $\theta = \pi/2$.

background black hole.

8.6 Discussion and Conclusions

We have calculated the superradiance spectrum of perturbations for a slowly rotating black hole in dCS gravity. We have found that the spectrum is composed of two contributions: one that is similar to the usual GR contribution from an (ℓ, m, n) mode, and another that includes additional contributions from the ℓth, the $(\ell+2)$th and the $(\ell-2)$th modes. The ℓth and $(\ell+2)$th modes are dominated by the $(\ell = 1, m = 1, n = 0)$ mode, and the $(\ell-2)$th mode is dominated by the $(\ell = 3, m = 1, n = 0)$ mode. The dCS corrections are subdominant to the leading order $\ell = 1$ GR contribution, and thus the angular dependence and overall shape of the scalar field cloud have small corrections which induce small deviations from GR.

Despite the lack of macroscopic distinction of the angular dependence of the scalar cloud between dCS gravity and GR, there are still many possible avenues toward determining potential observable signatures and placing constraints on dCS gravity. In general, superradiance can be used as a probe of ultralight scalars. These probes can equivalently be used to test dCS gravity by extending the analysis done for ultralight scalar superradiance sourced by a Kerr black hole to include the dCS corrections. In particular, it would be of interest to

determine the energy extraction due to the amplification of the scalar field and the resulting impact on the black hole Regge plane. It has also been suggested in [392] that including multiple modes in the analysis of the superradiant instability can impact the evolution of the scalar cloud. Presumably, the dCS activation of multiple modes would have a similar effect. This activation, in turn, could lead to stronger spontenous emission of gravitational waves, as the scalar cloud transitions between energy levels. These ideas could be interesting avenues for future exploration.

A puzzling finding of our results is that presence of the Chern-Simons caps do not seem to have an effect on the superradiant instability for the dCS black hole. One might expect that the behavior of the scalar field near the black hole would be altered due to the unique properties of the caps; however, we have found that the angular behavior of the scalar field in dCS gravity is similar to that in GR. One possible explanation is that the caps are located at the north and south poles of the black hole and extend out to about twenty degrees on each side. Superradiance is a process that is sourced by the rotation of the black hole, which is minimized at the poles where the effects of the caps are at a maximum. Due to this non-overlap of regions, the caps appear to be not relevant to the presence of the superradiant instability.

There are other avenues for future work related to superradiance in dCS gravity. One such avenue is to consider whether fermionic superradiance arises in dCS gravity. Fermions have been extensively studied in dCS gravity, in e.g. [341]. Given that fermions do not exhibit superradiant behavior in GR [397], the presence of fermionic superradiance would be an excellent test of dCS gravity from which one could potentially obtain an observable signature. One could also explore other couplings and interactions of the scalar field, such as a conformal coupling, or coupling between the Chern-Simons pseudo-scalar and the external ultralight scalar field. Lastly, now that we have determined that Chern-Simons caps do not play a role in the superradiance process in dCS, it may be of interest to explore other phenomena in which the caps impact the dynamics of matter near dCS black holes.

8.A Legendre Polynomial Recurrence and Coefficients

Here we provide details of the Legendre polynomial reccurrence relation and the derivation of the constant coefficients in Eq. (8.54) and Eq. (8.80).

8.A.1 Far Zone

In Eq. (8.53) on the right-hand side of our expression for the far zone, we have angular dependence $(3\cos^2\theta - 1)P_\ell^m(\cos\theta)$. Employing the recurrence relation

$$\begin{aligned}(2\ell+1)\cos\theta P_\ell^m(\cos\theta) = (\ell - m + 1)P_{\ell+1}^m(\cos\theta) \\ + (\ell + m)P_{\ell-1}^m(\cos\theta).\end{aligned} \tag{8.95}$$

twice to the first term and collecting coefficients, we find that

$$\begin{aligned}(3\cos^2\theta - 1)P_\ell^m(\cos\theta) = \frac{(\ell + \ell^2 - 3m^2)}{4\ell(\ell+1) - 3}P_\ell^m(\cos\theta) \\ + \frac{3(\ell - 1 + m)(\ell + m)}{8\ell^2 - 2}P_{\ell-2}^m(\cos\theta) \\ + \frac{3(\ell + 1 - m)(2 + \ell - m)}{8\ell(2+\ell) + 6}P_{\ell+2}^m(\cos\theta).\end{aligned} \tag{8.96}$$

We then define

$$A = \frac{(\ell + \ell^2 - 3m^2)}{4\ell(\ell+1) - 3}, \tag{8.97}$$

$$B = \frac{3(\ell - 1 + m)(\ell + m)}{8\ell^2 - 2}, \tag{8.98}$$

and

$$C = \frac{3(\ell + 1 - m)(2 + \ell - m)}{8\ell(2+\ell) + 6}. \tag{8.99}$$

8.A.2 Near-Horizon Zone

First, note that the constant coefficients in the expression for $\Box_{\rm dCS}$ for the resummed metric are

$$\hat{A}(r_+) = -\frac{149\,M^5 r_+}{2016} + \frac{445\,M^4 r_+^2}{2016} + \frac{235\,M^3 r_+^3}{1568} + \frac{3725\,M^2 r_+^4}{21168} + \frac{67\,M r_+^5}{896} + M^6 + \frac{67\,r_+^6}{2688}, \tag{8.100}$$

$$\hat{B}(r_+) = -\frac{M^7}{3} - \frac{733\,M^6 r_+}{6048} - \frac{155\,M^5 r_+^2}{2016} - \frac{2785\,M^4 r_+^3}{254016} - \frac{11075\,M^3 r_+^4}{508032} - \frac{97\,M^2 r_+^5}{16128} + \frac{37\,M r_+^6}{32256} + \frac{305\,r_+^7}{64512}, \tag{8.101}$$

$$\begin{aligned}\hat{C}(r_+) &= 24385536\,M^8 - 11662560\,M^7 r_+ + 4189248\,M^6 {r_+}^{*2} + 481680\,M^5 {r_+}^3 \\ &\quad + 821280\,M^4 {r_+}^4 - 53688\,M^3 {r_+}^5 + 50652\,M {r_+}^7,\end{aligned} \tag{8.102}$$

$$\begin{aligned}\hat{D}(r_+) &= -8128512\,M^8 + 924000\,M^7 r_+ - 264768\,M^6 {r_+}^2 + 335040\,M^5 r{+}^3 \\ &\quad - 132640\,M^4 r^4 + 19856\,M^3 r^5 - 16884\,M r^7 + 19215\,r{+}^8.\end{aligned} \tag{8.103}$$

Then, in Eq. (8.78), we have terms on the right-hand side proportional to $P_\ell^m(\cos\theta)$ and $\cos^2\theta P_\ell^m(\cos\theta)$. We perform the same procedure for the near-horizon zone in the previous section. Using the recurrence relation, we find the following coefficients:

$$\tilde{A} = \hat{B}(r_+) + \hat{A}(r_+)\frac{(-\ell + 2\ell(1+\ell) - 2m^2)}{-3 + 4\ell(\ell+1)}, \tag{8.104}$$

$$\tilde{B} = \hat{A}(r_+)\frac{(\ell - 1 + m)(\ell + m)}{-1 + 4\ell^2}, \tag{8.105}$$

$$\tilde{C} = \hat{A}(r_+)\frac{(1 + \ell - m)(2 + \ell - m)}{3 + 4\ell(2+\ell)}, \tag{8.106}$$

$$\bar{A} = \hat{D}(r_+) + \hat{C}(r_+)\frac{(-\ell + 2\ell(1+\ell) - 2m^2)}{-3 + 4\ell(\ell+1)}, \tag{8.107}$$

$$\bar{B} = \hat{C}(r_+)\frac{(\ell - 1 + m)(\ell + m)}{-1 + 4\ell^2}, \tag{8.108}$$

$$\bar{C} = \hat{C}(r_+)\frac{(1 + \ell - m)(2 + \ell - m)}{3 + 4\ell(2+\ell)}. \tag{8.109}$$

$\tilde{B}$, $\bar{B}$, $\tilde{C}$, and $\bar{C}$ are the analogous coefficients to $\tilde{A}$ and $\bar{A}$ for the $l-2$ and $l+2$ solutions, respectively.

8.B Details of Asymptotic Matching

Here we give further detail about the expansions presented in Section 8.4 C.

8.B.1 Far Zone

We will begin from Eq. (8.58). First, note that the Whittaker functions can be written in terms of ordinary and confluent hypergeometric functions as follows:

$$\begin{aligned} W(\nu, \ell+1/2, x) &\approx e^{-x/2} x^{\ell} U(\ell+1-\nu, 2\ell+2, x) \\ M(\nu, \ell+1/2, x) &\approx e^{-x/2} x^{\ell} {}_2F_1(\ell+1-\nu, 2\ell+2, x). \end{aligned} \tag{8.110}$$

We then want the small-x expansions of these expressions. Let us call the small-x expansion of the confluent hypergeometric $\tilde{U}$ and note that the ordinary ${}_2F_1$ is approximately one in the small-x limit. The relevant expansions in U are

$$\tilde{U}(\ell+1-\nu, 2\ell+2, x) \approx \frac{\Gamma(-1-2\ell)}{\Gamma(-\ell-\nu)} + x^{-1-2\ell} \frac{\Gamma(2\ell+1)}{\Gamma(1+\ell-\nu)}, \tag{8.111}$$

$$\tilde{U}(\ell-\nu, 2\ell+2, x) \approx \frac{\Gamma(-1-2\ell)}{\Gamma(-1-\ell-\nu)} + x^{-1-2\ell} \frac{\Gamma(2\ell+1)}{\Gamma(\ell-\nu)} \tag{8.112}$$

Then, the integrals become:

$$\begin{aligned} \mathcal{I}_1(x) &\approx \frac{\tilde{U}(\ell+1-\nu, 2\ell+2, x)}{\tilde{U}(\ell+1-\nu, 2\ell+2, x)(1+\ell+\nu) + \tilde{U}(\ell-\nu, 2\ell+2, x)} \\ &= \frac{1}{1+2\ell} + x^{2\ell+1} \frac{\Gamma(-1-2\ell)\Gamma(1+\ell-\nu)}{\Gamma(2+2\ell)\Gamma(-\ell-\nu)}, \end{aligned} \tag{8.113}$$

and

$$\begin{aligned} \mathcal{I}_2 &\approx \frac{\tilde{U}(\ell+1-\nu, 2\ell+2, x)^2}{\tilde{U}(\ell+1-\nu, 2\ell+2, x)(1+\ell+\nu) + \tilde{U}(\ell-\nu, 2\ell+2, x)} \\ &= \frac{2\gamma(-1-2\ell)}{(1+2\ell)\Gamma(-\ell-\nu)} + x^{-2\ell-1} \frac{\Gamma(2\ell+1)}{(1+2\ell)\Gamma(1+\ell-\nu)} \\ &+ x^{2\ell+1} \frac{\Gamma(-1-2\ell)^2\Gamma(1+\ell-\nu)}{\Gamma(2+2\ell)\Gamma(-\ell-\nu)^2}. \end{aligned} \tag{8.114}$$

We then perform the integrals and simplify the full expression to obtain

$$g_\ell^p \approx \frac{(1+\ell)\Gamma(-2\ell-2)}{\ell\Gamma(-\ell-\nu)}x^{\ell-1} + \frac{\ell\Gamma(2\ell)}{(1+\ell)\Gamma(1+\ell-\nu)}x^{-\ell-2}. \tag{8.115}$$

Lastly, we define $\nu = n+1+\ell+\delta\nu$ and expand in small $\delta\nu$ to obtain Eq. (8.87).

8.B.2 Near Zone

Now we will consider the large r expansion of the near zone solution. From Eq. (8.83), we note that the integrands $\mathcal{J}_1$ and $\mathcal{J}_2$ each have a common overall factor of complicated hypergeometric functions each multiplied by a different hypergeometric. We take the common factor, expand in large z and simplify. Then, expand each of the leftover hypergeometric functions as

$${}_2F_1([-\ell,\ell+1],[1+2iP],-z) \approx \frac{\Gamma(1+2\ell)\Gamma(1+2iP)}{\Gamma(1+\ell)\Gamma(1+\ell+2iP)}z^\ell + \frac{\Gamma(-1-2\ell)\Gamma(1+2iP)}{\Gamma(-\ell)\Gamma(-\ell+2iP)}z^{-\ell-1}, \tag{8.116}$$

$${}_2F_1([-\ell-2iP,\ell+1-2iP],[1-2iP],-z) \approx \frac{\Gamma(1+2\ell)\Gamma(1-2iP)}{\Gamma(1+\ell)\Gamma(1+\ell-2iP)}z^\ell + \frac{\Gamma(-1-2\ell)\Gamma(1-2iP)}{\Gamma(-\ell)\Gamma(-\ell-2iP)}z^{-\ell-1}. \tag{8.117}$$

Then, performing the integrals, collecting terms and simplifying yields Eq. (8.88).

8.B.3 Matching

Using well known properties of the Γ function, we now provide the details of simplifying the resulting expression from the matching condition. From the matching, we obtain

$$\delta\nu_\ell \approx \frac{2^{1-2\ell}(-1)^{1-n}[k(r_+-r_-)]^{2\ell+1}\sin(\pi\ell)\Gamma(-2\ell-1)^2\Gamma(\ell+2iP+1)}{\Gamma\left(\ell+\frac{1}{2}\right)^2\Gamma(n+1)\Gamma(-2\ell-n-1)\Gamma(2iP-\ell)}. \tag{8.118}$$

We have the relations:

$$\Gamma(-z-n) = (-1)^{n+1}\frac{\Gamma(-z)\Gamma(1+z)}{\Gamma(1+n-z)}, \tag{8.119}$$

$$\frac{\pi}{\sin(\pi z)} = \Gamma(1-z)\Gamma(z), \tag{8.120}$$

$$\Gamma(n+1/2) = \frac{(2n)!\sqrt{\pi}}{4^n n!}. \tag{8.121}$$

We also have the following:

$$\Gamma(1+\ell+2iP) = \Gamma(2iP)\prod_{j=0}^{\ell}(j+2iP), \tag{8.122}$$

$$\Gamma(-\ell+2iP) = \Gamma(2iP)\prod_{j=1}^{\ell}(-j+2iP)^{-1}, \tag{8.123}$$

$$\tag{8.124}$$

which leads to

$$\frac{\Gamma(1+\ell+2iP)}{\Gamma(-\ell+2iP)} = 2iP(-1)^{\ell}\prod_{j=1}^{\ell}(j^2+4P^2), \tag{8.125}$$

Putting all of this together and simplifying Eq. (8.118) , we obtain Eq. (8.89).

8.C Full d'Alembertian Operators

Here, for completeness we show the full expression for $\Box_{\rm dCS}$ for the general Kerr + dCS metric.

Consider the metric

$$g_{\mu\nu} = g^K_{\mu\nu} + g^{\rm dCS}_{\mu\nu}\left[\mathcal{O}(\zeta\chi^2)\right]. \tag{8.126}$$

We have that

$$\Box f(t,r,\theta,\phi) = \Big\{\Box_K + \Box_{\rm dCS}(\mathcal{O}\left[\zeta\chi\right)] \; + \Box_{\rm dCS}\left[\mathcal{O}(\zeta\chi^2)\right]\Big\} f(t,r,\theta,\phi).$$

$\Box_{\mathcal{K}}$ is just the usual expression for the Kerr d'Alembertian, and we then have at $\mathcal{O}(\zeta\chi)$

$$\Box_{\rm dCS}\left[\mathcal{O}(\zeta\chi)\right] f(t,r,\theta,\phi) = \frac{M^5\left(189\,M^2+120\,Mr+70\,r^2\right)\zeta\,\chi}{56\,r^6\Delta\left(r\right)}\frac{\partial^2 f\left(t,r,\theta,\phi\right)}{\partial t\partial\phi}.$$

At $\mathcal{O}(\zeta\chi^2)$, we have the following:

$$\begin{aligned}
\Box_{\rm dCS}\left[\mathcal{O}(\zeta\chi)\right]f(t,r,\theta,\phi) = \frac{27M^3\zeta\chi^2}{2r^{12}\Delta(r)^2\sin^2\theta}\Bigg[&\frac{-27\sin^2\theta r\Delta(r)^2}{8}\Bigg(-\frac{40\Delta(r)}{9}\left(\cos^2\theta-\frac{1}{3}\right)A(r)+Mr^2B(r)\Bigg)\\
&+2\sin^2\theta r^6\left(\frac{\sin^2\theta M^3\Delta(r)}{8}C(r)+\left(M-\frac{r}{2}\right)\cos^2\theta D(r)+E(r)\right)\frac{\partial^2 f}{dt^2}\\
&-2\sin^2\theta r\Delta(r)^2\left(\cos^2\theta-\frac{1}{3}\right)F(r)\frac{\partial^2 f}{\partial\theta^2}\\
&-2r\Delta(r)\left(G(r)\cos^2\theta\Delta(r)+H(r)\Delta(r)-\frac{\sin^2\theta r^3M^3}{8}I(r)\right)\frac{\partial^2 f}{\partial\phi^2}\\
&-\sin^2\theta\Delta(r)\Bigg(-15r\left(\cos^2\theta-\frac{1}{3}\right)J(r)\Delta(r)+\left(M-\frac{r}{2}\right)r^2\Big(K(r)\cos^2\theta+L(r)\Big)\frac{d\Delta(r)}{dr}\\
&+8\Delta(r)\Big(M(r)\Delta(r)\cos^2\theta+N(r)\Delta(r)+rO(r)\cos^2\theta+rP(r)\Big)\Bigg)\frac{\partial f}{\partial r}\\
&+2\sin\theta\cos\theta r\Delta(r)\Bigg(-\frac{17M\cos^2\theta\Delta(r)}{2}Q(r)+R(r)\Delta(r)-\left(M-\frac{r}{2}\right)\sin^2\theta rS(r)\Bigg)\frac{\partial f}{\partial\theta},
\end{aligned} \tag{8.127}$$

where the coefficients are given by

$$A(r) = M^6+\frac{5623\,M^5r}{30240}+\frac{379\,M^4r^2}{6048}-\frac{2579\,M^3r^3}{42336}-\frac{125\,M^2r^4}{15876}-\frac{1459\,Mr^5}{362880}-\frac{67\,r^6}{40320}, \tag{8.128}$$

$$B(r) = M^5-\frac{523\,M^4r}{10206}-\frac{55\,M^3r^2}{972}-\frac{805\,M^2r^3}{8748}-\frac{25\,Mr^4}{5832}-\frac{25\,r^5}{17496}, \tag{8.129}$$

$$C(r) = M^2+\frac{40\,Mr}{63}+\frac{10\,r^2}{27} \tag{8.130}$$

$$D(r) = M^6-\frac{149\,M^5r}{2016}+\frac{445\,M^4r^2}{2016}+\frac{235\,M^3r^3}{1568}+\frac{3725\,M^2r^4}{21168}+\frac{67\,Mr^5}{896}+\frac{67\,r^6}{2688}, \tag{8.131}$$

$$E(r) = -\frac{M^7}{3}+\frac{275\,M^6r}{6048}-\frac{197\,M^5r^2}{12096}+\frac{1745\,M^4r^3}{63504}-\frac{4145\,M^3r^4}{254016}+\frac{1241\,M^2r^5}{254016}+\frac{67\,Mr^6}{16128}+\frac{67\,r^7}{16128}, \tag{8.132}$$

$$F(r) = M^6+\frac{481\,M^5r}{2016}+\frac{5615\,M^4r^2}{28224}+\frac{185\,M^3r^3}{6048}+\frac{4727\,M^2r^4}{84672}+\frac{355\,Mr^5}{12096}+\frac{67\,r^6}{5376}, \tag{8.133}$$

$$G(r) = M^6+\frac{229\,M^5r}{2016}+\frac{375\,M^4r^2}{3136}-\frac{95\,M^3r^3}{6048}+\frac{4727\,M^2r^4}{84672}+\frac{355\,Mr^5}{12096}+\frac{67\,r^6}{5376}, \tag{8.134}$$

$$H(r) = -\frac{M^6}{3} + \frac{275\,M^5 r}{6048} + \frac{1105\,M^4 r^2}{84672} + \frac{655\,M^3 r^3}{18144} - \frac{4727\,M^2 r^4}{254016} - \frac{355\,M r^5}{36288} - \frac{67\,r^6}{16128}, \tag{8.135}$$

$$I(r) = M^2 + \frac{40\,M r}{63} + \frac{10\,r^2}{27}, \tag{8.136}$$

$$J(r) = M^6 + \frac{5623\,M^5 r}{30240} + \frac{379\,M^4 r^2}{6048} - \frac{2579\,M^3 r^3}{42336} - \frac{125\,M^2 r^4}{15876} - \frac{1459\,M r^5}{362880} - \frac{67\,r^6}{40320}, \tag{8.137}$$

$$K(r) = M^6 - \frac{149\,M^5 r}{2016} + \frac{445\,M^4 r^2}{2016} + \frac{235\,M^3 r^3}{1568} + \frac{3725\,M^2 r^4}{21168} + \frac{67\,M r^5}{896} + \frac{67\,r^6}{2688}, \tag{8.138}$$

$$L(r) = -\frac{M^6}{3} + \frac{9473\,M^5 r}{6048} + \frac{4115\,M^4 r^2}{6048} + \frac{17285\,M^3 r^3}{63504} - \frac{2255\,M^2 r^4}{63504} - \frac{1459\,M r^5}{72576} - \frac{67\,r^6}{8064}, \tag{8.139}$$

$$M(r) = M^7 - \frac{1157\,M^6 r}{2304} + \frac{1039\,M^5 r^2}{5376} + \frac{5575\,M^4 r^3}{225792} + \frac{8555\,M^3 r^4}{169344} - \frac{2237\,M^2 r^5}{451584} - \frac{67\,M r^6}{21504} - \frac{67\,r^7}{43008}, \tag{8.140}$$

$$N(r) = -\frac{67\,r^6}{43008} - \frac{6035\,M^5 r}{12096} - \frac{1381\,M r^5}{290304} - \frac{1975\,M^4 r^2}{10752} - \frac{11135\,M^2 r^4}{1016064} + \frac{45265\,M^3 r^3}{338688} - \frac{57\,M^6}{16}, \tag{8.141}$$

$$O(r) = M^7 - \frac{1157\,M^6 r}{2304} + \frac{1039\,M^5 r^2}{5376} + \frac{5575\,M^4 r^3}{225792} + \frac{8555\,M^3 r^4}{169344} - \frac{2237\,M^2 r^5}{451584} - \frac{67\,M r^6}{21504} - \frac{67\,r^7}{43008}, \tag{8.142}$$

$$P(r) = -\frac{9931\,M^6 r}{6912} + \frac{283\,M^5 r^2}{5376} + \frac{156175\,M^4 r^3}{2032128} + \frac{8825\,M^3 r^4}{127008} + \frac{6157\,M^2 r^5}{1354752} + \frac{953\,M r^6}{580608} + \frac{67\,r^7}{129024} - \frac{M^7}{3}, \tag{8.143}$$

$$Q(r) = M^5 + \frac{139\,M^4 r}{672} + \frac{220\,M^3 r^2}{2499} - \frac{3575\,M^2 r^3}{79968} - \frac{13\,M r^4}{34272} - \frac{13\,r^5}{137088}, \tag{8.144}$$

$$R(r) = -\frac{67\,r^6}{8064} + \frac{19343\,M^5 r}{12096} - \frac{2957\,M r^5}{145152} + \frac{26065\,M^4 r^2}{42336} - \frac{10273\,M^2 r^4}{254016} - \frac{101705\,M^3 r^3}{254016} + \frac{47\,M^6}{6}, \tag{8.145}$$

$$S(r) = M^6 - \frac{149\,M^5 r}{2016} + \frac{445\,M^4 r^2}{2016} + \frac{235\,M^3 r^3}{1568} + \frac{3725\,M^2 r^4}{21168} + \frac{67\,M r^5}{896} + \frac{67\,r^6}{2688}. \tag{8.146}$$

Chapter 9

Concluding Remarks

In this thesis, we have discussed a range of non-standard cosmological and gravitational theories and their theoretical applications. We began in the early universe, considering cosmological implications for higher spin fields in the context of the cosmological collider as well as dark matter. We then moved to the late universe and studied the impact of modified gravity theories on gravitational waves, binary pulsars, and black holes. This work has discussed many promising directions for future probes of such theories in both the cosmological and gravitational realms. There are still many open questions to be answered and much more to learn, but the work contained in this thesis represents the author's beginning contributions to the field.

Fin.

Bibliography

[1] N. Aghanim et al. Planck 2018 results. VI. Cosmological parameters. Astron. Astrophys., 641:A6, 2020. [Erratum: Astron.Astrophys. 652, C4 (2021)].

[2] Sean M. Carroll. Lecture notes on general relativity. 12 1997.

[3] B.P. Abbott et al. GW170817: Observation of Gravitational Waves from a Binary Neutron Star Inspiral. Phys. Rev. Lett., 119(16):161101, 2017.

[4] B. P. Abbott et al. Gravitational Waves and Gamma-rays from a Binary Neutron Star Merger: GW170817 and GRB 170817A. Astrophys. J. Lett., 848(2):L13, 2017.

[5] Abhirup Ghosh. Summary of Tests of General Relativity with GWTC-3. In 56th Rencontres de Moriond on Gravitation, 4 2022.

[6] R. A. Hulse and J. H. Taylor. Discovery of a pulsar in a binary system. Astrophys. J., 195:L51–L53, 1975.

[7] M. Kramer, Ingrid H. Stairs, R.N. Manchester, M.A. McLaughlin, A.G. Lyne, et al. Tests of general relativity from timing the double pulsar. Science, 314:97–102, 2006.

[8] Kazunori Akiyama et al. First M87 Event Horizon Telescope Results. I. The Shadow of the Supermassive Black Hole. Astrophys. J., 875(1):L1, 2019.

[9] V. C. Rubin, N. Thonnard, and W. K. Ford, Jr. Rotational properties of 21 SC galaxies with a large range of luminosities and radii, from NGC 4605 /R = 4kpc/ to UGC 2885 /R = 122 kpc/. Astrophys. J., 238:471, 1980.

[10] J. A. Peacock. Cosmological physics. 1999.

[11] Andrew R. Liddle. An introduction to modern cosmology. 1998.

[12] Y. Akrami et al. Planck 2018 results. I. Overview and the cosmological legacy of Planck. 2018.

[13] David Wands, Karim A. Malik, David H. Lyth, and Andrew R. Liddle. A New approach to the evolution of cosmological perturbations on large scales. Phys. Rev., D62:043527, 2000.

[14] Steven Weinberg. Adiabatic modes in cosmology. Phys. Rev., D67:123504, 2003.

[15] G. I. Rigopoulos and E. P. S. Shellard. The separate universe approach and the evolution of nonlinear superhorizon cosmological perturbations. Phys. Rev., D68:123518, 2003.

[16] David H. Lyth, Karim A. Malik, and Misao Sasaki. A General proof of the conservation of the curvature perturbation. JCAP, 0505:004, 2005.

[17] David Langlois and Filippo Vernizzi. Conserved non-linear quantities in cosmology. Phys. Rev., D72:103501, 2005.

[18] Valentin Assassi, Daniel Baumann, and Daniel Green. Symmetries and Loops in Inflation. JHEP, 02:151, 2013.

[19] Leonardo Senatore and Matias Zaldarriaga. The constancy of ζ in single-clock Inflation at all loops. JHEP, 09:148, 2013.

[20] Xingang Chen and Yi Wang. Quasi-Single Field Inflation and Non-Gaussianities. JCAP, 1004:027, 2010.

[21] Xingang Chen and Yi Wang. Large non-Gaussianities with Intermediate Shapes from Quasi-Single Field Inflation. Phys. Rev., D81:063511, 2010.

[22] Xingang Chen, Mohammad Hossein Namjoo, and Yi Wang. Quantum Primordial Standard Clocks. JCAP, 1602(02):013, 2016.

[23] Nima Arkani-Hamed and Juan Maldacena. Cosmological Collider Physics. arXiv e-prints, page arXiv:1503.08043, Mar 2015.

[24] Hayden Lee, Daniel Baumann, and Guilherme L. Pimentel. Non-Gaussianity as a Particle Detector. JHEP, 12:040, 2016.

[25] Ettore Majorana. Relativistic theory of particles with arbitrary intrinsic angular momentum. Nuovo Cim., 9:335–344, 1932.

[26] Toshifumi Noumi, Toshiaki Takeuchi, and Siyi Zhou. String Regge trajectory on de Sitter space and implications to inflation. 2019.

[27] Dieter Lust and Eran Palti. A Note on String Excitations and the Higuchi Bound. 2019.

[28] D. J. Gross. Strings at superPlanckian energies: In search of the string symmetry. 1988. [Phil. Trans. Roy. Soc. Lond.A329,401(1989)].

[29] Edward Witten. THE SEARCH FOR HIGHER SYMMETRY IN STRING THEORY. 1988. [Phil. Trans. Roy. Soc. Lond.A329,349(1989)].

[30] David J. Gross and Paul F. Mende. String Theory Beyond the Planck Scale. Nucl. Phys., B303:407–454, 1988.

[31] E. S. Fradkin and Mikhail A. Vasiliev. Candidate to the Role of Higher Spin Symmetry. Annals Phys., 177:63, 1987.

[32] Rudolf Haag, Jan T. Lopuszanski, and Martin Sohnius. All Possible Generators of Supersymmetries of the s Matrix. Nucl. Phys., B88:257, 1975. [,257(1974)].

[33] I. L. Buchbinder, S. James Gates Jr., and K. Koutrolikos. Superfield continuous spin equations of motion. Phys. Lett., B793:445–450, 2019.

[34] S. M. Kuzenko, A. G. Sibiryakov, and V. V. Postnikov. Massless gauge superfields of higher half integer superspins. JETP Lett., 57:534–538, 1993. [Pisma Zh. Eksp. Teor. Fiz.57,521(1993)].

[35] S. M. Kuzenko and A. G. Sibiryakov. Massless gauge superfields of higher integer superspins. JETP Lett., 57:539–542, 1993. [Pisma Zh. Eksp. Teor. Fiz.57,526(1993)].

[36] S. M. Kuzenko and A. G. Sibiryakov. Free massless higher superspin superfields on the anti-de Sitter superspace. Phys. Atom. Nucl., 57:1257–1267, 1994. [Yad. Fiz.57,1326(1994)].

[37] I. L. Buchbinder, S. M. Kuzenko, and A. G. Sibiryakov. Quantization of higher spin superfields in the anti-De Sitter superspace. Phys. Lett., B352:29–36, 1995.

[38] S. James Gates, Jr., Sergei M. Kuzenko, and Alexander G. Sibiryakov. N=2 supersymmetry of higher superspin massless theories. Phys. Lett., B412:59–68, 1997.

[39] S. James Gates, Jr., Sergei M. Kuzenko, and Alexander G. Sibiryakov. Towards a unified theory of massless superfields of all superspins. Phys. Lett., B394:343–353, 1997.

[40] S. James Gates, Jr. and Sergei M. Kuzenko. 4D, N = 1 higher spin gauge superfields and quantized twistors. JHEP, 10:008, 2005.

[41] S. James Gates, Jr. and Konstantinos Koutrolikos. On 4D, $\mathcal{N} = 1$ massless gauge superfields of arbitrary superhelicity. JHEP, 06:098, 2014.

[42] I. L. Buchbinder and K. Koutrolikos. BRST Analysis of the Supersymmetric Higher Spin Field Models. JHEP, 12:106, 2015.

[43] S. James Gates Jr. and Konstantinos Koutrolikos. From Diophantus to Supergravity and massless higher spin multiplets. JHEP, 11:063, 2017.

[44] Dmitri Sorokin and Mirian Tsulaia. Supersymmetric Reducible Higher-Spin Multiplets in Various Dimensions. Nucl. Phys., B929:216–242, 2018.

[45] Yu. M. Zinoviev. Massive N=1 supermultiplets with arbitrary superspins. Nucl. Phys., B785:98–114, 2007.

[46] I. L. Buchbinder, M. V. Khabarov, T. V. Snegirev, and Yu. M. Zinoviev. Lagrangian formulation of the massive higher spin N=1 supermultiplets in AdS_4 space. Nucl. Phys., B942:1–29, 2019.

[47] S. James Gates, Jr., Sergei M. Kuzenko, and Gabriele Tartaglino-Mazzucchelli. New massive supergravity multiplets. JHEP, 02:052, 2007.

[48] S. James. Gates, Jr. and Konstantinos Koutrolikos. A dynamical theory for linearized massive superspin 3/2. JHEP, 03:030, 2014.

[49] Clifford Cheung, Paolo Creminelli, A. Liam Fitzpatrick, Jared Kaplan, and Leonardo Senatore. The Effective Field Theory of Inflation. JHEP, 03:014, 2008.

[50] Eric A. Bergshoeff, Daniel Z. Freedman, Renata Kallosh, and Antoine Van Proeyen. Pure de Sitter Supergravity. Phys. Rev., D92(8):085040, 2015. [Erratum: Phys. Rev.D93,no.6,069901(2016)].

[51] Renata Kallosh and Timm Wrase. De Sitter Supergravity Model Building. Phys. Rev., D92(10):105010, 2015.

[52] Renata Kallosh. Matter-coupled de Sitter Supergravity. Theor. Math. Phys., 187(2):695–705, 2016. [Teor. Mat. Fiz.187,no.2,283(2016)].

[53] Luca V. Delacretaz, Victor Gorbenko, and Leonardo Senatore. The Supersymmetric Effective Field Theory of Inflation. JHEP, 03:063, 2017.

[54] S. James Gates, Jr., Marcus T. Grisaru, and Silvia Penati. Holomorphy, minimal homotopy and the 4-D, N=1 supersymmetric Bardeen-Gross-Jackiw anomaly. Phys. Lett., B481:397–407, 2000.

[55] S. James Gates, Jr., Marcus T. Grisaru, Marcia E. Knutt, Silvia Penati, and Hiroshi Suzuki. Supersymmetric gauge anomaly with general homotopic paths. Nucl. Phys., B596:315–347, 2001.

[56] S. James Gates, Jr., Marcus T. Grisaru, Marcia E. Knutt, and Silvia Penati. The Superspace WZNW action for 4-D, N=1 supersymmetric QCD. Phys. Lett., B503:349–354, 2001.

[57] Michael B. Green and John H. Schwarz. Anomaly Cancellation in Supersymmetric D=10 Gauge Theory and Superstring Theory. Phys. Lett., 149B:117–122, 1984.

[58] E. A. Bergshoeff and M. de Roo. The Quartic Effective Action of the Heterotic String and Supersymmetry. Nucl. Phys., B328:439–468, 1989.

[59] Cumrun Vafa and Edward Witten. A One loop test of string duality. Nucl. Phys., B447:261–270, 1995.

[60] M. J. Duff, James T. Liu, and R. Minasian. Eleven-dimensional origin of string-string duality: A One loop test. Nucl. Phys., B452:261–282, 1995. [,142(1995)].

[61] Edward Witten. Five-brane effective action in M theory. J. Geom. Phys., 22:103–133, 1997.

[62] Kasper Peeters, Pierre Vanhove, and Anders Westerberg. Supersymmetric higher derivative actions in ten-dimensions and eleven-dimensions, the associated superalgebras and their formulation in superspace. Class. Quant. Grav., 18:843–890, 2001.

[63] Michael B. Green and Michael Gutperle. Effects of D instantons. Nucl. Phys., B498:195–227, 1997.

[64] Juan Martin Maldacena. The Large N limit of superconformal field theories and supergravity. Int. J. Theor. Phys., 38:1113–1133, 1999. [Adv. Theor. Math. Phys.2,231(1998)].

[65] Daniel Baumann and Liam McAllister. Inflation and String Theory. Cambridge Monographs on Mathematical Physics. Cambridge University Press, 2015.

[66] Stephon H. S. Alexander. Inflation from D - anti-D-brane annihilation. Phys. Rev., D65:023507, 2002.

[67] Lisa Randall and Raman Sundrum. Out of this world supersymmetry breaking. Nucl. Phys., B557:79–118, 1999.

[68] Evan McDonough and Marco Scalisi. Inflation from Nilpotent Kähler Corrections. JCAP, 1611(11):028, 2016.

[69] Renata Kallosh, Andrei Linde, Diederik Roest, and Yusuke Yamada. $\overline{D3}$ induced geometric inflation. JHEP, 07:057, 2017.

[70] Sergio Ferrara, Renata Kallosh, and Andrei Linde. Cosmology with Nilpotent Superfields. JHEP, 10:143, 2014.

[71] Renata Kallosh and Andrei Linde. Inflation and Uplifting with Nilpotent Superfields. JCAP, 1501:025, 2015.

[72] Robert H. Brandenberger. Lectures on the theory of cosmological perturbations. Lect. Notes Phys., 646:127–167, 2004.

[73] Thomas Curtright. Massless Field Supermultiplets With Arbitrary Spin. Phys. Lett., 85B:219–224, 1979.

[74] Mikhail A. Vasiliev. 'Gauge' form of description of massless fields with arbitrary spin. (IN RUSSIAN). Yad. Fiz., 32:855–861, 1980. [Sov. J. Nucl. Phys.32,439(1980)].

[75] S. J. Gates Jr., Marcus T. Grisaru, M. Rocek, and W. Siegel. Superspace Or One Thousand and One Lessons in Supersymmetry. Front. Phys., 58:1–548, 1983.

[76] I. L. Buchbinder and S. M. Kuzenko. Ideas and methods of supersymmetry and supergravity: Or a w
1998.

[77] Atsushi Higuchi. Forbidden Mass Range for Spin-2 Field Theory in De Sitter Spacetime. Nucl. Phys., B282:397–436, 1987.

[78] Stanley Deser and A. Waldron. Partial masslessness of higher spins in (A)dS. Nucl. Phys., B607:577–604, 2001.

[79] Sergei M. Kuzenko, Ruben Manvelyan, and Stefan Theisen. Off-shell superconformal higher spin multiplets in four dimensions. JHEP, 07:034, 2017.

[80] I. L. Buchbinder, S. James Gates Jr., and Konstantinos Koutrolikos. Higher Spin Superfield interactions with the Chiral Supermultiplet: Conserved Supercurrents and Cubic Vertices. Universe, 4(1):6, 2018.

[81] Jessica Hutomo and Sergei M. Kuzenko. Non-conformal higher spin supercurrents. Phys. Lett., B778:242–246, 2018.

[82] Konstantinos Koutrolikos, Pavel KoÃÂÃÂ, and Rikard von Unge. Higher Spin Superfield interactions with Complex linear Supermultiplet: Conserved Supercurrents and Cubic Vertices. JHEP, 03:119, 2018.

[83] I. L. Buchbinder, S. James Gates Jr., and Konstantinos Koutrolikos. Interaction of supersymmetric nonlinear sigma models with external higher spin superfields via higher spin supercurrents. JHEP, 05:204, 2018.

[84] I. L. Buchbinder, S. James Gates Jr., and Konstantinos Koutrolikos. Conserved higher spin supercurrents for arbitrary spin massless supermultiplets and higher spin superfield cubic interactions. JHEP, 08:055, 2018.

[85] Evgeny I. Buchbinder, Jessica Hutomo, and Sergei M. Kuzenko. Higher spin supercurrents in anti-de Sitter space. JHEP, 09:027, 2018.

[86] I. L. Buchbinder, S. James Gates Jr., and K. Koutrolikos. Integer superspin supercurrents of matter supermultiplets. 2018.

[87] S. James Gates and K. Koutrolikos. Progress on cubic interactions of arbitrary superspin supermultiplets via gauge invariant supercurrents. 2019.

[88] Juan Martin Maldacena. Non-Gaussian features of primordial fluctuations in single field inflationary models. JHEP, 05:013, 2003.

[89] Xingang Chen. Primordial Non-Gaussianities from Inflation Models. Adv. Astron., 2010:638979, 2010.

[90] Peter Adshead, Richard Easther, and Eugene A. Lim. The 'in-in' Formalism and Cosmological Perturbations. Phys. Rev., D80:083521, 2009.

[91] Yi Wang. Inflation, cosmic perturbations and non-gaussianities. Communications in Theoretical Physics, 62(1):109–166, jul 2014.

[92] Alexander Altland and Ben D. Simons. Condensed Matter Field Theory. Cambridge University Press, 2 edition, 2010.

[93] Eiichiro Komatsu and David N. Spergel. Acoustic signatures in the primary microwave background bispectrum. Phys. Rev., D63:063002, 2001.

[94] Daniel Baumann, Garrett Goon, Hayden Lee, and Guilherme L. Pimentel. Partially Massless Fields During Inflation. JHEP, 04:140, 2018.

[95] Kevork N. Abazajian et al. CMB-S4 Science Book, First Edition. 2016.

[96] Hayden Lee. High-Energy Aspects of Inflationary Cosmology. PhD thesis, Cambridge U., DAMTP, 2017-07-21.

[97] David H. Lyth and David Roberts. Cosmological consequences of particle creation during inflation. Phys. Rev., D57:7120–7129, 1998.

[98] Nicola Bartolo, Alex Kehagias, Michele Liguori, Antonio Riotto, Maresuke Shiraishi, and Vittorio Tansella. Detecting higher spin fields through statistical anisotropy in the CMB and galaxy power spectra. Phys. Rev. D, 97(2):023503, Jan 2018.

[99] Azadeh Moradinezhad Dizgah, Gabriele Franciolini, Alex Kehagias, and Antonio Riotto. Constraints on long-lived, higher-spin particles from the galaxy bispectrum. Phys. Rev. D, 98(6):063520, Sep 2018.

[100] Azadeh Moradinezhad Dizgah and Cora Dvorkin. Scale-Dependent Galaxy Bias from Massive Particles with Spin during Inflation. JCAP, 1801(01):010, 2018.

[101] A. Moradinezhad Dizgah, H. Lee, J. B. Muñoz, and C. Dvorkin. Galaxy bispectrum from massive spinning particles. jcap, 5:013, May 2018.

[102] Lorenzo Bordin and Giovanni Cabass. Probing higher-spin fields from inflation with higher-order statistics of the CMB. arXiv e-prints, page arXiv:1902.09519, Feb 2019.

[103] Kazuhiro Kogai, Takahiko Matsubara, Atsushi J. Nishizawa, and Yuko Urakawa. Intrinsic galaxy alignment from angular dependent primordial non-Gaussianity. JCAP, 1808(08):014, 2018.

[104] Alex Kehagias and Antonio Riotto. On the Inflationary Perturbations of Massive Higher-Spin Fields. JCAP, 1707(07):046, 2017.

[105] Gabriele Franciolini, Alex Kehagias, and Antonio Riotto. Imprints of Spinning Particles on Primordial Cosmological Perturbations. JCAP, 1802(02):023, 2018.

[106] Gabriele Franciolini, Alex Kehagias, Antonio Riotto, and Maresuke Shiraishi. Detecting higher spin fields through statistical anisotropy in the CMB bispectrum. Phys. Rev., D98(4):043533, 2018.

[107] Donald Marolf, Luca Martucci, and Pedro J. Silva. Actions and Fermionic symmetries for D-branes in bosonic backgrounds. JHEP, 07:019, 2003.

[108] Donald Marolf, Luca Martucci, and Pedro J. Silva. Fermions, T duality and effective actions for D-branes in bosonic backgrounds. JHEP, 04:051, 2003.

[109] Luca Martucci, Jan Rosseel, Dieter Van den Bleeken, and Antoine Van Proeyen. Dirac actions for D-branes on backgrounds with fluxes. Class. Quant. Grav., 22:2745–2764, 2005.

[110] Keshav Dasgupta, Maxim Emelin, and Evan McDonough. Fermions on the antibrane: Higher order interactions and spontaneously broken supersymmetry. Phys. Rev., D95(2):026003, 2017.

[111] Xingang Chen, Hassan Firouzjahi, Mohammad Hossein Namjoo, and Misao Sasaki. A Single Field Inflation Model with Large Local Non-Gaussianity. EPL, 102(5):59001, 2013.

[112] R. Holman and Andrew J. Tolley. Enhanced Non-Gaussianity from Excited Initial States. JCAP, 0805:001, 2008.

[113] Nima Arkani-Hamed, Daniel Baumann, Hayden Lee, and Guilherme L. Pimentel. The Cosmological Bootstrap: Inflationary Correlators from Symmetries and Singularities. 2018.

[114] Edward Witten. String theory dynamics in various dimensions. Nucl. Phys., B443:85–126, 1995. [,333(1995)].

[115] Petr Horava and Edward Witten. Heterotic and type I string dynamics from eleven-dimensions. Nucl. Phys., B460:506–524, 1996. [,397(1995)].

[116] Chris Hull and Barton Zwiebach. Double Field Theory. JHEP, 09:099, 2009.

[117] P. Daniel Meerburg, Joel Meyers, Alexander van Engelen, and Yacine Ali-HaÃÂ¯moud. CMB B -mode non-Gaussianity. Phys. Rev., D93:123511, 2016.

[118] S. J. Gates, Jr. Sticking with SUSY. Physics World, 27(10):32–37, October 2014.

[119] Edward W. Kolb, Daniel J.H. Chung, and Antonio Riotto. WIMPzillas! AIP Conf. Proc., 484(1):91–105, 1999.

[120] Daniel J.H. Chung, Patrick Crotty, Edward W. Kolb, and Antonio Riotto. On the Gravitational Production of Superheavy Dark Matter. Phys. Rev. D, 64:043503, 2001.

[121] Daniel J.H. Chung. Classical Inflation Field Induced Creation of Superheavy Dark Matter. Phys. Rev. D, 67:083514, 2003.

[122] Daniel J.H. Chung, Edward W. Kolb, and Antonio Riotto. Production of massive particles during reheating. Phys. Rev. D, 60:063504, 1999.

[123] Edward W. Kolb, A.A. Starobinsky, and I.I. Tkachev. Trans-Planckian wimpzillas. JCAP, 07:005, 2007.

[124] Daniel J.H. Chung, Edward W. Kolb, and Antonio Riotto. Superheavy dark matter. Phys. Rev. D, 59:023501, 1998.

[125] Karim Benakli, John R. Ellis, and Dimitri V. Nanopoulos. Natural candidates for superheavy dark matter in string and M theory. Phys. Rev. D, 59:047301, 1999.

[126] Kristjan Kannike, Antonio Racioppi, and Martti Raidal. Super-heavy dark matter – Towards predictive scenarios from inflation. Nucl. Phys. B, 918:162–177, 2017.

[127] Edward W. Kolb and Andrew J. Long. Superheavy dark matter through Higgs portal operators. Phys. Rev. D, 96(10):103540, 2017.

[128] Lingfeng Li, Shiyun Lu, Yi Wang, and Siyi Zhou. Cosmological Signatures of Superheavy Dark Matter. JHEP, 07:231, 2020.

[129] Stephon Alexander, Gabriel Herczeg, Jinglong Liu, and Evan McDonough. Chiral Symmetry and the Cosmological Constant. Phys. Rev. D, 102(8):083526, 2020.

[130] Edward W. Kolb and Andrew J. Long. Completely Dark Photons from Gravitational Particle Production During Inflation. 9 2020.

[131] Edmund J. Copeland, Andrew R. Liddle, David H. Lyth, Ewan D. Stewart, and David Wands. False vacuum inflation with Einstein gravity. Phys. Rev. D, 49:6410–6433, 1994.

[132] Ran Ding and Yi Liao. Spin 3/2 Particle as a Dark Matter Candidate: an Effective Field Theory Approach. JHEP, 04:054, 2012.

[133] Chia-Feng Chang, Xiao-Gang He, and Jusak Tandean. Exploring Spin-3/2 Dark Matter with Effective Higgs Couplings. Phys. Rev. D, 96(7):075026, 2017.

[134] Marcos A.G. Gar cia, Yann Mambrini, Keith A. Olive, and Sarunas Verner. The case for decaying spin-3/2 dark matter. 2020.

[135] Katsuki Aoki and Kei-ichi Maeda. Condensate of Massive Graviton and Dark Matter. Phys. Rev. D, 97(4):044002, 2018.

[136] Luca Marzola, Martti Raidal, and Federico R. Urban. Oscillating Spin-2 Dark Matter. Phys. Rev. D, 97(2):024010, 2018.

[137] Juan Manuel Armaleo, Diana López Nacir, and Federico R. Urban. Binary pulsars as probes for spin-2 ultralight dark matter. JCAP, 01:053, 2020.

[138] Juan Manuel Armaleo, Diana López Nacir, and Federico R. Urban. Pulsar timing array constraints on Spin-2 ULDM. JCAP, 09:031, 2020.

[139] M. Asorey and D. García-Álvarez. Higher spin dark matter. AIP Conf. Proc., 1241(1):1192–1197, 2010.

[140] J. Asorey, M. Asorey, and D. García-Álvarez. Symplectic gauge fields and dark matter. Phys. Rev. D, 92(10):103517, 2015.

[141] Manuela Kulaxizi and Rakibur Rahman. Higher-Spin Modes in a Domain-Wall Universe. JHEP, 10:193, 2014.

[142] Nima Arkani-Hamed and Juan Maldacena. Cosmological Collider Physics. 3 2015.

[143] Daniel Baumann, Carlos Duaso Pueyo, Austin Joyce, Hayden Lee, and Guilherme L. Pimentel. The Cosmological Bootstrap: Weight-Shifting Operators and Scalar Seeds. 10 2019.

[144] Daniel Baumann, Carlos Duaso Pueyo, Austin Joyce, Hayden Lee, and Guilherme L. Pimentel. The Cosmological Bootstrap: Spinning Correlators from Symmetries and Factorization. 5 2020.

[145] Anson Hook, Junwu Huang, and Davide Racco. Searches for other vacua. Part II. A new Higgstory at the cosmological collider. JHEP, 01:105, 2020.

[146] Anson Hook, Junwu Huang, and Davide Racco. Minimal signatures of the Standard Model in non-Gaussianities. Phys. Rev. D, 101(2):023519, 2020.

[147] Soubhik Kumar and Raman Sundrum. Cosmological Collider Physics and the Curvaton. JHEP, 04:077, 2020.

[148] Tao Liu, Xi Tong, Yi Wang, and Zhong-Zhi Xianyu. Probing P and CP Violations on the Cosmological Collider. JHEP, 04:189, 2020.

[149] Lian-Tao Wang and Zhong-Zhi Xianyu. In Search of Large Signals at the Cosmological Collider. JHEP, 02:044, 2020.

[150] Yi Wang and Yuhang Zhu. Cosmological Collider Signatures of Massive Vectors from Non-Gaussian Gravitational Waves. JCAP, 04:049, 2020.

[151] Arushi Bodas, Soubhik Kumar, and Raman Sundrum. The Scalar Chemical Potential in Cosmological Collider Physics. 10 2020.

[152] Stephon Alexander, S. James Gates, Leah Jenks, K. Koutrolikos, and Evan McDonough. Higher Spin Supersymmetry at the Cosmological Collider: Sculpting SUSY Rilles in the CMB. JHEP, 10:156, 2019.

[153] Thomas Curtright. Massless Field Supermultiplets With Arbitrary Spin. Phys. Lett. B, 85:219–224, 1979.

[154] S.J. Gates, Marcus T. Grisaru, M. Rocek, and W. Siegel. Superspace Or One Thousand and One Lessons in Supersymmetry, volume 58. 1983.

[155] S.M. Kuzenko and A.G. Sibiryakov. Massless gauge superfields of higher integer superspins. JETP Lett., 57:539–542, 1993.

[156] S.M. Kuzenko, A.G. Sibiryakov, and V.V. Postnikov. Massless gauge superfields of higher half integer superspins. JETP Lett., 57:534–538, 1993.

[157] Jr. Gates, S.James, Sergei M. Kuzenko, and Alexander G. Sibiryakov. N=2 supersymmetry of higher superspin massless theories. Phys. Lett. B, 412:59–68, 1997.

[158] E.S. Fradkin and Mikhail A. Vasiliev. On the Gravitational Interaction of Massless Higher Spin Fields. Phys. Lett. B, 189:89–95, 1987.

[159] Mikhail A. Vasiliev. Consistent equation for interacting gauge fields of all spins in (3+1)-dimensions. Phys. Lett. B, 243:378–382, 1990.

[160] M.A. Vasiliev. Nonlinear equations for symmetric massless higher spin fields in (A)dS(d). Phys. Lett. B, 567:139–151, 2003.

[161] E.S. Fradkin and Mikhail A. Vasiliev. Superalgebra of Higher Spins and Auxiliary Fields. Int. J. Mod. Phys. A, 3:2983, 1988.

[162] V.E. Didenko and E.D. Skvortsov. Elements of Vasiliev theory. 1 2014.

[163] Dmitri Sorokin. Introduction to the classical theory of higher spins. AIP Conf. Proc., 767(1):172–202, 2005.

[164] Rakibur Rahman and Massimo Taronna. From Higher Spins to Strings: A Primer. 12 2015.

[165] Pan Kessel. The Very Basics of Higher-Spin Theory. PoS, Modave2016:001, 2017.

[166] Jr Gates, S.James and Konstantinos Koutrolikos. A Unified Spinorial Superfield Treatment of the Higher Superspin Superfield Formalism. 4 2010.

[167] Jr. Gates, S.James and Konstantinos Koutrolikos. A Codicil To Massless Gauge Superfields of Higher Half-Odd Integer Superspins. 3 2011.

[168] Jr. Gates, S.James and Konstantinos Koutrolikos. A Codicil To Massless Gauge Superfields of Higher Integer Superspins. 3 2011.

[169] Jr. Gates, S. James and Konstantinos Koutrolikos. On 4D, N = 1 Massless Gauge Superfields of Higher Superspin: Half-Odd-Integer Case. 10 2013.

[170] Jr. Gates, S.James and Konstantinos Koutrolikos. On 4D, $\mathcal{N} = 1$ massless gauge superfields of arbitrary superhelicity. JHEP, 06:098, 2014.

[171] Jr. Gates, S. James and Konstantinos Koutrolikos. A dynamical theory for linearized massive superspin 3/2. JHEP, 03:030, 2014.

[172] Konstantinos Koutrolikos. Aspects of Supersymmetric Higher Spins. PoS, CORFU2014:152, 2015.

[173] S. James Gates and Konstantinos Koutrolikos. From Diophantus to Supergravity and massless higher spin multiplets. JHEP, 11:063, 2017.

[174] I.L. Buchbinder, S. James Gates, and Konstantinos Koutrolikos. Higher Spin Superfield interactions with the Chiral Supermultiplet: Conserved Supercurrents and Cubic Vertices. Universe, 4(1):6, 2018.

[175] I.L. Buchbinder, S. James Gates, and Konstantinos Koutrolikos. Interaction of supersymmetric nonlinear sigma models with external higher spin superfields via higher spin supercurrents. JHEP, 05:204, 2018.

[176] I.L. Buchbinder, S. James Gates, and K. Koutrolikos. Integer superspin supercurrents of matter supermultiplets. JHEP, 05:031, 2019.

[177] Evgeny I. Buchbinder, Jessica Hutomo, and Sergei M. Kuzenko. Higher spin supercurrents in anti-de Sitter space. JHEP, 09:027, 2018.

[178] I.L. Buchbinder, S. James Gates, and Konstantinos Koutrolikos. Conserved higher spin supercurrents for arbitrary spin massless supermultiplets and higher spin superfield cubic interactions. JHEP, 08:055, 2018.

[179] S. James Gates and K. Koutrolikos. Progress on cubic interactions of arbitrary superspin supermultiplets via gauge invariant supercurrents. Phys. Lett. B, 797:134868, 2019.

[180] I.L. Buchbinder, S. James Gates, and K. Koutrolikos. Hierarchy of Supersymmetric Higher Spin Connections. 10 2020.

[181] I.L. Buchbinder and T.V. Snegirev. Lagrangian formulation of free arbitrary N-extended massless higher spin supermultiplets in 4D, AdS space. 9 2020.

[182] Nima Afkhami-Jeddi, Sandipan Kundu, and Amirhossein Tajdini. A Bound on Massive Higher Spin Particles. JHEP, 04:056, 2019.

[183] Jared Kaplan and Sandipan Kundu. Closed Strings and Weak Gravity from Higher-Spin Causality. 8 2020.

[184] Jared Kaplan and Sandipan Kundu. Causality Constraints in Large N QCD Coupled to Gravity. 9 2020.

[185] S. Weinberg. Photons and gravitons in s-matrix theory: Derivation of charge conservation and equality of gravitational and inertial mass. Physical Review, 135:338–345, 1964.

[186] Sidney Coleman and Jeffrey Mandula. All possible symmetries of the s matrix. Phys. Rev., 159:1251–1256, Jul 1967.

[187] Marcus T. Grisaru and H.N. Pendleton. Soft Spin 3/2 Fermions Require Gravity and Supersymmetry. Phys. Lett. B, 67:323–326, 1977.

[188] C. Aragone and Stanley Deser. Consistency Problems of Hypergravity. Phys. Lett. B, 86:161–163, 1979.

[189] Steven Weinberg and Edward Witten. Limits on Massless Particles. Phys. Lett. B, 96:59–62, 1980.

[190] M. Porrati. Universal Limits on Massless High-Spin Particles. Phys. Rev. D, 78:065016, 2008.

[191] Brando Bellazzini, Francesco Riva, Javi Serra, and Francesco Sgarlata. Massive Higher Spins: Effective Theory and Consistency. JHEP, 10:189, 2019.

[192] Marco Scalisi. Inflation, Higher Spins and the Swampland. Phys. Lett. B, 808:135683, 2020.

[193] Simone Giombi and Xi Yin. Higher Spins in AdS and Twistorial Holography. JHEP, 04:086, 2011.

[194] A. Sagnotti and M. Tsulaia. On higher spins and the tensionless limit of string theory. Nucl. Phys. B, 682:83–116, 2004.

[195] Matthias R Gaberdiel and Rajesh Gopakumar. Stringy Symmetries and the Higher Spin Square. J. Phys. A, 48(18):185402, 2015.

[196] Kevin Ferreira, Matthias R. Gaberdiel, and Juan I. Jottar. Higher spins on AdS_3 from the worldsheet. JHEP, 07:131, 2017.

[197] Lorenz Eberhardt, Matthias R. Gaberdiel, and Ingo Rienacker. JHEP, 03:097, 2018.

[198] Matthias R. Gaberdiel and Rajesh Gopakumar. Tensionless string spectra on AdS_3. JHEP, 05:085, 2018.

[199] David J. Gross and Paul F. Mende. The High-Energy Behavior of String Scattering Amplitudes. Phys. Lett. B, 197:129–134, 1987.

[200] D. Amati, M. Ciafaloni, and G. Veneziano. Superstring Collisions at Planckian Energies. Phys. Lett. B, 197:81, 1987.

[201] A. Sagnotti. Notes on Strings and Higher Spins. pages 183–221, 2013.

[202] L. H. Thomas. On unitary representations of the group of de sitter space. Annals of Mathematics, 42(1):113–126, 1941.

[203] T. D. Newton. A note on the representations of the de sitter group. Annals of Mathematics, 51(3):730–733, 1950.

[204] G. W. Gibbons and S. W. Hawking. Cosmological event horizons, thermodynamics, and particle creation. Phys. Rev. D, 15:2738–2751, May 1977.

[205] William H. Kinney. Cosmology, inflation, and the physics of nothing. NATO Sci. Ser. II, 123:189–243, 2003.

[206] A.S. Lapedes. Bogolyubov Transformations, Propagators, and the Hawking Effect. J. Math. Phys., 19:2289, 1978.

[207] Akihiro Nakayama. Notes on the Hawking Effect in De Sitter Space. 2. Phys. Rev. D, 37:354, 1988.

[208] Daniel Baumann. Primordial Cosmology. PoS, TASI2017:009, 2018.

[209] N. Aghanim et al. Planck 2018 results. VI. Cosmological parameters. Astron. Astrophys., 641:A6, 2020.

[210] David N. Spergel. The Motion of the Earth and the Detection of Wimps. Phys. Rev. D, 37:1353, 1988.

[211] F. Mayet et al. A review of the discovery reach of directional Dark Matter detection. Phys. Rept., 627:1–49, 2016.

[212] Riccardo Catena, Jan Conrad, Christian Döring, Alfredo Davide Ferella, and Martin B. Krauss. Dark matter spin determination with directional direct detection experiments. Phys. Rev. D, 97(2):023007, 2018.

[213] Riccardo Catena, K$\rho are Fridell, and Vanessa Zema. Direct detection of fermionic and vector dark matt$

[214] Nassim Bozorgnia, Graciela B. Gelmini, and Paolo Gondolo. Ring-like features in directional dark matter detection. JCAP, 06:037, 2012.

[215] Nassim Bozorgnia, Graciela B. Gelmini, and Paolo Gondolo. Inverted dipole feature in directional detection of exothermic dark matter. JCAP, 01:052, 2017.

[216] Dan Hooper and Lisa Goodenough. Dark Matter Annihilation in The Galactic Center As Seen by the Fermi Gamma Ray Space Telescope. Phys. Lett. B, 697:412–428, 2011.

[217] Juan Carlos Criado, Niko Koivunen, Martti Raidal, and Hardi Veermäe. Dark Matter of Any Spin – an Effective Field Theory and Applications. 10 2020.

[218] Stephon Alexander, Marina Cortes, Andrew R. Liddle, JoÃÂ£o Magueijo, Robert Sims, and Lee Smolin. Zero-parameter extension of general relativity with a varying cosmological constant. Phys. Rev., D100(8):083506, 2019.

[219] Stephon Alexander, Marina Cortes, Andrew R. Liddle, JoÃÂ£o Magueijo, Robert Sims, and Lee Smolin. Cosmology of minimal varying Lambda theories. Phys. Rev., D100(8):083507, 2019.

[220] Brian P. Dolan. Chiral fermions and torsion in the early Universe. Class. Quant. Grav., 27:095010, 2010. [Erratum: Class. Quant. Grav.27,249801(2010)].

[221] Simone Mercuri and Victor Taveras. Interaction of the Barbero–Immirzi Field with Matter and Pseudo-Scalar Perturbations. Phys. Rev., D80:104007, 2009.

[222] Peter Baekler, Friedrich W. Hehl, and James M. Nester. Poincare gauge theory of gravity: Friedman cosmology with even and odd parity modes. Analytic part. Phys. Rev., D83:024001, 2011.

[223] Nikodem J. Poplawski. Nonsingular, big-bounce cosmology from spinor-torsion coupling. Phys. Rev., D85:107502, 2012.

[224] Thomas Schucker and Andre Tilquin. Torsion, an alternative to the cosmological constant? Int. J. Mod. Phys., D21:1250089, 2012.

[225] Antonella Cid, Fernando Izaurieta, Genly Leon, Perla Medina, and Daniela Narbona. Non-minimally coupled scalar field cosmology with torsion. JCAP, 1804(04):041, 2018.

[226] Tom Zlosnik, Federico Urban, Luca Marzola, and Tomi Koivisto. Spacetime and dark matter from spontaneous breaking of Lorentz symmetry. Class. Quant. Grav., 35(23):235003, 2018.

[227] Eanna E. Flanagan. Palatini form of 1/R gravity. Phys. Rev. Lett., 92:071101, 2004.

[228] Thomas P. Sotiriou. Unification of inflation and cosmic acceleration in the Palatini formalism. Phys. Rev., D73:063515, 2006.

[229] Florian Bauer and Durmus A. Demir. Higgs-Palatini Inflation and Unitarity. Phys. Lett., B698:425–429, 2011.

[230] Shane Farnsworth, Jean-Luc Lehners, and Taotao Qiu. Spinor driven cosmic bounces and their cosmological perturbations. Phys. Rev., D96(8):083530, 2017.

[231] Andrea Addazi, Pisin Chen, and Antonino Marciano. Emergent inflation from a Nambu–Jona-Lasinio mechanism in gravity with non-dynamical torsion. Eur. Phys. J., C79(4):297, 2019.

[232] João Magueijo and Tom Zλośnik. $Parityviolating Friedmann Universes. Phys. Rev.$, $D100(8) : 08403$

[233] Markus Lazar and Friedrich W. Hehl. Cartan's spiral staircase in physics and, in particular, in the gauge theory of dislocations. Found. Phys., 40:1298–1325, 2010.

[234] M. Henneaux and C. Teitelboim. The Cosmological Constant and General Covariance. Phys. Lett., B222:195–199, 1989.

[235] Pavel Jirousek and Alexander Vikman. New Weyl-invariant vector-tensor theory for the cosmological constant. JCAP, 1904:004, 2019.

[236] Katrin Hammer, Pavel Jirousek, and Alexander Vikman. Axionic cosmological constant. 2020.

[237] Stephon Alexander, Joao Magueijo, and Lee Smolin. The Quantum Cosmological Constant. Symmetry, 11(9):1130, 2019.

[238] João Magueijo and Lee Smolin. A Universe that does not know the time. 2018.

[239] Lee Smolin and Chopin Soo. The Chern-Simons invariant as the natural time variable for classical and quantum cosmology. Nucl. Phys., B449:289–316, 1995.

[240] J. Richard Gott, III and Li-Xin Li. Can the universe create itself? Phys. Rev., D58:023501, 1998.

[241] Niayesh Afshordi, Daniel J. H. Chung, and Ghazal Geshnizjani. Cuscuton: A Causal Field Theory with an Infinite Speed of Sound. Phys. Rev., D75:083513, 2007.

[242] Rodrigo Aros, Mauricio Contreras, Rodrigo Olea, Ricardo Troncoso, and Jorge Zanelli. Conserved charges for gravity with locally AdS asymptotics. Phys. Rev. Lett., 84:1647–1650, 2000.

[243] Olivera Miskovic and Rodrigo Olea. Topological regularization and self-duality in four-dimensional anti-de Sitter gravity. Phys. Rev., D79:124020, 2009.

[244] Chung-Pei Ma and Edmund Bertschinger. Cosmological perturbation theory in the synchronous and conformal Newtonian gauges. Astrophys. J., 455:7–25, 1995.

[245] Planck Collaboration, P. A. R. Ade, N. Aghanim, M. Arnaud, M. Ashdown, J. Aumont, C. Baccigalupi, A. J. Banday, R. B. Barreiro, J. G. Bartlett, and et al. Planck 2015 results. XIII. Cosmological parameters. ArXiv e-prints, February 2015.

[246] Sean M. Carroll and Eugene A. Lim. Lorentz-violating vector fields slow the universe down. Phys. Rev. D, 70:123525, 2004.

[247] José Barrientos, Fabrizio Cordonier-Tello, Cristóbal Corral, Fernando Izaurieta, Perla Medina, Eduardo Rodríguez, and Omar Valdivia. Luminal Propagation of Gravitational Waves in Scalar-tensor Theories: The Case for Torsion. Phys. Rev., D100(12):124039, 2019.

[248] T. Baker, E. Bellini, P. G. Ferreira, M. Lagos, J. Noller, and I. Sawicki. Strong constraints on cosmological gravity from GW170817 and GRB 170817A. Phys. Rev. Lett., 119(25):251301, 2017.

[249] Paolo Creminelli and Filippo Vernizzi. Dark energy after gw170817 and grb170817a. Physical Review Letters, 119(25), Dec 2017.

[250] Jeremy Sakstein and Bhuvnesh Jain. Implications of the neutron star merger gw170817 for cosmological scalar-tensor theories. Physical Review Letters, 119(25), Dec 2017.

[251] Jose María Ezquiaga and Miguel Zumalacárregui. Dark energy after gw170817: Dead ends and the road ahead. Physical Review Letters, 119(25), Dec 2017.

[252] Giovanni Amelino-Camelia. Relativity in space-times with short distance structure governed by an observer independent (Planckian) length scale. Int. J. Mod. Phys., D11:35–60, 2002.

[253] Joao Magueijo and Lee Smolin. Lorentz invariance with an invariant energy scale. Phys. Rev. Lett., 88:190403, 2002.

[254] Joao Magueijo and Lee Smolin. Generalized Lorentz invariance with an invariant energy scale. Phys. Rev., D67:044017, 2003.

[255] J. Kowalski-Glikman and S. Nowak. Doubly special relativity theories as different bases of kappa Poincare algebra. Phys. Lett., B539:126–132, 2002.

[256] Michele Arzano, Giulia Gubitosi, and Joao Magueijo. Parity at the Planck scale. Phys. Lett., B781:510–516, 2018.

[257] Aindriú Conroy and Tomi Koivisto. Parity-Violating Gravity and GW170817 in Non-Riemannian Cosmology. 2019.

[258] Wen Zhao, Tao Zhu, Jin Qiao, and Anzhong Wang. Waveform of gravitational waves in the general parity-violating gravities. 2019.

[259] Wen Zhao, Tan Liu, Linqing Wen, Tao Zhu, Anzhong Wang, Qian Hu, and Cong Zhou. Model-independent test of the parity symmetry of gravity with gravitational waves. 2019.

[260] Stephon H. Alexander and Nicolas Yunes. Gravitational wave probes of parity violation in compact binary coalescences. Phys. Rev., D97(6):064033, 2018.

[261] Kent Yagi and Huan Yang. Probing Gravitational Parity Violation with Gravitational Waves from Stellar-mass Black Hole Binaries. Phys. Rev., D97(10):104018, 2018.

[262] Vera Gluscevic and Marc Kamionkowski. Testing parity-violating mechanisms with cosmic microwave background experiments. Physical Review D, 81(12), Jun 2010.

[263] Anzhong Wang, Qiang Wu, Wen Zhao, and Tao Zhu. Polarizing primordial gravitational waves by parity violation. Phys. Rev., D87(10):103512, 2013.

[264] Nicola Bartolo and Giorgio Orlando. Parity breaking signatures from a Chern-Simons coupling during inflation: the case of non-Gaussian gravitational waves. JCAP, 1707:034, 2017.

[265] Nicola Bartolo, Giorgio Orlando, and Maresuke Shiraishi. Measuring chiral gravitational waves in Chern-Simons gravity with CMB bispectra. JCAP, 1901(01):050, 2019.

[266] Keisuke Inomata and Marc Kamionkowski. Chiral photons from chiral gravitational waves. Phys. Rev. Lett., 123(3):031305, 2019.

[267] Kiyoshi Wesley Masui, Ue-Li Pen, and Neil Turok. Two- and Three-Dimensional Probes of Parity in Primordial Gravity Waves. Phys. Rev. Lett., 118(22):221301, 2017.

[268] Maresuke Shiraishi, Daisuke Nitta, and Shuichiro Yokoyama. Parity Violation of Gravitons in the CMB Bispectrum. Prog. Theor. Phys., 126:937–959, 2011.

[269] B. P. Abbott et al. Tests of general relativity with GW150914. Phys. Rev. Lett., 116(22):221101, 2016.

[270] Nicolas Yunes, Kent Yagi, and Frans Pretorius. Theoretical Physics Implications of the Binary Black-Hole Mergers GW150914 and GW151226. Phys. Rev., D94(8):084002, 2016.

[271] Emanuele Berti, Kent Yagi, and NicolÃ¡s Yunes. Extreme Gravity Tests with Gravitational Waves from Compact Binary Coalescences: (I) Inspiral-Merger. Gen. Rel. Grav., 50(4):46, 2018.

[272] Emanuele Berti, Kent Yagi, Huan Yang, and NicolÃ¡s Yunes. Extreme Gravity Tests with Gravitational Waves from Compact Binary Coalescences: (II) Ringdown. Gen. Rel. Grav., 50(5):49, 2018.

[273] B.P. Abbott et al. Tests of General Relativity with the Binary Black Hole Signals from the LIGO-Virgo Catalog GWTC-1. Phys. Rev. D, 100(10):104036, 2019.

[274] B.P. Abbott et al. Tests of General Relativity with GW170817. Phys. Rev. Lett., 123(1):011102, 2019.

[275] Chao Zhang, Xiang Zhao, Anzhong Wang, Bin Wang, Kent Yagi, Nicolas Yunes, Wen Zhao, and Tao Zhu. Gravitational waves from the quasicircular inspiral of compact binaries in Einstein-aether theory. Phys. Rev. D, 101(4):044002, 2020.

[276] Remya Nair, Scott Perkins, Hector O. Silva, and Nicolás Yunes. Fundamental Physics Implications for Higher-Curvature Theories from Binary Black Hole Signals in the LIGO-Virgo Catalog GWTC-1. Phys. Rev. Lett., 123(19):191101, 2019.

[277] Kei Yamada, Tatsuya Narikawa, and Takahiro Tanaka. Testing massive-field modifications of gravity via gravitational waves. PTEP, 2019(10):103E01, 2019.

[278] Zack Carson and Kent Yagi. Parametrized and inspiral-merger-ringdown consistency tests of gravity with multiband gravitational wave observations. Phys. Rev. D, 101(4):044047, 2020.

[279] Sharaban Tahura and Kent Yagi. Parameterized Post-Einsteinian Gravitational Waveforms in Various Modified Theories of Gravity. Phys. Rev. D, 98(8):084042, 2018. [Erratum: Phys.Rev.D 101, 109902 (2020)].

[280] M. Kramer et al. Tests of general relativity from timing the double pulsar. Science, 314:97–102, 2006.

[281] Emanuele Berti et al. Testing General Relativity with Present and Future Astrophysical Observations. Class. Quant. Grav., 32:243001, 2015.

[282] Hartland S. Snyder. Quantized space-time. Phys. Rev., 71:38–41, Jan 1947.

[283] Alain Connes. Non-commutative differential geometry. Publications MathÃ©matiques de l'Institut des Hautes Ãtudes Scientifiques, 62:41–144, 1985.

[284] Michael R. Douglas and Nikita A. Nekrasov. Noncommutative field theory. Rev. Mod. Phys., 73:977–1029, 2001.

[285] Richard J. Szabo. Quantum field theory on noncommutative spaces. Phys. Rept., 378:207–299, 2003.

[286] M. Chaichian, P. Presnajder, M.M. Sheikh-Jabbari, and A. Tureanu. Noncommutative standard model: Model building. Eur. Phys. J. C, 29:413–432, 2003.

[287] Masud Chaichian, Archil Kobakhidze, and Anca Tureanu. Spontaneous reduction of noncommutative gauge symmetry and model building. Eur. Phys. J. C, 47:241–245, 2006.

[288] X. Calmet, B. Jurco, P. Schupp, J. Wess, and M. Wohlgenannt. The Standard model on noncommutative space-time. Eur. Phys. J. C, 23:363–376, 2002.

[289] Paolo Aschieri, Branislav Jurco, Peter Schupp, and Julius Wess. Noncommutative GUTs, standard model and C,P,T. Nucl. Phys. B, 651:45–70, 2003.

[290] F. Ardalan, H. Arfaei, and M.M. Sheikh-Jabbari. Noncommutative geometry from strings and branes. JHEP, 02:016, 1999.

[291] Nathan Seiberg and Edward Witten. String theory and noncommutative geometry. JHEP, 09:032, 1999.

[292] Archil Kobakhidze, Cyril Lagger, and Adrian Manning. Constraining noncommutative spacetime from GW150914. Phys. Rev. D, 94(6):064033, 2016.

[293] Luc Blanchet and Guillaume Faye. Lorentzian regularization and the problem of point - like particles in general relativity. J. Math. Phys., 42:4391–4418, 2001.

[294] William Nelson, Joseph Ochoa, and Mairi Sakellariadou. Constraining the Noncommutative Spectral Action via Astrophysical Observations. Phys. Rev. Lett., 105:101602, 2010.

[295] William Nelson, Joseph Ochoa, and Mairi Sakellariadou. Gravitational Waves in the Spectral Action of Noncommutative Geometry. Phys. Rev., D82:085021, 2010.

[296] Xue-Mei Deng. Solar System and stellar tests of noncommutative spectral geometry. Eur. Phys. J. Plus, 132(2):85, 2017.

[297] Lawrence E. Kidder, Clifford M. Will, and Alan G. Wiseman. Spin effects in the inspiral of coalescing compact binaries. Phys. Rev., D47(10):R4183–R4187, 1993.

[298] Lawrence E. Kidder. Coalescing binary systems of compact objects to postNewtonian 5/2 order. 5. Spin effects. Phys. Rev., D52:821–847, 1995.

[299] Kunihito Ioka and Keisuke Taniguchi. Gravitational waves from inspiralling compact binaries with magnetic dipole moments. Astrophys. J., 537:327, 2000.

[300] Kent Yagi. Scientific Potential of DECIGO Pathfinder and Testing GR with Space-Borne Gravitational Wave Interferometers. Int. J. Mod. Phys. D, 22:1341013, 2013.

[301] Thibault Damour, Bala R. Iyer, and B.S. Sathyaprakash. A Comparison of search templates for gravitational waves from binary inspiral. Phys. Rev. D, 63:044023, 2001. [Erratum: Phys.Rev.D 72, 029902 (2005)].

[302] B.P. Abbott et al. GWTC-1: A Gravitational-Wave Transient Catalog of Compact Binary Mergers Observed by LIGO and Virgo during the First and Second Observing Runs. Phys. Rev. X, 9(3):031040, 2019.

[303] Clifford M. Will. Theory and Experiment in Gravitational Physics. Cambridge University Press, 9 2018.

[304] Clifford M. Will. Testing general relativity with compact-body orbits: a modified Einstein–Infeld–Hoffmann framework. Class. Quant. Grav., 35(8):085001, 2018.

[305] Ingrid H. Stairs. Testing general relativity with pulsar timing. Living Rev. Rel., 6:5, 2003.

[306] Laura Sampson, Nicolas Yunes, and Neil Cornish. A Rosetta Stone for Parameterized Tests of Gravity. 2013.

[307] R. Jackiw and S.Y. Pi. Chern-Simons modification of general relativity. Phys. Rev. D, 68:104012, 2003.

[308] S. Alexander and N. Yunes. Chern-Simons modified general relativity. Phys. Rep., 480:1–55, August 2009.

[309] Luis Alvarez-Gaume and Edward Witten. Gravitational anomalies. Nuclear Physics B, 234(2):269–330, 1984.

[310] J. Polchinski. String theory. Vol. 2: Superstring theory and beyond. Cambridge Monographs on Mathematical Physics. Cambridge University Press, 12 2007.

[311] Stephon H. S. Alexander, Michael E. Peskin, and M. M. Sheikh-Jabbari. Leptogenesis from gravity waves in models of inflation. Phys. Rev. Lett., 96:081301, Feb 2006.

[312] Stephon H. S. Alexander and Jr. Gates, S. James. Can the string scale be related to the cosmic baryon asymmetry? JCAP, 0606:018, 2006.

[313] Michael B. Green, J. H. Schwarz, and Edward Witten. Superstring Theory. Vol. 2: Loop Amplitides, Anomalies and Phenomenology. Cambridge University Press, Cambridge, UK, 1987.

[314] R. Jackiw and S. Y. Pi. Chern-Simons modification of general relativity. Phys. Rev., D68:104012, 2003.

[315] Bruce A. Campbell, M.J. Duncan, Nemanja Kaloper, and Keith A. Olive. Gravitational dynamics with lorentz chern-simons terms. Nuclear Physics B, 351(3):778–792, 1991.

[316] David Guarrera and A. J. Hariton. Papapetrou energy-momentum tensor for chern-simons modified gravity. 2007.

[317] Daniel Grumiller and Nicolas Yunes. How do Black Holes Spin in Chern-Simons Modified Gravity? Phys. Rev., D77:044015, 2008.

[318] Nicolas Yunes and Frans Pretorius. Dynamical Chern-Simons Modified Gravity. I. Spinning Black Holes in the Slow-Rotation Approximation. Phys. Rev. D, 79:084043, 2009.

[319] Kent Yagi, Nicolas Yunes, and Takahiro Tanaka. Slowly Rotating Black Holes in Dynamical Chern-Simons Gravity: Deformation Quadratic in the Spin. Phys. Rev. D, 86:044037, 2012. [Erratum: Phys.Rev.D 89, 049902 (2014)].

[320] Andrea Maselli, Paolo Pani, Roberto Cotesta, Leonardo Gualtieri, Valeria Ferrari, and Luigi Stella. Geodesic models of quasi-periodic-oscillations as probes of quadratic gravity. Astrophys. J., 843(1):25, 2017.

[321] Roger Penrose. Gravitational collapse and space-time singularities. Phys. Rev. Lett., 14:57–59, 1965.

[322] S. W. Hawking and R. Penrose. The Singularities of gravitational collapse and cosmology. Proc. Roy. Soc. Lond. A, 314:529–548, 1970.

[323] Robert Delbourgo and Abdus Salam. The gravitational correction to pcac. Phys. Lett. B, 40:381–382, 1972.

[324] Stephon Alexander. A Quantum gravitational relaxation of the cosmological constant. Phys. Lett. B, 629:53–59, 2005.

[325] Hector O. Silva, A. Miguel Holgado, Alejandro Cárdenas-Avendaño, and Nicolás Yunes. Astrophysical and theoretical physics implications from multimessenger neutron star observations. 4 2020.

[326] Thomas E. Riley et al. A *NICER* View of PSR J0030+0451: Millisecond Pulsar Parameter Estimation. Astrophys. J. Lett., 887(1):L21, 2019.

[327] M. C. Miller et al. PSR J0030+0451 Mass and Radius from *NICER* Data and Implications for the Properties of Neutron Star Matter. Astrophys. J. Lett., 887(1):L24, 2019.

[328] Kent Yagi, Leo C. Stein, Nicolas Yunes, and Takahiro Tanaka. Isolated and Binary Neutron Stars in Dynamical Chern-Simons Gravity. Phys. Rev. D, 87:084058, 2013. [Erratum: Phys.Rev.D 93, 089909 (2016)].

[329] Renata Kallosh, Andrei D. Linde, Dmitri A. Linde, and Leonard Susskind. Gravity and global symmetries. Phys. Rev. D, 52:912–935, 1995.

[330] Tetsuya Shiromizu and Kentaro Tanabe. Static spacetimes with/without black holes in dynamical Chern-Simons gravity. Phys. Rev. D, 87:081504, 2013.

[331] GRTensorII. This is a package which runs within Maple but distinct from packages distributed with Maple. It is distributed freely on the World-Wide-Web from the address: `http://grtensor.org`.

[332] Terence Delsate, Carlos Herdeiro, and Eugen Radu. Non-perturbative spinning black holes in dynamical Chern–Simons gravity. Phys. Lett. B, 787:8–15, 2018.

[333] Andrew Sullivan, Nicolás Yunes, and Thomas P. Sotiriou. Numerical Black Hole Solutions in Modified Gravity Theories: Axial Symmetry Case. 9 2020.

[334] Ibrahima Bah and Pierre Heidmann. Topological Stars and Black Holes. 11 2020.

[335] Amalkumar Raychaudhuri. Relativistic Cosmology. I. Physical Review, 98(4):1123–1126, May 1955.

[336] A Borde. Geodesic focusing, energy conditions and singularities. Classical and Quantum Gravity, 4(2):343–356, mar 1987.

[337] Stephon Alexander, Leah Jenks, and Nicolas Yunes. To appear. *To Appear,*, 2021.

[338] Stephon Alexander, Gregory Gabadadze, Leah Jenks, and Nicolas Yunes. In Preparation. *To Appear,*, 2021.

[339] Stephon Alexander and Nicolas Yunes. A new PPN parameter to test Chern-Simons gravity. Phys. Rev. Lett., 99:241101, 2007.

[340] Stephon Alexander and Nicolas Yunes. Parametrized post-newtonian expansion of chern-simons gravity. Phys. Rev., D75:124022, 2007.

[341] Stephon Alexander and Nicolas Yunes. Chern-Simons Modified Gravity as a Torsion Theory and its Interaction with Fermions. Phys. Rev., D77:124040, 2008.

[342] Carlos F. Sopuerta and Nicolas Yunes. Extreme and Intermediate-Mass Ratio Inspirals in Dynamical Chern-Simons Modified Gravity. Phys.Rev., D80:064006, 2009.

[343] Vitor Cardoso and Leonardo Gualtieri. Perturbations of Schwarzschild black holes in Dynamical Chern-Simons modified gravity. Phys. Rev., D80:064008, 2009. [Erratum-ibid.D81:089903,2010].

[344] Kohkichi Konno, Toyoki Matsuyama, and Satoshi Tanda. Rotating black hole in extended Chern-Simons modified gravity. Prog.Theor.Phys., 122:561–568, 2009.

[345] Leonardo Amarilla, Ernesto F. Eiroa, and Gaston Giribet. Null geodesics and shadow of a rotating black hole in extended Chern-Simons modified gravity. Phys. Rev., D81:124045, 2010.

[346] Songbai Chen and Jiliang Jing. Geodetic precession and strong gravitational lensing in the dynamical Chern-Simons modified gravity. Class. Quant Grav., 27:225006, 2010.

[347] David Garfinkle, Frans Pretorius, and Nicolas Yunes. Linear Stability Analysis and the Speed of Gravitational Waves in Dynamical Chern-Simons Modified Gravity. Phys. Rev. D, 82:041501, 2010.

[348] C. Molina, Paolo Pani, Vitor Cardoso, and Leonardo Gualtieri. Gravitational signature of Schwarzschild black holes in dynamical Chern-Simons gravity. Phys. Rev., D81:124021, 2010.

[349] Nicholas Loutrel, Takahiro Tanaka, and Nicolas Yunes. Spin-Precessing Black Hole Binaries in Dynamical Chern-Simons Gravity. 2018.

[350] Pratik Wagle, Alexander Saffer, and Nicolas Yunes. Polarization modes of gravitational waves in Quadratic Gravity. Phys. Rev. D, 100(12):124007, 2019.

[351] Pratik Wagle, Nicolas Yunes, and Hector O. Silva. Quasinormal modes of slowly-rotating black holes in dynamical Chern-Simons gravity. 3 2021.

[352] Yuya Nakamura, Daiki Kikuchi, Kei Yamada, Hideki Asada, and Nicolas Yunes. Weakly-gravitating objects in dynamical Chern–Simons gravity and constraints with gravity probe B. Class. Quant. Grav., 36(10):105006, 2019.

[353] Scott E. Perkins, Remya Nair, Hector O. Silva, and Nicolas Yunes. Improved gravitational-wave constraints on higher-order curvature theories of gravity. Phys. Rev. D, 104(2):024060, 2021.

[354] Stephon Alexander, Gregory Gabadadze, Leah Jenks, and Nicolás Yunes. The Chern-Simons Caps for Rotating Black Holes. 3 2021.

[355] R. H. Dicke. Coherence in spontaneous radiation processes. Phys. Rev., 93:99–110, Jan 1954.

[356] Ya. B. Zel'Dovich. Generation of Waves by a Rotating Body. Soviet Journal of Experimental and Theoretical Physics Letters, 14:180, August 1971.

[357] Ya. B. Zel'Dovich. Amplification of Cylindrical Electromagnetic Waves Reflected from a Rotating Body. Soviet Journal of Experimental and Theoretical Physics, 35:1085, January 1972.

[358] A. A. Starobinsky. Amplification of waves reflected from a rotating "black hole". Sov. Phys. JETP, 37(1):28–32, 1973.

[359] William H. Press and Saul A. Teukolsky. Floating Orbits, Superradiant Scattering and the Black-hole Bomb. Nature, 238:211–212, 1972.

[360] James M. Bardeen, William H. Press, and Saul A Teukolsky. Rotating black holes: Locally nonrotating frames, energy extraction, and scalar synchrotron radiation. Astrophys. J., 178:347, 1972.

[361] I. M. Ternov, V. R. Khalilov, G. A. Chizhov, and Alex B. Gaina. Finite motion of massive particles in the Kerr and Schwarzschild fields. Sov. Phys. J., 21:1200–1204, 1978.

[362] T. J. M. Zouros and D. M. Eardley. INSTABILITIES OF MASSIVE SCALAR PERTURBATIONS OF A ROTATING BLACK HOLE. Annals Phys., 118:139–155, 1979.

[363] Steven L. Detweiler. KLEIN-GORDON EQUATION AND ROTATING BLACK HOLES. Phys. Rev. D, 22:2323–2326, 1980.

[364] Sam R. Dolan. Instability of the massive Klein-Gordon field on the Kerr spacetime. Phys. Rev. D, 76:084001, 2007.

[365] Asimina Arvanitaki, Savas Dimopoulos, Sergei Dubovsky, Nemanja Kaloper, and John March-Russell. String Axiverse. Phys. Rev. D, 81:123530, 2010.

[366] Asimina Arvanitaki and Sergei Dubovsky. Exploring the String Axiverse with Precision Black Hole Physics. Phys. Rev. D, 83:044026, 2011.

[367] Sam R. Dolan. Superradiant instabilities of rotating black holes in the time domain. Phys. Rev. D, 87(12):124026, 2013.

[368] Hirotaka Yoshino and Hideo Kodama. Gravitational radiation from an axion cloud around a black hole: Superradiant phase. PTEP, 2014:043E02, 2014.

[369] Richard Brito, Vitor Cardoso, and Paolo Pani. Black holes as particle detectors: evolution of superradiant instabilities. Class. Quant. Grav., 32(13):134001, 2015.

[370] Richard Brito, Vitor Cardoso, and Paolo Pani. Superradiance: New Frontiers in Black Hole Physics. Lect. Notes Phys., 906:pp.1–237, 2015.

[371] Masha Baryakhtar, Marios Galanis, Robert Lasenby, and Olivier Simon. Black hole superradiance of self-interacting scalar fields. Phys. Rev. D, 103(9):095019, 2021.

[372] Joao G. Rosa and Sam R. Dolan. Massive vector fields on the Schwarzschild spacetime: quasi-normal modes and bound states. Phys. Rev. D, 85:044043, 2012.

[373] Paolo Pani, Vitor Cardoso, Leonardo Gualtieri, Emanuele Berti, and Akihiro Ishibashi. Perturbations of slowly rotating black holes: massive vector fields in the Kerr metric. Phys. Rev. D, 86:104017, 2012.

[374] Paolo Pani, Vitor Cardoso, Leonardo Gualtieri, Emanuele Berti, and Akihiro Ishibashi. Black hole bombs and photon mass bounds. Phys. Rev. Lett., 109:131102, 2012.

[375] William E. East. Superradiant instability of massive vector fields around spinning black holes in the relativistic regime. Phys. Rev. D, 96(2):024004, 2017.

[376] Masha Baryakhtar, Robert Lasenby, and Mae Teo. Black Hole Superradiance Signatures of Ultralight Vectors. Phys. Rev. D, 96(3):035019, 2017.

[377] Daniel Baumann, Horng Sheng Chia, John Stout, and Lotte ter Haar. The Spectra of Gravitational Atoms. JCAP, 12:006, 2019.

[378] Richard Brito, Vitor Cardoso, and Paolo Pani. Massive spin-2 fields on black hole spacetimes: Instability of the Schwarzschild and Kerr solutions and bounds on the graviton mass. Phys. Rev. D, 88(2):023514, 2013.

[379] Richard Brito, Sara Grillo, and Paolo Pani. Black Hole Superradiant Instability from Ultralight Spin-2 Fields. Phys. Rev. Lett., 124(21):211101, 2020.

[380] Cheng-Yong Zhang, Shao-Jun Zhang, Peng-Cheng Li, and Minyong Guo. Superradiance and stability of the regularized 4D charged Einstein-Gauss-Bonnet black hole. JHEP, 08:105, 2020.

[381] Mohsen Khodadi. Black Hole Superradiance in the Presence of Lorentz Symmetry Violation. Phys. Rev. D, 103(6):064051, 2021.

[382] Mohsen Khodadi, Alireza Talebian, and Hassan Firouzjahi. Black Hole Superradiance in f(R) Gravities. 2 2020.

[383] Shao-Jun Zhang. Massive scalar field perturbation on Kerr black holes in dynamical Chern–Simons gravity. Eur. Phys. J. C, 81(5):441, 2021.

[384] R. Penrose and R. M. Floyd. Extraction of rotational energy from a black hole. Nature, 229:177–179, 1971.

[385] Lam Hui. Wave Dark Matter. 1 2021.

[386] Asimina Arvanitaki, Masha Baryakhtar, and Xinlu Huang. Discovering the QCD Axion with Black Holes and Gravitational Waves. Phys. Rev. D, 91(8):084011, 2015.

[387] Asimina Arvanitaki, Peter W. Graham, Jason M. Hogan, Surjeet Rajendran, and Ken Van Tilburg. Search for light scalar dark matter with atomic gravitational wave detectors. Phys. Rev. D, 97(7):075020, 2018.

[388] Asimina Arvanitaki, Masha Baryakhtar, Savas Dimopoulos, Sergei Dubovsky, and Robert Lasenby. Black Hole Mergers and the QCD Axion at Advanced LIGO. Phys. Rev. D, 95(4):043001, 2017.

[389] Richard Brito, Shrobana Ghosh, Enrico Barausse, Emanuele Berti, Vitor Cardoso, Irina Dvorkin, Antoine Klein, and Paolo Pani. Gravitational wave searches for ultralight bosons with LIGO and LISA. Phys. Rev. D, 96(6):064050, 2017.

[390] Daniel Baumann, Horng Sheng Chia, and Rafael A. Porto. Probing Ultralight Bosons with Binary Black Holes. Phys. Rev. D, 99(4):044001, 2019.

[391] Matthew J. Stott and David J. E. Marsh. Black hole spin constraints on the mass spectrum and number of axionlike fields. Phys. Rev. D, 98(8):083006, 2018.

[392] Giuseppe Ficarra, Paolo Pani, and Helvi Witek. Impact of multiple modes on the black-hole superradiant instability. Phys. Rev. D, 99(10):104019, 2019.

[393] Robert McNees, Leo C. Stein, and NicolÃÂ¡s Yunes. Extremal black holes in dynamical Chern?Simons gravity. Class. Quant. Grav., 33(23):235013, 2016.

[394] William E. East, Fethi M. Ramazanoğlu, and Frans Pretorius. Black Hole Superradiance in Dynamical Spacetime. Phys. Rev. D, 89(6):061503, 2014.

[395] William E. East and Frans Pretorius. Superradiant Instability and Backreaction of Massive Vector Fields around Kerr Black Holes. Phys. Rev. Lett., 119(4):041101, 2017.

[396] Milton Abramowitz and Irene A. Stegun. Handbook of Mathematical Functions with Formulas, Graphs, and Mathematical Tables. Dover Publications, Mineola, New York, 1972.

[397] W. G. Unruh. Second quantization in the Kerr metric. Phys. Rev. D, 10:3194–3205, 1974.